

**The complete genome sequence of *Rhizobium* sp.
NGR234 reveals a surprisingly large number of
quorum quenching associated genes**

Dissertation

zur Erlangung der Würde des Doktors der Naturwissenschaften

des Fachbereichs Biologie, der Fakultät für Mathematik, Informatik und Naturwissenschaften,

der Universität Hamburg

vorgelegt von

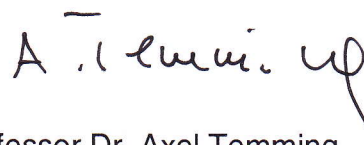
Dagmar Krysciak

aus Kreuzburg / Polen

Hamburg 2011

Genehmigt vom Fachbereich Biologie
der Fakultät für Mathematik, Informatik und Naturwissenschaften
an der Universität Hamburg
auf Antrag von Prof. Dr. W. STREIT
Weiterer Gutachter der Dissertation:
Prof. Dr. B. BISPING
Tag der Disputation: 26. August 2011

Hamburg, den 11. August 2011

A handwritten signature in black ink, appearing to read 'A. Temming' with a stylized flourish at the end.

Professor Dr. Axel Temming
Leiter des Fachbereichs Biologie



Universität Hamburg

Universität Hamburg • 22609 Hamburg

Department Biologie
Molekularbiologie Mikrobieller Konsortien

junProf. Dr. Mirjam Perner

Telefon (040) 42816 – 444
Fax (040) 42816 – 459
E-Mail mirjam.perner@uni-hamburg.de

Biozentrum Klein Flottbek
Ohnhorststr. 18
22609 Hamburg

Raum 3.156

Datum 19. Juli 2012

**Bestätigung der sprachlichen Korrektheit der Dissertation von
MSc Dagmar Krysciak**

Hiermit bestätige ich die sprachliche Korrektheit (englisch) der vorliegenden Dissertation, verfasst von MSc Dagmar Krysciak mit dem Titel: **The complete genome sequence of *Rhizobium* sp. NGR234 reveals a surprisingly large number of quorum quenching associated genes.**

Mit freundlichen Grüßen

junProf. Dr. Mirjam Perner

Jun. Prof. Dr. Mirjam Perner
Universität Hamburg
Biozentrum Klein Flottbek • Mikrobiologie
Ohnhorststraße 18 • D-22609 Hamburg
Tel: ++49-40-428 16 444
Fax: ++49-40-428 16 459

The results of this research have been published in the following journals:

Krysciak, D., Schmeisser, C., Preuss, S., Riethausen, J., Quitschau, M., Grond, S. and Streit, W. R. (2011). Multiple loci are involved in quorum quenching of autoinducer I molecules in the nitrogen-fixing symbiont (*Sino-*) *Rhizobium* sp. NGR234. *Applied and Environmental Microbiology* **55** (15): 5089-99.

Schmeisser, C.*; Liesegang, H.*; **Krysciak, D.***, Bakkou, N., Le Quere, A., Wollherr, A., Heinemeyer, I., Morgenstern, B., Pommerening-Röser, A., Flores, M., Palacios, R., Brenner, S., Gottschalk, G., Schmitz, R. A., Broughton, W. J., Perret, X., Strittmatter, A. W. and Streit, W. R. (2009). *Rhizobium* sp. strain NGR234 possesses a remarkable number of secretion systems. *Applied and Environmental Microbiology* **75** (12): 4035-45.

*** contributed equally to this study**

Table of Contents

I.	Introduction	1
1.	Cell-to-cell communication	1
1.1.	AHL-dependent QS mechanisms of Gram-negative bacteria	2
1.2.	Peptide-mediated QS in Gram-positive bacteria	2
1.3.	Interspecies cell-to-cell communication	3
1.4.	Interkingdom signaling systems	4
1.5.	Quorum sensing in rhizobia	4
2.	Quorum quenching – The evolutive advantage	6
2.1.	Blockade of autoinducer synthases	7
2.2.	Inhibition of autoinducer receptors	7
2.3.	Mechanisms of enzymatic degradation of signal molecules	8
2.3.1	Signal degradation by AHL lactonases - AHLases	9
2.3.2	Signal degradation by AHL amidases	12
2.4.	Modification of AHL signal molecules by oxidoreductases	13
2.5.	QQ in plant-associated bacteria and their eukaryotic hosts	14
2.5.1	Interaction of plant-associated bacteria	14
2.5.2	QQ-mediated defense mechanisms of eukaryotic hosts	15
3.	The α -proteobacterium <i>Rhizobium</i> sp. NGR234	15
4.	Aims of the research	17
II.	Material and Methods	18
1.	Bacterial strains, vectors and primers	18
2.	Culture media, supplements and solutions	20
2.1.	Culture media	20
2.1.1	LB medium for <i>Escherichia coli</i> (Sambrook 2001)	21
2.1.2	AT medium for <i>Agrobacterium tumefaciens</i> NTL4	21
2.1.3	YEM medium for <i>Rhizobium</i> sp. NGR234	22
2.1.4	TY medium for <i>Rhizobium</i> sp. NGR234 (Streit <i>et al.</i> 2004, modified)	22
2.1.5	YDC agar for <i>Chromobacterium violaceum</i> ChV2	23
2.2.	Antibiotics and supplements	23
2.3.	Solutions and buffers	24
2.3.1	TE buffer	24
2.3.2	Potassium phosphate buffer (0.1 M)	24
2.3.3	Hoagland solution (Hoagland and Arnon 1950)	25
3.	Cell culture, strain collection and growth conditions	26
3.1.	Cultivation of bacteria	26
3.1.1	Cultivation of <i>Escherichia coli</i> (<i>E. coli</i>)	26
3.1.1.1	<i>E. coli</i> cell cultures	26
3.1.1.2	<i>E. coli</i> expression cultures	26
3.1.1.3	<i>E. coli</i> cosmid clone cultures	26
3.1.2	Cultivation of <i>Rhizobium</i> sp. NGR234	27
3.1.3	Cultivation of <i>A. tumefaciens</i> NTL4	27
3.1.4	Cultivation of <i>C. violaceum</i> ChV2 and CV026	27
3.1.5	Cultivation of <i>Pseudomonas aeruginosa</i> PAO1	27
3.2.	Strain collection	27
3.2.1	Maintenance and strain collection of pure cultures	27
3.2.2	Maintenance and preservation of the cosmid clone library	28
3.3.	Determination of cell density	28
4.	Standard techniques for working with DNA	28
4.1.	Isolation of DNA	28
4.1.1	Isolation of plasmid and cosmid DNA by commercial kits	28

4.1.2	Isolation of plasmid DNA by alkaline cell lysis.....	29
4.1.3	Isolation of plasmid DNA by cracking.....	30
4.1.4	Isolation of cosmid DNA by the quick and dirty method.....	31
4.1.5	Isolation of genomic DNA with AquaPure Genomic DNA kit.....	31
4.1.6	Classical isolation of genomic DNA.....	31
4.2.	DNA fragment isolation and purification by extraction from agarose gels.....	32
4.3.	Determination of DNA concentration and purity.....	32
4.4.	Agarose gel electrophoresis.....	32
4.5.	Enzymatic modification of nucleic acids.....	33
4.5.1	Digestion of DNA by restriction endonucleases.....	33
4.5.1.1	Complete digestion.....	33
4.5.1.2	Partial digestion of genomic DNA.....	34
4.5.2	Dephosphorylation of complementary ends.....	35
4.5.3	Complementation of overhangs with Klenow polymerase.....	35
4.5.4	Purification and concentration of nucleic acids after enzymatic modification..	36
4.5.5	Ligation of DNA.....	36
4.5.5.1	Ligation of DNA fragments with T4 DNA ligase.....	36
4.5.5.2	Ligation of PCR products in pDrive Cloning Vector.....	37
4.6.	Amplification of DNA by PCR.....	37
4.6.1	Oligonucleotide primers.....	37
4.6.2	Standard PCR.....	38
4.6.3	Direct colony PCR.....	38
4.6.4	Purification of PCR products.....	39
4.7.	Transposon mutagenesis.....	40
4.8.	Construction of a cosmid clone library.....	40
4.8.1	Preparation of genomic DNA fragments.....	40
4.8.2	Ligation.....	41
4.8.3	<i>In vitro</i> Packaging.....	41
4.8.4	Transduction.....	41
5.	DNA transfer techniques.....	42
5.1.	Transformation of <i>E. coli</i> cells.....	42
5.1.1	Preparation of heat competent and <i>E. coli</i> DH5 α cells.....	42
5.1.2	Chemical preparation of heat competent <i>E. coli</i> XL1 blue and BL21 (DE3) cells by the CaCl ₂ method.....	42
5.1.3	Heat shock transformation of <i>E. coli</i> DH5 α , XL1 blue and BL 21 (DE3).....	43
5.2.	Transformation of <i>Rhizobium</i> sp. NGR234.....	43
5.2.1	Preparation of electrocompetent <i>Rhizobium</i> sp. NGR234 cells.....	43
5.2.2	Electroporation of <i>Rhizobium</i> sp. NGR234.....	43
6.	Biochemical methods for working with proteins.....	44
6.1.	Standard techniques.....	44
6.1.1	Quantitative determination of protein content (Bradford 1976).....	44
6.1.2	SDS-Polyacrylamide gel electrophoresis (SDS-PAGE).....	44
6.1.2.1	Composition of SDS-PAGE gels.....	45
6.1.2.2	Preparation of protein samples and SDS-PAGE gel electrophoresis.....	46
6.1.2.3	Coomassie staining of SDS-PAGE gels.....	46
6.2.	Protein purification.....	47
6.2.1	Crude cell extract preparation.....	47
6.2.1.1	Ultrasonication.....	47
6.2.1.2	French Pressure Cell.....	47
6.2.2	Purification of histidine-tagged proteins by Protino [®] Ni-TED columns.....	48
6.2.3	Dialysis of purified protein extracts.....	48
6.2.4	Concentration of protein solutions.....	48
6.2.4.1	Concentration by Vivaspin concentrator.....	48
6.2.4.2	Concentration by flow filtration capsule.....	48
6.3.	Western blotting.....	49
6.3.1	Preparation of membrane and blotting.....	49

6.3.2	Blocking of membrane and binding of antibodies.....	49
6.3.3	Detection of His-tagged proteins.....	49
7.	Methods for detection of QQ activity	50
7.1.	Homoserine lactone solutions.....	50
7.1.1	<i>N</i> -(butanoyl)-L-homoserine lactone	50
7.1.2	<i>N</i> -(3-oxohexanoyl)-L-homoserine lactone.....	51
7.1.3	<i>N</i> -(3-oxooctanoyl)-L-homoserine lactone.....	51
7.1.4	<i>N</i> -(3-oxododecanoyl)- L-homoserine lactone	51
7.2.	ATsoft screening using <i>A. tumefaciens</i> NTL4 (Schipper <i>et al.</i> 2009).....	51
7.2.1	Preparation of ATsoft screening agar	51
7.2.2	ATsoft screening procedure.....	52
7.2.2.1	Determination of required HSL concentration	52
7.2.2.2	Preparation of <i>E. coli</i> cosmid clone samples	52
7.2.2.3	Screening procedure	53
7.3.	Inhibition of swarming motility in <i>E. coli</i>	53
7.3.1	Swarming motility of <i>E. coli</i> in liquid medium	53
7.3.1.1	Preparation of liquid swarming medium.....	53
7.3.1.2	Screening procedure	53
7.3.2	Swarming motility of <i>E. coli</i> on solid medium	54
7.3.2.1	Preparation of solid swarming medium.....	54
7.3.2.2	Screening procedure	54
7.4.	Inhibition of motility in <i>P. aeruginosa</i> PAO1	55
7.4.1	Swarming and swimming motility in <i>P. aeruginosa</i> PAO1	55
7.4.1.1	Preparation of swarming/swimming agar for <i>P. aeruginosa</i> PAO1.....	55
7.4.1.2	Screening procedure	56
7.4.2	Biofilm inhibition assay with <i>P. aeruginosa</i> PAO1	57
7.5.	Pigment inhibition assays with <i>C. violaceum</i> ChV2 and CV026	57
7.5.1	Pigment inhibition of solid YDC medium with ChV2	57
7.5.2	Pigment inhibition in liquid medium with ChV2 and CV026	57
7.6.	Enzyme activity assays.....	58
7.6.1	β -Galactosidase activity assay using reporter strain <i>A. tumefaciens</i> NTL4	58
7.6.2	Pyocyanine assay.....	59
7.6.3	Degradation of β -lactam antibiotics.....	60
8.	HPLC analysis	60
8.1.	Preparation of protein samples	60
8.2.	Detection of cleavage products by HPLC-MS-DAD analysis	60
9.	Rhizobial colonization experiments.....	61
9.1.	Germination and inoculation of cowpea seeds.....	61
9.2.	Cell harvesting and cell counts	62
10.	Sequence analysis of DNA	62
10.1.	Sequencing of ORFs, plasmids and cosmids	62
10.2.	Complete genome sequencing.....	62
11.	Software	63
11.1.	Databases.....	63
11.2.	Programs	63
III.	Results	65
1.	Sequencing and complete genome analysis of <i>Rhizobium</i> sp. NGR234	65
1.1.	General features and highlights hidden in the genome of the NGR234.....	66
1.2.	Diverse secretion systems are encoded by the 6.9 Mbp genome	67
1.3.	Cell-to-cell communication apparatus comprised by NGR234.....	68
1.3.1	AHL-mediated cell-to-cell communication present in NGR234.....	69
1.3.2	The LuxS/AI-2 signaling system in NGR234.....	70
1.3.3	The autoinducer 3 molecule based signaling system.....	71
1.4.	QQ mechanisms found in NGR234.....	71

1.4.1	Putative QQ genes belonging to AHLases.....	72
1.4.2	Five putative QQ genes can be possibly grouped to AHL amidases.....	73
1.4.3	Other hydrolases related to QQ.....	74
2.	Genome wide functional analysis of genes/enzymes interfering with QS systems.....	74
2.1.	Construction of a genomic NGR234 cosmid clone library.....	74
2.2.	Functional-based screening of the genomic library on AHL degrading ability.....	75
2.2.1	ATsoft screening procedure using <i>A. tumefaciens</i> NTL4.....	75
2.2.2	Inhibition of swarming motility in <i>E. coli</i>	76
2.2.2.1	Screening for inhibition of swarming motility in <i>E. coli</i> EPI100.....	76
2.2.2.2	Screening for inhibition of swarming motility in <i>E. coli</i> XL1 blue.....	77
2.2.3	Inhibition of motility in <i>P. aeruginosa</i> PAO1.....	78
2.2.3.1	Inhibition of swarming motility in <i>P. aeruginosa</i> PAO1.....	78
2.2.3.2	Biofilm inhibition in <i>P. aeruginosa</i> PAO1.....	78
3.	Five functional NGR234 cosmid clones reveal AHL degradation or modification.....	80
3.1.	Chromosomal loci <i>hitR-hydR</i> , <i>qsdR2</i> and <i>aldR</i> appeared to be involved in QQ in <i>Rhizobium</i> sp. NGR234.....	81
3.1.1	Locus <i>hitR-hydR</i> reveals AHL-degrading or modifying ability.....	81
3.1.1.1	Construction of pWEB-TNC-A5 transposon mutant bank.....	82
3.1.1.2	Initial motility assays in <i>E. coli</i> XL1 blue and <i>P. aeruginosa</i> PAO1.....	82
3.1.1.3	Identification of <i>hitR-hydR</i> locus by sequencing of conspicuous transposon mutants.....	83
3.1.1.4	Sequence analysis of locus <i>hitR-hydR</i>	84
3.1.1.5	Direct cloning and initial screening of the QQ active <i>hitR-hydR</i> locus.....	85
3.1.1.6	Functional verification of locus <i>hitR-hydR</i>	85
3.1.2	The AHLase related <i>qsdR2</i> gene is able to degrade AHLs.....	87
3.1.2.1	Detailed analysis of the conserved motif on <i>qsdR2</i> attributed to QQ.....	87
3.1.2.2	Sequence-based comparison to known AHLases.....	88
3.1.2.3	Functional screenings confirm QQ activity of <i>qsdR2</i>	88
3.1.3	An acetaldehyde dehydrogenase, AldR, a novel lactone hydrolyzing enzyme.....	89
3.1.3.1	Construction of a pWEB-TNC-G2 transposon mutant bank and initial motility assays.....	90
3.1.3.2	Identification and detailed sequence analysis of the <i>aldR</i> locus.....	91
3.1.3.3	Functional verification of QQ activity of AldR.....	92
3.2.	Verification and biochemical characterization of putative QQ genes <i>dlhR</i> and <i>qsdR1</i> located on the megaplasmid of NGR234.....	93
3.2.1	DlhR, a dienelactone hydrolase capable of inactivating AHLs.....	94
3.2.1.1	Subcloning and identification of candidate ORFs on pWEB-TNC-B2.....	94
3.2.1.2	Sequence analysis revealed the presence of <i>dlhR</i> on pWEB-TNC-B2.....	95
3.2.1.3	Overexpression and purification of DlhR.....	96
3.2.1.4	Inhibition of motility in <i>P. aeruginosa</i> PAO1 by DlhR.....	97
3.2.1.4.1	Swarming and swimming test with <i>P. aeruginosa</i> PAO1 and DlhR.....	98
3.2.1.4.2	Complementation experiments with <i>P. aeruginosa</i> PAO1 and external AHLs.....	99
3.2.2	Gene <i>qsdR1</i> is involved in QQ of AI-1 molecules.....	100
3.2.2.1	Subcloning and identification of candidate ORFs on pWEB-TNC-C6.....	100
3.2.2.2	Sequence analysis and comparison to representatives of the AHLase group.....	101
3.2.2.3	Overexpression and purification of QsdR1.....	102
3.2.2.4	Analysis of the QQ activity of QsdR1.....	104
3.2.2.4.1	Inhibition of motility in <i>P. aeruginosa</i> PAO1.....	104
3.2.2.4.2	Pigment inhibition assay with <i>C. violaceum</i> ChV2.....	104
3.2.2.4.3	Determination of β -lactam degrading ability of QsdR1.....	106
3.2.3	Biochemical characterization of QQ associated proteins, DlhR and QsdR1.....	106
3.2.3.1	Verification of QQ effects of DlhR and QsdR1 by the β -galactosidase assay.....	106

3.2.3.2	Characterization of DIhR and QsdR1 responsible for biofilm phenotypes in the rhizosphere	107
3.2.3.3	Uncovering the cleaving mechanisms of DIhR and QsdR1 by HPLC-MS analysis	110
IV.	Discussion	113
1.	The number of secretion systems correlates to the host range of <i>Rhizobium</i> sp. NGR234	114
2.	Quorum sensing in NGR234 and selected rhizobia.....	115
2.1.	AHL-mediated cell-to-cell communication	116
2.2.	AI-2 and AI-3 signaling systems can contribute to the broad host range of NGR234	118
2.2.1	AI-2-mediated signaling systems found in NGR234.....	118
2.2.2	AI-3 molecule based signaling systems	119
2.3.	Correlation of QS-mediated communication in NGR234 and its number of symbiotic partners.....	120
3.	QQ in <i>Rhizobium</i> sp. NGR234	120
3.1.	Multiple QQ associated genes owned by NGR234 collaborate with its broad host range.....	121
3.2.	The functional approach revealed a surprisingly high number of QQ related genes hidden in the genome of NGR234	124
3.3.	Wealth of loci involved in QQ is a unique feature of NGR234	125
3.3.1	Chromosomal loci <i>hitR-hydR</i> , <i>qsdR2</i> and <i>aldR</i> encode for novel lactone hydrolyzing enzymes	126
3.3.1.1	Locus <i>hitR-hydR</i> reveals AHL degrading/modifying activity	126
3.3.1.2	The metal-dependent hydrolase, QsdR2, is able to degrade AHL signal molecules.....	128
3.3.1.3	AldR, an acetaldehyde dehydrogenase represents a novel lactone hydrolyzing enzyme.....	129
3.3.2	Biochemical characterization of DIhR and QsdR1 located on the pNGR234 <i>b</i>	129
3.3.2.1	The dienelactone hydrolase, DIhR, constitutes a new member of the AHLases	130
3.3.2.2	QsdR1 extends the list of functionally characterized AHLases of the metallo- β -lactamase family.....	131
3.3.3	DIhR and QsdR1 associated with biofilm phenotypes in the rhizosphere.....	133
4.	Concluding remarks and outlook.....	134
V.	Abstract	135
VI.	References	137
VII.	Appendix	147
VIII.	Abbreviations	159
	Acknowledgements	164

List of Figures

Figure 1: Model of QS gene regulation in NGR234.....	6
Figure 2: Three main mechanisms of AHL degrading enzymes.....	9
Figure 3: The α -proteobacterium <i>Rhizobium</i> sp. NGR234.....	16
Figure 4: Map of the genome of <i>Rhizobium</i> sp. NGR234.....	67
Figure 5: Conserved cluster of QS systems found in <i>Rhizobium</i> sp. NGR234	70
Figure 6: Examples of ATsoft screening procedure and swarming motility assay in <i>E. coli</i> ..	77
Figure 7: Swarming behavior of cosmid clones in <i>E. coli</i> XL1 blue cells on solid medium....	77
Figure 8: <i>P. aeruginosa</i> PAO1 motility and biofilm assays.....	79
Figure 9: Identification of AHL-degrading cosmid clones on cNGR234.....	81
Figure 10: Motility assays accomplished with transposon mutants in <i>E. coli</i> XL1 blue and PAO1.	83
Figure 11: β -Galactosidase assay with NTL4 and violacein inhibition assay with CV026.....	86
Figure 12: BioEdit alignment of QsdR2 and published AHLases sharing conserved regions	88
Figure 13: β -Galactosidase assay with NTL4 and violacein inhibition assay with CV026.....	89
Figure 14: Motility assays accomplished with transposon mutants in <i>E. coli</i> XL1 blue and PAO1	91
Figure 15: β -Galactosidase assay with NTL4 and violacein inhibition assay with CV026.....	93
Figure 16: Identification of AHL-degrading cosmid clones on pNGR234 <i>b</i>	94
Figure 17: Localization of identified domains and motifs on the deduced AA sequence of DlhR and a predicted protein model	96
Figure 18: SDS-PAGE of His-tag purification and western blot analysis of DlhR	97
Figure 19: <i>P. aeruginosa</i> PAO1 motility assays	98
Figure 20: BioEdit alignment of QsdR1 and published AHLases sharing conserved regions	102
Figure 21: SDS-PAGE of overexpression and western blot analysis of QsdR1.	103
Figure 22: <i>P. aeruginosa</i> PAO1 swarming/biofilm assay and pigment inhibition in <i>C. violaceum</i> ChV2	105
Figure 23: β -Galactosidase assay with NTL4.....	107
Figure 24: Biofilm phenotype of NGR234 in medium and the rhizosphere triggered by extra copies of <i>dlhR</i> and <i>qsdR1</i>	109

Figure 25: HPLC-MS analysis of recombinant DIhR and QsdR1.	111
Figure 26: Phylogenetic relationships of rhizobia.....	116
Figure 27: Reactions catalyzed by ELH and dienelactone hydrolases with structure of substrates and products	130
Figure 28: Straight calibration for determination of protein content (Bradford assay)	148
Figure 29: Definition of the motility of <i>E. coli</i> XL1 blue and of <i>P. aeruginosa</i> PAO1 on agar plates.	148
Figure 30: Motility assays accomplished with pDrive:: <i>qsdR2</i> in <i>E. coli</i> XL1 blue and PAO1..	151
Figure 31: Motility assays accomplished with pDrive:: <i>aldR</i> in <i>E. coli</i> XL1 blue and PAO1..	152
Figure 32: Complementation assay with 3-oxo-C8-HSL and 5 µg/mL DIhR	152

List of Tables

Table 1: Functionally characterized AHLases found in diverse microorganisms and metagenomes.....	11
Table 2: Uncovered AHL amidases found in diverse Gram-negative and Gram-positive strains.....	12
Table 3: Bacterial strains used in this study	18
Table 4: Vectors and constructs used and established in this study.....	18
Table 5: Primers used in this study	20
Table 6: Antibiotics and supplements used in this study	23
Table 7: Solutions and composition of 1L Hoagland solution	25
Table 8: Commercial Mini- and Midiprep DNA isolation kits	29
Table 9: Temperature conditions for PCR with <i>Pfu</i> polymerase	38
Table 10: Temperature conditions for PCR with <i>Taq</i> polymerase	39
Table 11: Composition of SDS-PAGE gels used in this study	46
Table 12: Composition of 100 mL swarming and swimming agar.....	56
Table 13: Genes/ORFs involved in synthesis of secretion systems in <i>Rhizobium</i> sp. NGR234	68
Table 14: Possible QQ genes identified by alignment analyses with public databases	72
Table 15: Five candidate cosmid clones identified in this study with their properties and positions	80
Table 16: Complementation experiments with PAO1, external AHLs and DIhR	99
Table 17: QQ inventory of NGR234 and selected rhizobial microbes.....	123
Table 18: Hydrolases found in the genome of NGR234 by sequence analysis	149
Table 19: β -Lactam degradation assay with pET24c:: <i>qsdr1</i>	153

I. Introduction

1. Cell-to-cell communication

Environmental sensing systems that enable bacteria to monitor their own population density to subsequently synchronize group behavior are termed quorum sensing (QS) systems. This cell-to-cell signaling process conveys by small chemical molecules the status of the single cell and its extracellular environment to the population, allowing bacteria to collectively make decisions with respect to gene expression (Fuqua *et al.* 2001; Miller and Bassler 2001). Essential components of the QS circuits are small, diffusible signaling molecules, called autoinducers (AI), which are released by diffusion or active transport into the environment and sensed by surrounding bacteria (Redfield 2002). The accumulation of a threshold autoinducer concentration in the extracellular environment has two consequences: First, AIs bind to a regulator protein leading to a population-wide alternation of gene expression and secondly, AI uptake results in a positive feedback loop, increasing the production of signal molecules (Waters and Bassler 2005; Gonzalez and Keshavan 2006). Since such vital biological functions as virulence, plasmid transfer and/or biofilm formation coordinated by QS are unproductive when accomplished by an individual bacterium, they require a concentrated action of numerous cells to become effective (Henke and Bassler 2004), which is accomplished by cell-to-cell communication using AIs. Until today many structurally diverse QS signals have been described which can be distinguished into intra- and interspecies AIs. Various Gram-negative bacteria rely on *N*-acylhomoserine lactones (AHLs), representing the most prevalent and best studied class of AI-1. AHL structures have a common homoserine lactone (HSL) ring moiety and an acyl side chain varying in length (ranging from 4 to 14 carbons) and substituent on the third carbon (Fuqua *et al.* 2001). In contrast, small modified oligopeptides facilitate QS in Gram-positive bacteria such as *Bacillus subtilis* and *Staphylococcus aureus* by interaction with a two-component histidine protein kinase signal transduction system (Grossman 1995; Yarwood *et al.* 2004). The autoinducer 2 (AI-2) represents a species nonspecific class of signal molecules found to be produced by a wide range of Gram-negative and Gram-positive bacteria. Based on this fact the novel furanosyl borate diester is proposed to be a universal signal of interspecies cell-to-cell communication (Xavier and Bassler 2003). Finally, the aromatic autoinducer 3 (AI-3) together with eukaryotic cell signals represent the hormonal interkingdom signaling between microbes and their hosts. A closer look on the accepted QS circuits will be given in the following.

1.1. AHL-dependent QS mechanisms of Gram-negative bacteria

Investigations on AHL-dependent QS mechanisms were initiated over forty years ago by studies of Nealson and coworkers on cell density dependent bioluminescence regulation in the marine bacterium *Vibrio fischeri* (Nealson *et al.* 1970). The luciferase operon *luxCDABE* encodes for enzymes responsible for the light production in light organs of squids and is regulated by two main proteins: LuxI, an AHL-synthase and LuxR, an autoinducer receptor protein. Deduced from the bioluminescence regulatory network, this QS process is considered to be the paradigm for most Gram-negative bacteria. AHL-specific QS in these bacteria involves the two mentioned components. The AHL-synthase, a LuxI homologue which constitutively produces the autoinducer 1 at low levels, requires for its synthesis S-adenosylmethionine (SAM) and fatty acyl carrier proteins (Acyl-ACP) (Hanzelka and Greenberg 1996). After reaching a critical threshold concentration, AI-1 associates with its AHL response transcription factor, a LuxR homologue. This LuxR-AHL complex binds to DNA promoter sequences (called *lux* boxes), induces the AHL synthase creating a positive induction loop as well as regulates the expression of QS target genes (Waters and Bassler 2005). Since the initial description of the luciferase operon, AHL-mediated QS including homologs of LuxR/LuxI has been demonstrated in over 70 different Gram-negative bacteria (Czajkowski and Jafra 2009) and is perhaps present in many more. Beside free-living bacteria, QS mechanisms were also associated with microorganisms living in symbiosis with higher organisms, such as humans and plants. In this context, the intricate signaling between rhizobial symbionts and their host was intensively studied, as different symbiotic processes were connected to the complex QS network (Wisniewski-Dye and Downie 2002; Marketon *et al.* 2003).

1.2. Peptide-mediated QS in Gram-positive bacteria

Gram-positive bacteria employ a common cell-to-cell signaling structure using small, modified oligopeptides to coordinate such processes as virulence response in *Staphylococcus aureus* (Yarwood *et al.* 2004) and genetic competence in *Bacillus subtilis* (Grossman 1995). The signal molecules also termed autoinducer polypeptides (AIPs) are synthesized in the cytoplasm as precursor peptides are then further modified and subsequently exported from the bacterium by ABC-transporters (Taga and Bassler 2003). The concentration of AIPs in the extracellular surroundings increases as a response to changing environmental conditions and as a function of cell density. Subsequently, the AIPs are recognized by membrane-bound receptors of a two-component signal transduction system (Kleerebezem *et al.* 1997; Federle and Bassler 2003). These sensor kinases detect and transmit the extracellular information (AIPs) by a phosphorylation cascade to response

regulator proteins. When phosphorylated, this response regulator binds to promoter DNA and alters the transcription of QS controlled target genes. Similar to the AHL-driven QS circuit, the fundamental two-component QS circuit among Gram-positive bacteria is conserved. Nevertheless, adaption to certain environments entailed many differences in the regulation of the AIP signaling mechanism (Lazazzera and Grossman 1998; Miller and Bassler 2001).

1.3. Interspecies cell-to-cell communication

Beyond intraspecies communication, the discovery of the AI-2 signaling molecule postulated the presence of a communication between bacterial species. Evidence came from initial genetic analyses of the marine bacterium *Vibrio harveyi* which revealed a hybrid QS system controlling the bioluminescence by two different AIs (Bassler *et al.* 1994). Interestingly its QS circuit comprises components found in Gram-negative and Gram-positive QS systems. The genome of *V. harveyi* harbors genes attributed to production (LuxLM) and recognition of AHL-like AIs (LuxN). The AHL synthase LuxM does not share homologies to LuxI-type proteins however, its biosynthetic pathway is identical to LuxI synthases. The AI-1 molecule is recognized by a two-component sensor kinase termed LuxN (Ng and Bassler 2009). In contrast, the recognition of AI-2 demands for two proteins: LuxP a periplasmic binding protein which associates with AI-2 and further connects to LuxQ (hybrid sensor kinase) to transmit the AI-2 signal. The sensor information from LuxN as well as LuxPQ is channeled to a complex phosphorelay system, transferring the signal from the shared receptor LuxU to the response regulator LuxO. At a low cell density (AIs are absent) LuxO is present in the phosphorylated form, repressing the expression of *luxCDABE* genes, at high cell densities unphosphorylated LuxO activates expression of those genes, which results in production of light (Bassler *et al.* 1993; Federle and Bassler 2003; Reading and Sperandio 2006). The assumed “species-nonspecific” AI-2 signal molecule is produced by the LuxS synthase, which constitutes a complex biosynthesis pathway where the precursor DPD (4,5-dihydroxy-2,3-pentanedione) is spontaneously cyclized to form a furanone ring formation including the active AI-2 (Czajkowski and Jafra 2009; Schauder *et al.* 2001). Detailed sequence analyses of different bacterial genomes uncovered the presence of highly conserved *luxS* homologues in numerous microorganisms and many species have been shown to constitute AI-2 activity (Miller and Bassler 2001). The production and response to AI-1 was observed in only closely related species of *V. harveyi*, whereas AI-2 and its *luxS* synthase were found in a wide variety of Gram-negative and Gram-positive bacteria, suggesting that AI-1 mediates intraspecies communication and AI-2 could be a common mechanism employed for interspecies cell-to-cell communication (Schauder *et al.* 2001).

1.4. Interkingdom signaling systems

Coordination of gene expression within a population by bacterial QS signaling is not restricted to a conversation between bacterial cells but also enables communication between bacteria and their hosts. This interkingdom signaling is accomplished by means of a hormone-like autoinducer (Hughes and Sperandio 2008). Studies on expression of virulence genes in food-borne pathogen enterohemorrhagic *E. coli* (hereafter EHEC) serotype O157:H7 could reveal a molecule controlled by LuxS, being not similar to AI-2 (Walters *et al.* 2006). EHEC produces a previously not described aromatic autoinducer (AI-3) which is chemically distinct from AI-2. Surprisingly, continuative studies uncovered that EHEC *luxS* mutants were able to respond to eukaryotic cell signals present in the gastrointestinal tract and could further activate the expression of virulence genes (Kendall *et al.* 2007; Sperandio *et al.* 2003). These signals identified as mammalian hormones epinephrine and norepinephrine have shown to cross communicate with AI-3. Both QS signals are sensed by a two-component signal transduction system, the sensor kinase QseC which phosphorylates QseB and activates expression of the flagella regulon. Another two-component transduction system (proposed to be QseEF) senses these signals, transmitting the information to transcriptional factors (QseA and QseD) which induce regulation of pathogenicity islands required for the production of toxins and attaching/effacing lesions (Reading and Sperandio 2006; Walters and Sperandio 2006). These findings suggest a link between the bacterial cell-to-cell communication mediated by AI-3 and the eukaryotic cell-to-cell signaling mediated by hormones by which microbes and host cells can establish a beneficial communication.

1.5. Quorum sensing in rhizobia

AHL-based signaling mechanisms enable bacteria to sense their local environment to coordinate certain genes. Such a synchronized gene expression is of great importance in particular for bacterial symbionts and pathogens. The successful infection of eukaryotic hosts as well as the ability to establish an effective symbiosis with plant hosts requires QS-dependent signaling (Bauer and Mathesius 2004; Loh *et al.* 2002b; Wisniewski-Dye and Downie 2002). One emerging research field concentrates on plant-associated bacteria living in a pathogenic, nonpathogenic or symbiotic interaction with eukaryotic hosts. Beside the opportunistic human pathogen *Pseudomonas aeruginosa* (Passador *et al.* 1993), plant pathogens like *Ralstonia solanacearum* (Flavier *et al.* 1997), *Erwinia carotovora* (Pirhonen *et al.* 1993) and *Agrobacterium tumefaciens* (Zhang *et al.* 1993), different members of the family *Rhizobiaceae* forming symbiotic nodules on leguminous plants are of special interest (Brelles-Marino and Bedmar 2001). Most QS circuits found in these symbiotic rhizobia are similar in structure however, the subordinated genes mediating physiological processes are

diverse. In addition, these underlying signaling systems are often complex due to incorporation of multiple AHL synthase and response proteins and their organization in a regulatory hierarchy (Soto *et al.* 2006). Several representatives among the *Rhizobiaceae* prevalently using QS systems for signal communication were studied in more detail, like *Rhizobium leguminosarum* bv. *viciae*, *Rhizobium etli* CNPAF512 and CFN42, *Sinorhizobium meliloti*, *Bradyrhizobium japonicum* (for a detail review see Gonzalez and Marketon 2003 and Wisniewski-Dye and Downie 2002). An outstanding and unique candidate is portrayed by *Rhizobium* sp. NGR234 (hereafter NGR234) forming nitrogen-fixing nodules with over 120 genera of legumes (Pueppke and Broughton 1999). Detailed analyses of NGR234's genomic information revealed among striking secretory and transport associated features a cluster of gene homologs to QS components (*tral-trb* operon) of *A. tumefaciens* (Freiberg *et al.* 1997). Investigations accomplished with NGR234 *tral* mutants still producing a compound related to *N*-3-oxooctanoyl-homoserine lactone (hereafter 3-oxo-C8-HSL) along with another more hydrophobic compound, indicated that additional AHL synthases and response regulators may be present elsewhere (He *et al.* 2003). The complex regulatory QS present in NGR234 which is connected to symbiosome development, nitrogen fixation as well as nodule formation is shown in Figure 1 and serves as a paradigm QS circuit in this chapter.

The QS regulators Tral, TraR and TraM found in NGR234 (Figure 1A) are functional similar to *A. tumefaciens* Ti plasmid QS regulators. At a low cell density Tral produces AHL signals, verified to be 3-oxo-C8-HSL, which are transferred into the environment at a basal concentration. With an increasing density of a population of NGR234 AHLs accumulate in the environment until reaching a threshold value. Subsequently, 3-oxo-C8-HSL interacts with TraR acting as a positive transcription regulator. The TraR-AHL complex binds to DNA promoter regions and initiates a positive feedback loop as well as the expression of conjugal plasmid transfer (*trb*) genes (Gonzalez and Marketon 2003; He *et al.* 2003). Based on the experimental findings of He and colleagues, a recent detailed sequence analysis of NGR234 genes revealed an additional QS system on the chromosome of NGR234, composed of NgrI/NgrR (LuxI/LuxR homologous) and a hypothetical protein. This novel QS system might be the missing regulatory network responsible for the synthesis/response to a compound related to 3-oxo-C8-HSL or the long-chain AHL (He *et al.* 2003).

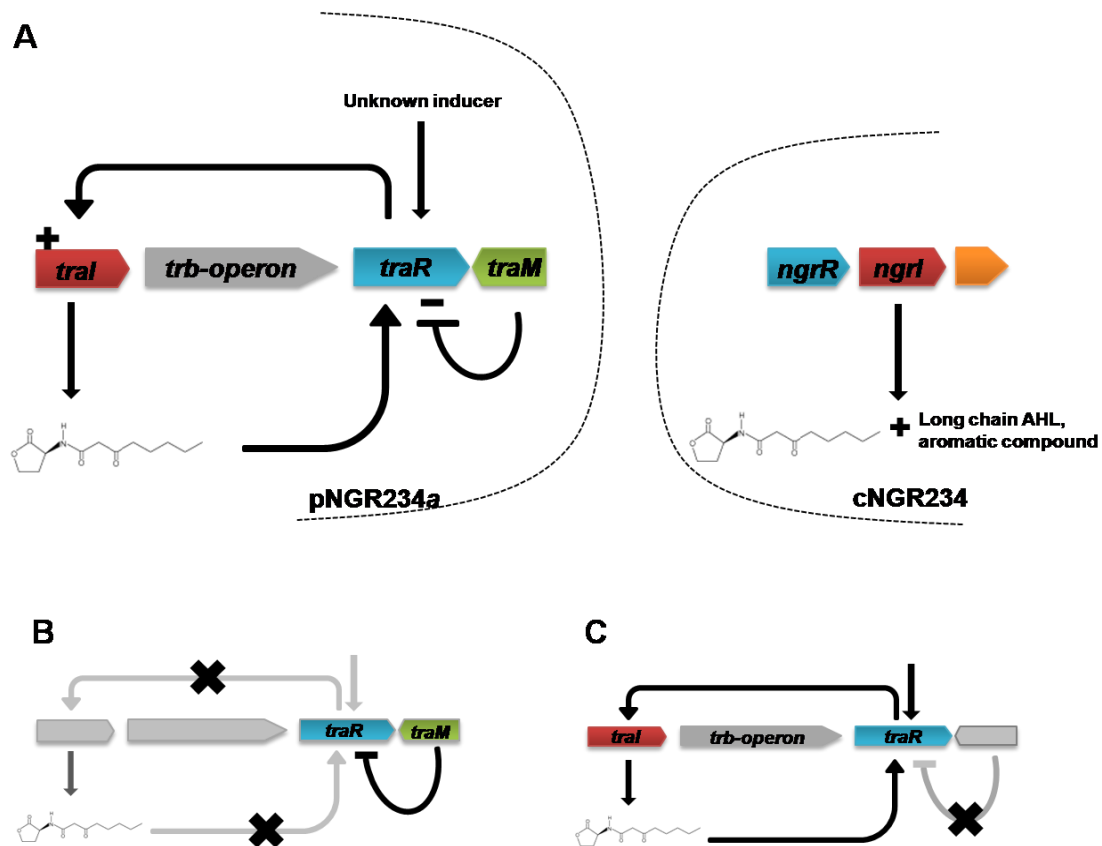


Figure 1: Model of QS gene regulation in *Rhizobium* sp. NGR234. (A) The AHL synthase *Tral* (NGR_a04220, red) directs the synthesis of 3-oxo-C8-HSL which associates with the response regulator *TraR* (NGR_a04090, blue). *TraM* (NGR_a04080, green) functions as a suppressor, preventing *TraR* from activating target genes under non-inducing conditions. The *trb* genes (NGR_a04210-NGR_a04100) are shaded dark grey. The second QS system identified on the cNGR234 composed of *NgrI* (NGR_c16900, red)/*NgrR* (NGR_c16890, blue) and the hypothetical protein (NGR_c16910, orange). (B) QS circuit suppressed by activity of *TraM*. (C) QS circuit under non-suppressing conditions expressing *tral* and *trb* genes.

2. Quorum quenching – The evolutive advantage

The limited availability of nutrients and energy resources in changing and challenging environments forces the competition in mixed populations of both prokaryotes and eukaryotes. Gaining the upper hand under such competing conditions could give one bacterial species an advance over another. Since bacteria evolved the ability to communicate via diverse QS systems, it is reasonable that these microbes also evolved the ability to rival with each other by means of QS and the corresponding signal molecules. Consequently, bacteria emerged various defense strategies to protect themselves as well as to disarm competitors to colonize nutrient and energy rich niches by efficiently interfering with the key components of QS mechanisms. This process is termed quorum quenching (QQ). These anti-QS strategies are also tracked by eukaryotic hosts to fend pathogenic microbes whose invasion and colonization is QS-regulated. Targets for such QQ process can be either

AHL synthases which are disarmed and blocked by certain substances, the signal molecule itself which can be removed/inactivated or the cognate LuxR-type regulator which can be blocked by mimics thus inhibit expression of target genes. A range of living organisms, including bacteria, algae and plants evolved multiple QS interference strategies aimed not to destroy the competitors or invaders but to impair the expression of certain genes for example to down regulate expression of virulence genes involved in plant-microbe interactions. The recently discovered and well studied QQ processes will be described in the following.

2.1. Blockade of autoinducer synthases

Until today only few research groups addressed their investigations to the inhibition of AHL signal generation. The AHL synthesis involves in the reaction mechanism SAM as a donor for the HSL ring and acyl-ACP as a precursor of the acyl chain. Extensive studies of the AHL synthase RhIL (comprised by *P. aeruginosa*) uncovered analogs of SAM such as S-adenosylhomocysteine, sinefungin and butyryl-SAM which effectively repress the synthase action (Parsek *et al.* 1999). In addition, triclosan inhibits the enoyl-ACP reductase in *P. aeruginosa* whose product is one essential intermediate in the synthesis of AHL (Hoang and Schweizer 1999). Concerning two-component signal transduction systems of Gram-positive bacteria, phenolic substances such as closantel and RWJ-49815 were found to act on histidine kinases by structural alternation and further protein aggregation (Stephenson *et al.* 2000). Finally, certain macrolide antibiotics such as erythromycin or azithromycin are also capable to inhibit AHL synthesis, e.g. in *P. aeruginosa* (Pechere 2001; Tateda *et al.* 2001), but it is still unclear how in detail they effect QS -regulated processes.

2.2. Inhibition of autoinducer receptors

Attenuation of competitors by disturbing the crucial signal transmission became a promising QQ strategy for prokaryotes as well as eukaryotic hosts and was also implemented as a pharmacological approach to overcome bacterial infections (Givskov *et al.* 1996). The suppression of the signal transduction can be achieved by either competitive molecules which imitate AHL structures and occupy the AHL-binding site consequently not activating the receptor or noncompetitive molecules which are not similar to AHL structures and bind to different sites of the receptor. The most intensively studied example are halogenated furanones which are structural AHL analogs produced by the seaweed *Delisea pulchra* and were found to interact directly with LuxR-type receptors. The natural AHL mimics compete with AHLs for the LuxR AI binding site and after binding accelerate the proteolytic degradation of the LuxR transcriptional factor (Manefield *et al.* 2002). This marine alga *D. pulchra* produces over 30 different types of natural furanones halogenated by bromide,

chloride or iodide at various positions which are for example able to disturb the colonization by marine bacteria (de Nys *et al.* 1993) or inhibit swarming motility in *Serratia liquefaciens* MG1 (Rasmussen *et al.* 2000). Additionally one representative of these *D. pulchra*-borne natural furanones was able to inhibit QS systems based on AI-1 as well as AI-2 in *V. harveyi* and *E. coli* (Ren *et al.* 2001). Furthermore, in various studies synthetic derivatives of natural furanones revealed an even more pronounced inhibitory effect on QS based communication in different microorganisms. The imitating AHL structure was evaluated in *P. aeruginosa* - E 30/E 56 where the application of the synthetic furanone resulted in a biofilm more susceptible to antibiotics and SDS (Hentzer *et al.* 2003; Wu *et al.* 2004). The filamentous bacterium *Streptomyces antibioticus* produces furanone as an intermediate in butenolide production. These furanone compounds as well as the synthetic derivatives were assayed in *Chromobacterium violaceum* CV026 and also found to possess an inhibitory effect on the QS-regulated violacein production (Martinelli *et al.* 2004). Such synthetic furanones were also effective in *Salmonella enterica* serovar Typhimurium (Janssens *et al.* 2008) and *Streptococcus* spp. (Lonn-Stensrud *et al.* 2007).

Beyond structural analogs of halogenated furanones, synthetic compounds modeled on AHL structures were assayed in various studies where single components, side chains or rings of common AHLs were substituted by other compounds. Substitution within as well as at the end of the acyl chain yielded in effective inhibitors of QS (Castang *et al.* 2004; Persson *et al.* 2005; Schaefer *et al.* 1996). Substitution of the HSL ring by alternative ring structures like phenyl or benzyl compounds turned out to be also very potent inhibiting structures (Reverchon *et al.* 2002; Smith *et al.* 2003). Supplementary, a lot of other chemical modifications of AHLs were undertaken and employed often yielding in a loss of inhibition but in most cases delivering an accelerated inhibition of QS (Frezza *et al.* 2006; Morohoshi *et al.* 2007; Persson *et al.* 2005).

Finally, some evidence was obtained on receptor associated interference mechanisms involved in two-component systems. Analogs of AIPs as well as truncated AIP structures were found to function like AHL mimics, directly acting on the AIP receptor (Lyon *et al.* 2000).

2.3. Mechanisms of enzymatic degradation of signal molecules

Since the AHL-driven cell-to-cell communication is widespread and conserved in many microorganisms, this signaling mechanism is attractive for many QQ targeted processes. Beside the repression of signal generation and inhibition of signal reception, the inactivation of the signal molecule itself is a very potent strategy to silence QS. The chemical structure of AHL signal molecules offers a number of sites that can be enzymatically cleaved or modified:

Degradation of the HSL ring - lactone hydrolysis mediated by AHL lactonases, cleaving the acyl chain off the HSL moiety - amide bond hydrolysis mediated by AHL amidases and finally, modification of the acyl chain - oxidoreduction mediated by oxidases and/or reductases. These main enzymatic mechanisms are depicted in Figure 2 and are described in detail in the following sections.

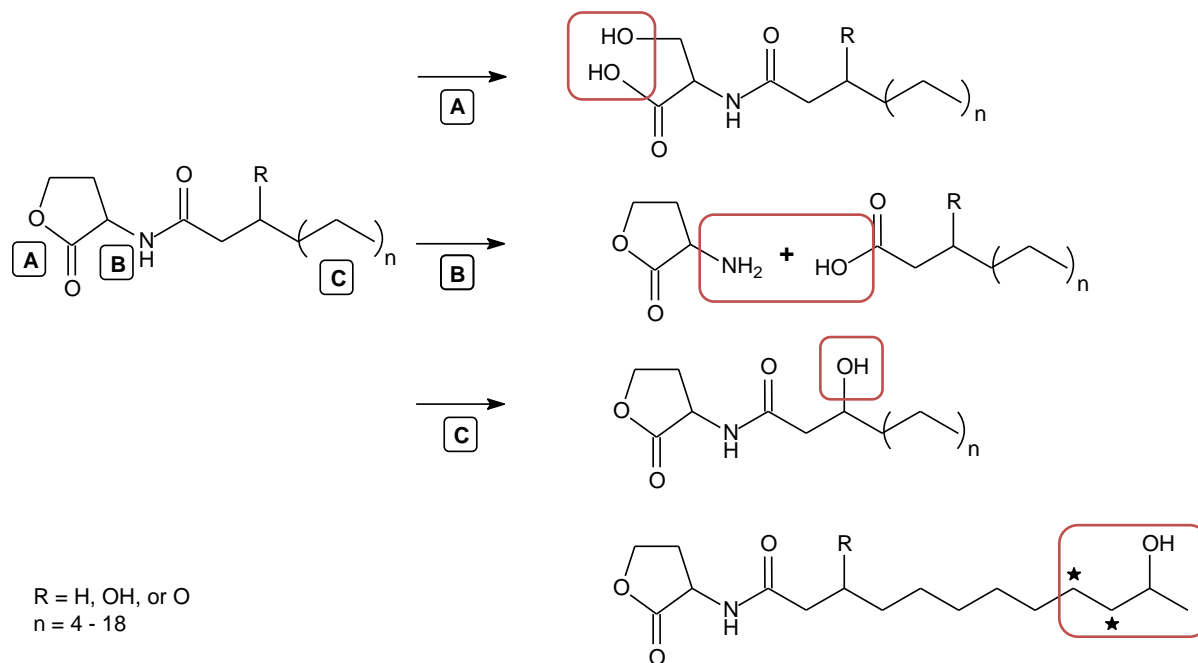


Figure 2: Three main mechanisms of AHL degrading enzymes. (A) Mode of AHL lactonase action, resulting in a hydrolysis of the lactone ring in the homoserine moiety. **(B)** Mode of AHL amidase action, resulting in a hydrolysis of the amide bond between homoserine moiety and acyl side chain. **(C)** Mode of oxidoreductase action, modifying the acyl side chain by reducing a single/several oxo-groups, * display radicals.

2.3.1 Signal degradation by AHL lactonases - AHLases

The AHL lactonases hydrolyze the lactone ring in the homoserine moiety of the AHL not affecting the rest of the molecule (Figure 2A). This ring opening causes an inactivation of the AHL signal (Dong *et al.* 2001), thus the signal molecules are incapable of binding to their target regulator and consequently QS-mediated conversation is blocked. As the AHLase-driven reaction is identical to the pH-dependent lactonolysis this reaction can be reversed by acidification (Yates *et al.* 2002). The first lactonase activity was demonstrated by AiiA from *Bacillus* sp. 240B1 and was found to hydrolyze a range of AHLs varying in chain length (C4 - C14-HSL) and substitution at C_3 position (Dong *et al.* 2000). The research group proposed AiiA as a member of the metallohydrolases [EC 3.5.-.-]. At this time, sequence alignments did not reveal significant similarities to known enzymes but indicated the presence of two main amino acid motifs among the AiiA sequence.

The first motif “¹⁰⁴HXHXDHAG¹¹¹” which was found to be conserved within metal-dependent β -lactamases [EC 3.5.2.6] and the second region “¹⁶⁵HTPGHTPGH¹⁷³” was similar to the zinc-binding motif of metal-dependent hydrolases (Dong *et al.* 2000). During recent years more bacteria were uncovered featuring an AHLase activity and surprisingly the conserved “HXHX~DH” region (comprised by AiiA) was found in many poorly related species. Different alignment studies revealed this short region to be a characteristic of metallo- β -lactamases [EC 3.5.2.6], glyoxalases II [EC 3.1.2.6] and arylsulfatases [EC 3.1.6.1]. Metallo- β -lactamases are hydrolases featuring a binuclear zinc center and additional residues that coordinate the two zinc atoms which all are invariant in metallo- β -lactamases (Wang *et al.* 2004). The second pattern “HTPGHTPGH” is moderate conserved among AiiA-related proteins and is proposed to coordinate the second zinc atom in metallo- β -lactamases, glyoxalases II and arylsulfatases. Although the zinc-binding motif is found in a number of metal-dependent β -lactamases, studies of Wang and colleagues in 2004 indicated that AHLases are not metalloproteins relying on zinc or other metal ions for activity (Wang *et al.* 2004). These findings were rather unlikely and in contrast to studies of Kim *et al.* 2005 and Thomas *et al.* 2005 which presented the evidence that AHLases from *Bacillus thuringiensis* are in fact metalloproteins requiring Zn^{2+} .

Enzymes featuring an AHLase activity are not only limited to *Bacillus* species. Homologous of AiiA as well as new lactonase members were identified in microorganisms living in various habitats like soil, biofilms and plants. A novel class of AHLases was uncovered by studies on *Rhodococcus erythropolis* W2, clearly belonging to the phosphotriesterases (PTE) of zinc-dependent metalloproteins and totally unrelated to published AHLases or AHL amidases. QsdA was found to exhibit a lactonolytic pathway, consequently extending the number of AHL degrading enzymes to the PTE family (Uroz *et al.* 2008).

Beyond lactonases in bacteria, AHL degradation was also observed in eukaryotes. Studies on mammalian cells revealed a strong AHL inactivation by paraoxonases (PONs) (Yang *et al.* 2005). These PONs are a family of mammalian lactone hydrolases with a distinct substrate specificity. PON1, PON2 and PON3 are highly conserved (Draganov *et al.* 2005) and can use AHL molecules as substrates by hydrolyzing their lactone ring. These findings suggest that higher organisms like humans and other mammalian species evolved certain mechanisms to disarm QS-mediated communication, most likely to counteract pathogenic colonization or invasion.

The subsequent Table 1 summarizes already identified and published AHL degrading enzymes counted among the AHLases, spanning prokaryotic and eukaryotic organisms.

Table 1: Functionally characterized AHLases found in diverse organisms and metagenomes

Name	Species/Source	Protein family	Conserved motif	Reference
AiiA	<i>Bacillus</i> sp. 240B1	Metallo- β -lactamase superfamily	HXHX-DH	Dong et al. 2000
	<i>Bacillus thuringiensis</i>	Metallo- β -lactamase superfamily	HXHX-DH	Dong et al. 2000
	<i>Bacillus cereus</i>	Metallo- β -lactamase superfamily	HXHX-DH	Dong et al. 2000
	<i>Bacillus mycooides</i>	Metallo- β -lactamase superfamily	HXHX-DH	Dong et al. 2000
	<i>Bacillus thuringiensis</i> (subspecies)	Metallo- β -lactamase superfamily	HXHX-DH	Lee et al. 2002
	<i>Bacillus anthracis</i>	Metallo- β -lactamase superfamily	HXHX-DH	Ulrich 2004
AiiB	<i>Agrobacterium tumefaciens</i> C58	Metallo- β -lactamase superfamily	HXHX-DH	Carlier et al. 2003
AttM	<i>Agrobacterium tumefaciens</i>	Metallo- β -lactamase superfamily	HXHX-DH	Zhang et al. 2002
AhID	<i>Arthrobacter</i> sp. IBN110	Metallo- β -lactamase superfamily	HXHX-DH	Park et al. 2003
AhIK	<i>Klebsiella pneumoniae</i>	Metallo- β -lactamase superfamily	HXHX-DH	Park et al. 2003
QlcA	Soil metagenome	Metallo- β -lactamase superfamily	HXHX-DH	Riaz et al. 2008
QsdR1	<i>Rhizobium</i> sp. NGR234	Metallo- β -lactamase superfamily	HXHX-DH	Krysciak et al. 2011
QsdR2	<i>Rhizobium</i> sp. NGR234	Metallo- β -lactamase superfamily	HXHX-DH	Krysciak et al. 2011
AiiM	<i>Microbacterium testaceum</i> SILB037	α/β Hydrolase fold family	NF	Wang et al. 2010
AidH	<i>Ochrobactrum</i> sp. T63	α/β Hydrolase fold family	GX-Nuc-XG	Mei et al. 2010
BpiB01	Soil metagenome	Hypothetical protein	NF	Schipper et al. 2009
BpiB05	Soil metagenome	Hypothetical protein	NF	Bijtenhoorn 2011
QsdA	<i>Rhodococcus erythropolis</i> W2	Phosphotriesterase superfamily	PTE	Uroz et al. 2008
BpiB04	Soil metagenome	Glycosyl hydrolase family	NF	Schipper et al. 2009
BpiB07	Soil metagenome	Dienelactone hydrolase family	NF	Schipper et al. 2009
DihR	<i>Rhizobium</i> sp. NGR234	Dienelactone hydrolase family	GSD(L)	Krysciak et al. 2011
Unknown	<i>Acinetobacter</i> sp. C1010	NF	NF	Kang et al. 2004
HitR-HydR	<i>Rhizobium</i> sp. NGR234	Histidine triad (HIT) protein; NUDIX hydrolase	HXHXHXX; NUDIX	Krysciak et al. 2011
AidR	<i>Rhizobium</i> sp. NGR234	Acetaldehyde dehydrogenase	motif segments	Krysciak et al. 2011
PON1,2,3	Mammalian cells	Paraoxonase family	NF	Ozer et al. 2005

NF: not found

2.3.2 Signal degradation by AHL amidases

The enzymatic mechanism of AHL amidases is based on hydrolysis of the amino bond between the acyl side chain and the HSL moiety in the AHL molecule (Figure 2B). The side chain is irreversibly released from the intact HSL which leads to an inactivation of the signal molecule and, like in AHLases, to a suppression of QS-mediated communication. There are many different types of amidases known differing in their substrate specificity for the side chain. Biochemically these AHL cleaving enzymes are amidases and should consequently be called AHL amidases [EC 3.5.1.4]. Nevertheless, researchers use the term AHL acylases in this context (Czajkowski and Jafra 2009; Uroz *et al.* 2009). Shortly after the discovery of the first AHLase in *Bacillus* sp., the strain *Variovorax paradoxus* was found to degrade AHL molecules, while releasing HSLs it utilized the fatty acids as a sole source of carbon and nitrogen (Leadbetter and Greenberg 2000). However, the gene responsible for AHL degradation was not identified until today. After this first AHL amidase determined in *Variovorax*, a range of other bacterial amidases were uncovered. Until today, altogether fourteen AHL amidases have been reported whereas nine have been described in detail (Table 2).

Table 2: Uncovered AHL amidases found in diverse Gram-negative and Gram-positive strains

Name	Species / Source	Protein family	Reference
AiiD	<i>Ralstonia</i> sp. XJ12B	Ntn-hydrolase superfamily	Lin <i>et al.</i> 2003
QuiP	<i>Pseudomonas aeruginosa</i> PAO1	Ntn-hydrolase superfamily	Huang <i>et al.</i> 2006
PvdQ	<i>Pseudomonas aeruginosa</i> PAO1	Ntn-hydrolase superfamily	Huang <i>et al.</i> 2003
PA0305	<i>Pseudomonas aeruginosa</i> PAO1	Ntn-hydrolase superfamily	Wahjudi <i>et al.</i> 2011
HacA	<i>Pseudomonas syringae</i> pathovar <i>syringae</i> B728a	Ntn-hydrolase superfamily	Shepherd and Lindow 2009
HacB	<i>Pseudomonas syringae</i> pathovar <i>syringae</i> B728a	Ntn-hydrolase superfamily	Shepherd and Lindow 2009
AhIM	<i>Streptomyces</i> sp. M664	Ntn-hydrolase superfamily	Park <i>et al.</i> 2005
AiiO	<i>Ochrobactrum</i> sp. A44	Carboxylic ester hydrolases	Czajkowski <i>et al.</i> 2011
AiiC	<i>Anabaena</i> sp. PCC 7120	NF	Romero <i>et al.</i> 2008
Aac	<i>Ralstonia solanacearum</i> GMI1000	NF	Chen <i>et al.</i> 2009
Unknown	<i>Shewanella</i> sp. MIB015	NF	Morohoshi <i>et al.</i> 2007
Unknown	<i>Rhodococcus erythropolis</i> W2	NF	Uroz <i>et al.</i> 2005
Unknown	<i>Variovorax paradoxus</i> VAI-C	NF	Leadbetter and Greenberg 2000
Unknown	<i>Comamonas</i> sp. D1	NF	Uroz <i>et al.</i> 2007

NF: not found

Table 2 summarizes the current published and identified AHL amidases. Sequence analyses of the in detail studied amidase representatives revealed a common characteristic of the N-terminal nucleophilic (Ntn) hydrolases (Dong *et al.* 2007; Lin *et al.* 2003) except of AiiO which represents a novel class of AHL amidases. The Ntn-hydrolases are known to undergo post-translational processing into two enzymatically active subunits after cleavage of the signal (Duggleby *et al.* 1995; Oinonen and Rouvinen 2000). Only seven AHL amidases share this post-translational modification pattern as well as other conserved regions comprised by most Ntn-hydrolases like penicillin or cephalosporin amidases. To date no sequence alignment of the remaining five amidases was accomplished in order to uncover similarities to Ntn-hydrolases.

2.4. Modification of AHL signal molecules by oxidoreductases

The chemical structure of AHL signal molecules provides a third way of AHL modification which is mediated by oxidoreductases [EC 1.-.-.-]. These enzymes target the acyl side chain itself by oxidative or reducing activities (Figure 2C). In contrast to AHLases and AHL amidases this enzymatic reaction catalyzes the chemical modification of AHL molecules but not the degradation of those. Additionally, AHL signals undergone AHLase and amidase activities can also be modified by such oxidoreductases. Nevertheless, the chemical modification interferes indirectly with QS-mediated communication as the signal recognition might be affected. To date, only two such enzymes with oxidoreductase activity were uncovered and biochemically characterized. In 2005, Uroz and colleagues described beside the amidolytic activity a novel oxidoreductase action in *Rhodococcus erythropolis* W2. This strain was able to reduce *N*-acyl side chains ranging from C8 to C14 and convert them into their 3-hydroxy derivatives (Uroz *et al.* 2005). The second enzyme is a monooxygenase originating from *Bacillus megaterium* which was able to oxidize fatty acids but acyl homoserine lactones emerged to be better substrates. CYP102A1 (cytochrome P450) is capable of oxidizing long-chain saturated and unsaturated fatty acids at the ω -1, ω -2 and ω -3 position (Chowdhary *et al.* 2007). The impact of oxidoreductases by chemical alternation of AHL signal molecules results in an indirect blockade of AHL-mediated cell-to-cell communication. Nevertheless, this modification might be as profitable as lactonolytic or amidolytic pathways aiming to combat pathogenic competitors in the environment.

2.5. QQ in plant-associated bacteria and their eukaryotic hosts

In natural environments like the soil, where plants especially in the rhizosphere are constantly exposed to bacteria, the establishment of an effective symbiosis is beneficial for both. While nitrogen-fixing bacteria initiate the development of root nodules to assure the access to nutrients and to profit from a plant-associated community, plants benefit from these root nodules which enable them to fix nitrogen from the surrounding soil (Bever and Simms 2000). The conversation of plant-associated bacteria by means of AHLs is crucial for the interaction of pathogens and symbionts with their eukaryotic host and requires the action of both partners: On the one hand plant-associated bacterial communities produce AHL signal molecules to synchronize group behavior and to communicate with their eukaryotic host. In addition they are able to degrade AHL signals to rival with other microbes for a successful symbiosis. On the other hand eukaryotic hosts e.g. plants detect and respond to AHLs to enable a successful symbiosis with its desirable partner or to counteract the establishment of a harmful pathogenic correlation (Teplitski *et al.* 2011).

2.5.1 Interaction of plant-associated bacteria

Particularly in the rhizosphere the interaction among different bacterial species results in a competition for the plant host and the ecological niche. The strategy of AHL degradation by lactonases, amidases or oxidoreductases was found to play a significant role in obtaining a competitive advantage for its producer over other present microbes (Dong and Zhang 2005; Krysciak *et al.* 2011). Supplementary, rhizosphere bacteria use this strategy to protect their plant host from pathogens that utilize AHLs for control of virulence genes. It has recently been shown that plant-associated strains comprising AHLases or amidases were able to suppress other plant pathogens in their virulence activity. Such examples are *Bacillus thuringiensis* (Dong *et al.* 2004), *Pseudomonas fluorescens* (Molina *et al.* 2003) and *Arthrobacter* sp. (Park *et al.* 2003) which were either modified or naturally featuring an AHLase activity. These strains when co-inoculated with *Erwinia carotovora* affected its virulence and thus reduced the pathogenicity of *E. carotovora* in several plant models. Inverted studies accomplished with pathogens like *P. aeruginosa* PAO1 or *E. carotovora* expressing an AHLase and amidase revealed that both strains were significantly impaired in their virulence to infect eukaryotes (Reimann *et al.* 2002). Most surprisingly studies carried out with transgenic plants expressing the AiiA lactonase demonstrated to be also resistant to QS-regulated infection by *E. carotovora* (Dong *et al.* 2001). These results demonstrate that AHL signal degradation is of great importance for microbe-microbe as well as pathogen-host interactions. Prokaryotes use this QQ strategy to overcome competing conditions in the rhizosphere. While pathogens have a selective advantage and the possibility to infect the

plant, symbionts mostly defend themselves and protect the plant by means of lactonases and amidases from pathogenic competitors.

2.5.2 QQ-mediated defense mechanisms of eukaryotic hosts

Eukaryotic hosts like plants have the ability to detect AHL signal molecules transmitted by their bacterial partners and are capable to respond to those. However, plants are also able to produce and exudate AHL mimics that disrupt or manipulate different bacterial behaviors (Teplitski *et al.* 2000). Since such important biological functions like production of virulence factors, control of nitrogen fixation, or plasmid transfer regulated by QS might impair the plant, it is not surprising that even eukaryotic hosts have evolved different defense strategies to overcome the negative effects of symbiosis (Bauer and Mathesius 2004). The model legume *Medicago truncatula* can detect AHL synthesized by its symbiont *Sinorhizobium meliloti* and responds by an accelerated expression of root and defense related proteins which potentially interfere with bacterial QS (Mathesius *et al.* 2003). Such a production of defense related proteins was also observed in pea seedlings (*Pisum sativum*) which released several AHL mimics that were capable of inhibiting QS-regulated behaviors in strains like *C. violaceum* and simultaneously stimulating QS-regulated swarming behavior in *Serratia liquefaciens* (Teplitski *et al.* 2000). A research from 2010 aiming to find alternative strategies to antibiotic usage against bacterial infections uncovered several extracts of edible plants and fruits displaying a significant reduction of pigment production in *C. violaceum* as well as different QS-regulated functions in *P. aeruginosa* PAO1 (Musthafa *et al.* 2010). In summary, various studies employing AHL signal mimics produced by eukaryotic hosts could prove that these compounds are important and beneficial for the success of interaction between plants and pathogenic/symbiotic bacteria.

3. The α -proteobacterium *Rhizobium* sp. NGR234

Rhizobium sp. NGR234 is outstanding and unique among the rhizobia with its ability to nodulate a very broad range of legumes and even one nonlegume. NGR234 (Figure 3) was first uncovered in 1965 in Papua New Guinea and isolated from *Lablab purpureus* nodules as the only fast-growing strain among 30 isolates (Trinick 1980). Shortly after this discovery its broad host range attracted great interest.

Several studies were accomplished to describe NGR234's hosts in comparison to other symbiotic soil bacteria, in particular to the phylogenetic closely related strain *Sinorhizobium fredii* USDA257, revealing a wealth of symbiotic partners. Over 120 different genera of

legumes were identified to symbiotically interact with NGR234 in order to facilitate their access to mineral nitrogen via root nodules. In addition, *Parasponia andersonii* is the only non legume which undergoes symbiosis with NGR234 (Pueppke and Broughton 1999).

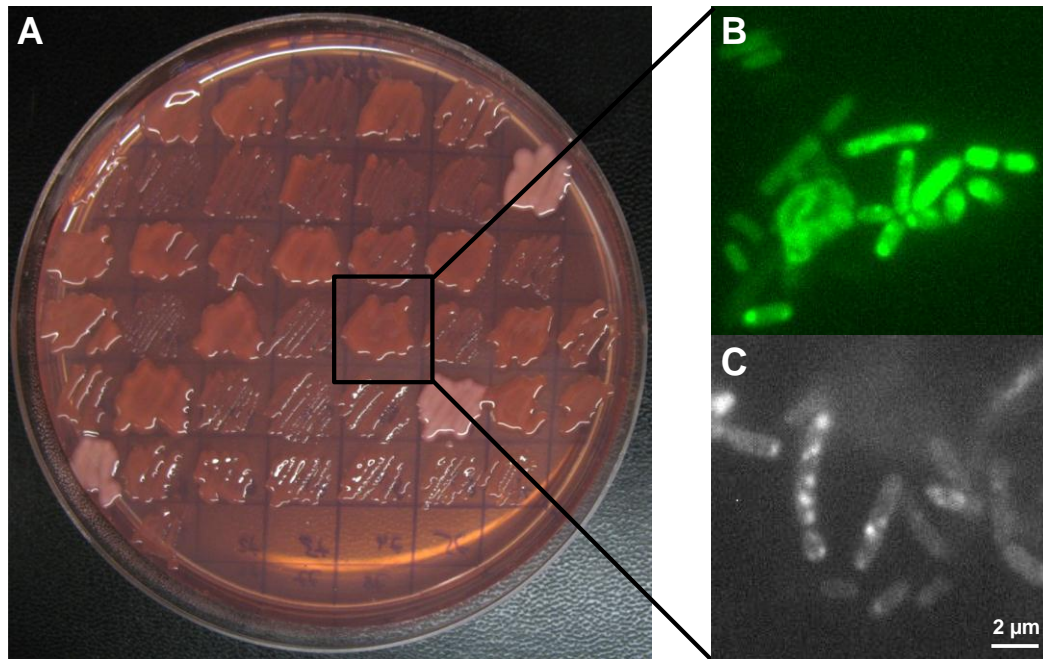


Figure 3: The α -proteobacterium *Rhizobium* sp. NGR234. (A) Phenotype of *Rhizobium* sp. NGR234 on a TY agar plate supplemented with congo red. (B) Microscopic analysis of NGR234 harboring a *tral::evoglow* fusion (Evocat, Duesseldorf, Germany). (C) Microscopic analysis of a liquid culture of NGR234 grown in TY medium supplemented with rifampicin.

Early studies with derivatives as well as spontaneous resistance mutants of NGR234 gave evidence that genes required for an effective symbiosis with leguminous plants are located exclusively on the symbiotic (sym) plasmid. A NGR234 derivative (ANU265) which was deprived of pNGR234a by heat curing was not impaired in its growth but failed to nodulate any of its hosts (Morrison *et al.* 1983). Consequently, the sym plasmid of NGR234 lacks essential genes required for growth and survival control but comprises genes for nitrogen fixation (*nif/fix*) and synthesis of nodulation (Nod) factors equipping this microbe with the ability to symbiotically associate with legumes (Freiberg *et al.* 1997). In a symbiotic relationship like NGR234 undergoes with leguminous plants, root-hair curling, induction of nodulation as well as the entry of bacteria into the root are strictly dependent on secreted Nod factors. These Nod factors might play a role in the host range of symbiotic soil bacteria and especially in NGR234 (Viprey *et al.* 2000). Thus, the host range of different rhizobia might directly correlate with genes that are involved in Nod factor production. NGR234 and USDA257 have only small differences in their number of nodulation genes but this difference

results in NGR234 secreting a larger amount of diverse Nod factors than USDA257 (Pueppke and Broughton 1999).

Researches accomplished in the recent years addressed their questions to NGR234's broad range of symbiotic partners and delivered a couple of interesting but still incomplete answers. Major approaches to illuminate the broad host range of NGR234 might involve the Nod factor production, protein secretion as a key component of efficiency of nitrogen fixation as well as differences in the utilized secretion machinery (Deakin and Broughton 2009; Freiberg *et al.* 1997; Pueppke and Broughton 1999). Furthermore, one major key of the broad host spectrum of NGR234 might be the poorly understood and studied inter-/intra-cellular communication as well as its ability to disrupt other communication systems as a defense strategy to obtain a competitive advantage for its producer over other present symbiotic soil bacteria. More knowledge is needed on the appointed key approaches in this research field which might then deliver first and possibly concrete answers of NGR234's broad host spectrum.

4. Aims of the research

The goal of the present research was the investigation of the QQ potential owned by *Rhizobium* sp. NGR234 combining sequence-based and function-based approaches. Primarily the completion of the genome sequence of NGR234 should provide the profound basis for initial sequencing and experimental analyses. Detailed alignment and comparative analyses using the newly established genomic data set of NGR234 should answer the question of novel QS-based communication systems as well as QQ-based strategies and enzymes comprised by NGR234.

The second goal of this research was the implementation and advancement of a published function-based screening initially used to search for AHL degrading enzymes in metagenomes. The objective was to confirm the sequentially detected QQ-associated genes found in NGR234 and furthermore to verify novel functional active ORFs which were not detected by initial comparative analyses. For this purpose a NGR234 cosmid clone library had to be established and screened on cosmids conferring AHL degrading ability. The identified cosmid clones had to be further investigated to localize the responsible ORF. Finally, the most promising proteins had to be biochemically characterized including a HPLC-MS analysis to uncover their underlying AHL cleaving mechanism.

II. Material and Methods

1. Bacterial strains, vectors and primers

The following bacterial strains, vectors, clones and primers were used in this study (Table 3 to Table 5).

Table 3: Bacterial strains used in this study

Strain	Description	Source/Reference
EPI100™-T1 ^R Phage T1-resistant <i>E. coli</i> strain	F ⁻ mcrA Δ(<i>mrr-hsdRMS-mcrBC</i>) Φ80Δ <i>lacZ</i> ΔM15 Δ <i>lacX74</i> <i>recA1</i> <i>endA1</i> <i>araD139</i> Δ(<i>ara, leu</i>)7697 <i>galU</i> <i>galK</i> λ ⁻ <i>rpsL</i> <i>nupG</i>	Epicentre Technologies, Madison, Wisconsin, USA
<i>E. coli</i> XL1 blue	<i>recA1</i> <i>endA1</i> <i>gyrA96</i> <i>thi-1</i> <i>hsdR17</i> <i>supE44</i> <i>relA1</i> <i>lac</i> [F ['] <i>proAB</i> <i>lacI</i> ^q ΔM15 Tn10 (Tet ^R)]	Stratagene, La Jolla, Canada
<i>E. coli</i> DH5α	<i>supE44</i> , Δ <i>lacU169</i> (Φ80 <i>lacZ</i> ΔM15) <i>hsdR17</i> <i>recA1</i> <i>endA1</i> <i>gyrA96</i> <i>thi-1</i> <i>relA1</i>	Gibco Bethesda Research Laboratories, Eggenstein, Germany
<i>E. coli</i> BL21 (DE3)	F ⁻ <i>ompT</i> <i>hsdS_B</i> (<i>r_B⁻</i> <i>m_B⁻</i>) <i>gal</i> <i>dcm</i> , (DE3)	Novagen, Darmstadt, Germany
<i>Rhizobium</i> sp. NGR234	Wild type New Guinea isolate, Rif ^R	Trinick 1980
<i>Pseudomonas aeruginosa</i> PAO1	Wild type <i>P. aeruginosa</i> , Amp ^R	Holloway <i>et al.</i> 1979
<i>Agrobacterium tumefaciens</i> NTL4	Reporter strain for AHL detection, <i>traI::lacZ</i> , Tet ^R , Sp ^R	Fuqua and Winans 1994 Fuqua and Winans 1996 Luo <i>et al.</i> 2001
<i>Chromobacterium violaceum</i> ChV2	Wild type <i>C. violaceum</i>	Reference stock of the laboratory
<i>Chromobacterium violaceum</i> CV026	Mini-Tn5 mutant of <i>C. violaceum</i> wild type strain ATCC 31532	McClellan <i>et al.</i> 1997

Table 4: Vectors and constructs used and established in this study

Vectors/Constructs	Description	Source/Reference
pWEB-TNC™	Cosmid cloning vector derived from pWE15, linearized with <i>Sma</i> I, ColE1, <i>cos</i> site, T7 promoter, Amp ^R , Cm ^R	Epicentre Technologies, Madison, Wisconsin, USA
pWEB-TNC-A5	pWEB-TNC™ with a 40.5 kb insert from <i>Rhizobium</i> sp. NGR234	This study
pWEB-TNC-B2	pWEB-TNC™ with a 34.0 kb insert from <i>Rhizobium</i> sp. NGR234	This study
pWEB-TNC-B9	pWEB-TNC™ with a 42.0 kb insert from <i>Rhizobium</i> sp. NGR234	This study

Vectors/Constructs	Description	Source/Reference
pWEB-TNC-C2	pWEB-TNC™ with insert from <i>Rhizobium</i> sp. NGR234	This study
pWEB-TNC-C6	pWEB-TNC™ with a 37.7 kb insert from <i>Rhizobium</i> sp. NGR234	This study
pWEB-TNC-D9	pWEB-TNC™ with insert from <i>Rhizobium</i> sp. NGR234	This study
pWEB-TNC-D10	pWEB-TNC™ with insert from <i>Rhizobium</i> sp. NGR234	This study
pWEB-TNC-F9	pWEB-TNC™ with insert from <i>Rhizobium</i> sp. NGR234	This study
pWEB-TNC-F10	pWEB-TNC™ with insert from <i>Rhizobium</i> sp. NGR234	This study
pWEB-TNC-G2	pWEB-TNC™ with a 33.3 kb insert from <i>Rhizobium</i> sp. NGR234	This study
pDrive Cloning Vector (pDrive)	F', Tn10(Tet ^R), <i>lacI</i> ^f , <i>lacZ</i> ΔM15, <i>recA1</i> , <i>endA1</i> , <i>hscR17</i> , <i>lac</i> , <i>glnV44</i> , <i>thi-1</i> , <i>gyrA96</i> , <i>relA1</i> , Amp ^R	QIAGEN, Hilden, Germany
pDrive:: <i>hitR-hydR</i>	pDrive Cloning Vector with <i>hitR-hydR</i> locus from pWEB-TNC-A5 ligated via A/U-overhangs	This study
pDrive:: <i>hitR</i>	pDrive Cloning Vector with <i>hitR</i> gene from pWEB-TNC-A5 ligated via A/U-overhangs	This study
pDrive:: <i>hydR</i>	pDrive Cloning Vector with <i>hydR</i> gene from pWEB-TNC-A5 ligated via A/U-overhangs	This study
pDrive:: <i>qsdR2</i>	pDrive Cloning Vector with <i>qsdR2</i> gene from pWEB-TNC-B9 ligated via A/U-overhangs	This study
pDrive:: <i>aldR</i>	pDrive Cloning Vector with <i>aldR</i> gene from pWEB-TNC-G2 ligated via A/U-overhangs	This study
pTZ19R::Cm (pTZ19R)	Cloning vector, Δ <i>bla-cat</i> , Cm ^R	Amersham Pharmacia Biotech, Essex, United Kingdom
pTZ19R::fr44	pTZ19R::Cm containing the 4.4 kb <i>EcoRI</i> fragment from pWEB-TNC-B2 cloned into <i>EcoRI</i> restriction site	This study
pTZ19R::fr55	pTZ19R::Cm containing the 5.5 kb <i>HindIII</i> fragment from pWEB-TNC-C6 cloned into <i>HindIII</i> restriction site	This study
pBluescript II SK+ (pSK+)	<i>lacPOZ</i> ⁺ , high copy cloning vector, Amp ^R	Stratagene, Heidelberg, Germany
pSK+:: <i>dlhR</i>	pSK+ containing <i>Pfu</i> amplified PCR product of <i>dlhR</i> cloned into <i>EcoRV</i> site	This study
pSK+:: <i>qsdR1</i>	pSK+ containing <i>Pfu</i> amplified PCR product of <i>qsdR1</i> cloned into <i>EcoRV</i> site	This study
pET21a	His ₆ -tagged expression vector, Amp ^R	Novagen, Darmstadt Germany
pET21a:: <i>dlhR</i>	pET21a containing the <i>dlhR</i> gene cloned into <i>NdeI</i> and <i>HindIII</i> restriction sites	This study
pET21a:: <i>qsdR1</i>	pET21a containing the <i>qsdR1</i> gene cloned into <i>NdeI</i> and <i>XhoI</i> restriction sites	This study
pET21a:: <i>conT</i>	pET21a containing a control protein (glycosyl transferase with frame shift) cloned into <i>NdeI</i> and <i>XhoI</i> restriction sites	This study
pET24c	His ₆ -tagged expression vector, Kan ^R	Novagen, Darmstadt Germany
pET24c:: <i>qsdR1</i>	pET24c containing the <i>qsdR1</i> gene cloned into <i>NdeI</i> and <i>XhoI</i> restriction sites	This study
pBBR1MCS (pBBR)	Broad host range vector, low copy, Cm ^R	Kovach <i>et al.</i> 1995

Vectors/Constructs	Description	Source/Reference
pBBR1MCS-5 (pBBR-5)	Broad host range vector, low copy, Gm ^R	Kovach <i>et al.</i> 1995
pBBR1:: <i>dlhR</i>	pBBR1MCS containing the <i>dlhR</i> fragment amplified by T7 promoter/T7 terminator primer from pET21a:: <i>dlhR</i> and cloned into <i>EcoRV</i> restriction site	This study
pBBR1:: <i>qsdR1</i>	pBBR1MCS containing the <i>qsdR1</i> fragment amplified by T7 promoter/T7 terminator primer from pET21a:: <i>qsdR1</i> and cloned into <i>EcoRV</i> restriction site	This study

Table 5: Primers used in this study

Primer	Sequence (5'-3')	Length [bp]	GC content [%]	Tm [°C]
M13_for	CGCCAGGGTTTTCCAGTCACGAC	24	62.5	67.8
T7 promoter	TAATACGACTCACTATAGGG	20	40	53.2
T7 terminator	GCTAGTTATTGCTCAGCGG	19	52.6	56.7
M13_20	GTAAAACGACGGCCAGT	17	52.9	52.8
M13_rev	GGAAACAGCTATGACCATG	19	47.4	54.5
KAN-2 FP-1	ACCTACAACAAAGCTCTCATCAACC	25	44	61.3
KAN-2 RP-1	GCAATGTAACATCAGAGATTTTGAG	25	36	58.1
hitR-hydR_for	GGTTTCTCGACGGTTGAAACTG	22	50	60.3
hitR-hydR_rev	AGCACCTGGAGGAGATCGATG	21	57.1	61.8
hitR_for	GGTTTCTCGACGGTTGAAACTG	22	50	60.3
hitR_rev	CGTGCTGCAAATGCCTGATG	20	55	59.4
hydR_for	GCTTCATGTGCACGTCATCG	20	55	59.4
hydR_rev	AGCACCTGGAGGAGATCGATG	21	57.1	61.8
qsdR2_for	CTTCCGCGGCAAGCGTAAC	20	60	61.4
qsdR2_rev	CGCATCTCTAACTGGCTCATATGTC	25	48	63
aldR_for	CTATCCGGTTCGGACAAGGACTGG	24	58.3	66.1
aldR_rev	ATGAGAAAGTGCAGCGGTTTGAC	24	50	62.7
dlhR_for	<u>CATATGATT</u> CCTTCGCATGTTCC	23	43.5	58.9
dlhR_rev	<u>AAGCTT</u> GACCTTACGAAGGCTC	22	50	60.3
qsdR1_for	CGCCATAT <u>G</u> CCGCATGCAGAAACAA	25	52	64.6
qsdR1_rev	ACTGCTCGAGTGAGTCCCAGACGA	24	58.3	66.1

Oligonucleotide primers were ordered by Operon Biotechnologies (Eurofins MWG GmbH, Ebersberg, Germany). Inserted restriction sites are underlined.

2. Culture media, supplements and solutions

2.1. Culture media

All media and heat stable supplements were prepared as described below with bidistilled water and autoclaved at 121°C for 30 min before use. Antibiotics and heat sensitive

supplements were added sterile filtered (Rotilabo[®]-Spritzenfiter (CME, sterile, 0.22 µm), Roth, Karlsruhe, Germany) after the media cooled down to 56°C. For solid culture media preparation, 1.5% (w/v) of agar was added prior to autoclaving. Culture media were stored at 4°C.

2.1.1 LB medium for *Escherichia coli* (Sambrook 2001)

Tryptone	10 g
Yeast extract	5 g
NaCl	10 g
H ₂ O _{bidest}	ad 1000 mL

2.1.2 AT medium for *Agrobacterium tumefaciens* NTL4

The following components were autoclaved or filtered sterile and afterwards combined according to the details below. For 1 L AT medium, 50 mL AT salt solution (20x), 50 mL AT buffer (20x), 10 mL glucose solution (50%) and 890 mL H₂O_{bidest} were combined under sterile conditions.

AT salt solution (20x)

(NH ₄) ₂ SO ₄	40 g
MgSO ₄ x 7 H ₂ O	3.2 g
CaCl ₂ x 2 H ₂ O	0.2 g
FeSO ₄ x 7 H ₂ O	0.1 g
MnSO ₄ x 7 H ₂ O	0.024 g
H ₂ O _{bidest}	ad 1000 mL

AT buffer (20x)

KH ₂ PO ₄	214 g
H ₂ O _{bidest}	ad 1000 mL
pH	7.0

Glucose solution (50%, sterile filtered)

Glucose	50 g
H ₂ O _{bidest}	ad 100 mL

2.1.3 YEM medium for *Rhizobium* sp. NGR234

Mannitol	10 g
Yeast extract	1 g
K ₂ HPO ₄	0.5 g
MgSO ₄ x 7 H ₂ O	0.2 g
NaCl	0.1 g
CaCl ₂ (0.325 g/mL)	2 mL
FeCl ₃ x 6 H ₂ O (0.01 g/mL)	1 mL
H ₂ O _{bidest}	ad 1000 mL
pH 6.8 – 7.0	

All components were autoclaved except the FeCl₃ x 6 H₂O, CaCl₂ and the congo red solution. These solutions were prepared separately, filtered sterile and added to the YEM medium after autoclaving. For differentiation between rhizobia and *E. coli* or other bacteria, autoclaved YEM medium was complemented with congo red solution (Table 6).

2.1.4 TY medium for *Rhizobium* sp. NGR234 (Streit *et al.* 2004, modified)

Tryptone	5 g
Yeast extract	2 g
CaCl ₂ (1M)	5 mL
H ₂ O _{bidest}	ad 1000 mL
pH 7.0	

The TY medium was completed, similar to YEM medium, with CaCl₂ and congo red solution (Table 6) after autoclaving. For germination of sterilized seeds in colonization experiments, 0.5x TY medium was prepared without supplementation with CaCl₂.

2.1.5 YDC agar for *Chromobacterium violaceum* ChV2

KAT (Yeast extract)	10 g
Glucose	10 g
CaCO ₃	4 g
Agar	18 g
H ₂ O _{bidest}	ad 1000 mL

2.2. Antibiotics and supplements

Antibiotics and not autoclavable supplements were prepared as 1000-fold stock solutions with bidistilled water, ethanol (EtOH), methanol (MetOH) or dimethylformamide (DMF), filtered sterile and stored in aliquots of 1-5 mL at -20°C. Antibiotics as well as supplements were added to culture media at a temperature less than 55°C.

The concentration of antibiotics and supplements in solid and liquid media used for cultivation of bacterial strains are listed in Table 6. IPTG (Isopropyl-β-D-1-thiogalactopyranoside) was prepared as a 1000-fold stock solution in H₂O_{bidest} and used in concentrations of 100-500 μM in media.

Table 6: Antibiotics and supplements used in this study

Antibiotic/ Supplement	Stock solution [mg/mL]	End concentration in medium [μg/mL]				Solvent
		<i>E. coli</i>	<i>P. aeruginosa</i>	<i>A. tumefaciens</i>	<i>Rhizobium</i> sp.	
Ampicillin (Amp)	100	50-100	100		100	H ₂ O _{bidest}
Chloramphenicol (Cm)	25	25-50			50	EtOH
Gentamycin (Gm)	50	10			10	H ₂ O _{bidest}
Kanamycin (Kan)	25	20-25		100	25	H ₂ O _{bidest}
Rifampicin (Rif)	25				25-50	MetOH
Spectinomycin (Sp)	50			50	50	H ₂ O _{bidest}
Tetracycline (Tet)	5	5		4.5		H ₂ O _{bidest} / 70% EtOH
Congo Red	0.5				2.5	H ₂ O _{bidest}
X-Gal*	50	50	50	60		DMF

*X-Gal : 5-bromo-4-chloro-3-indolyl-β-D-galactopyranoside

2.3. Solutions and buffers

Solutions and buffers used in this study are summarized in the following section. Unless otherwise specified, solutions and buffers were filtered sterile.

2.3.1 TE buffer

For the preparation of crude cell extracts from *E. coli* BL21 (DE3) cells harboring cosmid clones, harvested cells were resuspended in autoclaved 1-fold TE buffer. When instead of H₂O_{bidest} buffer was needed for resuspending dry plasmid/cosmid/ chromosomal DNA pellets, TE buffer was used.

1x TE buffer

Tris	0.606 g
EDTA	0.146 g
H ₂ O _{bidest}	ad 500 mL
pH 8	

2.3.2 Potassium phosphate buffer (0.1 M)

Potassium phosphate buffer was used for dialysis of purified protein extracts as well as a buffer control for different QQ assays.

Mono-potassium salt solution (0.2 M)

KH ₂ PO ₄	27.2 g
H ₂ O _{bidest}	ad 1000 mL

Di-potassium salt solution (0.2 M)

K ₂ HPO ₄	34.8 g
H ₂ O _{bidest}	ad 1000 mL

Potassium phosphate buffer (0.1 M)

Mono salt solution	39 mL
Di salt solution	61 mL
H ₂ O _{bidest}	100 mL
pH 7.0	

Potassium phosphate buffer (0.1 M)

Mono salt solution	16 mL
Di salt solution	84 mL
H ₂ O _{bidest}	100 mL
pH 7.5	

2.3.3 Hoagland solution (Hoagland and Arnon 1950)

For cultivation of cowpeas in vermiculite a 0.25-fold Hoagland solution was used to supply the seedlings with nutrients. Therefore stock solutions were prepared as given below and stored separately. For the Hoagland solution all components were added to 800 mL H₂O_{bidest} according to Table 7 and filled up to 1L under sterile conditions.

Table 7: Solutions and composition of 1L Hoagland solution

Constituent	Stock solution	Volume of stock solution (mL) for 1L Hoagland
KNO ₃ (2 M)	202 g/L	2.5
Ca(NO ₃) ₂ x 4 H ₂ O (2 M)	236 g/0.5 L	2.5
MgSO ₄ x 7 H ₂ O (2 M)	493 g/L	1
KH ₂ PO ₄ (1 M)	136 g/L	1
NH ₄ NO ₃ (1 M)	80 g/L	1
Fe-EDTA solution	see below	20
Trace element solution	see below	1

Fe-EDTA solution

FeCl₃ x 6 H₂O 0.121 g

EDTA 0.375 g

H₂O_{bidest} ad 250 mL

Trace element solution

H₃BO₃ 2.86 g

MnCl₂ x 4 H₂O 1.81 g

ZnSO₄ x 7 H₂O 0.22 g

CuSO₄ x 5 H₂O 0.08 g

Na₂MoO₄ x 2 H₂O 0.09 g

H₂O_{bidest} ad 1000 mL

3. Cell culture, strain collection and growth conditions

3.1. Cultivation of bacteria

Liquid cultures were grown in Erlenmeyer flasks, test tubes or deep well plates at 140-200 rpm in rotary shakers (Infors HT, Minitron, Bottmingen, Switzerland). Cultures were inoculated by either single colonies from agar plates or aliquots of culture material from the strain collection. Inoculation was carried out with a sterile pipette tip or an inoculation loop.

3.1.1 Cultivation of *Escherichia coli* (*E. coli*)

3.1.1.1 *E. coli* cell cultures

E. coli was grown overnight at 37°C in LB medium supplemented with appropriate antibiotics. Therefore liquid 5 or 30 mL LB cultures of *E. coli* were inoculated as described earlier. For higher volumes of cultures first 30 mL precultures were grown, volumes of 100-2000 mL were then inoculated with a 1-5% aliquot of the preculture.

3.1.1.2 *E. coli* expression cultures

For purification of His-tagged proteins from *E. coli* BL21 (DE3) cells harboring pET-constructs, cell cultures with volumes of 100-2000 mL were used. Therefore 30 mL precultures were cultivated in LB medium supplemented with ampicillin (100 µg/mL) overnight at 37°C. The precultures were used to inoculate 100-2000 mL LB main cultures, where the optical density (OD₆₀₀) was adjusted to 0.1 (II.3.3). Expression cultures were grown at 37°C to an OD₆₀₀ of 0.6-0.8 and expression was induced by addition of 100-500 µM IPTG. The main cultures were incubated overnight at 17-37°C with shaking at 140 rpm. Cells were harvested and purified as described in II.6.2.

3.1.1.3 *E. coli* cosmid clone cultures

E. coli cosmid clones (NGR234 genomic library stored in 96-well microtiter plates) were inoculated in deep well plates containing 1-1.2 mL LB medium supplemented with ampicillin (100 µg/mL) using a sterile stamp. The deep well plates were sealed off with sterile permeable tissues (Greiner Bio-One, Frickenhausen, Germany) and incubated at 37°C on a rotary shaker at 350 rpm for 20 h.

3.1.2 Cultivation of *Rhizobium* sp. NGR234

Rhizobium sp. NGR234 was grown at 30°C on either YEM or TY medium supplemented with rifampicin (25 µg/mL) and other appropriate antibiotics. Cultures grown in media with rifampicin were incubated for two days, cultures grown in media with rifampicin and additional antibiotics were incubated between three–five days. For cultivation of higher volumes of rhizobial cells first 30 mL precultures were grown and volumes of 100-500 mL were then inoculated with a 1-5% aliquot of the preculture. The inoculation procedure was carried out as described previously in II.3.1 with respective media.

3.1.3 Cultivation of *A. tumefaciens* NTL4

Liquid 5 mL LB precultures of *A. tumefaciens* NTL4 (hereafter NTL4) were inoculated from glycerin stocks or plates and grown overnight at 30°C. The following day 5 mL of AT medium were inoculated with an 1-5% aliquot of the LB overnight culture supplemented with appropriate antibiotics and grown overnight at 30°C.

3.1.4 Cultivation of *C. violaceum* ChV2 and CV026

Cultures of *C. violaceum* ChV2 and CV026 (hereafter ChV2 and CV026) were inoculated as described before and grown overnight at 30°C either in liquid 5 mL LB medium with shaking at 200 rpm (both strains) or on YDC plates (ChV2).

3.1.5 Cultivation of *Pseudomonas aeruginosa* PAO1

Liquid cultures of *P. aeruginosa* PAO1 (hereafter PAO1) were established in 5 mL LB medium or on LB agar plates supplemented with ampicillin (Table 6) and incubated overnight at 37°C. Inoculation was carried out as described in II.3.1. For determination of pyocyanine levels produced by PAO1, plates as well as liquid cultures were incubated at 30°C overnight.

3.2. Strain collection

3.2.1 Maintenance and strain collection of pure cultures

Strains which were maintained for short-term storage were grown on agar plates. Therefore Petri dishes were sealed with Parafilm and stored at 4°C up to four weeks. For conservation purposes glycerol stocks were prepared to preserve strains for long-term storage. For these stocks, cultures were grown in liquid medium overnight at appropriate temperatures, an aliquot was mixed 1:1 with 87% sterile glycerol in screw-cap tubes and stored at -70°C.

3.2.2 Maintenance and preservation of the cosmid clone library

Colonies obtained by construction of the cosmid clone library were picked from agar plates into sterile microtiter plates (96-wells) containing 150 μ L LB broth supplemented with ampicillin (100 μ g/mL). The microtiter plates were incubated at 37°C overnight without shaking. For preservation 50 μ L sterile glycerol (87%) were added to each well, mixed well and stored at -70°C.

3.3. Determination of cell density

Growth of liquid cell cultures was determined by optical density (OD) measurement with an Eppendorf BioPhotometer (Eppendorf, Hamburg, Germany). The OD was measured at a wavelength of 600 nm (OD_{600}) using one-way cuvettes (10x4x45 mm, Sarstedt, Nuembrecht, Germany) with a path length of 1 cm. Pure medium was used as reference. Cell cultures were diluted when required so a measured optical density of 0.8 was not exceeded. An OD_{600} of 0.1 corresponds to a cell density of approximately 1×10^8 cells/mL for *E. coli*.

4. Standard techniques for working with DNA

For the inactivation of nucleases heat stable solutions and devices were autoclaved at 121°C for 20 min. Heat unstable devices were rinsed with 70% ethanol and solutions were filtered sterile.

4.1. Isolation of DNA

Before the isolation of plasmid, cosmid or genomic DNA, cells from cultures were harvested by centrifugation either using a miniSpin plus centrifuge/centrifuge 5415D (Eppendorf, Hamburg, Germany) or when cooling was required a centrifuge 5417R (Eppendorf, Hamburg, Germany). Higher volumes of cell cultures were pelleted using a Sorvall® RC 6+™ centrifuge with Sorvall® SS-34 and SLA-150 Super-Lite® autoclavable rotors (Thermo Electron Corporation, Langenselbold, Germany).

4.1.1 Isolation of plasmid and cosmid DNA by commercial kits

Highly pure plasmids or cosmids were isolated by appliance of different purchased DNA isolation kits given in Table 8. Culture volumes of 5 mL were sufficient for isolation of plasmid DNA, in contrast cosmid DNA preparation demanded for culture volumes up to 30 mL. The application of these DNA isolation kits was done according to manufacturer's instructions.

Cosmids were treated as low copy plasmids, the procedure for isolation of low copy vector DNA was given in the corresponding manuals. When a higher yield of plasmid or cosmid DNA was required, Midiprep DNA isolation kits were used according to manufacturer's instructions. Obtained plasmid and cosmid DNA could be used for further restriction, PCR (polymerase chain reaction) or sequencing purposes.

Table 8: Commercial Mini- and Midiprep DNA isolation kits

Kit Name	Sample size	Company
QIAprep® Spin Miniprep kit	1-5 mL	QIAGEN, Hilden, Germany
QIAGEN® Plasmid Midi kit	100-500 mL	QIAGEN, Hilden, Germany
peqGOLD Plasmid Miniprep kit	1-5 mL	PEQLAB Biotechnology, Erlangen, Germany
NucleSpin® Plasmid QuickPure	1-5 mL	Macherey-Nagel, Dueren, Germany
Wizard® Plus SV Miniprep DNA Purification System	1-5 mL	Promega, Madison, Wisconsin, USA

4.1.2 Isolation of plasmid DNA by alkaline cell lysis

Alkaline cell lysis is used for isolation and separation of plasmid DNA from genomic DNA. This method generates plasmid DNA in sufficient quality and quantity for further manipulation.

A preculture of *E. coli* harboring the desired plasmid was grown in 5 mL LB medium with appropriate antibiotic concentration at 37°C. 2-4 mL of this overnight culture were centrifuged for 3 min at 13000 rpm. Then the pellet was resuspended in 200 µL P1 buffer and cells were lysed by addition of 200 µL P2 buffer. After incubating at RT for maximum 5 min, the mixture was neutralized with 300 µL of P3 buffer and centrifuged for 10 min at 13000 rpm. The supernatant containing plasmid DNA was transferred into a new 1.5 mL Eppendorf Cup (hereafter E-Cup) and mixed with 500 µL chloroform/isoamyl alcohol (24:1, v/v). The two phases were mixed by shaking and for a new separation centrifuged for 5 min at 13000 rpm. Then the upper layer was transferred into a new 1.5 mL E-Cup and plasmid DNA was precipitated with 500 µL cold isopropanol. The mixture was incubated on ice or at -20°C for 15 min and then centrifuged for 20 min at 13000 rpm, 4°C. The supernatant was pipetted off and the obtained pellet was washed two times each with 1 mL 70% ethanol by following centrifugation for 2 min at 13000 rpm, 4°C. The supernatant was discarded. The pellet was dried either at 37°C for 10-30 min or in a vacuum concentrator 5301 (Eppendorf, Hamburg, Germany) at 45°C for 3-5 min. The plasmid DNA was resuspended in 50 µL H₂O_{bidest.}

P1 buffer (sterile filtered)

Tris-HCl	1.21 g
EDTA	0.74 g
RNase	100 µg/mL
H ₂ O _{bidest}	ad 200 mL
pH 8.0	

P2 buffer (sterile filtered)

NaOH	4.0 g
SDS	5.0 g
H ₂ O _{bidest}	ad 500 mL

P3 buffer (sterile filtered)

Kac	62.73 g
H ₂ O _{bidest}	ad 200 mL
pH 5.5 (adjusted with acetic acid)	

4.1.3 Isolation of plasmid DNA by cracking

Cracking is a very fast procedure resulting in unpurified plasmid DNA, thus this method is not suitable for further analysis such as sequencing. This procedure only provides information about the absence or presence of a plasmid.

As the cracking analysis requires little cell material, colonies had to be grown on LB plates containing appropriate antibiotics. Cell material was collected from the LB plate with a sterile pipette tip or a toothpick and resuspended in 25 µL 10 mM EDTA (pH 8.0). Then 25 µL freshly prepared cracking buffer were added and mixed well. The cell suspension was incubated for 5 min at 70°C and cooled on ice. Two µL of freshly prepared cracking dye were added and mixed. After incubation for 5 min on ice the cell suspension was centrifuged for 10 min at 13000 rpm, 4°C. Then, 20 µL of the supernatant were loaded on a 0.8% agarose gel (II.4.4) and electrophoresed at 100 V (Volt) for 1 h (hour).

Cracking buffer

2 N NaOH	100 µL
SDS (10%)	50 µL
Sucrose	0.2 g
H ₂ O _{bidest}	850 µL

Cracking dye

4 M KCl	150 μ L
Bromophenol blue (0.4%)	50 μ L

4.1.4 Isolation of cosmid DNA by the quick and dirty method

Quick and dirty isolation of cosmid DNA is based on the alkaline cell lysis method, which was already described in (II.4.1.2) with some minor modifications. Same buffers (P1, P2 and P3) were used for this cosmid DNA isolation.

A preculture of *E. coli* harboring the cosmid was grown in 5 mL LB medium with appropriate antibiotic concentration at 37°C. Five mL of this overnight culture were centrifuged for 30 sec at 9000 rpm. The pellet was resuspended in 100 μ L P1 buffer and incubated at 37°C for 30 min up to 2 h. Cells were lysed by addition of 200 μ L P2 buffer and incubated at room temperature (RT) for 1 min. After addition of 200 μ L chloroform, the mixture was neutralized with 150 μ L of P3 buffer, vortexed and centrifuged for 2 min at 13000 rpm. The supernatant containing cosmid DNA (approximately 400 μ L) was transferred into a new 1.5 mL E-Cup and mixed with 1 mL ice cold 96% EtOH (corresponding to 2-3 volumes of supernatant). The phases were mixed by inverting several times and incubated at -20°C for 30 min. For a new separation, centrifugation was carried out for 20 min at 13000 rpm, 4°C. Then the supernatant was pipetted off and the obtained pellet was dried a few minutes at 37°C. The dry pellet was washed with 200 μ L 70% ethanol by following centrifugation for 2 min at 13000 rpm, 4°C. The supernatant was discarded and the pellet was dried either at 37°C for 10-30 min or in a vacuum concentrator 5301 (Eppendorf, Hamburg, Germany) at 45°C for 3-5 min. The cosmid DNA was resuspended in 20 μ L H₂O_{bidest.}

4.1.5 Isolation of genomic DNA with AquaPure Genomic DNA kit

Purified genomic DNA from NGR234 was required for PCR amplification, sequencing and cloning. Therefore the AquaPure Genomic DNA kit (Bio-Rad Laboratories, Hercules, Canada) was applied according to manufacturer's instructions.

4.1.6 Classical isolation of genomic DNA

A preculture of NGR234 was grown in 30 mL TY medium with rifampicin at 30°C for 2-3 days. Then 5-10 mL of this preculture were centrifuged for 30 sec at 9000 rpm. To remove excess medium and antibiotics, the pellet was resuspended in 1 mL NaCl. Then, cells were

harvested for 30 sec at 9000 rpm and resuspended in 250 μ L TE-sucrose buffer (20% sucrose dissolved in 1x TE buffer by heating in microwave). After adding 250 μ L TE buffer containing lysozyme (10 mg/mL) and RNAase (1 mg/mL) the mixture was incubated for 1 h at 37°C. Proteinase K (1 mg/mL) as well as sarcosyl (overall volume of 5%) were added to the suspension and incubated for at least 1 h. After adding 250 μ L phenol/chloroform (1:1) the suspension was mixed well until a white emulsion appeared. The emulsion was centrifuged for 20 min at 13000 rpm and the supernatant was carefully transferred into a new E-Cup. The phenol/chloroform step was repeated twice. Then, 250 μ L of chloroform were added to the supernatant, mixed well and centrifuged for 2 min. The supernatant was transferred into a fresh E-Cup and participated with 2.5 volume of 96% EtOH and 0.3 M NaOAc. The E-Cup was inverted several times and incubated at -70°C for 10 min. After centrifugation for 20 min at 13000 rpm, the supernatant was decanted and mixed with 1 mL 70% EtOH and centrifuged again. This step was repeated once more. The DNA pellet was then dried, resuspended in 100 μ L 1x TE buffer or H₂O_{bidest} and incubated for 1 h at 60°C or at RT overnight.

4.2. DNA fragment isolation and purification by extraction from agarose gels

For isolation and purification purposes DNA fragments gained by PCR or restriction were separated depending on their size on 0.8-2% agarose gels, excised and purified by the Wizard[®] SV Gel and PCR Clean-Up System (Promega, Madison, Wisconsin, USA) or HiYield[®] PCR Clean-Up/Gel Ex kit (SLG Laborbedarf, Gauting, Germany) according to the instructions.

4.3. Determination of DNA concentration and purity

The quality and quantity of DNA solutions was determined with an Eppendorf BioPhotometer. Therefore the concentration of DNA solutions was measured at 260 nm in UV cuvettes (Carl Roth GmbH, Karlsruhe, Germany) against pure H₂O_{bidest} as a reference. An extinction of 1.0 corresponds to 50 μ g/mL. The purity of DNA was indicated by the ratio of extinction at 260 nm/280 nm, where the aimed ratio was 1.8-2.0.

4.4. Agarose gel electrophoresis

For size determination, purification and separation of DNA obtained by PCR, restriction and DNA isolation, 0.8-2% agarose gels in 1x TAE buffer were used. Concentration of agarose gels was selected corresponding to the expected DNA size. The electrophoresis was performed with an electrophoresis power supply EPS 301 (Amersham Biosciences, USA) at

100 V for 35-90 min in an electrophoresis gel chamber (Hoefer™ HE-33 mini horizontal submarine unit, Amersham Biosciences, USA) filled with 1x TAE buffer. Prior to electrophoresis the samples were mixed with 1/10 volume of loading dye. Gels were stained for 5 - 15 min in an ethidium bromide solution (10 µg/mL) and destained in water to remove excess ethidium bromide. Visualization and documentation of nucleic acids were carried out with UV light in a gel documentation device (Bio-Rad Laboratories, Munich Germany) and printed with a Seiko VP-1200 thermo printer (Seiko Precision GmbH, Hamburg, Germany). Evaluation of the size of DNA fragments was performed by the comparison to the standard GeneRuler™ 1 kb DNA Ladder or GeneRuler™ 100 bp DNA Ladder (Fermentas, St. Leon-Rot, Germany, see VII.1.1) directly on the agarose gel.

50x TAE buffer

Tris	2 M
EDTA (pH 8.0)	100 mM
H ₂ O _{bidest}	ad 1000 mL
pH 8.1 (adjusted with acetic acid)	

Loading dye

Glycerol (30%)	60 mL
EDTA (pH 8.0)	50 mM
Bromophenol blue (0.25%)	0.5 g
Xylencyanol (0.25%)	0.5 g
H ₂ O _{bidest}	ad 200 mL

4.5. Enzymatic modification of nucleic acids

4.5.1 Digestion of DNA by restriction endonucleases

For digestion of plasmids/cosmids/DNA fragments and for partial digestion of high molecular weight DNA, type II restriction endonucleases were used supplied by Fermentas (St. Leon-Rot, Germany).

4.5.1.1 Complete digestion

For the complete digestion of DNA, different restriction enzymes were used. The analytical restriction analysis, like determination of orientation and size of inserts/plasmids/cosmids, was carried out with a total volume of 10 µL. For preparative analysis like gel extraction or restriction for further ligation, higher volumes of DNA were needed, therefore the volume was increased to 50 µL.

Reaction for analytical restriction analysis (10 µL)

DNA solution	0.5-1 µg
Reaction buffer (10x)	1 µL
Restriction enzyme	0.3 µL (corresponding to 3 U of enzyme)
H ₂ O _{bidest}	ad 10 µL

Reaction for preparative restriction analysis (50 µL)

DNA solution	2-5 µg
Reaction buffer (10x)	5 µL
Restriction enzyme	1 µL (corresponding to 10 U of enzyme)
H ₂ O _{bidest}	ad 50 µL

Temperatures were specific for the particular enzymes. The incubation time for the analytical reactions was 1-3 h, preparative reactions were incubated overnight. Inactivation was carried out for 20 min at 65°C or 80°C depending on the used enzyme.

4.5.1.2 Partial digestion of genomic DNA

To construct a cosmid clone library, DNA fragments (prior to ligation into pWEB-TNC™ cosmid vector) had to be prepared by partial digestion to obtain complementary ends. Therefore genomic DNA from NGR234 was isolated with the AquaPure Genomic DNA kit. The DNA was digested with certain dilutions of the restriction enzyme *Bsp143I*. A master mix was prepared:

Master mix (100 µL)

<i>Bsp143I</i> buffer (10x)	10 µL
DNA solution	depending on DNA conc.
H ₂ O _{bidest}	ad 100 µL

The master mix was split in 9 µL aliquots and 1 µL of a stepwise increasing *Bsp143I* dilution was added. The enzyme dilutions ranged from 1:5000 to 1:160000. The reaction was incubated at 37°C for 20 min and the enzyme was inactivated by incubation at 65°C for 20 min. Undigested genomic DNA functioned as a control. To verify the correct size of DNA fragments all dilutions were separated by agarose gel electrophoresis. The reaction with the

enzyme dilution producing the desired DNA fragments (20-40 kb) was chosen, scaled up to 50 μ L and purified as further described in II.4.8.

4.5.2 Dephosphorylation of complementary ends

To avoid religation of enzymatically linearized plasmids or cosmids and to enhance ligation performance, dephosphorylation was performed with Antarctic phosphatase (New England BioLabs Inc., Frankfurt a. M., Germany).

Dephosphorylation reaction (70 μ L)

Preparative reaction	50 μ L
Phosphatase buffer (10x)	7 μ L
Antarctic phosphatase	1 μ L
H ₂ O _{bidest}	12 μ L

After incubation for 1 h at 37°C, the phosphatase was inactivated for 5 min at 65°C. Further treatment of the reaction was extraction from agarose gels (II.4.2) or purification and concentration according to II.4.5.4.

4.5.3 Complementation of overhangs with Klenow polymerase

When needed for blunt end ligation, DNA fragments with 3'-/5'-overhanging ends produced by restriction endonucleases were filled with nucleotides using the Klenow enzyme (Roche, Penzberg, Germany).

Klenow filling reaction (30 μ L)

DNA solution	23.7 μ L
Klenow buffer	3 μ L
dNTPs (10 nM)	3 μ L
Klenow enzyme	0.3 μ L

The reaction was incubated for 1 h at 37°C and heat inactivated for 10 min at 70°C. For further ligations digested DNA was purified using the purification protocol according to II.4.5.4 or extraction from agarose gels (II.4.2).

4.5.4 Purification and concentration of nucleic acids after enzymatic modification

After treatment of nucleic acids with enzymes NaOAc was added to the reaction with an end concentration of 0.3 M. For protein extraction DNA solutions were mixed with 1 volume of chloroform/isoamyl alcohol (24:1, v/v), vortexed and centrifuged for 5 min at 13000 rpm. The upper layer was transferred into a new 1.5 mL E-Cup. For DNA precipitation the upper layer was mixed with 2.5 volumes of 96% ethanol and incubated on ice for 20 min. After centrifugation for 20 min at 13000 rpm, 4°C the supernatant was pipetted off and the pellet was resuspended in 1 mL of 70% ethanol. After incubation for 10 min on ice the DNA solution was centrifuged for 5 min at 13000 rpm, 4°C. The supernatant was pipetted off, the pellet was dried either at RT 1-2 h or in the vacuum concentrator at 45°C for 3-5 min. The dried pellet was hydrated with 20 µL H₂O_{bidest} and stored at -20°C.

4.5.5 Ligation of DNA

The direct ligation of inserts or cosmid fragments into linearized vectors was accomplished with T4 DNA ligase (Fermentas, St. Leon-Rot, Germany). For subcloning purposes, obtained PCR products were ligated with QIAGEN® PCR Cloning kit (QIAGEN, Hilden, Germany).

4.5.5.1 Ligation of DNA fragments with T4 DNA ligase

Linear DNA fragments obtained by restriction or PCR amplification with *Pfu* polymerase (Fermentas, St. Leon-Rot, Germany) were recombined by either sticky end or blunt end ligation. A standard ligation reaction is listed below, vector and insert DNA were applied in a molar ratio of 1:2.

Ligation reaction (20 µL)

Vector DNA	x µL
Insert DNA	y µL
Ligase buffer (10x)	2 µL
T4 ligase (for sticky ends)	0.5 µL
T4 ligase (for blunt ends)	1 µL
H ₂ O _{bidest}	ad 20 µL

The ligation reaction was incubated overnight at 16°C or at 4°C and used directly for transformation into *E. coli* or rhizobial competent cells.

4.5.5.2 Ligation of PCR products in pDrive Cloning Vector

For subcloning purposes and for insertion of additional restriction sites, purified PCR products obtained by *Taq* polymerase were ligated with the QIAGEN® PCR Cloning kit into pDrive Cloning Vector (linearized and equipped with U-overhangs) according to manufacturer's instructions.

pDrive ligation (10 µL)

PCR product	0.5-2 µL
pDrive vector	0.5 µL
Ligation master mix	2.5 µL
H ₂ O _{bidest}	ad 5 µL

The ligation reaction was incubated at 16°C for 2 h and continued with transformation into *E. coli* cells as described in II.5.1.3.

4.6. Amplification of DNA by PCR

The PDR was used for amplification of DNA fragments. PCR products which were amplified with *Pfu* polymerase (Fermentas, St. Leon-Rot, Germany) were used for further subcloning. PCR products gained by amplification with *Taq* polymerase (Fermentas, St. Leon-Rot, Germany) were used as a first control of ligations or for direct cloning into the pDrive vector. The PCR was carried out either with a Mastercycler personal or gradient (Eppendorf, Hamburg, Germany).

4.6.1 Oligonucleotide primers

Primers used for PCR amplification are listed in Table 5. Primer annealing is performed at varying temperatures (T_{ann}) due to the melting temperature of the employed primer pair. The melting temperature (T_m) was calculated according to Chester and Marshak 1993:

$$T_m (^{\circ}\text{C}) = 69.3 + 0.41 * (\% \text{ GC}) - (650/\text{bp}_{\text{Primer}})$$

$$T_{ann} (^{\circ}\text{C}) = T_m - 5^{\circ}\text{C}$$

% GC = percentage content of bases guanine and cytosine in primer sequence

bp_{Primer} = base pairs, length of primer

4.6.2 Standard PCR

The standard PCR was carried out with prior isolated DNA and *Pfu* polymerase which produces blunt end PCR products and has due to the 3'/5'-exonuclease activity a very low error probability. Volumes and conditions for the standard reaction are given below.

Standard PCR reaction (50 μ L)

DNA (template)	1 μ L (corresponding to ~ 1 μ g)
<i>Pfu</i> buffer (10x)	5 μ L
dNTPs (10 mM)	1 μ L
Primer forward	0.5 μ L
Primer reverse	0.5 μ L
DMSO	2 μ L
<i>Pfu</i> polymerase	1 μ L (corresponding to 2.5 U)
H ₂ O _{bidest}	ad 50 μ L

The PCR reaction was pipetted together on ice. For the temperature program (Table 9) the annealing temperature was calculated based on the melting temperature (II.4.6.1), whereas the lower T_m value of the used primer pair was used. Elongation time was chosen based on the length of the target DNA sequence and based on the elongation efficiency of 500 bp per min (*Pfu* polymerase).

Table 9: Temperature conditions for PCR with *Pfu* polymerase

	Initial Denaturation	95°C	5-10 min
30-35 cycles	Denaturation	95°C	1 min
	Annealing	48-63°C	45 sec
	Elongation	72°C	2 min/kb
	Final Elongation	72°C	5-10 min

4.6.3 Direct colony PCR

The direct colony PCR was used for verification of positive clones and their correct inserts directly from colonies growing on agar plates. Therefore, the colonies were picked and resuspended in 20 μ L of a master mix serving as DNA templates for PCR amplification with *Taq* polymerase. Volumes and conditions for the direct colony reaction are given below.

Direct colony reaction (master mix, 500 μ L)

<i>Taq</i> buffer (10x)	50 μ L
dNTPs (10 mM)	10 μ L
Primer forward	5 μ L
Primer reverse	5 μ L
<i>Taq</i> polymerase	5 μ L
H ₂ O _{bidest}	425 μ L

The direct colony reactions were prepared and left on ice until DNA templates (colonies) were added. The temperature conditions are given in Table 10. The calculation of T_m was carried out as described in II.4.6.1, elongation efficiency for *Taq* polymerase is 1 kb per min.

Table 10: Temperature conditions for PCR with *Taq* polymerase

	Initial Denaturation	95°C	5 min
25-30 cycles	Denaturation	95°C	1 min
	Annealing	48-63°C	45 sec
	Elongation	72°C	1 min/kb
	Final Elongation	72°C	5 min

4.6.4 Purification of PCR products

Prior to further cloning of PCR products into prepared restricted plasmids or cosmids products had to be cleaned from enzymes, primers and remaining nucleotides. The purification was carried out either by isopropanol precipitation as described in the following paragraph or by extraction from agarose gels (II.4.2). For isopropanol precipitation the PCR reaction was transferred into a 1.5 mL E-Cup. After addition of an equal volume of ice-cold isopropanol the reaction was incubated on ice for 10 min. The PCR product was harvested by centrifugation at 13000 rpm and 4°C for 20 min. The isopropanol was pipetted off and the pellet was dried at 50°C for approximately 10 min. Rehydration of the pellet was carried out by addition of 25 μ L H₂O_{bidest} and incubation at 70°C. The purified PCR product was stored at -20°C until required for ligation.

4.7. Transposon mutagenesis

In order to identify and localize potential QQ candidate genes on cosmid clones (*in vitro*) transposon mutagenesis was accomplished. Therefore the *in vitro* transposon mutagenesis EZ-Tn5™ <KAN-2> Insertion kit (Epicentre Biotechnologies, Madison, Wisconsin, USA) was used. To apply the same amount of transposon to the reaction mix, the amount of target DNA (cosmid) was calculated according to the equation:

$$\mu\text{mol target DNA} = \mu\text{g target DNA}/(\text{bp target DNA} \times 660)$$

Then, 0.2 µg target DNA as well as the molar equivalent of the transposon were added to the reaction mix together with reaction buffer, transposase and sterile H₂O_{bidest.} The *in vitro* transposon insertion reaction was carried out according to the manufacturer's protocol. After transformation of 1 µL transposon reaction into *E. coli* XL1 blue cells, selection was employed on LB agar containing kanamycin. All obtained clones were transferred into a 96-well plate and preserved as described in II.3.2.2.

4.8. Construction of a cosmid clone library

For the construction of a NGR234 cosmid clone library, the pWEB-TNC™ Cosmid Cloning kit (Epicentre Biotechnologies, Madison, Wisconsin, USA) was used whereby the provided protocol was slightly modified (modifications are stated below).

4.8.1 Preparation of genomic DNA fragments

Genomic DNA of NGR234 was isolated as described in II.4.1.5 using a commercial AquaPure kit. The construction of the NGR234 cosmid clone library demanded for at least 10 µg of genomic DNA already fractioned in 20-40 kb fragments. To generate required DNA fragments, partial digestion with *Bsp*143I (II.4.5.1.2) was accomplished using enzyme dilutions ranging from 1:5000 to 1:160000. The enzyme dilution of 1:30000 turned out to be suitable as separated on a agarose gel this dilution generated the desired DNA fragments with sizes between 30-45 kb (compared to a cosmid control standard and undigested genomic DNA). Prior to the end repair, the genomic DNA fragments were purified as described in II.4.5.4. The end repair reaction was carried out with ~10 µg of the fragmented NGR234 DNA as specified in the instructions, followed by a dialysis against water for 2 h for purification purposes and to enhance ligation efficiency.

4.8.2 Ligation

The purified and dialyzed DNA fragments were then ligated into blunt-ended pWEB-TNC™ cosmid vector. Therefore, the double volume of each reagent (provided by the kit) was combined in the order listed in the manual and mix thoroughly. A molar ratio of 10:1 and 5:1 of pWEB-TNC vector to genomic DNA fragments was established. After incubation at RT for 2 h and inactivation of Fast-Link ligase at 70°C for 10 min, a 5 µL aliquot of the ligation was separated on an agarose gel to verify the successful ligation. Dialyzed DNA was used as a control.

4.8.3 *In vitro* Packaging

To transfer heterologous DNA into an *E. coli* host phages were used. To package obtained cosmid DNA into λ phage particles, the MaxPlax Packaging Extracts (provided with pWEB-TNC™ Cosmid Cloning kit). Packaging was done according to the instructions except from the extract, the dialyzed ligation, the phage dilution buffer and chloroform, which were halved for the reaction. The obtained supernatant could be stored at 4°C up to one month.

Phage dilution buffer

Tris-HCl (pH 8.3)	10 mM
NaCl	100 mM
MgCl ₂	10 mM

4.8.4 Transduction

Phage competent cells were prepared from *E. coli* EPI100™-T1^R Phage T1-resistant cells (hereafter EPI100). Therefore, 50 mL LB medium supplemented with 10 mM MgSO₄ and 0.2% (w/v) maltose were inoculated with a single colony. Cells were grown at 37°C with shaking until they reached an OD₆₀₀ of 1. Then, cells were pelleted by centrifugation at 2000 rpm, 4°C for 10 min and resuspended in 25 mL of sterile 10 mM MgSO₄, diluting the cells to an OD₆₀₀ of 0.5. After adding 5-10 µL of the prepared packaging mix to 100 µL of prepared EPI100 phage competent cells, the mixture was incubated for 30 min at 37°C. Aliquots were plated on LB medium with ampicillin and incubated overnight at 37°C. Obtained colonies were picked with sterile toothpicks, transferred into 96-well microtiter plates containing 150 µL liquid LB medium with ampicillin and incubated 20-24 h at 37°C.

5. DNA transfer techniques

Depending on the target organism, different transfer techniques were applied in this study for transformation of DNA. Heat shock and electroporation were accomplished to transfer the ligated plasmid or cosmid DNA into competent *E. coli* cells. For transformation of plasmid or cosmid DNA into competent *Rhizobium* sp. NGR234 electroporation or conjugation were carried out.

5.1. Transformation of *E. coli* cells

5.1.1 Preparation of heat competent *E. coli* DH5 α cells

Prepared heat competent *E. coli* DH5 α cell were supplied by the laboratory.

5.1.2 Chemical preparation of heat competent *E. coli* XL1 blue and BL21 (DE3) cells by the CaCl₂ method

A preculture of *E. coli* XL1 blue or BL21 (DE3) was grown in 5 mL LB medium at 37°C overnight. In a 1 L flask 250 mL prewarmed LB medium were inoculated with 2.5 mL of the preculture and incubated with shaking at 37°C until an OD₆₀₀ of 0.5 was reached. The culture was cooled on ice for 5 min and then centrifuged for 5 min at 4000 rpm, 4°C. The supernatant was discarded and the pellet was cooled on ice. The cells were then resuspended in 75 mL ice cold TFB1 buffer and left on ice for 90 min. After centrifugation at 4000 rpm, 4°C for 5 min, the supernatant was discarded and the cells were resuspended in 10 mL ice cold TFB2 buffer. The competent cells were distributed in aliquots of 100 μ L and stored at -70°C until needed for transformation.

TFB1 buffer

RbCl 0.91 g

MnCl₂ x 4 H₂O 0.74 g

Potassium acetate 0.22 g

CaCl₂ x 2 H₂O 0.11 g

Glycerin 11.25 mL

H₂O_{bidest} ad 75 mL

pH 5.8 (adjust with diluted acetic acid)

TFB2 buffer

MOPS 0.042 g

RbCl 0.0242 g

CaCl₂ x 2 H₂O 0.221 g

Glycerin 3 mL

H₂O_{bidest} ad 20 mL

pH 6.8 (adjust with diluted KOH)

5.1.3 Heat shock transformation of *E. coli* DH5 α , XL1 blue and BL 21 (DE3)

Competent *E. coli* cells were thawed on ice for 5 min. Five μ L of plasmid or cosmid DNA were added to the competent cells and incubated on ice for 30 min. The heat shock was performed for exactly 90 sec at 42°C. The cells were transferred back on ice for 5 min, resuspended in 1 mL LB broth and incubated for 1 h at 37°C. Volumes between 50 and 200 μ L of the cell suspension were plated on selective LB agar plates and incubated overnight at 37°C.

5.2. Transformation of *Rhizobium* sp. NGR234

5.2.1 Preparation of electrocompetent *Rhizobium* sp. NGR234 cells

50 mL YEM medium were inoculated with a fresh culture of rhizobial cells and incubated at 30°C for two days to an OD₆₀₀ of 0.4-0.6. In every following step cells had to be kept on ice. Rhizobial cells were chilled for 30 min on ice and then harvested by centrifugation for 10 min at 9000 rpm, 4°C. The supernatant was discarded and the pellet was washed four times with 40 mL cold sterile H₂O_{bidest.} Finally, the pellet was washed with 10% glycerol, centrifuged for 10 min at 9000 rpm, 4°C and resuspended in 1 mL 10% glycerol. The cell suspension was distributed in aliquots of 90 μ L and conserved at -70°C until required for electroporation.

5.2.2 Electroporation of *Rhizobium* sp. NGR234

Electrocompetent NGR234 cells were thawed on ice for 5 min. After adding 2 μ L of target DNA to the cells, the mixture was vortexed for 10 sec at high speed and incubated on ice for 30 min. A chilled electroporation cuvette was loaded with the cell-DNA mixture and subjected to a single pulse of high voltage according to the following parameters:

Electroporation parameters *Rhizobium* sp. NGR234

Voltage	2400 V
Resistance	200 Ω
Condenser capacity	25 μ F

After delivering the pulse the cuvette was kept on ice for 10 min. The cell-DNA mixture was then resuspended in 1 mL of sterile TY broth and incubated overnight at 30°C. Afterwards different volumes of the cell suspension were plated on selective and non selective YEM agar plates. Selective plates were used for calculation of the number of transformants and non selective plates were used to calculate the number of survivors.

6. Biochemical methods for working with proteins

6.1. Standard techniques

6.1.1 Quantitative determination of protein content (Bradford 1976)

The measurement of the concentration of protein solutions was carried out using the Bradford protein assay. This method is based on the shift of the absorbance in the Coomassie Brilliant Blue G-250 dye (absorbs at 595 nm), when the previously red form of the Coomassie reagent (absorbs at 465 nm) changes and stabilizes into Coomassie blue.

10 μ L of the purified protein were added to 1 mL Bradford solution (see below), mixed well and incubated for 15 min at RT in the dark. The extinction was measured at a wavelength of 595 nm in a one-way cuvette with an Eppendorf BioPhotometer or a SmartSpec™ Plus Spectrometer. The buffer used for dialysis served as a reference. A direct correlation between extinction and protein concentration was only given in the range of linearity of the calibration curve. Samples above this range were diluted either with buffer or H₂O_{bidest}. Prior to the measurements, a calibration curve was generated. The calibration curve is given in VII.2.1 (Figure 28 in appendix).

Bradford solution (sterile filtered)

Coomassie Brilliant Blue G-250	100 mg
Ethanol (95%, v/v)	50 mL
H ₃ PO ₄ (85%, w/v)	100 mL
H ₂ O _{bidest}	ad 1000 mL

6.1.2 SDS-Polyacrylamide gel electrophoresis (SDS-PAGE)

After dialysis, the eluted proteins were separated due to their molecular weight by SDS-PAGE. The proteins were treated with SDS (sodium dodecyl sulfate), which neutralizes and covers them with a negative charge. The SDS-PAGE was carried out in gel electrophoresis chambers (Bio-Rad Laboratories, Munich, Germany).

6.1.2.1 Composition of SDS-PAGE gels

For preparation of the SDS-PAGE gel the following solutions had to be prepared:

Acrylamide stock solution

Acrylamide 30 g

Bisacrylamide 0.8 g

H₂O_{bidest} ad 100 mL

Ammonium Persulfate (APS)

10% (w/v) in H₂O_{bidest}

N,N,N',N'-Tetramethylene ethylene diamine

(TEMED) supplied by Bio-Rad Laboratories (Munich, Germany)

Resolving gel stock solution (4-fold)

Tris (1.5 M) 45.4 g

SDS (0.4%, w/v) 1 g

H₂O_{bidest} ad 250 mL

pH 8.8 (with HCl_{conc.})

Stacking gel stock solution (4-fold)

Tris (500 mM) 6.1 g

SDS (0.4%, w/v) 0.4 g

H₂O_{bidest} ad 100 mL

pH 6.8 (with HCl_{conc.})

10x Electrophoresis buffer

Tris 30.3 g

Glycine 144.1 g

SDS 10 g

H₂O_{bidest} ad 1000 mL

pH 8.4 (with Glycine)

4x SDS loading buffer

Glycerol 7.5 mL

β-mercaptoethanol 2.5 mL

SDS 1.2 g

Bromophenol blue (0.2%,w/v) 0.5 mL

Tris 0.4 g

H₂O_{bidest} ad 50 mL

pH 6.8 (with HCl_{conc.})

The resolving and stacking gels were prepared as depicted in the following Table 11. The percentage of both gels dependent on the specific application of the SDS-PAGE. After mixing all components in a falcon tube, the resolving gel was poured between two glass plates, which were previously cleaned with 70% ethanol and inserted into a stand. Water was poured on the top of the resolving gel to level the gel edge. After the resolving gel polymerized, water was decanted and all components for the stacking gel were mixed. Then, the gel was poured over the resolving gel and the comb was inserted. After polymerization of

the stacking gel the comb was removed. The gel was used immediately or was stored at 4°C in wet tissues.

Table 11: Composition of SDS-PAGE gels used in this study

Component	Resolving gel		Stacking gel 7%
	12%	15%	
Resolving gel stock solution	1.25 mL	1.25 mL	-
Stacking gel stock solution	-	-	0.48 mL
Acrylamide stock solution	1.5 mL	1.88 mL	0.35 mL
APS	23 µL	28 µL	10 µL
TEMED	5 µL	6 µL	3 µL
H ₂ O	2.23 mL	1.84 mL	1.17 mL

6.1.2.2 Preparation of protein samples and SDS-PAGE gel electrophoresis

Aliquots of 20 µL of obtained protein extracts were mixed with 4 µL SDS loading buffer and incubated at 95°C for 5 min. For detection of molecular masses, protein markers were used in order to compare the masses on the SDS gels. When using protein marker #SM0431 (Fermentas, St.Leon-Rot, Germany, see also VII.1.2) it had to be incubated at 95°C for 5 min, when using the prestained protein marker #SM0671 (Fermentas, St.Leon-Rot, Germany, see also VII.1.2), the marker was loaded directly into the gel pocket. When cell pellets were used for SDS-PAGE analysis, pellets were resuspended in 4 M urea and diluted 1:100. Prior to loading of samples, the gel was inserted into the electrophoresis chamber (Bio-Rad Laboratories, Munich, Germany) and the chamber was filled with 1x electrophoresis buffer. Aliquots of 20 µL from each sample were then loaded carefully into the gel pockets and electrophoresis was carried out at 20 mA for the stacking gel and was increased to 40 mA for the resolving gel.

6.1.2.3 Coomassie staining of SDS-PAGE gels

After the electrophoresis, the gel was carefully removed from the glass plates and stained with Coomassie overnight under gentle shaking. Destaining of the gel was accomplished with 20% acetic acid until bands were visible.

Coomassie stain (1 L)

Coomassie brilliant blue powder	1 g
Acetic acid	100 mL
Ethanol	400 mL
H ₂ O _{bidest}	500 mL

6.2. Protein purification

6.2.1 Crude cell extract preparation

To obtain crude cell extracts from cosmid clones, *E. coli* harboring the clone was cultivated as described in II.3.1.1.1. For purification of His-tagged proteins, *E. coli* BL21 (DE3) cells harboring target DNA were cultivated as described in II.3.1.1.2. Cells were then harvested by centrifugation at 10000 rpm, 4°C for 20 min, washed and resuspended in either 1x TE buffer (II.2.3.1) or 1x LEW buffer (Macherey-Nagel, Dueren, Germany), where 2 mL of buffer were used per 1 g cell pellet. The cells were disrupted either by ultrasonication or by a French press.

6.2.1.1 Ultrasonication

When crude cell extracts (from *E. coli* BL21 (DE3) cells harboring cosmid clones) were needed without further His-tag purification, harvested cells were resuspended in 1x TE buffer, otherwise 1x LEW buffer was used. Cells were disrupted on ice through ultrasonication with a microtip S2 (UP200S Ultrasonic Processor, Hielscher Ultrasound Technologies, Teltow, Germany) at 50% amplitude and cycle 0.5 for up to 30 min (with 2 min cooling steps per 10 min sonication). The lysate was centrifuged at 13000 rpm, 4°C for 30 min, the obtained supernatant was filtered sterile with 0.45 µm PVDF filters (Rotilabo®-Spritzenfilter, Carl Roth GmbH, Karlsruhe, Germany) and stored on ice until further use.

6.2.1.2 French Pressure Cell

The crude cell extract was produced in three-five intervals of 1000 psi each with a French Pressure Cell Press® (American Instrument Company, Silver Spring, Maryland, USA). After cell disruption, the lysate was transferred into sterile centrifugation tubes or E-Cups and centrifuged at 10000 rpm, 4°C for 30 min. The supernatant was filtered sterile with a 0.45 µm PVDF filter and stored on ice until further use.

6.2.2 Purification of histidine-tagged proteins by Protino[®] Ni-TED columns

The obtained supernatants were purified under native conditions using Protino[®] Ni-TED 2000 packed columns (Macherey-Nagel, Dueren, Germany) following the manufacturers protocol. First, the column was equilibrated with 1x LEW buffer, the clarified lysate was loaded on the column and allow draining by gravity. The bound protein was then eluted with 1x elution buffer containing imidazole. If necessary, a dialysis was carried out to remove excess imidazole from the eluted proteins. The level of protein purity as well as the molecular mass were determined by SDS-PAGE (II.6.1.2).

6.2.3 Dialysis of purified protein extracts

To remove excess imidazole as well as to change the buffer and pH value of protein eluates, a dialysis was carried out. The obtained protein eluates were placed into dialysis tubings (MWCO 7 kDa, ø 22mm, Serva Membran-Cel[™], Heidelberg, Germany), which were boiled for 10 min prior to usage. The ends were sealed off and the tubing was placed into 200-fold volume of potassium phosphate buffer (II.2.3.2) with a pH value according to the used protein. Dialysis was carried out overnight at 4°C under stirring, the buffer was changed once after 1 h. Subsequently, the protein eluate could be used for activity tests.

6.2.4 Concentration of protein solutions

For further assays and the HPLC analysis, high concentrated protein extracts were needed, therefore Vivaspin concentrators were used.

6.2.4.1 Concentration by Vivaspin concentrator

The Vivaspin 6 concentrator (50000 MWCO PES, Satorius Stedim Biotech GmbH, Goettingen, Germany) was filled with max. 15 mL of the protein extract and centrifuged at 5000 rpm, 4°C until the desired concentration was reached. The supernatant was removed from the concentrator and could be used for further assays.

6.2.4.2 Concentration by flow filtration capsule

In order to obtain protein extracts from supernatants of liquid medium with up to 1 L overall volume, the Minimate[™] TFF (tangential flow filtration) Capsule (PALL Life Sciences, Michigan, USA) was used. NGR234 was cultivated as described in II.3.1.2 and centrifuged at 9000 rpm, 4°C for 30 min. The supernatant was filled in the sample reservoir and the concentration of protein extract was done according to the manufacturer's instructions.

6.3. Western blotting

The western blot analysis was used to detect specific proteins which are able to bind to antibodies and were prior separated by SDS-PAGE. Therefore, proteins were transferred to a membrane by electroblotting.

6.3.1 Preparation of membrane and blotting

Prior to preparation of the western blot, proteins were separated on a SDS-PAGE gel as described earlier (II.6.1.2), using a prestained molecular marker but not stained with Coomassie. The gel and the solid nitrocellulose membrane (Schleicher & Schuell, Dassel, Germany) were compressed between a sandwich of tissue paper (three/side) in a provided cassette. This cassette was closed and inserted into the chamber filled with a small volume of 1x blotting buffer. The right position of the cassette and the chamber was checked. The transfer was employed for 90 min at 300 mA.

6.3.2 Blocking of membrane and binding of antibodies

After electrophoretic transfer, the membrane was removed from the cassette, washed two times for 10 min with 1x TBS buffer and then incubated with the blocking solution (5% milk powder in TBST buffer) overnight at 4°C to saturate the remaining free hydrophobic binding sites. After washing the membrane three times for 10 min with TBST buffer, the first antibody (penta His-tag, diluted 1:5000 in TBST) was incubated with the membrane for 2.5 h at 4°C. Again, the membrane was washed three times for 10 min with TBST buffer and afterwards incubated with the second antibody (anti-Rabbit IgG, diluted 1:10000 in the 5% milk powder-TBST solution) for 1 h at RT. Finally, the membrane was washed three times with TBST buffer.

6.3.3 Detection of His-tagged proteins

For the detection of antibodies, first the membrane was equilibrated for three minutes with the reaction buffer. Then, 10 mL of reaction buffer were mixed with 35 µL BCIP (5-bromo-4-chloro-3'-indolyphosphate p-toluidine salt, X-phosphate) and 45 µL NBT (nitro-blue tetrazolium chloride), added to the membrane and incubated until bands were clearly visible.

5x Blotting buffer

Tris	250 mM
Glycine	1.9 M
SDS (w/v)	0.5%
H ₂ O _{bidest}	ad 1000 mL

1x Blotting buffer

5x Blotting buffer	200 mL
Methanol	200 mL
H ₂ O _{bidest}	ad 1000 mL

1x TBS buffer

Tris	100 mM
NaCl (w/v)	0.9%
H ₂ O _{bidest}	ad 1000 mL

TBST buffer

Tris	100 mM
NaCl (w/v)	0.9%
Tween-20 (v/v)	0.1%
H ₂ O _{bidest}	ad 1000 mL

Reaction buffer

Tris	100 mM
NaCl	100 mM
MgCl ₂	50 mM
H ₂ O _{bidest}	ad 100 mL
pH	9.5

7. Methods for detection of QQ activity**7.1. Homoserine lactone solutions****7.1.1 *N*-(butanoyl)-L-homoserine lactone**

A stock solution of 1 M *N*-(butanoyl)-L-homoserine lactone (hereafter C4-HSL; Sigma-Aldrich, Heidelberg, Germany) was prepared in ice cold ethyl acetate. When required for complementation assays in PAO1, dilution series ranging from 10⁻⁴ to 10⁻⁷ M were established in ethyl acetate and used immediately.

7.1.2 *N*-(3-oxohexanoyl)-L-homoserine lactone

Dilutions of *N*-(3-oxohexanoyl)-L-homoserine lactone (hereafter 3-oxo-C6-HSL; Sigma-Aldrich, Heidelberg, Germany) were prepared in ice cold ethyl acetate. For pigment inhibition assays with CV026 dilutions were established in liquid LB medium and used immediately. A final concentration of 0.1 μ M 3-oxo-C6-HSL was required.

7.1.3 *N*-(3-oxooctanoyl)-L-homoserine lactone

Dilutions of *N*-(3-oxooctanoyl)-L-homoserine lactone (hereafter 3-oxo-C8-HSL; Sigma-Aldrich, Heidelberg, Germany) were prepared in ice cold ethyl acetate or in DMSO, when required for HPLC analysis. Dilution steps ranging from 4.1×10^{-1} to 4.1×10^{-12} mol/L were prepared and stored in screw bottles at -20°C . When larger volumes of HSL were needed for assays, these stock solutions were used for further dilutions which were then established in liquid LB medium.

7.1.4 *N*-(3-oxododecanoyl)-L-homoserine lactone

A stock solution of 1 M *N*-(3-oxododecanoyl)-L-homoserine lactone (hereafter 3-oxo-C12-HSL; Cayman Chemical Company, Ann Arbor, USA) was prepared in ice cold ethyl acetate. When required for complementation assays in PAO1, dilution series ranging from 10^{-4} to 10^{-7} M were established in ethyl acetate and used immediately.

7.2. ATsoft screening using *A. tumefaciens* NTL4 (Schipper *et al.* 2009)

The ATsoft screening was employed for detection of AHLs directly in cosmid clone cultures. Therefore, ATsoft screening agar in combination with the biosensor strain *A. tumefaciens* NTL4 were used. NTL4 possesses a plasmid-based *traR* and a gene fusion (*tral::lacZ*) which allows a blue-white screening. In the presence of AHLs, the enzyme β -galactosidase is released and converts X-Gal present in the agar into a blue dye. The medium remains white in the absence of AHLs.

7.2.1 Preparation of ATsoft screening agar

Prior to preparation of ATsoft agar, Eiken agar (Eiken Chemical CO. LTD., Tokyo, Japan) was added to $\text{H}_2\text{O}_{\text{bidest}}$, autoclaved and cooled to 42°C . The components (given below) were either autoclaved or filtered sterile and added to the agar (for AT buffer (20x) and AT salt solution (20x) see II.2.1.2). A preculture of NTL4 was grown in 5 mL AT medium with

appropriate antibiotics 20 h at 28°C and then added with a final cell density of 10^7 cells/mL to the ATsoft agar.

Composition of ATsoft agar (100 mL)

Eiken agar	1 g in 89 mL
AT buffer (20x)	5 mL
AT salt solution (20x)	5 mL
Glucose solution (50x)	1 mL
Spectinomycin (60 mg/mL)	100 μ L
X-Gal (60 mg/mL)	100 μ L

The ATsoft agar was kept in a water bath at 42°C while adding the components. Then, 200 μ L of the agar were pipetted into each wells of a 96-well microtiter plate and agar was allowed to cool and solidify under sterile conditions. The 96-well plates were stored not longer than 2 h.

7.2.2 ATsoft screening procedure

7.2.2.1 Determination of required HSL concentration

First, control experiments were carried out to determine the minimal amount of HSL required by NTL4 to switch on QS and the maximal amount of HSL which is inactivated by EPI100 cells harboring NGR234 cosmid clones during 20 h incubation. Therefore, dilutions of 3-oxo-C8-HSL were prepared as described previously, ranging from 4.1×10^{-1} to 4.1×10^{-12} mol/L. Five mL of each dilution were pipetted on the solidified ATsoft agar, sealed airtight and incubated at 30°C overnight. The 3-oxo-C8-HSL concentration used for the ATsoft agar screening was increased compared to the determined threshold concentration. Consequently, the following screening was carried out with a 3-oxo-C8-HSL concentration of 4.1×10^{-6} mol/L.

7.2.2.2 Preparation of *E. coli* cosmid clone samples

Prior to preparation of ATsoft agar, *E. coli* cosmid clones (NGR234 genomic library) were cultivated in deep well plates as described in II.3.1.1.3. After incubation for 20 h at 37°C, 100 μ L culture from each well were transferred into a new, sterile 96-well plate and mixed with 100 μ L of the previously prepared 3-oxo-C8-HSL solution (4.1×10^{-6} mol/L in LB medium).

The 96-well plates were sealed airtight with PCR foil (Henze Laborbedarf, Elmshorn, Germany) and incubated 20 h at 28°C.

7.2.2.3 Screening procedure

Five µL of the cell-AHL mixture were pipetted on the solidified ATsoft agar and incubated at 30°C overnight without shaking. The 96-well plates were prepared in triplicate. Development of the blue color indicated an unimpaired QS activity and wells that remained colorless indicated possible QQ enzyme present on the cosmid clone. For a better development of possible blue wells, the plates were stored several hours at 4°C. All positive NGR234 cosmid clones were collected in a new 96-well plate.

7.3. Inhibition of swarming motility in *E. coli*

To narrow the number of cosmid clones tested positively in the ATsoft screening, the influence of these candidate clones on the QS-dependent swarming motility directly in their *E. coli* EPI100 and *E. coli* XL1 blue hosts was analyzed.

7.3.1 Swarming motility of *E. coli* in liquid medium

The determination of a modified swarming behavior was carried out in deep well plates followed by an incubation in 96-well plates equipped with a round bottom.

7.3.1.1 Preparation of liquid swarming medium

The basic medium was liquid LB medium supplemented with glucose and casamino acids. Both solutions were prepared as stocks, filtered sterile and added to the liquid LB medium after autoclaving.

LB with 2.5% (w/v) glucose was designated as LB-G

LB with 2.5% (w/v) glucose and 5% (w/v) casamino acids was designated as LB-G/C

7.3.1.2 Screening procedure

Candidate cosmid clones were cultivated in deep well plates as described in II.3.1.1.3 directly in their *E. coli* EPI100 or *E. coli* XL1 blue host. After incubation for 20 h at 37°C, three sterile deep well plates were filled with LB medium and the two above described media (LB-G, LB-G/C) and inoculated with a 5-10% aliquot of the pre-deep well culture. These plates

were sealed with permeable tissues and again incubated for 20 h at 37°C on a rotary shaker (350 rpm). Aliquots of 100 µL culture from each well were transferred to 96-well plates with a round bottom, sealed airtight with PCR foil and incubated at 28°C for 24 h and 48 h without shaking. Altered swarming motility was evaluated visually.

7.3.2 Swarming motility of *E. coli* on solid medium

Swarming motility assays on solid medium were carried out only with candidate cosmid clones which displayed an altered swarming motility in the previous test as this assay was established in Petri dishes. When the cosmid clones were present in EPI100 cells, they had to be transferred to *E. coli* XL1 blue cells.

7.3.2.1 Preparation of solid swarming medium

Soild swarming agar for *E. coli* was prepared from LB medium solidified with 0.4% Eiken agar. As supplements either nutrient broth (18 g/L), glucose (4 g/L) or a combination of both were used. Glucose was prepared as a stock solution, filtered sterile and added to swarming agar after autoclaving.

Swarming agar for *E. coli*

Tryptone	10 g
Yeast extract	5 g
NaCl	10 g
Eiken agar	4 g
H ₂ O _{bidest}	ad 1000 mL

7.3.2.2 Screening procedure

Selected cosmid clones were cultivated in 30 mL LB medium with ampicillin overnight at 37°C. The OD₆₀₀ was measured and aliquots corresponding to 1x10⁹ cells/mL were configured in sterile E-Cup and centrifuged shortly. The supernatant was pipetted off completely and the pellet was resuspended in 10 µL fresh LB medium. The agar plates were prepared and allowed to solidify under sterile conditions. Then, 1 µL of the cell suspension was pipetted on the center of each plate. Incubation was carried out at 30°C and 37°C for 20 h. Swarming behavior was evaluated visually according to the scheme given in VII.2.2 (Figure 29 in appendix).

7.4. Inhibition of motility in *P. aeruginosa* PAO1

For motility assays PAO1 was used as its motility like swarming and swimming or biofilm formation are QS-dependent.

7.4.1 Swarming and swimming motility in *P. aeruginosa* PAO1

7.4.1.1 Preparation of swarming/swimming agar for *P. aeruginosa* PAO1

For the determination of swarming/swimming motility of PAO1, the following solutions were prepared and combined according to Table 12.

Solution 1

Glucose 4 g
H₂O_{bidest} ad 100 mL

Solution 2

MgSO₄ x 7 H₂O 2 g
H₂O_{bidest} ad 100 mL

Solution 3

CaCl₂ x 2 H₂O 0.2 g
H₂O_{bidest} ad 100 mL

Solution 4a

Na₂HPO₄ 7 g
KH₂PO₄ 3 g
NaCl 0.5 g
H₂O_{bidest} ad 100 mL

Solution 4b

Na₂HPO₄ 7 g
KH₂PO₄ 3 g
NaCl 0.5 g
NH₄Cl 1 g
H₂O_{bidest} ad 100 mL

Solution 5

C₅H₈NNaO₄ x H₂O 5.5% (w/v)
H₂O_{bidest} ad 100 mL

The solutions were sterile filtered and stored at RT. For 100 mL of swarming or swimming medium, the following volumes were added to freshly autoclaved Eiken agar.

Table 12: Composition of 100 mL swarming and swimming agar

Constituent	Volumes [mL]	
	Swarming agar	Swimming agar
Solution 1	10	10
Solution 2	1	1
Solution 3	1	1
Solution 4a	10	-
Solution 4b	-	10
Solution 5	1	-
Eiken agar	0.5% in 77 mL	0.3% in 78 mL

7.4.1.2 Screening procedure

Selected cosmid clones were cultivated in 30 mL LB medium with ampicillin overnight at 37°C. Crude cell extracts from cosmid clones were established as described in II.6.2.1. When swarming and swimming tests were carried out with pure protein extracts, purification was done according to II.6.2.2. A preculture of PAO1 was necessary for the assay therefore, it was cultivated as described in II.3.1.5.

Either crude cell or protein extracts were added to the agar. Therefore, the swarming or swimming agar was prepared as described above, autoclaved and cooled to 40°C. Extracts were then added to the agar, gently vortexed and poured into Petri dishes. After 3 h at RT, the plates could be used for inoculation with PAO1.

Alternatively, extracts were spread over the surface of already solidified swarming or swimming agar. Plates were dried under sterile condition until the extracts were completely absorbed by the agar surface.

The prepared swarming or swimming agar plates supplemented with either crude cell or protein extract were inoculated with PAO1. Therefore, the OD₆₀₀ was measured and an aliquot corresponding to an OD₆₀₀ of 1 was configured from the preculture in a sterile E-Cup. The cells were harvested, the supernatant was pipetted off and cells were resuspended in 10 µL fresh LB medium. One µL of the PAO1 cell suspension was pipetted exactly in the center of each swarming or swimming agar plate and the plates were incubated at 37°C for 16 h. Swarming behavior was evaluated visually according to scheme given in VII.2.2 (Figure 29 in appendix).

7.4.2 Biofilm inhibition assay with *P. aeruginosa* PAO1

Further motility tests on glass surfaces of test tubes were measuring the capability of PAO1 to form biofilms and the ability of selected cosmid clones or purified proteins to inhibit the biofilm formation of PAO1.

Therefore, a preculture of PAO1 was cultivated as described in II.3.1.5. The test tubes were filled with 5 mL liquid LB medium and supplemented with either crude cell extracts or protein extracts in varying concentrations. The supplemented test tubes were inoculated with a 5% aliquot of the PAO1 preculture and incubated at 37°C, 140 rpm for 16 h. Biofilm formation or inhibition was monitored visually.

7.5. Pigment inhibition assays with *C. violaceum* ChV2 and CV026

Two different assays were carried out in this study to analyze the effect of putative cosmid clones or protein extracts on the production of violacein associated with *C. violaceum* ChV2 and CV026. Strain ChV2 does not require AHLs in the medium for the production of violacein. Assays employed with strain CV026 required the addition of 3-oxo-C6-HSL. When AHLs are absent in the medium, due to degradation by putative QQ active cosmid clones, the medium becomes white otherwise it turns to purple.

7.5.1 Pigment inhibition of solid YDC medium with ChV2

A preculture of ChV2 was cultivated on solid YDC agar as described in II.3.1.4. Little cell material was resuspended in 500 µL sterile LB medium. Then, 2 µL of the cell mixture were added to crude cell extracts as well as protein extracts and to buffer controls. These samples were plated on YDC agar plates and incubated at 30°C up to 48 h. The production or inhibition of the pigment violacein was determined visually.

7.5.2 Pigment inhibition in liquid medium with ChV2 and CV026

A preculture of ChV2 was cultivated in LB medium as described in II.3.1.4. Fresh LB medium was inoculated with 0.1%, 0.5% and 1% aliquots of the ChV2 preculture and 50 µL of each suspension were filled into the wells of a 96-well plate. Different volumes of crude cell extracts and buffer controls were added to the ChV2 suspensions. The 96-well plates were sealed airtight and incubated overnight at 30°C. When AHLs were absent in the medium or were degraded by putative QQ active cosmid clones, the medium became white, otherwise it

turned to purple. For assays with CV026, a preculture was cultivated in LB medium as described for ChV2. To turn on violacein production, 0.1 μM 3-oxo-C6-HSL had to be present in the medium. For the inhibition assay, 500 μL of crude cell extracts of constructs or cosmids were mixed with five μL of 3-oxo-C6-HSL (0.1 mM) and incubated for 3 h. Then fresh LB medium was inoculated with a 1% aliquot of the CV026 preculture supplemented with the crude extract-HSL mixture and again incubated overnight at 30°C.

7.6. Enzyme activity assays

To quantify the QQ ability of identified cosmid clones or proteins, different enzyme activity assays were employed in this study. The tests were based on the degradation of substrates by QQ active clones which were necessary for a visible/measurable reaction.

7.6.1 β -Galactosidase activity assay using reporter strain *A. tumefaciens* NTL4

ONPG (*ortho*-nitrophenyl- β -D-galactopyranoside, Karl Roth GmbH, Karlsruhe, Germany) was used to determine the presence or absence of the enzyme β -galactosidase in solutions which is released in the presence of AHLs in the strain NTL4. The β -galactosidase hydrolyses lactose to form galactose and glucose. If β -galactosidase is present, the colorless ONPG, which has a similar structure to lactose, is cleaved into galactose and *ortho*-nitrophenol, a yellow compound which can be measured at a wavelength of 420 nm. This hydrolytic cleavage of ONPG was used for liquid assays to monitor the increasing or decreasing levels of β -galactosidase which correspond to AHL levels.

Prior to the main assay, the required 3-oxo-C8-HSL concentration had to be determined. Therefore, five μL of different dilutions of 3-oxo-C8-HSL (4.1×10^{-1} to 4.1×10^{-12} M) were added to 100 μL potassium phosphate buffer (100 mM). These mixtures were then added to five mL of AT medium containing 10^7 cells/mL of freshly grown NTL4 (obtained from a preculture cultivated as described in II.3.1.3). The test tubes were incubated for 30 h at 30°C and subjected to the main assay, given below. The required concentration of 3-oxo-C8-HSL was detected to be 4.1×10^{-8} mol/L.

For the analysis of putative proteins, five μL of a 4.1×10^{-8} M solution of 3-oxo-C8-HSL were added to 1-100 μL purified protein extracts (400 $\mu\text{g}/\text{mL}$) and incubated for 1.5 h at 30°C in 100 potassium phosphate buffer (100 mM, pH 7.0-7.5). Then, the AHL-protein mixture was added to five mL of a freshly grown NTL4 culture in AT medium, where the cells were adjusted to 1×10^7 cells/mL prior to the assay. After incubation at 30°C for 17 h, the cell density was measured at OD_{600} . Then one mL of the cell suspension was mixed with 20 μL

toluene and vortexed for 3 min. After transferring 800 μL of the lower layer into a new E-Cup, 200 μL of the ONPG solution (4 mg/mL ONPG in Z-buffer) were added. After incubation for 20 min at RT the reaction was stopped by adding 400 μL of a 1 M Na_2CO_3 solution, then the mixture was centrifuged for 2 min at 13000 rpm. The absorbance of the resulting upper layer was measured at 420 nm with a SmartSpec™ Plus Spectrometer (Bio-Rad Laboratories, Munich, Germany).

Z-buffer

$\text{Na}_2\text{HPO}_4 \times 7 \text{ H}_2\text{O}$	16.1 g
$\text{NaH}_2\text{PO}_4 \times 7 \text{ H}_2\text{O}$	5.5 g
KCl	0.75 g
$\text{MgSO}_4 \times 7 \text{ H}_2\text{O}$	0.246 g
β -mercaptoethanol	2.7 mL
$\text{H}_2\text{O}_{\text{bidest}}$	ad 1000 mL
pH 7.0 (storage at 4°C)	

7.6.2 Pyocyanine assay

The blue compound pyocyanine produced by PAO1 in cultures is also regulated by QS-dependent processes and is subordinated to biofilm formation. In the absence of QQ active compounds in PAO1 cultures, the blue compound is produced which is why cultures appear to be green. By extraction with chloroform this compound gives a strong blue color, while inhibited production of pyocyanine results in colorless or pale blue extracts.

The pyocyanine assay was carried out as already described in the biofilm inhibition assay. A preculture of PAO1 was cultivated, test tubes were filled with five mL LB medium and supplemented with either crude cell extracts or protein extracts in varying concentrations. The supplemented test tubes were inoculated with a 5% aliquot of the preculture and incubated at 30°C, 140 rpm for 16 h. Then, two mL of these cultures were extracted with the same volume of ice cold chloroform, by vortexing for 5 min at highest speed. The color of extracts was evaluated visually.

7.6.3 Degradation of β -lactam antibiotics

To verify a β -lactamase degrading activity for the identified protein, a test with different β -lactam antibiotics was carried out. The candidate protein was cloned into pET24c expression vector and transformed into *E. coli* BL21 (DE3) cells. To ensure a good expression of the gene, the construct was cultivated in its *E. coli* host overnight. Then 200 μ L were plated onto LB agar containing 100 μ M IPTG with/without kanamycin 50 μ g/mL, covering the whole surface. Small filter discs (Oxoid, Basingstoke, England) with different β -lactam antibiotics and concentrations were placed on the agar surface and incubated overnight at 37°C. The size of inhibition halos was measured.

8. HPLC analysis

HPLC-MS-DAD (high performance liquid chromatography-mass spectrometry-diode array detector) analysis was established in cooperation with the Institute for Organic Chemistry at the University of Tuebingen. The HPLC analysis was employed to reveal the underlying mechanism of AHL degradation of two possible QQ active proteins. Sample preparation as well as the incubation with AHLs was done in our lab. The chemical analysis was carried out in the lab of Dr. S. Grond (University of Tuebingen, Germany).

8.1. Preparation of protein samples

The sample preparation as well as the analysis were done as previously published in Bijtenhoorn *et al.* 2011 and Schipper *et al.* 2009 with minor modifications. For the chemical analysis a 10.5 mM 3-oxo-C8-HSL stock solution was prepared in DMSO (corresponding to 0.2 mg of 3-oxo-C8-HSL/ μ L DMSO). The protein extracts were obtained as described previously (II.6.2). Different protein amounts were mixed with 20 μ L of the 3-oxo-C8-HSL stock solution in 100 mM potassium phosphate buffer. After incubation for 20 h at 30°C the mixtures were extracted twice with one volume ice cold ethyl acetate and obtained extract were combined, sealed airtight and send to Tuebingen for analysis.

8.2. Detection of cleavage products by HPLC-MS-DAD analysis

For HPLC analysis each extract was dissolved in 110 μ L methanol. HPLC-MS-DAD analysis of the solutions was performed using a Grom Supersphere 100 RP-18 endcapped column (4 μ m; 100x2 mm, Alltech Grom GmbH, Rottenburg-Hailfingen, Germany), a Flux instruments Rheos 4000 pump (HiTechTrader, Mount Holly, New York, USA), a PDA

detector Finnigan Surveyor and a mass spectrometer Finnigan LCQ (70 eV) with the software package Finnigan Xcalibur (Thermo Finnigan LLC, San Jose, California, USA). A gradient program with solvent A (0.05% aqueous HCOOH) and B (0.05% HCOOH in MeOH) was used to detect the 3-oxo-C8-HSL and the cleaved product (retention times 8.6 min and 7.9 min, respectively): gradient from 20% B to 100% B in solvent A in 20 min, 10 min 100% B to 20% B in 2 min, 8 min 20% B (total: 40 min program) at a flow rate of 300 μ L/min. HPLC-MS-Tandem mass analyses were recorded on a Finnigan LCQ spectrometer (impact energy 25%); high-resolution mass spectra (electrospray ionization [ESI]) on a Bruker APEX-Q 7T IV spectrometer (Bruker BioSciences Corp, Billerica, Massachusetts, USA); preselected ion peak matching at a resolution (R) of $\gg 10000$ were within 2 ppm of the exact masses. *N*-(3-oxooctanoyl)-L-homoserine was synthesized by chemical hydrolysis of the corresponding acyl-homoserine lactone (5.8 mg) in 60 μ L dimethyl sulfoxide with 1 N NaOH (1.5 equivalents, 36 μ L) for 16 h at RT (Dong *et al.* 2001).

9. Rhizobial colonization experiments

To analyze the importance of the putative AHL degrading proteins for the plant rhizosphere colonization, extra copies of the two candidate proteins were clones into pBBR1MCS, transferred into NGR234 cells and colonization with cowpea roots was employed. Rhizosphere colonization tests were done as described by Streit *et al.* 1996.

9.1. Germination and inoculation of cowpea seeds

Cowpea seeds (*Vigna unguiculata* subs. *unguiculata*) were treated 15 min with 70% ethanol and rinsed three times with sterile H₂O_{bidest.}. The sterilized seeds were placed on 0.5x TY agar lacking CaCl₂ (II.2.1.4) and germinated at 30°C. After 18 h, germinating seeds with no visible contamination were transferred into sterile 50 mL falcon tubes filled with ~10 g autoclaved vermiculite and 5 mL 0.25x Hoagland solution (II.2.3.3). NGR234 inocula consisted of NGR234 cells harboring control plasmids or pBBR1MCS constructs. NGR234 inocula were grown in 250 mL YEM medium with appropriate antibiotics 3-4 days, cell densities were determined by OD₆₀₀ and adjusted in fresh medium to 10³ or 10⁵ cells/mL. A volume of 100 μ L of the bacterial suspensions was used to inoculate the germinated seedlings. Therefore, bacterial solutions of NGR234 carrying the control plasmid and the constructs were used in combination, mixed 1:1 before inoculation. For control purposes, NGR234 with the control plasmid as well as the constructs were inoculated separately. Falcon tubes with the inoculated seeds were incubated in a light and humidity controlled

incubator (Rumed Rubarth Apparate GmbH, Laatzen, Germany) under the following conditions: day/night, 24/19°C, 16/8 h, 50% relative humidity.

9.2. Cell harvesting and cell counts

The roots were harvested after 4 days of incubation, therefore roots were shaken to remove vermiculite, cutted into segments and placed in 1.5 mL E-Cups containing 1 mL of extraction buffer. Appropriate dilutions of the extraction mixture were plated on YEM agar plates containing congo red and the required antibiotics. Plates were incubated at 30°C for 5-7 days and cell numbers were recorded.

Extraction buffer

Tween 20	0.01%
H ₂ O _{bidest}	ad 100 mL

10. Sequence analysis of DNA

10.1. Sequencing of ORFs, plasmids and cosmids

The sequence analysis was used to verify the presence of correct insert/orientation/mutation as well as to obtain the location of cosmid clone inserts and transposons inserted into the genome. Automated sequencing was realized with an ABI 3730XL DNA Analyser (Applied Biosystems, Foster City, California, USA) based on the Sanger technique and accomplished at the group of Prof. R. Schmitz-Streit (University of Kiel, Germany). Sequence samples were purified with commercial kits (II.4.1.1) and adjusted to a concentration of 100 ng/μL for plasmid and 300 ng/μL for cosmid DNA in H₂O_{bidest}. Respective primers (Table 5) were adjusted to 4.8 μM. Three μL of DNA and 1 μL primer were sent separately packed.

10.2. Complete genome sequencing

The complete genome of *Rhizobium* sp. NGR234 was accomplished at the G2L laboratories of the University of Goettingen with PCR-based techniques as well as a single 454 sequencing run. For detailed information of sequencing see Schmeisser *et al.* 2009.

11. Software

Nucleotide as well as AA sequence evaluations and comparisons were accomplished using the listed databases and programs (predominantly publicly available).

11.1. Databases

BRENDA (Enzyme database)	http://www.brenda-enzymes.info/
EMBL-EBI (InterPro Scan)	http://www.ebi.ac.uk/embl/
ERGO (Database/annotation software)	Overbeek <i>et al.</i> 2003
ExpASY (Proteomics server)	http://expasy.org/
• UniProt (Swiss-Prot and TrEMBL)	http://www.uniprot.org/
• PROSITE (Protein domains)	http://expasy.org/prosite/
• SWISS-MODEL (Protein structure)	http://swissmodel.expasy.org/repository/
KEGG (Encyclopedia of genes/genomes)	http://www.genome.jp/kegg/
NCBI (Database)	http://www.ncbi.nlm.nih.gov/
• BLAST (Alignment tool)	http://blast.ncbi.nlm.nih.gov/Blast.cgi
• COG (Classification of proteins)	http://www.ncbi.nlm.nih.gov/COG/
• GenBank [®] (Sequence database)	http://www.ncbi.nlm.nih.gov/genbank/
RAST (Annotation server)	http://rast.nmpdr.org/
RCSB PDB (Protein data bank)	http://www.rcsb.org/pdb/explore.do
Signal IP (Signal peptide prediction)	http://www.cbs.dtu.dk/services/SignalP/

11.2. Programs

BioEdit

(Sequence alignment editor) <http://www.mbio.ncsu.edu/bioedit/bioedit.html>

Chromas Lite

(Process of chromatogram files) http://www.technelysium.com.au/chromas_lite.html

Clone Manager Suite 7

(Edition of sequence files) Sci-Ed Software (Licensed)

Quality One

(Gel documentation software) Bio-Rad Laboratories, Munich, Germany

GAP4 software package v4.5/v4.6

(DNA sequence edit/assembly) <http://staden.sourceforge.net/>

EndNote

(Literature) <http://www.endnote.com/> (Licensed)

III. Results

The scope of the present research was to investigate the inventory of QQ associated systems and enzymes comprised by the α -proteobacterium *Rhizobium* sp. NGR234, which was initiated by the completion of its genome sequence. Illuminating whole genome sequences of unique and ubiquitous microorganisms provides access to a large pool of sequence data for comparative genomics. Where functional based analyses fail to uncover single genes, gene operons or complex correlations responsible for certain processes, genome wide analyses answer these questions. The sequencing, closure and comparative analysis of the genome of unique microbe *Rhizobium* sp. NGR234 provided deeper insights into mechanisms involved in transport, secretion and communication revealing some puzzles of its broad host range (Schmeisser *et al.* 2009). Focusing on cell-to-cell communication in NGR234, the genome uncovered one novel QS system and a wealth of genes linked to degradation of AI-1 molecules. One main goal of the research was to employ a function-based approach to confirm these findings. Therefore, a NGR234 cosmid clone library was constructed and screened on cosmids conferring AHL degrading ability. This first approach combined with further motility assays and sequence analyses delivered five genes/loci involved in AHL degradation or modification. Two out of the five proteins were biochemically characterized in detail and subjected to HPLC-MS analysis in order to uncover the underlying cleaving mechanism. Comparing the sequential and functional results there is evidence that the genome of NGR234 comprises a high number of genes involved in QQ and that at least five genes are functional, interfering with QS systems of different biosensor strains. The detailed characterization of two genes, *dIhR* and *qsdR1*, proved that the megaplasmid of NGR234 encodes true lactonases not described in earlier studies (Krysciak *et al.* 2011).

1. Sequencing and complete genome analysis of *Rhizobium* sp. NGR234

Around 5,000 microbial genomes have been sequenced and completed according to the NCBI genome database (<http://www.ncbi.nlm.nih.gov/sites/genome>) but only twelve of the entries concern diverse rhizobia. With a large group of symbiotic partners, NGR234 is a suitable candidate organism for extraction of crucial sequence data to give first answers for its broad host range as well as specify secretion and communication pathways.

The sequencing project began with a shotgun library and assembling of overlapping sets of cosmids. This first sequencing approach led to the elucidation of the symbiotic plasmid

(pNGR234a) which was published in 1997 (Freiberg *et al.* 1997). Some genetic snapshots of the genome became available by shotgun sequencing of the derivative strain of NGR234, *Rhizobium* sp. ANU265, which is cured of pNGR234a (Viprey *et al.* 2000). The available sequence data set of an ordered cosmid library forced the assembly of larger sections of the pNGR234b by Streit and colleagues in 2004 (Streit *et al.* 2004).

The completion of the whole genome of NGR234 in 2009 with over 100 gaps was initiated by PCR-based techniques using the shotgun library and the ordered cosmid library. To facilitate the gap closure, pyrosequencing was employed. A single 454 sequencing run generated 110 Mbp of raw data. All available contigs were assembled to close the remaining gaps. Polishing as well as necessary editing of the sequence was accomplished with the Gap4 software. The prediction of coding sequences (CDS) and open reading frames (ORFs) was done by the aid of ORF finders Glimmer, Critica and Z-values (Schmeisser *et al.* 2009). The annotation of the whole genome was carried out in ERGO and was based on comparison of CDSs with publicly available databases like EMBL-EBI, ExPASy, GenBank, KEGG and NCBI.

1.1. General features and highlights hidden in the genome of the NGR234

The genome of NGR234 has an overall size of 6,891,900 bp and is composed of three replicons depicted in the following Figure 4. The chromosome (cNGR234) totals to 3,925,702 bp with an average G+C content of 62.8%. This replicon encodes for 3,633 ORFs and comprises most of the essential genes of NGR234. Major genes of catabolic and metabolic functions like the Entner-Doudoroff pathway, genes associated with the degradation of larger polymers as well as genes linked to the biosynthesis of cobalamin and riboflavin were found on the cNGR234. The megaplasmid pNGR234b with 2,430,033 bp has a G+C content of 62.3% and comprises 2,342 ORFs. This replicon carries relatively few genes that encode for essential functions like the cofactor pathways and fatty acid synthesis. In contrast, pNGR234b carries most genes associated with polysaccharide synthesis and 50% of all transporters present on the NGR234 genome, making the replicon of great importance for growth and survival under different environmental conditions. The smallest replicon pNGR234a is 536,165 bp in size and has comparatively a lower G+C content of 58.4%. This replicon carries important genes for symbiosis, as discovered by heat curing experiments (Viprey *et al.* 2000), however the symbiotic plasmid does not comprise genes encoding for essential functions.

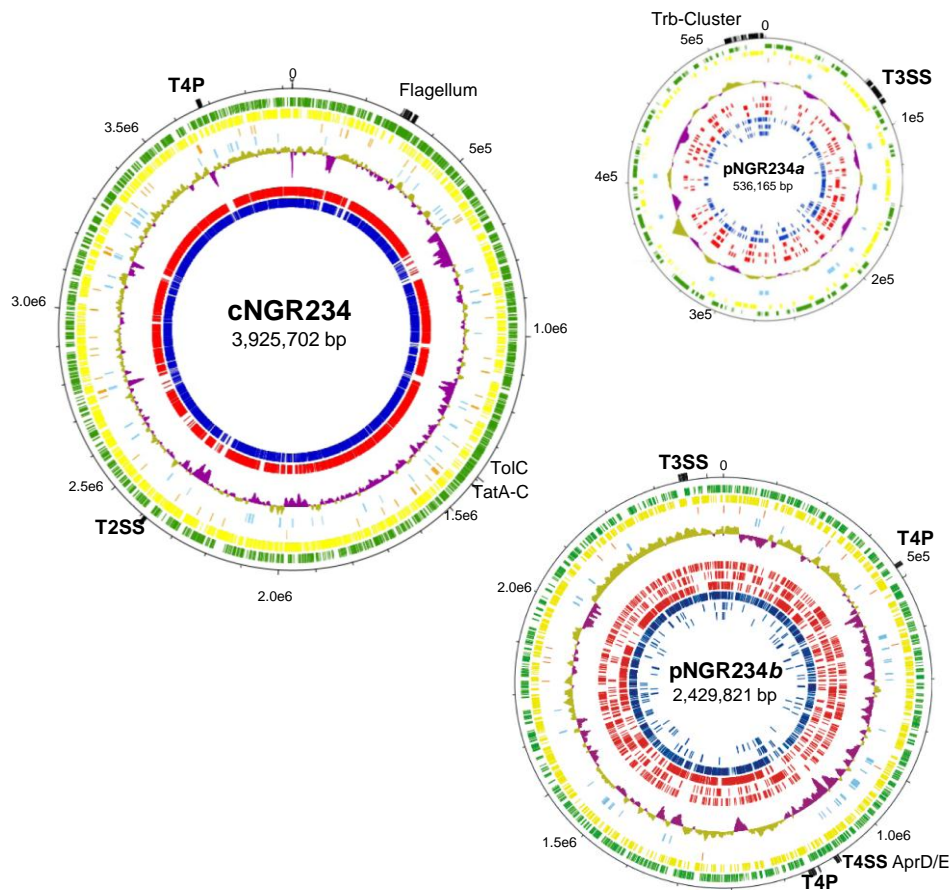


Figure 4: Map of the genome of *Rhizobium* sp. NGR234, displaying the chromosome (cNGR234), the megaplasmid (pNGR234b) and the sym plasmid (pNGR234a). Outer circle: Coordinates of selected genes. Second/third circle: ORFs on the leading and lagging strands. Next inner circle: sncRNAs (light red) followed by position of repeats (light blue). Next inner circle: G+C content (dark yellow and purple). The following innermost circles are described in detail in Schmeisser *et al.* 2009.

1.2. Diverse secretion systems are encoded by the 6.9 Mbp genome

Speculating on the correlation between the host range of NGR234 and the presence and number of genes associated or involved in the secretion apparatus comprised by this microbe, a detailed sequence and comparison analysis revealed surprising support. Table 13 summarizes genes and proteins comprised by NGR234 involved in the synthesis of secretion systems. Astonishing, NGR234 carries 132 genes spread over the three replicons which are associated with protein secretion and hereby portrays a unique plant microbe within the order of Rhizobiales.

Table 13: Genes/ORFs involved in synthesis of secretion systems in *Rhizobium* sp. NGR234

Secretion system	Number of ORFs/genes linked to secretion systems
Type I	
AprD/E	2
TolC	1
PrtD	1
PrtE, HlyD family	1
Type I secretion related protein	1
Type II	
General secretion pathway (Gsp)	13
Sec-pathway (Sec)	7
Type III (Hrp, Rhc)	
Rhc-pili	42
Type IV	
F-type (conjugation, Vir, Trb)	23
P-type (Flp and attachment)	35
Type V	
Autotransporter (Aut)	-
Type VI	
Type VI secretion protein	-
TAT (twin arginine)	
TatA/B/C	3
SRP	
Signal recognition particle	3
Total:	132

Different secretion apparatuses were reported to participate in interactions between plant-associated bacteria and their host. The genome of NGR234 revealed the presence of proteins involved in general and export pathways as well as a twin arginine translocase secretion system. This microbe also carries six type I transporter genes, one functional and one putative type III system, three type IV attachment systems as well as two putative type IV conjugation pili. No type V and VI transporters were found in the genome. Compared to NGR234, *S. meliloti* and *R. leguminosarum* comprise less than half of the 132 proteins involved in secretion processes.

1.3. Cell-to-cell communication apparatus comprised by NGR234

Establishing a symbiosis between nitrogen-fixing rhizobia and their legume host requires a complex signaling network, which is still poorly understood. Certainly, rhizobial cells have to concentrate in and around plant root hairs as well as in nodules in order to undergo a successful symbiotic interaction with the host plant. The increase of cell density is mediated by the exchange of signals. Among *Rhizobiaceae*, the QS system, induced by AHLs, is

prevalent as signal communication. The ability of NGR234 to nodulate over 120 plant genera and one non-legume raised the question of presence and absence of such QS systems, their number and their similarity to already published systems.

1.3.1 AHL-mediated cell-to-cell communication present in NGR234

A previous work of He and colleagues already described the *Tral/TraR* QS system in NGR234 (Figure 1) sharing similarities with its counterparts on the Ti plasmid of *A. tumefaciens* (He *et al.* 2003). Beside regions encoding for plasmid replication and conjugal transfer, the QS regulators *tral*, *traR*, and *traM* can be found on pNGR234a, all orthologous of *A. tumefaciens*. The investigation of He and coworkers revealed that *tral* mutants of NGR234 or strain ANU265 (cured of pNGR234a) still produce low levels of a compound related to 3-oxo-C8-HSL along with another more hydrophobic compound, suggesting that additional AHL synthases and also possible LuxR-like proteins might be present elsewhere on the genome.

The sequenced genome of NGR234 provided access to data answering the raised question of novel communication systems. The first attempt of comparison was accomplished with NGR234's own *tral/R* genes, continuing with publicly available QS systems of *V. harveyi* (LuxI/R), *A. tumefaciens* (Tral/R), *S. meliloti* (SinI/R), *Burkholderia cepacia* (Cvil/R) and *R. etli* (Rail/R). The obtained data set uncovered the presence of a chromosome borne QS system, designated as NgrI/R, where the *luxI* homolog *ngrI* possibly encodes a novel type of AHL synthase and *luxR* homolog *ngrR* displays its possible regulator. Figure 5 displays the uncovered cell-to-cell communication systems of NGR234. However, the direct comparison of both reveals an inverted order of synthases and regulators. The alignment with the SinI/R system comprised by *S. meliloti* SM1021 and the CinI/R system of *R. leguminosarum* (AF210630) uncovered an adjacent small hypothetical protein (NGR_c16910) also possibly linked to QS. The orientation of the NgrI/R system with NGR_c16910 present on cNGR234 is similar to CinI/R and adjacent CinS in *R. leguminosarum*.

Beside *Tral/R* homologous on pNGR234a and the novel *NgrI/R* system on cNGR234, additional copies of LuxR-type regulators were found on both replicons. Collectively, five response regulators featuring an autoinducer binding domain similar to those found on *TraR* and *NgrR* were identified (NGR_a01900; NGR_a04090; NGR_c04390; NGR_c04400; NGR_c32870). No further AHL synthases could be detected which is in contrast to findings of He and colleagues who speculated about three synthases being responsible for the AHLs produced by NGR234.

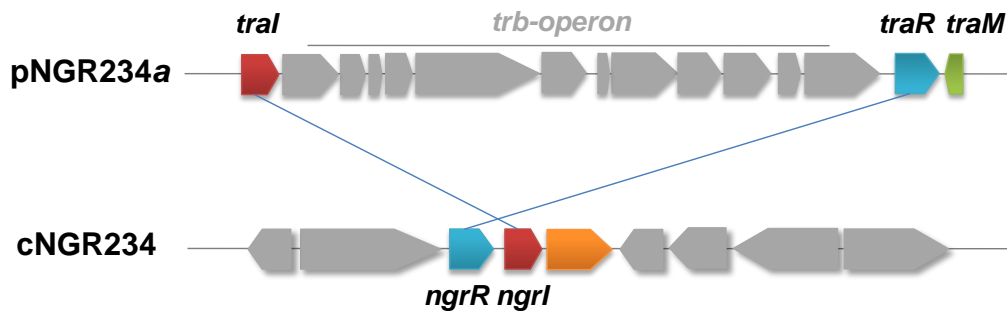


Figure 5: Conserved cluster of QS systems found in *Rhizobium* sp. NGR234. The AHL synthase (NGR_a04220, red) directs the synthesis of 3-oxo-C8-HSL which associates with the response regulator TraR (NGR_a04090, blue) and activates transcription. TraM (NGR_a04080, green) functions as a suppressor, preventing TraR from activating target genes under non inducing conditions. The *trb* genes (*trbB* to *trbI*, NGR_a04210 to NGR_a04100, shaded grey) are involved in the conjugal plasmid transfer. The additional QS system identified on the chromosome is composed of NgrI (NGR_c16900, red) and NgrR (NGR_c16890, blue) and the small hypothetical protein (NGR_c16910, orange) probably involved in QS.

1.3.2 The LuxS/AI-2 signaling system in NGR234

In mixed populations, microorganisms sense themselves by AHL-type molecules and respectively coordinate their behavior. It seems likely that in such populations bacteria also need mechanisms to detect the presence of other species. The evidence of the existence of signals used for interspecies cell-to-cell communication was provided by studies on *V. harveyi* (Bassler *et al.* 1994). Available sequences of the all members of the *V. harveyi* AI-2 QS circuit were used for alignments with NGR234. A gene weakly similar to the first AI-2 binding protein, LuxP (building a complex with AI-2) was identified on pNGR234b, however an E-value of only $3e^{-5}$ (NGR_b22070) lead to rejection of the gene as a positive hit. Several orthologous were uncovered in the genome of NGR234 for the second component of AI-2 recognition, the LuxQ hybrid sensor kinase (acceptor of the LuxP-AI-2 complex) with the best hit of E-value of $4e^{-54}$ for NGR_b14580. The signal information is further transduced to a complex phosphorelay system composed of the shared receptor LuxU and the subsequent LuxO, a response regulator protein. High similarities could be detected for LuxO (E-value $3e^{-75}$ for NGR_c28410) but no analogs of LuxU were found elsewhere. In addition, the genome of NGR234 did not reveal the AI-2 synthase LuxS, which would complete the LuxS/AI-2 circuit. In summary, NGR234 seems to lack the gene for the AI-2 synthase, but possesses several receptor proteins, possibly enabling NGR234 to respond to AI-2 supplied by other bacteria. These findings are in line with the research of Sun and colleagues in 2004 where comparative genomic and phylogenetic analyses of the AI-2 circuit revealed similar presence and absence of the key genes involved in the signaling cascade of detection of AI-2 (Sun *et al.* 2004).

1.3.3 The autoinducer 3 molecule based signaling system

AI-3 molecules are suggested to be aromatic compounds and probably involved in interspecies signaling not only limited to EHEC. The AI-3 as well as epinephrine and norepinephrine are sensed by two-component signal transduction systems composed of QseBC and QseEF together with the transcriptional factors QseA and QseD. Several hits for QseC ($3e^{-31}$; NGR_b20590) and QseE ($5e^{-87}$; NGR_b21890) were found within the NGR234 genome, which resemble response regulators. The sensor histidine kinases were also comprised by NGR234, QseB with $1e^{-46}$ (NGR_c07760) and QseF with $3e^{-21}$ (NGR_c07870). The transcriptional factors QseA (best hit: $3e^{-38}$; NGR_c29280) and QseD (best hit: $1e^{-10}$; NGR_c15650) were existing in many copies. These findings indicated on the first sight, that NGR234 comprises such an AI-3 based signaling system, nevertheless the sequential similarities have to be put into another perspective. Both transcriptional factors belong to the LysR family, which are found to regulate genes and complexes in diverse prokaryotes. LysR type transcriptional regulators may be the most common type of positive regulators in prokaryotes. Thus, it is not surprising that NGR234 carries at least 50 transcriptional regulators grouped to the LysR family. This conclusion can also be applied for the regulators and histidine kinases found within the genome of NGR234. Both enzymes are ubiquitous in prokaryotic organisms and spread in NGR234 as well. A quick look through the three replicons of NGR234 revealed at least 45 response regulators and 20 sensor histidine kinases most resembling two-component systems, all found by their annotated function.

Consequently, similarities to QseA and QseD as well as QseBC/QseEF may arise only from sequence similarities on the protein level but not from a true similarity to an AI-3 based signal system. Nevertheless, a support on the functional level of all components is absolute necessarily to confirm or even reject this speculation.

1.4. QQ mechanisms found in NGR234

Regarding the multiple enzymes and gene operons participating in cell-to-cell communication systems comprised by the genome of NGR234, it was hypothesized that this microbe might also have developed strategies to compete with other bacterial species for limited nutrient and energy resources by disrupting foreign cell-to-cell communication. To obtain global information about QQ associated genes and loci in NGR234, a detailed sequence alignment analysis was realized. The ERGO database was used to compare the genome of NGR234 to publicly available nucleotide and amino acid sequences of already characterized AHL degrading enzymes which are already summarized in Table 1 in the introduction (I.2.3.1). To assure a dataset of candidate genes as complete as possible, different conserved motifs

attributed to a QQ activity were also used for this alignment analysis. Overall, 23 putative QQ genes were identified on the megaplasmid and the chromosome of NGR234, none were found on the sym plasmid. Eighteen of these 23 putative genes were grouped to the AHLases, based on their common “HXHX~DH” motif or on their annotation indicating a possible enzymatic degradation of AHLs. The remaining five identified QQ genes could be grouped to AHL amidases. Surprisingly no oxidoreductases were uncovered by the alignment which might be due to the lack of published sequences within this group of AHL degrading enzymes. The predicted and annotated functions as well as existing conserved motifs of the putative QQ genes are depicted in Table 14.

Table 14: Possible QQ genes identified by alignment analyses with public databases

ORF ID	Possible and/or annotated function	Conserved motif	Size of protein (no. of AA)
NGR_c10650	metallo- β -lactamase family protein	HXHX~DH	556
NGR_b16870	putative metallo- β -lactamase family protein	HXHX~DH	321
NGR_b15850	metallo- β -lactamase family protein	HXHX~DH	312
NGR_b12260	metallo- β -lactamase family protein	HXHX~DH	277
NGR_c22830	putative β -lactamase family protein	HXHX~DH	214
NGR_c27960	metal-dependent hydrolase	-	280
NGR_c05660	metallo- β -lactamase family protein	HXHX~DH	304
NGR_c03760	metallo- β -lactamase family protein	HXHX~DH	383
NGR_c05950	putative β -lactamase family protein	HXHX~DH	254
NGR_c16020	metal-dependent hydrolase	HXHX~DH	279
NGR_c00430	putative metal-dependent hydrolase	-	174
NGR_c08460	metal-dependent phosphohydrolase	-	219
NGR_c06480	metal-dependent hydrolase	HXHX~DH	289
NGR_c32270	putative β -lactamase family protein	HXHX~DH	336
NGR_c17430	metallo- β -lactamase family protein	HXHX~DH	306
NGR_c10940	metal-dependent hydrolase	HXHX~DH	235
NGR_b22150	dienelactone hydrolase-like	GDSL	358
NGR_c03800	dienelactone hydrolase-like	-	292
NGR_c01920	metal-dependent amidase	-	390
NGR_c28580	putative amidohydrolase	-	479
NGR_c27330	putative amidohydrolase family protein	-	388
NGR_c18520	putative amidohydrolase	-	384
NGR_c33720	amidohydrolase 2	-	279

1.4.1 Putative QQ genes belonging to AHLases

Twelve of the putative QQ genes were grouped to metal-dependent hydrolases including seven proteins belonging to the metallo- β -lactamase family and three ORFs belonging to the putative β -lactamase family proteins. One ORF was annotated as a metal-dependent

phosphohydrolase, thus direct alignment was accomplished with the AHL degrading phosphotriesterase QsdA identified in *Rhodococcus erythropolis* W2 (Uroz *et al.* 2008), revealing no similarities. Altogether 13 of these proteins shared the “HXHX~DH” pattern which is found in several members of these metallohydrolases including metallo- β -lactamases, glyoxalases II, arylsulfatases and was proved to be essential for AHL degrading activity. Metal-dependent hydrolases belong to the best studied group of QQ enzymes acting on AHL-signaling molecules by hydrolysing the lactone ring in the homoserine moiety.

In addition to the putative QQ genes which could be clearly grouped to the metal-dependent hydrolases/AHLases, two diene lactone hydrolase-like proteins were found. The ORFs NGR_b22150 and NGR_c03800 do not provide sequential similarities to published QQ enzymes, but both comprise a predicted diene lactone hydrolase domain (COG0412/COG4188) allowing the speculation that these proteins might belong to the lactonases.

1.4.2 Five putative QQ genes can be possibly grouped to AHL amidases

Among the 23 identified QQ genes, five ORFs (NGR_c01920, NGR_c28580, NGR_c27330, NGR_c18520, and NGR_c33720) were related to amidases/amidohydrolases which were grouped to the amidases of AHL degrading enzymes. The NCBI BLAST sequence alignments revealed that these five ORFs hold conserved domains of the metal-dependent hydrolase superfamily, amidohydrolases or peptidase family proteins. This is in contrast to the published AHL amidases, which mostly share common characteristics of Ntn-hydrolases. However no intensive investigations were accomplished for the remaining published amidases, thus no conclusions in respect to other conserved domains attributed to an amidolytic pathway can be drawn. Only AiiO (Czajkowski *et al.* 2011) constitutes an exception with its similarity to the carboxylic ester hydrolases, but in this case no similarities were observed to this enzyme. Consequently, the insufficient analysed group of AHL amidases only offers a conserved domain originating from N-terminal nucleophilic hydrolases, no other speculations about further common motifs within the amidases were hypothesized to date. Nevertheless, the five identified putative QQ genes were added to the AHL amidases, based on their annotation. A rearrangement of these five ORFs to the group of AHL lactonases can not be excluded, but requires more detailed sequence information as well as functional data.

1.4.3 Other hydrolases related to QQ

Additionally, 14 genes and ORFs (VII.2.3, Table 18 in appendix) were identified that encode for possible hydrolases with no clear function assigned. The selection of these ORFs was exclusively based on the annotation as a hydrolase, because other hydrolases like AiiM from *Microbacterium testaceum* and AidH originating from *Ochrobactrum* sp. were already identified to have a QQ impact on different organisms. How far these 14 hydrolases can be taken into account as putative QQ genes remains unknown. More sequential and experimental data might group these ORFs to lactonases or amidases, but this has to be proven.

2. Genome wide functional analysis of genes/enzymes interfering with QS systems

The completion of the genome of NGR234 provided the access to a large pool of sequence data, revealing several remarking features hidden in the genetic information of this microbe. Especially, the surprisingly large number of candidate genes possibly involved in QQ processes raised the question of their functionality. To identify the active and functional genes and ORFs *in vitro* involved in QQ in NGR234, an already published screening (Schipper *et al.* 2009) was employed. Previously, a cosmid clone library of NGR234 had to be constructed and a combination of different screening procedures was conducted to obtain the most promising genes and ORFs.

2.1. Construction of a genomic NGR234 cosmid clone library

The cosmid clone library was generated using the pWEB-TNC Cosmid Cloning kit as described in material and methods (II.4.8). After establishing the end-repair reaction with the desired genomic DNA fragments, a ligation was accomplished using molar ratios of 10:1 and 5:1 (cosmid vector to dialyzed DNA fragments). As both ligation reactions worked well, both were packaged according to the provided protocol. Nevertheless, the efficiency of obtained cosmid clones generated by the transinfection of the 10:1 ligation into EPI100 cell was 2-fold increased. To determine the extent of the cosmid clone bank as well as its coverage of the NGR234 genome, several calculations had to be accomplished using the formula given in the manual.

The generated NGR234 cosmid clones comprised insert sizes ranging from 33-42 kb and had an experimentally determined insert rate of 95%. The calculation revealed that a

minimum of 600 clones had to be established within the library to reach the optimal number of clones (considering also empty clones). Consequently, a total of 603 cosmid clones was generated, ensuring a 95% probability of a given DNA sequence of NGR234 being contained within the library composed of 33-42 kb inserts. The constructed NGR234 cosmid clone library, when using the average insert size, covers at least 96.3% of the 6.9 Mbp NGR234 genome. Considering lower/upper limits of insert sizes, the overall coverage of the NGR234 genome ranges between 94.4% and 97.5%. The detailed calculation of all parameters is given in VII.2.4 in the appendix.

2.2. Function-based screening of the genomic library on AHL degrading ability

Functional verification of putative QQ genes/ORFs within the NGR234 library required the application of several subsequent screening procedures to reduce the number of positive candidate genes to the most promising ones. The number of 603 NGR234 cosmid clones could be narrowed to five functional clones capable of AHL degradation or modification by the following in detail described screening steps.

2.2.1 ATsoft screening procedure using *A. tumefaciens* NTL4

As described in the material and method section (II.7.2) this screening was used for the detection of an AHL degrading ability of cosmid clones directly in their *E. coli* host. The ATsoft screening combines the ability of NTL4 to sense AHLs and AHL degrading cosmid clones. When externally added AHLs are degraded by putative QQ active cosmids, the ATsoft agar remains white, otherwise it turns blue.

First, the screening procedure had to be adjusted and optimized to conditions required by the NGR234 cosmid library, the employed cosmid vector as well as the *E. coli* host to establish a successful screening. Therefore, several parameters were tested and changed prior to the screening: type of agar, solvent of AHL, incubation time and temperature and the detection threshold of AHL in this assay. In summary, Eiken agar in combination with incubation at 28°C for 20 h and 3-oxo-C8-HSL dilutions prepared in LB liquid medium from an ethyl acetate stock solution proved to be the best conditions. Further control experiments delivered the threshold concentration of 3-oxo-C8-HSL of 1×10^{-6} mol/L being suitable to be still detected by NTL4 in ATsoft agar. As described in material and methods (II.3.1.1.3) NGR234 cosmid clones were grown in deep well plates, mixed with 3-oxo-C8-HSL and pipetted on the solidified ATsoft agar. When after incubation (cosmid clones with AHLs) AHL was still

present, β -galactosidase was released and converted X-Gal (present in agar) into a blue dye. The medium remained white in the absence of AHLs.

The screening procedure was accomplished for all 603 NGR234 cosmid clones twice directly in their EPI100 host. In each run microtiter plates were tested in triplicates to assure a high coverage of putative positive cosmids. All wells which remained white were listed and transferred into a new 96-well microtiter plate (named: W-AHL). Wells displaying a bright blue color or a blue color with a small white halo were also counted as positive and collected in the W-AHL plate. An example of a positively tested cosmid clone is depicted in Figure 6A. In sum, 72 cosmid clones were counted as putative positive (corresponding to 12% of the cosmid library) and collected in the W-AHL plate. The microtiter plate was stored at -70°C for subsequent assays.

2.2.2 Inhibition of swarming motility in *E. coli*

To further limit the relatively high number of cosmid clones verified positive in the previous screening, motility assays in *E. coli* should decrease the candidate clones as motility like swarming and swimming are regulated by QS processes.

2.2.2.1 Screening for inhibition of swarming motility in *E. coli* EPI100

To determine a modified swarming behavior triggered by the cosmid clones directly in their EPI100 host, a swarming assay in *E. coli* was set up using different media and 96-well plates equipped with a round bottom. Candidate cosmid clones from the W-AHL plate were cultivated in the respective media (LB-G and LB-G/C) and further treated as described in material and methods (II.7.3). After incubation at 28°C for 24 h the swarming behavior of the candidate cosmid clones was determined. A cosmid clone tested negative in the previous screening served as a control. All 72 putative cosmid clones were tested at least in three runs each employed in triplicate. Cosmid clones displaying a deviant swarming behavior compared to the control cosmid were treated as a positive hit and were taken into account for further motility tests. An example of such a deviant swarming behavior in wells is depicted in Figure 6B. Collectively, 33 cosmid clones were selected as candidates for accomplishing further screening steps.

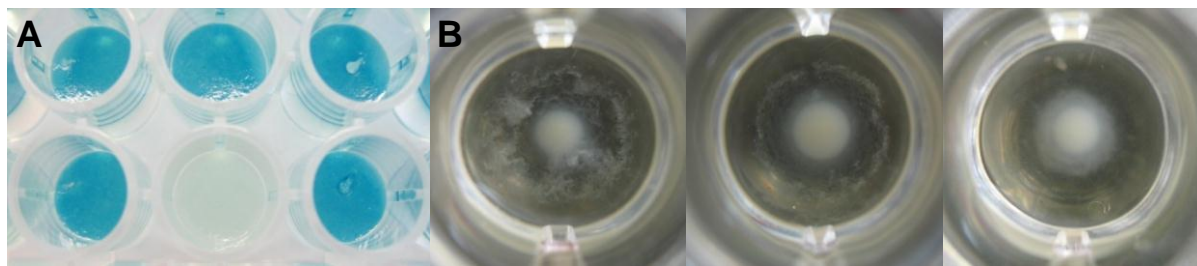


Figure 6: Examples of ATsoft screening procedure and swarming motility assay in *E. coli*. (A) Selected section of an ATsoft screening plate, displaying blue wells with cosmid clones that are not able to degrade 3-oxo-C8-HSL and a white well displaying a positive clone degrading 3-oxo-C8-HSL. (B) Motility assay displaying exemplary selected swarming behaviors. Left: Control (negative clone), Middle / Right: Cosmid clones revealing deviant swarming behavior in their EPI100 host.

2.2.2.2 Screening for inhibition of swarming motility in *E. coli* XL1 blue

The investigation of the swarming motility on solid medium was realized for the 33 candidate cosmid clones, which were previously detected. To assure a consistent swarming performance, the cosmid DNA of all 33 candidate clones was isolated and transferred via heat shock into *E. coli* XL1 blue cells. The clones in their new *E. coli* XL1 blue host were grown overnight at 37°C, aliquots of 1×10^9 cells/mL were configured and pipetted on solidified LB plates (prepared with Eiken agar). *E. coli* XL1 blue cells without a vector were used as a control. Different swarming appearances were observed for the cosmids, ranging from a complete inhibited swarming behavior (Figure 7B) to a modified, frayed appearing edge of the culture (Figure 7C). Figure 7 summarizes different observed appearances of cosmid cultures which were used for evaluation the QQ ability of the candidate clones.

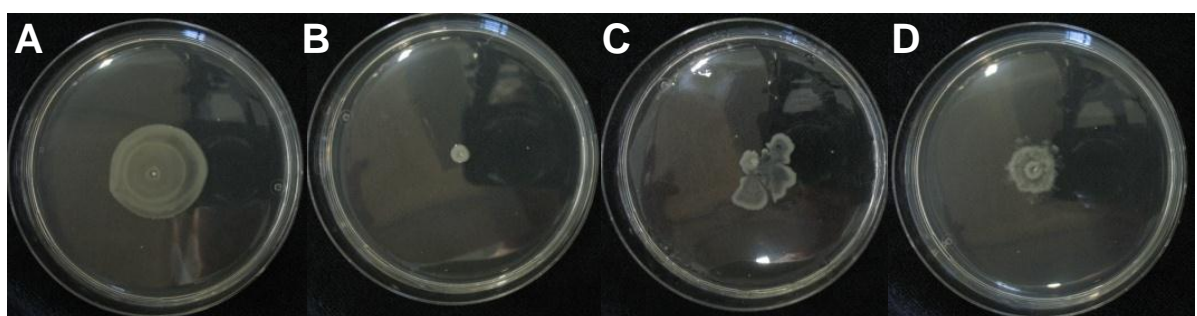


Figure 7: Swarming behavior of cosmid clones in *E. coli* XL1 blue cells on solid medium. (A) Control: *E. coli* XL1 blue cells without vector. (B-D) Examples of altered / inhibited swarming ability of *E. coli* XL1 blue conferred by cosmid clones.

Only ten out of the 33 cosmid clones reproducibly revealed an inhibition or modification of *E. coli* XL1 blue's swarming ability. This QQ ability of all ten clones could be reproduced in all media supplemented with either glucose, nutrient broth or in medium containing a

combination of both. However, best inhibition of *E. coli* XL1 blue swarming motility by the candidates was observed on solid LB medium supplemented with 1.8% glucose. The positions of the ten positively tested cosmids originating from the W-AHL plate are: A5, B2, B9, C2, C6, D9, D10, F9, F10 and G2. All subsequent specifications and details refer to this nomenclature originating from the W-AHL plate. For simplification purposes, the positions of the ten candidate clones were chosen as their designation. The resulting cosmids designated pWEB-TNC-A5, pWEB-TNC-B2, pWEB-TNC-B9, pWEB-TNC-C2, pWEB-TNC-C6, pWEB-TNC-D9, pWEB-TNC-D10, pWEB-TNC-F9, pWEB-TNC-F10 and pWEB-TNC-G2 were subjected to further motility assays in PAO1.

2.2.3 Inhibition of motility in *P. aeruginosa* PAO1

To further verify the influence of the isolated cosmids on QS-dependent processes in other Gram-negative bacteria, PAO1 motility assays were used, as motility like swarming and swimming or biofilm formation is QS-dependent in PAO1.

2.2.3.1 Inhibition of swarming motility in *P. aeruginosa* PAO1

To monitor a possible altered PAO1 motility phenotype triggered by positively tested cosmid clones, the following swarming motility assay was performed similar to the previous test. Crude cell extracts from cultures of *E. coli* XL1 blue cells harboring the cosmid clones were established as described in II.6.2.1. After preparation of PAO1 swarming plates, different amounts of cell crude extracts were spread over the agar surface and allowed to absorb. Then, 1×10^8 cells of an overnight PAO1 culture were applied on the middle of the agar and plates were incubated at 37°C for up to 24 h. Swarming ability of the PAO1 isolate was strongly altered after incubation with cosmid crude cell extracts. Only eight out of the ten clones could significantly reduce swarming motility of PAO1 and additionally alter the phenotype of the PAO1 isolate. The control which was *E. coli* XL1 blue carrying a randomly chosen, negatively tested pWEB-TNC cosmid was treated as the other cosmids. However, PAO1 was not affected in its swarming capabilities by the control. Figure 8A depicts the control and exemplary five cosmids displaying a conspicuous altered swarming motility of PAO1. Similar to motility tests in *E. coli* XL1 blue, appearance of PAO1 swarming halo triggered by added cosmid crude cell extracts was very diverse.

2.2.3.2 Biofilm inhibition in *P. aeruginosa* PAO1

Tests monitoring biofilm phenotypes of PAO1 caused by cosmid clones were accomplished in test tubes containing LB liquid medium supplemented with appropriate antibiotics and 1×10^8 cells of freshly grown PAO1. For this test, 5-100 µg of previously prepared crude cell

extracts of the eight cosmids were added to the inoculated test tubes and incubated at 37°C, 140 rpm for at least 16 h. Controls were either empty *E. coli* XL1 blue or XL1 blue carrying a randomly chosen, negatively tested cosmid. Visually evaluated biofilms on glass surfaces suggested that the crude cell extracts of the cosmids pWEB-TNC-A5, -B2, -B9, -C6 and -G2 influenced biofilm formation. In all test tubes supplemented with crude cells extracts from the five cosmid clones a less permanent biofilm formation was visible, no such effect was observed in the control tube (Figure 8B). Monitoring the biofilm formation ability of PAO1 by addition of different amounts of cosmid crude cell extracts resulted in the correlation: The higher the amount of added crude cell extract the less the biofilm forming capability. Collectively, pWEB-TNC-A5, -B2, -B9, -C6 and -G2 could reproducibly inhibit biofilm formation in PAO1. Figure 8B depicts on the left the *E. coli* XL1 blue control followed by the five cosmid clones inhibiting PAO1s ability to form a permanent biofilm in test tubes. Cosmids pWEB-TNC-B2 and -C6 could completely disrupt the biofilm, whereas pWEB-TNC-A5,-B9 and -G2 revealed a less developed biofilm compared to the control test tube.

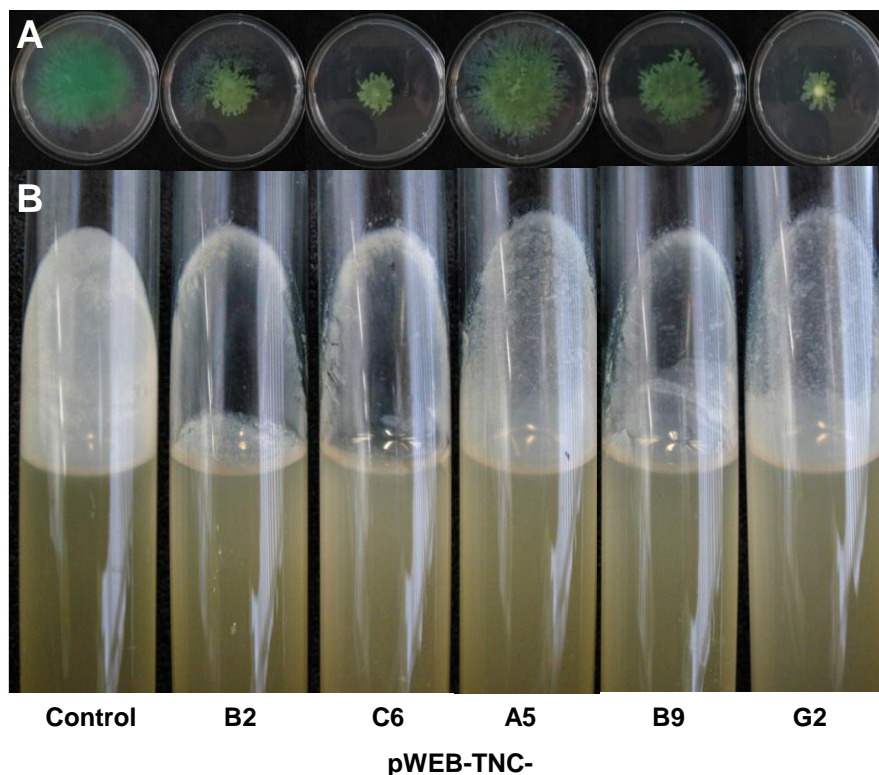


Figure 8: *P. aeruginosa* PAO1 motility and biofilm assays. (A) Altered swarming motility of PAO1 on swarming plates supplemented with crude cell extracts of cosmids pWEB-TNC-B2, -C6, -A5, -B9, and -G2. Plates were supplemented with 5-100 µg of crude cell extract of *E. coli* XL1 blue harboring the QQ cosmids. **(B)** Biofilm assays in test tubes filled with LB medium and supplemented with 5-100 µg of crude cell extracts of cosmid clones. All tubes were inoculated with PAO1. For overview purposes only one control was displayed.

3. Five functional NGR234 cosmid clones reveal AHL degradation or modification

The initial function-based screening procedure revealed after tests on ATsoft agar with *A. tumefaciens* NTL4 72 putative positive cosmids. The considerable cosmid clones had to be subjected to motility assays in *E. coli* and PAO1 in order to decrease the relatively high number to few candidates. Accumulated data from several repetitions of functional screenings identified five cosmid clones that consistently gave a positive result. All five clones reproducibly stayed colorless in the NTL4 assay and displayed a deviant phenotype in both motility assays compared to the negative controls.

Further screening steps demanded for localization of the candidates on the NGR234 genome sequence. Therefore, all five cosmid clones were end-sequenced with M13_for and T7 promoter primers (Table 5) and their positions were determined by comparison to the complete genome sequence of NGR234 in the ERGO database. The results are summarized in Table 15 highlighting their significant characteristics.

Table 15: Five candidate cosmid clones identified in this study with their properties and positions

Cosmid clone	Location	ORF ID	Coordinates [bp]	Insert size [bp]	No. of ORFs
pWEB-TNC-A5	cNGR234	NGR_c35340-NGR_c35730	3 752 569 – 3 793 031	40462	39
pWEB-TNC-B2	pNGR234b	NGR_b21920-NGR_b22210	2 252 689 – 2 286 730	34041	30
pWEB-TNC-B9	cNGR234	NGR_c15790-NGR_c16240	1 630 075 – 1 671 235	41160	45
pWEB-TNC-C6	pNGR234b	NGR_b16700-NGR_b17020	1 696 835 – 1 734 543	37708	33
pWEB-TNC-G2	cNGR234	NGR_c23130-NGR_c23380	2 397 554 – 2 430 912	33358	26

All clones carried inserts ranging from 33-42 kb, three of the cosmid clones were mapped on cNGR234 (i.e. pWEB-TNC-A5, -B9 and -G2) and two on pNGR234b (pWEB-TNC-B2 and -C6). The number of ORFs located on the respective cosmids ranged from 26 ORFs on pWEB-TNC-G2 up to 45 on pWEB-TNC-B9. Detailed listings of cosmid clones and their corresponding ORFs are given in the appendix (V.II.3). For functional detection of the respective ORFs involved in QS inhibition, different strategies were employed including *in vitro* transposon mutagenesis, subcloning, direct cloning and detailed sequence analyses. Therefore, the following results were subdivided into two sections. The first section concentrates on the identification of putative QQ active genes located on the chromosome and their first experimental verification of functionality. The second section concentrates on the two candidate genes located on the megaplasmid and their detailed functional and biochemical verification.

3.1. Chromosomal loci *hitR-hydR*, *qsdR2* and *aldR* appeared to be involved in QQ in *Rhizobium* sp. NGR234

To identify the genes responsible for the observed phenotypes in the specified bioassays, a detailed analysis of the insert sequences of these cosmid clones was combined with *in vitro* transposon mutagenesis and direct cloning. Altogether, these tests identified locus *hitR-hydR* on pWEB-TNC-A5, gene *qsdR2* on pWEB-TNC-B9 and gene *aldR* on pWEB-TNC-G2. Partial physical maps of the identified putative genes and their flanking regions are presented in Figure 9. The detailed sequential and experimental verification of these identified genes is described in the following.

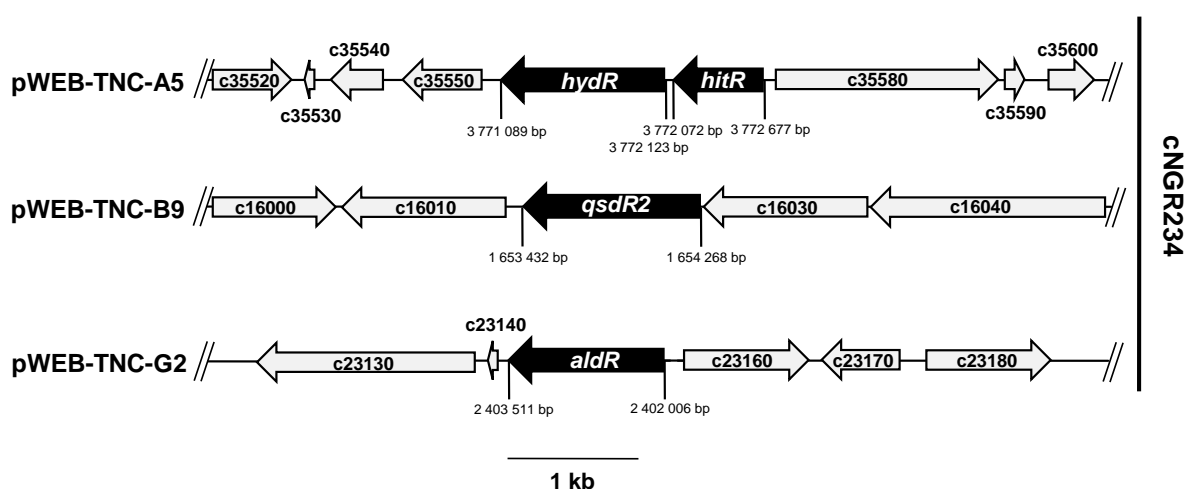


Figure 9: Identification of AHL-degrading cosmid clones on cNGR234. Partial maps of identified cosmid clones pWEB-TNC-A5, -B9 and -G2 carrying putative loci *hitR-hydR*, *qsdR2* and *aldR*. Black arrows indicate the ORFs that were involved in QQ, gray shaded arrows indicate flanking ORFs that were not linked to QQ phenotypes. ORFs were designated using ORF IDs from GenBank entries CP000874 and CP001389 (prefix NGR_~). The scale bar represents 1 kb.

3.1.1 Locus *hitR-hydR* reveals AHL-degrading or modifying ability

The QQ based impact of cosmid clone pWEB-TNC-A5 was verified in several bioassays described previously. The subsequent sequence analysis should uncover one candidate ORF being attributed to this QQ activity. Cosmid pWEB-TNC-A5 with its size of 40.5 kb comprised 39 ORFs. Beside genes with clear assigned functions, this cosmid clone contained several hypothetical proteins related to membranes and transport or harboring phospholipid-binding domains. Since the sequence approach revealed several considerable ORFs, *in vitro* transposon mutagenesis should deliver one definite candidate.

3.1.1.1 Construction of pWEB-TNC-A5 transposon mutant bank

Prior to construction of the mutant library, cosmid DNA was isolated by a commercial kit from an overnight culture of pWEB-TNC-A5 grown under given conditions. *In vitro* transposon mutagenesis was accomplished with EZ-Tn5™ <KAN-2> Insertion kit as described in the material and methods section (II.4.7). The reaction was carried out with 0.2 µg cosmid DNA of pWEB-TNC-A5 and a molar equivalent of the transposon. After heat shock transformation of *E. coli* XL1 blue with generated transposon mutants, the successful insertion was verified on LB agar supplemented with kanamycin. Collectively, 220 mutants could be obtained by the *in vitro* transposon mutagenesis which could be subjected to primarily motility assays.

3.1.1.2 Initial motility assays in *E. coli* XL1 blue and *P. aeruginosa* PAO1

Swarming motility triggered by transposon mutants of pWEB-TNC-A5 was monitored directly in *E. coli* XL1 blue as well as by addition of PAO1 cells. These tests were accomplished as already described in III.2.2.2 and III.2.2.3.1. Mutants harboring a transposon insertion in their QQ active ORF would restore the original *E. coli* XL1 blue and PAO1 phenotype of swarming behavior due to the disrupted activity. The transposon mutants were cultivated in their *E. coli* XL1 blue host and firstly subjected to swarming assays in liquid medium (II.7.3.1) giving 20 candidate clones. These 20 transposon mutants were secondly subjected to swarming assays on solid medium (II.7.3.2) where aliquots of 1×10^9 cells/mL (cosmid clones in *E. coli* XL1 blue) were pipetted on solidified LB plates (prepared with Eiken agar). For further PAO1 motility tests, crude cell extracts of these mutants were established and different concentrations (ranging from 0.1 to 10 mg/mL) were mixed with the PAO1 swarming agar. After solidification, 1×10^8 cells of an overnight PAO1 culture were applied on the middle of the agar and incubated under given conditions. In both assays, *E. coli* XL1 blue harboring pWEB-TNC-A5 served as a positive control and *E. coli* XL1 blue cells without a vector served as a negative control. Out of the 220 generated transposon mutants of pWEB-TNC-A5, nine mutants could restore the *E. coli* XL1 blue as well as the PAO1 phenotype of swarming behavior consequently, harboring a transposon insertion in a putative QQ ORF. While cosmid clone pWEB-TNC-A5 could significantly reduce swarming motility, the nine transposon mutants were able to recover the motility of *E. coli* XL1 blue and PAO1. Figure 10 displays results obtained from both motility assays. While images A/D display the negative controls and images B/E depict the positive control pWEB-TNC-A5, images C/F show exemplary a transposon mutant not impairing the motility of both hosts.

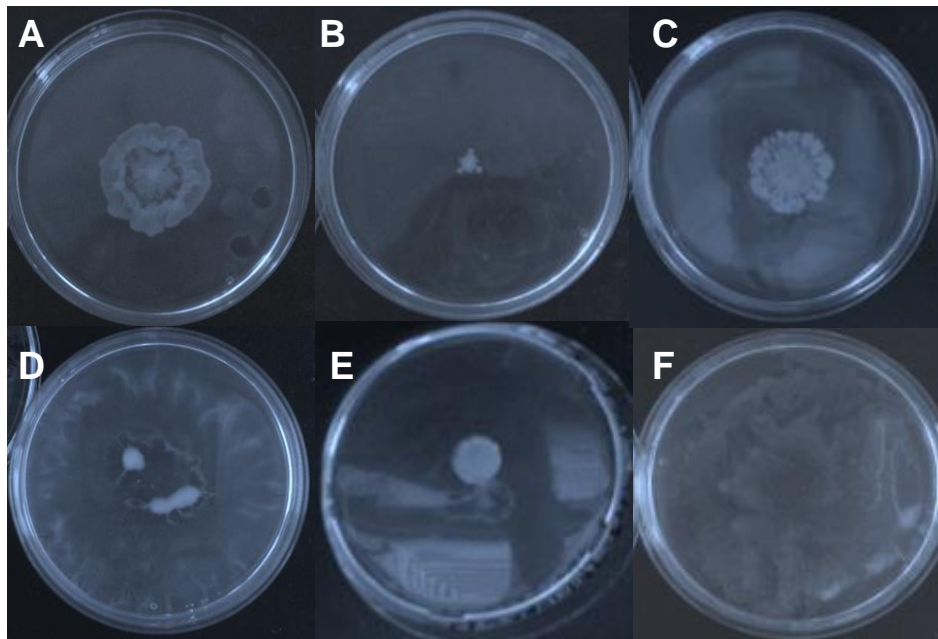


Figure 10: Motility assays accomplished with transposon mutants in *E. coli* XL1 blue and PAO1. (A) Negative control: *E. coli* XL1 blue cells without vector. (B) Positive control: *E. coli* XL1 blue harboring pWEB-TNC-A5. (C) Transposon mutant B10 in *E. coli* XL1 blue, exemplary. (D) Negative control: PAO1 cells. (E) Positive control: Crude cell extract of pWEB-TNC-A5 with PAO1. (F) Crude cell extract of transposon mutant F1 with PAO1, exemplary.

3.1.1.3 Identification of *hitR-hydR* locus by sequencing of conspicuous transposon mutants

Localization of transposon insertions of all nine mutants of pWEB-TNC-A5 was realized by bidirectional sequencing using transposon specific primers (KAN-2 FP-1 and KAN-2 RP-1 (Table 5), Epicentre Technologies, Madison, Wisconsin, USA). Only a few obtained sequences could be evaluated, indicating a transposon insertion within the first ORF of pWEB-TNC-A5 (NGR_c35340) but also insertions in the second antibiotic resistance gene (chloramphenicol) of pWEB-TNC were detected, making the sequencing results incompatible. Based on this data in combination with the first sequencing approach of pWEB-TNC-A5 for identification of the inserted NGR234 fragment, NGR_c35340 could be excluded as a positive QQ gene due to its incomplete sequence on the inserted NGR234 fragment. Consequently, the several hypothetical proteins were analysed in more detail using their DNA as well as the deduced amino acid sequence. Two ORFs draw the attention, NGR_c35570 encoding a putative histidine triad (HIT) protein revealing a similar HIT pattern as the QQ associated gene BpiB06 (Schipper 2009) and NGR_c35560 encoded for a predicted NUDIX hydrolase with no similarities to published QQ related hydrolases. Both genes were sequentially overlapping, thus it was considered that both proteins might be attributed to pWEB-TNC-A5's QQ activity and pursued the strategy of an operon. Therefore, both proteins designated as the *hitR-hydR* locus were treated as one ORF and subjected to

functional tests and additionally were cloned and tested separately. First, both ORFs were subjected to a detailed sequence analysis.

3.1.1.4 Sequence analysis of locus *hitR-hydR*

The ORF NGR_c35570 encodes for a **h**istidine **t**riad protein from *Rhizobium* sp. NGR234 (referred to as *hitR*) which is 609 bp in size. Prior to the predicted start codon of *hitR*, a putative ribosome binding site was identified (AGGACG, 6 bp upstream of GTG) being well conserved. Gene *hitR* is also preceeded by a possible promoter sequence, however -10 and -35 positions were found to be linked by a 20 nt region instead of 17 nt (MacLellan *et al.* 2006). The HitR protein (203 AA) was found by NCBI BLAST to be highly similar to homologous proteins in *S. meliloti* SM1021 (E-value $1e^{-104}$). The deduced amino acid sequence of HitR revealed a C-terminal HIT-like domain, named for the motif which is related to the sequence "HXHXHX" of histidine triad (HIT) proteins. This pattern is highly conserved in a variety of organisms and is associated with a zinc-binding site. HIT proteins are a superfamily of nucleotide hydrolases and transferases that act on the α -phosphate of ribonucleotides (Seraphin 1992).

The predicted NUDIX **h**ydrolase originating from *Rhizobium* sp. NGR234 (referred to as *hydR*) is encoded by ORF NGR_c35560. Sequentially, genes *hydR* and *hitR* were overlapping with 55 bp, thus a clear ribosome binding site as well as a promoter sequence could not be identified. Nevertheless, some sections were partially matching to predicted promoter sequences. HydR with a deduced AA size of 346 had the highest similarity to a NUDIX hydrolase of *S. medicae* WSM419 and *S. meliloti* SM1021 with E-values of 0.0. In nature, NUDIX hydrolases catalyze the hydrolysis of nucleoside diphosphates (NUDI) linked to other moieties (X). These enzymes carry a highly conserved structural motif that functions as a catalytic and metal binding site thus requiring a divalent cation for their activity. HydR comprises a N-terminal NADH pyrophosphatase-like NUDIX domain and a C-terminal NADH pyrophosphatase domain, NADH pyrophosphatases constitute members of NUDIX hydrolases. A zinc ribbon domain is found between both domains and the structural motif (active/metal binding site) could be mapped by the NCBI BLAST search.

Although there is no experimental evidence, it is highly possible that *hitR* and *hydR* genes form an operon due to their overlapping sequences. Surprisingly, the detailed sequence analysis of both genes did not reveal any significant similarities to known and published QQ related hydrolases.

3.1.1.5 Direct cloning and initial screening of the QQ active *hitR-hydR* locus

Treating *hitR* and *hydR* as an operon, a primer pair was designed to amplify both proteins as one amplicon. The PCR reaction was employed with *Taq* polymerase, genomic DNA from NGR234 and the primer pair *hitR-hydR_for/hitR-hydR_rev* (Table 5). The obtained ~1.8 kb PCR product was cloned into the pDrive vector and transformed into *E. coli* XL1 blue cells. In parallel, gene *hitR* was amplified under the same conditions using the *hitR_for/hitR_rev* primer pair (Table 5), resulting in a 770 bp fragment. Gene *hydR* was amplified using the primer pair *hydR_for/hydR_rev* resulting in a ~1.3 kb fragment. Both separated genes were cloned into the pDrive vector and transformed into *E. coli* XL1 blue cells. After verification of the correct insert sizes and their orientation, these three constructs (pDrive::*hitR-hydR*, pDrive::*hitR*, pDrive::*hydR*) were subjected to different functional screenings in order to determine the gene responsible for QQ activity.

3.1.1.6 Functional verification of locus *hitR-hydR*

First motility assays with construct pDrive::*hitR-hydR* (carried out as described previously) in *E. coli* XL1 blue and with PAO1 revealed a considerable inhibition of the swarming behavior. Based on the active *hitR-hydR* operon, the further AHL degradation assays were accomplished only with constructs pDrive::*hitR* and pDrive::*hydR*.

The β -galactosidase assay was employed to quantify the QQ ability of HitR and HydR proteins, where hydrolytic cleavage of ONPG substrate was used to monitor the level of AHL degradation. Crude cell extracts of the pDrive::*hitR* and pDrive::*hydR* constructs were prepared as described in II.6.2.1. Crude cell extracts corresponding to 1.3 mg/mL of total protein content were mixed with 5 μ L 3-oxo-C8-HSL (4.1×10^{-8} M) and the ONPG enzyme assay was then accomplished as described in II.7.6.1. The ratio of cell density at OD₆₀₀ to absorbance at 420 nm was calculated to compare the levels of AHL detection and to configure the bar chart. Collectively, after this short incubation time both constructs displayed a significantly lower level of detected AHLs compared to the buffer controls. These results are summarized in Figure 11A given below. In average less than 48% of the added 3-oxo-C8-HSL could be measured for pDrive::*hitR*. The β -galactosidase assay employed with crude cell extract of pDrive::*hydR* revealed an even slightly increased 3-oxo-C8-HSL degradation. In general, 45% of the added AHLs could be detected after incubation. In summary, the ONPG based screening confirmed the ability of HitR and HydR to degrade AHLs, whereas both displayed a very effective degradation rate of more than 50% of 3-oxo-C8-HSL.

A second AHL degradation assay was accomplished to confirm these findings. The pigment inhibition assay combining crude cell extracts, HSL and a culture of *C. violaceum* CV026 was employed. The *Chromobacterium* mutant CV026 only produces the purple pigment violacein in the presence of 3-oxo-C6-HSL. Therefore, freshly inoculated cultures of CV026 were supplemented with 5 μ L 3-oxo-C6-HSL (100 μ M) and 500 μ L of obtained crude cell extracts of pDrive::*hitR* and pDrive::*hydR* (corresponding to \sim 1.3 mg/mL protein content). Volumes of 200 μ L of the overnight cultures were extracted with butanole and the absorbance was measured. The ratio of cell density at OD₆₆₀ and absorbance at 585 nm was calculated to compare the levels of 3-oxo-C6-HSL degradation. Figure 11B summarizes the results obtained in the violacein inhibition assay. Both proteins could significantly inhibit the production of violacein in CV026 compared to the buffer controls. A good AHL degradation rate of 49% could be measured for pDrive::*hydR*. The assay employed with crude cell extract of pDrive::*hitR* revealed an even more pronounced violacein inhibition of almost 60%. Collectively, both proteins (present in crude cell extracts of pDrive::*hitR*/pDrive::*hydR*) were able to significantly degrade 3-oxo-C6-HSL and consequently quench the violacein production in CV026.

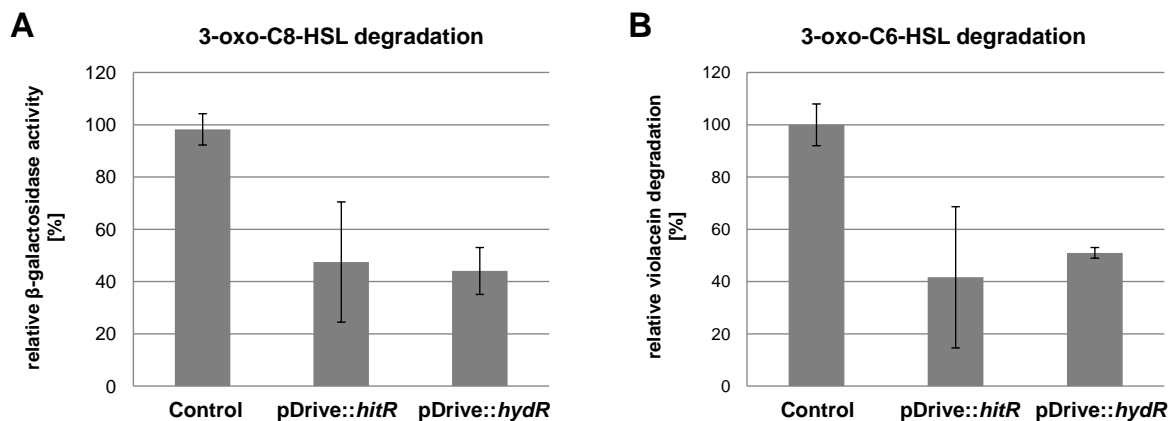


Figure 11: β -Galactosidase assay with NTL4 and violacein inhibition assay with CV026. (A) ONPG assay carried out with 1.4 mg crude extract from pDrive::*hitR* and pDrive::*hydR*, NTL4 without addition of 3-oxo-C8-HSL was employed as a control. **(B)** Violacein inhibition assay carried out with same amounts of crude extract from pDrive::*hitR* and pDrive::*hydR*, TE buffer was used as the control.

In summary, both proteins, HitR and HydR, found on cosmid clone pWEB-TNC-A5 were considered to be involved in QQ processes, although the detailed sequence analysis did not reveal any significant similarities to known and published QQ related hydrolases. Thus, the functional and sequential results support the conclusion that *hitR* and *hydR* represent novel QQ functional active proteins which cannot be grouped into any known division of QQ proteins.

3.1.2 The AHLase related *qsdR2* gene is able to degrade AHLs

Restriction as well as sequencing analyses revealed an overall size of 41.2 kb of cosmid pWEB-TNC-B9 which was mapped on cNGR234. This cosmid comprised 45 ORFs holding around 12 ORFs which were annotated as hypothetical, transporter, transmembrane or lipoproteins, in sum all not assigned to a clear function. Within these 12 hypothetical proteins one ORF stood out by its annotated function as a metal-dependent hydrolase (NGR_c16020). As described in the introduction (1.2.3.1), QQ associated proteins from the AHLase domain often are metallohydrolases and this delivered the first indication for this ORF being possibly attributed to the QQ activity of pWEB-TNC-B9. In fact, this metal-dependent hydrolase was already uncovered in the sequence-based screening of NGR234 described in III.1.4.1. Verification of ORF NGR_c16020 by the sequence-based as well as function-based screening delivered the most probable ORF attributed to an interference with QS.

3.1.2.1 Detailed analysis of the conserved motif on *qsdR2* attributed to QQ

The ORF NGR_c16020 (837 bp) encodes QsdR2 (for **q**uorum-sensing **s**ignal **d**egrading enzyme from *R*hizobium sp. NGR234) a 279-amino acid protein which was assigned to the metal-dependent hydrolases. Prior to the putative ATG start codon, a AGGAGA ribosome-binding site as well as a possible -10 and -35 promoter sequence could be identified according to the published rhizobial consensus sequences (MacLellan *et al.* 2006). QsdR2 showed a very high similarity to a hypothetical protein from *S. meliloti* SM1021 (SMc01194) with an E-value of $3e^{-146}$ and a β -lactamase domain-containing protein of *Sinorhizobium medicae* WSM419 (E-value $4e^{-146}$). Although the NCBI database in general revealed high homologies to rather conserved β -lactamase domain proteins, no significant similarity to known AHLases of the metallohydrolase family at either nucleotide or peptide sequence level could be identified. However, *qsdR2* shares one short conserved motif within the AHLases. Alignment analyses should answer the question of *qsdR2* lacking a clear similarity to AHLases but harboring a conserved zinc-binding domain of these metallohydrolases.

3.1.2.2 Sequence-based comparison to known AHLases

The program BioEdit was used to accomplish sequence alignment studies with *qsdR2* and other representatives of AHLases.



Figure 12: BioEdit alignment of QsdR2 and published AHLases sharing conserved regions. Positions of first AA in QsdR2: 80; AiiA: 101; AiiB/AttM: 93; AhID: 114; AhIK: 101.

Highly conserved motifs comprised by AiiA homologous are depicted in Figure 12 and indicated by black boxes. The deduced AA sequence of *qsdR2* uncovered the pattern “⁸³HAHADH⁸⁹” which is similar those of AiiA, AhID and QlcA and represents the conserved “HXHX~DH” motif existing among metallo- β -lactamases (introduction, 1.2.3.1). This conserved motif is proposed as a zinc-binding domain and holds beside the “HXHX~DH” region at least three other conserved residues, which are all present in AiiA, AiiB/AttM, AhID and AhIK but are absent in *qsdR2* (data not shown). Sequence alignment of the second moderately conserved region (black box) among AiiA-related proteins also uncovered the absence of this pattern in *qsdR2*, the respective AA sequence is highlighted in gray. Other residues completely conserved in AHLases of this family could not be related.

3.1.2.3 Functional screenings confirm QQ activity of *qsdR2*

Direct cloning was used to functionally verify the QQ activity of QsdR2. Therefore, gene *qsdR2* (1152 bp) was amplified with *Taq* polymerase (primer pair *qsdR2_for/qsdR2_rev*, Table 5) from genomic NGR234 DNA and ligated into the pDrive Cloning Vector. The resulting construct was transformed into *E. coli* XL1 blue and the correct size was verified by restriction analysis. In motility assays accomplished with *E. coli* XL1 blue harboring pDrive::*qsdR2* as well as with PAO1 and crude cell extract of pDrive::*qsdR2* (1.8 mg/mL total protein content) this construct displayed a clear inhibition of the swarming behavior (VII.2.5.1, Figure 30 in appendix).

The AHL degradation experiments using NTL4 and CV026 were employed as described in III.3.1.1.6 and revealed similar reduction rates as already recorded for HitR and HydR. The quantification of the QQ ability of QsdR2 was accomplished by the degradation of 3-oxo-C8-HSL and 3-oxo-C6-HSL. Figure 13 shows that QsdR2 was able to reduce the level of both AHLs compared to the buffer controls. Only 62.3% of 3-oxo-C6-HSL could be detected after incubation of QsdR2 with CV026. An even more pronounced degradation of 3-oxo-C8-HSL was measured in the NTL4 assay where less than 43% of the added AHL could be detected after the incubation time of 30 h.

Collectively, QsdR2 comprised by cosmid clone pWEB-TNC-B9 was first identified by a detailed sequence-based approach. These sequence similarities were supported by an inhibited motility of *E. coli* XL1 blue/PAO1 and were further confirmed by clearly reduced AHL levels in the enzyme activity assays. Although *qsdR2* comprises the zinc-binding motif common in AHLases, crucial conserved residues are absent in its sequence indicating that QsdR2 might constitute a new member of the family.

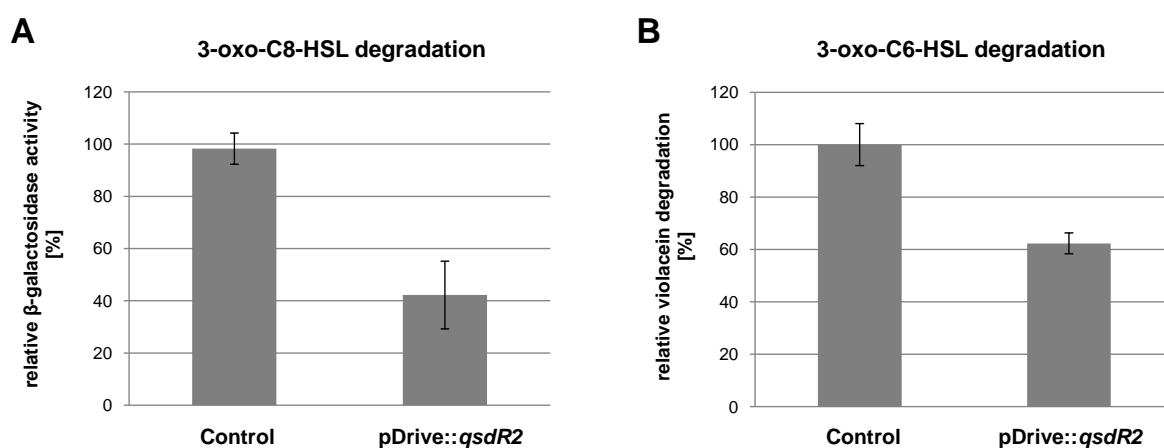


Figure 13: β -Galactosidase assay with NTL4 and violacein inhibition assay with CV026. (A) ONPG assay carried out with crude extract from pDrive::*qsdR2*, NTL4 without addition of 3-oxo-C8-HSL was employed as a control. **(B)** Violacein inhibition assay carried out with same amounts of crude extract from pDrive::*qsdR2*, TE buffer was used as the control.

3.1.3 An acetaldehyde dehydrogenase, AldR, a novel lactone hydrolyzing enzyme

The last chromosomal locus was identified on cosmid clone pWEB-TNC-G2. Initial function-based screenings revealed its ability to quench swarming motility in *E. coli* and biofilm production in PAO1. A subsequent sequence analysis demonstrated an overall size of 33.4 kb for pWEB-TNC-G2 only including 26 ORFs. Among these ORFs several could not be classified in detail and were annotated as hypothetical proteins. Since direct cloning of all

potential ORFs would be time-consuming, the *in vitro* transposon mutagenesis approach was pursued to localize the responsible ORF.

3.1.3.1 Construction of a pWEB-TNC-G2 transposon mutant bank and initial motility assays

The *in vitro* transposon mutagenesis was carried out as already described for pWEB-TNC-A5. The reaction was accomplished with 0.2 µg of pWEB-TNC-G2 cosmid DNA and the corresponding molar equivalent of the transposon. Generated transposon mutants were transferred via heat shock into *E. coli* XL1 blue cells and verified on LB agar supplemented with kanamycin. Collectively, 95 mutants were established for cosmid clone pWEB-TNC-G2.

Obtained transposon mutants were analyzed by functional assays directly in *E. coli* XL1 blue and using PAO1. First, mutants were cultivated in their *E. coli* XL1 blue host and subjected to liquid swarming motility tests as described in II.7.3.1. Best swarming results were obtained using LB-G/C liquid medium, yielding 30 clones which were able to recover the original phenotype of *E. coli* XL1 blue. Using assays on solid swarming plates, to monitor a deviant phenotype displayed by transposon mutants, narrowed the 30 candidate cosmid clones to five which reproducibly restored the swarming ability of *E. coli* XL1 blue and PAO1. Cultures and conditions were chosen as previously described in III.3.1.1.2. The cosmid clone pWEB-TNC-G2 was used as a positive control and could significantly reduce swarming motility in both tests. Figure 14 displays results obtained from *E. coli* XL1 blue assays exemplarily, while the positive control pWEB-TNC-G2 shows a phenotype triggered by its putative QQ gene (14B-14E), image C shows a transposon mutant not impairing the motility of *E. coli* XL1 blue host. Same results were obtained for assays accomplished with respective clones and PAO1 (Figure 14D-14F).

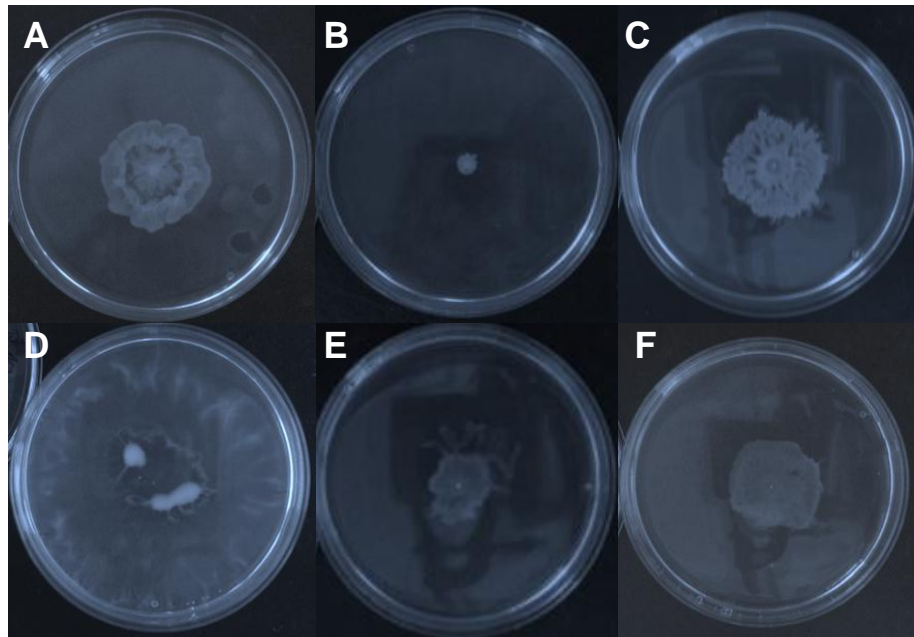


Figure 14: Motility assays accomplished with transposon mutants in *E. coli* XL1 blue and PAO1. (A) Control: *E. coli* XL1 blue cells without vector. **(B)** Positive control: *E. coli* XL1 blue harboring pWEB-TNC-G2. **(C)** Transposon mutant A8 in *E. coli* XL1 blue, exemplarily. **(D)** Control: PAO1 cells. **(E)** Positive control: Crude cell extract of pWEB-TNC-G2 impairing PAO1 growth. **(F)** Crude cell extract of transposon mutant A8 with PAO1, exemplarily.

3.1.3.2 Identification and detailed sequence analysis of the *aldR* locus

All five candidate pWEB-TNC-G2 mutants were sequenced bidirectional using transposon specific primers (KAN-2 FP-1 and KAN-2 RP-1, Table 5). Sequences obtained for three out of the five cosmid mutants could be assigned to ORF NGR_c23150, one to ORF NGR_c23270 and one could not be assigned. Supported by the three sequences, a detailed analysis of ORF NGR_c23150 was accomplished.

The predicted ORF NGR_c23150 (1509 bp) encodes an acetaldehyde dehydrogenase, a 503-AA protein, which was designated as AldR (for acetaldehyde dehydrogenase from *Rhizobium* sp. NGR234). A putative ribosome binding site was located 12 bp upstream of the predicted ATG start codon (AGGGAGG) and AldR is preceded by at least three possible promoter sequences, in general moderately conserved at both positions (-10/-35). As already uncovered for *hitR*, the best matching promoter sequence of these three was found to be linked by a 20 nt region and not as expected by a 17-18 nt region (MacLellan *et al.* 2006). Experimental data is needed to elucidate the most probable promoter region. NCBI BLAST searches of NGR_c23150 demonstrated high similarities to proteins present in *S. meliloti* SM1021 (SMc02689), *S. medicae* WSM419 (Smed 2260), *Rhizobium etli* CFN42 (RHE CH03723), *R. leguminosarum* bv. *trifolii* WSM2304 (Rleg2 3506) and *M. loti* MAFF303099 (ml6639) with a max. identity up to 100% and E-values of 0.0. The deduced

AA sequence of AldR features a highly conserved region counted to the NAD(P)⁺ dependent aldehyde dehydrogenase superfamily comprising the three crucial sides: NAD(P)⁺ cofactor binding site and a catalytic and bridging domain. NAD(P)⁺ dependent enzymes are involved in the oxidation of aromatic/aliphatic aldehydes and participate in diverse metabolic pathways.

3.1.3.3 Functional verification of QQ activity of AldR

To support the previous results obtained with cosmid pWEB-TNC-G2 and their mutants, gene *aldR* was cloned into pDrive Cloning Vector and subjected to further screenings. Therefore, the PCR reaction was accomplished with *Taq* polymerase and the primer pair *aldR_for/aldR_rev* (Table 5). The resulting PCR product (~ 1.8 kb) was ligated into the pDrive vector via A/U overhangs and transformed into *E. coli* XL1 blue cells. The correct insert and size was verified by restriction analysis.

In first motility assays accomplished with *E. coli* XL1 blue, the construct pDrive::*aldR* displayed a clear inhibition of the swarming behavior of the *E. coli* host. These results could be also repeatedly demonstrated for assays carried out with crude cell extracts of pDrive::*aldR* (1.3 mg/mL total protein content) and PAO1 (VII.2.5.2, Figure 31 in appendix). Additionally, a reduced level of the pyocyanine pigment could be observed for pDrive::*aldR* compared to the negative control, verifying a possible QQ activity.

AHL degradation experiments were employed to confirm the previous motility assays. The experiments were carried out as described in II.7.6.1. Quantification of the QQ ability of AldR was accomplished by measuring the degradation level of 3-oxo-C8-HSL using NTL4 and 3-oxo-C6-HSL using CV026 as already described for HitR, HydR and QsdR2. The β -galactosidase assay was accomplished using ONPG substrate and crude cell extract of pDrive::*aldR* with a total protein content of 1.3 mg/mL. NTL4 was used as a positive control. Collectively, after an incubation time of 30 h less than 71% of the added 3-oxo-C8-HSL could be detected compared to the positive control. An even more pronounced degradation of AHLs could be detected in the CV026 assay. Compared to the control (empty pDrive Cloning Vector), only 62.8% of the introduced 3-oxo-C6-HSL could be detected after 30 h incubation of AldR with CV026. The degradation levels measured for AldR are equal to those observed for QsdR2, both are depicted in Figure 15 given below.

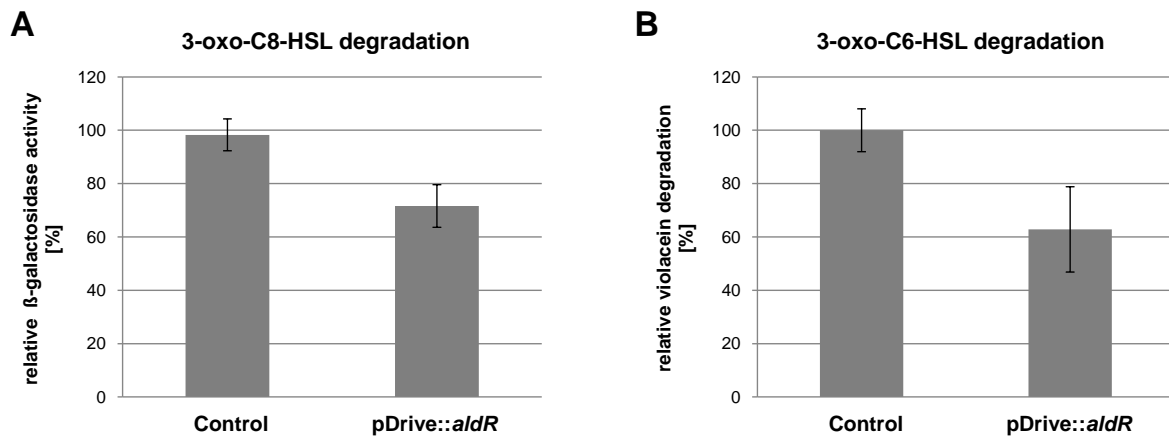


Figure 15: β -Galactosidase assay with NTL4 and violacein inhibition assay with CV026. (A) ONPG assay carried out with crude extract from pDrive::*aldR*, NTL4 without 3-oxo-C8-HSL was used as a control. **(B)** Violacein inhibition assay carried out with same amounts of crude extract from pDrive::*aldR*, TE buffer was used as the control.

In summary, AldR comprised by cosmid clone pWEB-TNC-G2 was identified by a combination of transposon mutagenesis and a subsequent cloning of the candidate ORF NGR_c23150. Although the detailed sequence analysis did not reveal any similarities to already published QQ associated proteins, motility as well as enzyme activity assays could clearly show AldR's ability to interfere with diverse QS systems in *E. coli* XL1 blue, PAO1 and CV026. Thus, this acetaldehyde dehydrogenase originating from NGR234 might constitute a novel enzyme associated with a QQ activity.

3.2. Verification and biochemical characterization of putative QQ genes *dlhR* and *qsdR1* located on the megaplasmid of NGR234

The following section concentrates on QQ associated loci identified on the megaplasmid pNGR234*b*. As discussed previously the megaplasmid of NGR234 is of great importance for growth and survival under fluctuating environmental conditions. Consequently, novel pNGR234*b*-borne enzymes involved in QQ might increase the knowledge on this research field and especially the understanding of symbiosis and communication of NGR234. Using the initial function-based screening procedure, the replicon pNGR234*b* uncovered two candidate genes, *dlhR* present on pWEB-TNC-B2 and *qsdR1* present on pWEB-TNC-C6, which reproducibly quenched QS-regulated processes. Partial physical maps of both identified genes together with their flanking regions are depicted in Figure 16. The detailed functional and biochemical verification of both identified proteins is described in the following sections, in which chapter III.3.2.1 and III.3.2.2 describe assays employed only with DlhR and QsdR1, respectively and chapter III.3.2.3 summarizes assays accomplished with both proteins.

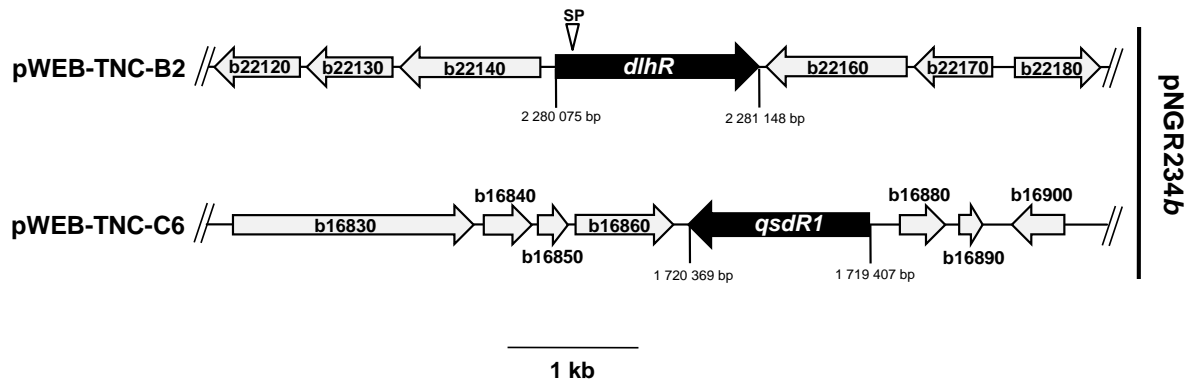


Figure 16: Identification of AHL-degrading cosmid clones on pNGR234b. Partial maps of identified cosmid clones pWEB-TNC-B2 and -C6 carrying the putative genes *dlhR* and *qsdr1*. Black arrows indicate the ORFs that are associated with QQ. Gray shaded arrows indicate flanking ORFs that are not linked to the QQ phenotypes. ORFs are designated using ORF ID from GenBank entries CP000874 and CP001389 (prefix NGR_~). SP: signal peptide. The scale bar represents 1 kb.

3.2.1 *DlhR*, a diene lactone hydrolase capable of inactivating AHLs

A detailed restriction analysis as well as first sequencing approaches revealed an overall size of 34 kb of cosmid pWEB-TNC-B2. A comparison of the sequence to the ERGO database uncovered that this cosmid clone harbors 30 ORFs. Only few ORFs could be annotated with an assigned function, several were only weakly specified or annotated as a putative protein. Since the first sequence-based revision revealed several considerable ORFs, subcloning was performed in order to narrow these candidates ORFs to one responsible for QQ activity.

3.2.1.1 Subcloning and identification of candidate ORFs on pWEB-TNC-B2

For subcloning purposes, cosmid clone pWEB-TNC-B2 was cultivated as described in II.3.1.1.3 in LB medium which was supplemented with ampicillin. Cosmid DNA was isolated using commercial kits and was initially digested with several enzymes in order to find optimal fragment sizes for cloning. Restriction enzyme *EcoRI* proved to deliver fragments between 1-8 kb which could be further subcloned into pTZ19R. *EcoRI* fragments were generated by a preparative restriction and purified as described under II.4.5.4. Vector pTZ19R was prepared identically and the random *EcoRI* fragments were ligated into the vector using T4 DNA ligase. All obtained subclones of pTZ19R with the *EcoRI* fragments of pWEB-TNC-B2 were isolated and verified by restriction analysis. In order to identify one or several subclones harboring a putative QQ gene, motility assays in *E. coli* XL1 blue cells were accomplished as described in II.7.3.2. All obtained subclones were subjected to the described motility test, uncovering one putative QQ active subclone, pTZ19R::fr44, which was able to alter the motility of *E. coli* XL1 blue. This subclone contained a 4.4 kb *EcoRI* insert of pWEB-TNC-B2 and showed repeatedly an inhibition of the swarming motility in its *E. coli* XL1 blue host on

solid swarming medium. Detailed sequence and ORF analyses were established for the identification of ORFs present on the 4.4 kb fragment of subclone pTZ19R::fr44.

3.2.1.2 Sequence analysis revealed the presence of *dlhR* on pWEB-TNC-B2

For the identification and verification of putative ORFs present on the promising 4.4 kb fragment, subclone pTZ19R::fr44 was end-sequenced using M13_20/M13_rev primer (Table 5). The obtained sequence data was compared to the complete genome of NGR234 within the ERGO database and revealed the presence of four ORFs (NGR_b22140, NGR_b22150, NGR_b22160, and NGR_b22170). All four ORFs were studied in more detail using their DNA as well as their deduced AA sequence. Within the four, two ORFs were annotated as putative transcriptional regulators (NGR_b22140 and NGR_b22170) and NGR_b22160 was assigned to a senescence marker protein. The most interesting ORF was NGR_b22150 annotated as a diene lactone hydrolase-like protein, which was already identified in the previous sequence alignment (III.1.4.1). Additionally, this ORF revealed functional and sequential similarities to a previously published biofilm inhibiting ORF *bpiB07* (Schipper *et al.* 2009). Since NGR_b22150 appeared to be the most promising hit on pTZ19R::fr44, the following experiments focused on this putative QS inhibiting ORF. Nevertheless, before subjecting this candidate to continuative functional assays, a detailed sequence analysis was necessary.

The AA analysis of ORF NGR_b22150 (1074 bp) encoding **DlhR** (for **d**iene**l**actone **h**ydrolase from **R**hizobium sp. NGR234) revealed that this gene was most similar to a hypothetical protein (Atu0247) from *Agrobacterium tumefaciens* str. C58. The observed similarity was 75% and the identity was 58% with an E-value of $3e^{-89}$. The deduced AA sequence of DlhR contained a multi-domain COG4188 spanning nearly the whole protein and a smaller Pfam03403 domain structure. COG4188 represents a predicted diene lactone hydrolase domain, whereas Pfam03403 is involved in a subfamily of phospholipases A2, responsible for the inactivation of platelet-activating factor through cleavage of an acetyl group. In addition, a conserved GSD(L) motif containing the active-site serine residue typical for GDSL esterases (family II of lipolytic enzymes) was identified (Arpigny and Jaeger 1999). Further analysis of the upstream sequence of the predicted ATG start codon of *dlhR* revealed a possible ribosome-binding site (AGAGG) as well as both promoter regions (-10/-35). Additionally, the prediction of presence and location of a signal peptide (SignalP 3.0 server, <http://www.cbs.dtu.dk/services/SignalP/>) on *dlhR* uncovered a 99% probability for a cleavage site between AA 22 and 23 (beginning by methionine). The predicted signal peptide on *dlhR* is: MIPSHVPAALALAVAFAPCHAF. All identified and localized motifs and domains are depicted in Figure 17.

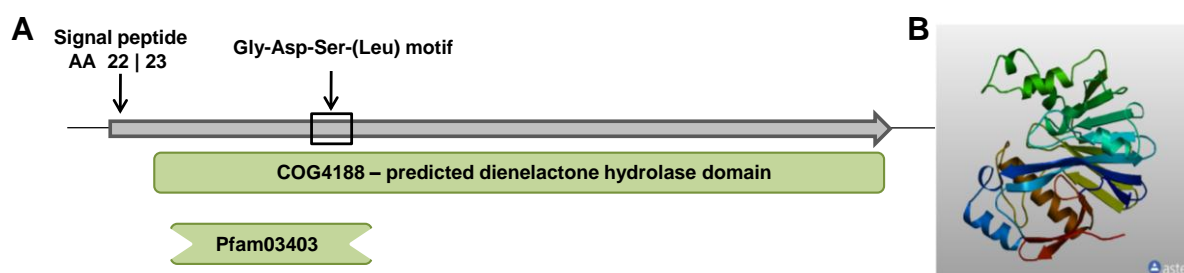


Figure 17: Localization of identified domains and motifs on the deduced AA sequence of DIhR and a predicted protein model. (A) COG4188 shows a predicted diene lactone hydrolase domain. Pfam003403 depicts the incomplete domain structure of platelet-activating factor. The GSD(L) motif is bordered by the black box. The identified signal peptide is indicated with the arrow, giving the possible cleavage site between AA 22 and 23. **(B)** Calculated comparative protein model of DIhR (Swiss-Model).

3.2.1.3 Overexpression and purification of DIhR

To functionally analyze the DIhR protein, gene *dlhR* was cloned into vector pBluescript II SK+ (referred to as pSK+) and then cloned directional into the expression vector pET21a using *HindIII/NdeI*. The primer pair *dlhR_for/dlhR_rev* (Table 5) was designed with appropriate restriction sites and used to amplify the *dlhR* gene with *Pfu* polymerase from genomic NGR234 DNA. The PCR product was ligated (blunt end) with T4 ligase into *EcoRV* digested pSK+. After verifying the correct size of the insert in pSK+, a preparative restriction was carried out to obtain the *dlhR* gene flanked by *HindIII* and *NdeI* sites. Subsequently, the purified *dlhR* 1.1 kb insert was ligated into the prepared pET21a expression vector (digested with *HindIII/NdeI*) and transformed into *E. coli* BL21 (DE3) cells. Prior to purification, the construct pET21a::*dlhR* was verified by restriction and sequence analysis.

For His-tag purification of the pET-construct, main expression cultures of *E. coli* BL21 (DE3) harboring pET21a::*dlhR* were cultivated as specified earlier (II.3.1.1.2). Growth conditions for a max. protein yield in the main expression cultures were determined in small expression cultures with volumes of 100 mL. Growth temperatures between 10-37°C and IPTG concentrations for induction between 100-500 μ M were tested in combination resulting in best expression of DIhR at 17°C and supplementation with 100 μ M IPTG. Furthermore, crude cell extracts of the expression cultures were established either by ultrasonication or French Pressure Cell preparation as described previously (II.6.2.1.1 and II.6.2.1.2). The obtained supernatants were purified using Protino[®] packed columns under native conditions and the bound DIhR protein was eluted with 5 mL 1x elution buffer. To subsequently use the DIhR protein eluate for activity assays, excess imidazole was removed by dialysis against potassium phosphate buffer (pH 7.5) (II.6.2.3) and the protein content was quantitatively determined using Bradford (II.6.1.1). Establishing the His-tag purification under optimal

growth and inducing conditions (17°C and 100 µM IPTG) resulted in DIhR protein concentrations of 300-400 µg/mL. Accordingly, a control culture (*E. coli* BL21 (DE3) with an empty pET21a vector) was grown and incubated under identical conditions and used as a negative control in the following assays.

The expected molecular weight of 39.9 kDa for the His-tagged DIhR protein as well as the protein purity were confirmed by SDS-PAGE. Figure 18A shows a SDS-PAGE gel with DIhR and the control. Figure 18A, column 1 displays the purified DIhR with a clear band at ~40 kDa. In contrast, the band pattern of the control (18A, column 2) lacks the band at the corresponding molecular weight. To confirm a successful tagging of DIhR with the desired His-tag, a western blot analysis was carried out after separating the protein by SDS-PAGE. Figure 18B shows in column 1 a clear dyed band at a weight of about 40 kDa, ensuring a successfully His-tagged DIhR.

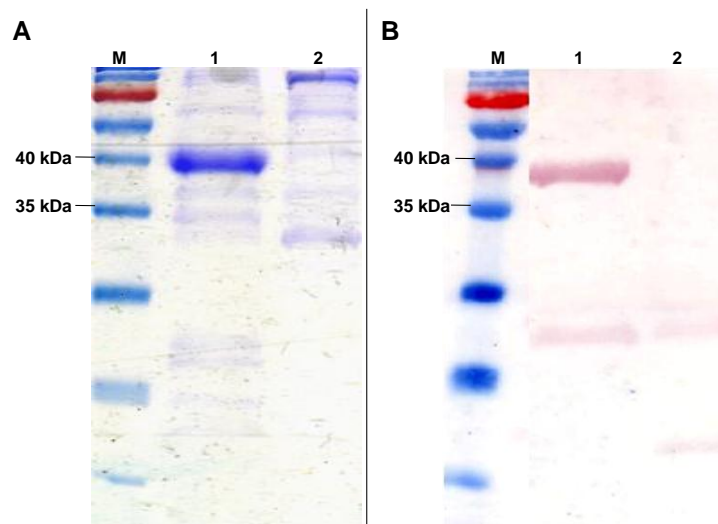


Figure 18: SDS-PAGE of His-tag purification and western blot analysis of DIhR. (A) M: Protein marker PageRuler™ Prestained Protein Ladder #SM0671. **1:** 20 µL of eluate of pET21a::*dlhR*. **2:** 20 µL of eluate of pET21a (control culture). **(B) M:** Prestained Protein Ladder #SM0671. **1:** 20 µL of eluate of pET21a::*dlhR* stained with western blot. **2:** 20 µL of eluate of pET21a (control culture).

When necessary for functional assays, the His-tag purified DIhR protein was filtered sterile and concentrated as described in material and methods (II.6.2.4).

3.2.1.4 Inhibition of motility in *P. aeruginosa* PAO1 by DIhR

Previous functional assays employing PAO1 strengthen the putative QQ activity of DIhR comprised by the cosmid clone pWEB-TNC-B2 and subclone pTZ19R::fr44. Both constructs

were able to significantly alter the motility of PAO1, accordingly these functional assays were repeated with the purified DlhR protein.

3.2.1.4.1 Swarming and swimming test with *P. aeruginosa* PAO1 and DlhR

To verify the QQ activity of the His-tag purified DlhR, swarming as well as swimming tests using PAO1 were accomplished as already described for screening of candidate cosmid clones in III.2.2.3. The purified DlhR protein extract was established as specified earlier. Different from the swarming and swimming tests accomplished with the cosmid clones, the protein extract was added directly to the agar and was not spread over the agar surface. Consequently, swarming or swimming agars for PAO1 were prepared as stated in material and methods (II.7.4.1.1) and supplemented with DlhR. Therefore, 1-10 $\mu\text{g}/\text{mL}$ DlhR were added to the agar, mixed gently and filled into the petri dishes. Then, 1×10^8 cells of an overnight PAO1 culture were applied on the middle of the agar and plates were incubated at 37°C for up to 24 h. As a negative control potassium phosphate buffer instead of protein eluate was used and incubated under identical conditions.

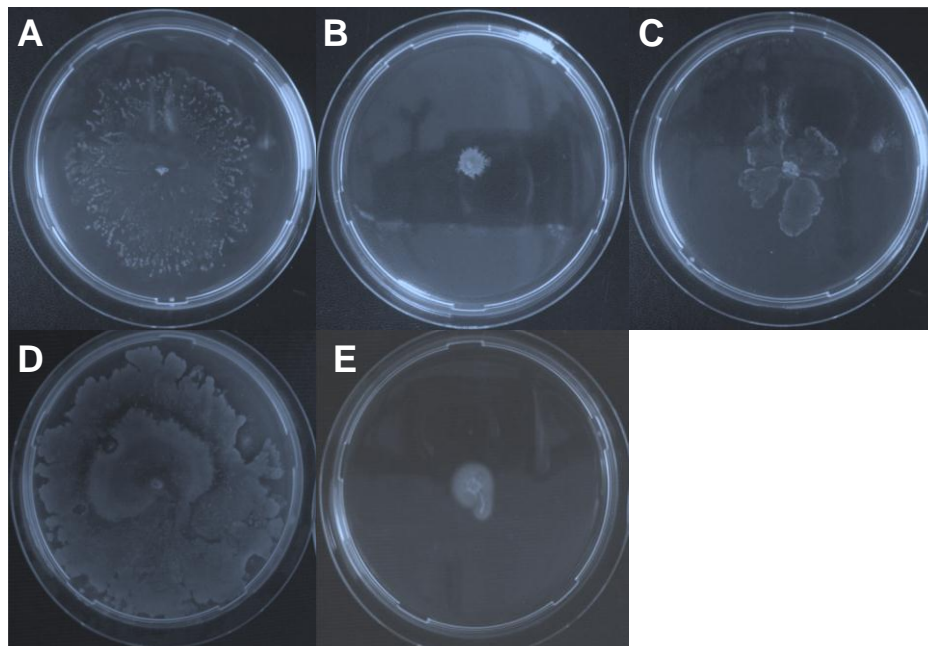


Figure 19: *P. aeruginosa* PAO1 motility assays (swarming/swimming behavior). (A) Control: PAO1 on swarming plates with potassium phosphate buffer. (B) PAO1 inhibited swarming behavior triggered by 5 $\mu\text{g}/\text{mL}$ DlhR. (C) PAO1's inhibited swarming behavior triggered by 1 $\mu\text{g}/\text{mL}$ DlhR. (D) Control: PAO1 on swimming plates with potassium phosphate buffer. (E) PAO1 inhibited swimming behavior triggered by 5 $\mu\text{g}/\text{mL}$ DlhR.

As monitored for swarming assays carried out with pWEB-TNC-B2 and pTZ19R::fr44, the purified DlhR also displayed a strong and clear inhibition of the swarming behavior of PAO1. These results could also repeatedly be demonstrated for assays carried out with PAO1 and

DlhR on swimming agar plates. The evaluation of all accomplished motility assays with PAO1 and the purified DlhR protein resulted in a min. DlhR protein amount of 5 µg/mL which was still able to impair the motility of PAO1. Applying less than 5 µg/mL of DlhR in those assays led to a partial or no inhibition of motility. Figure 19 summarizes results monitored for both motility assays. While images A/D display the negative controls (PAO1 inoculated on swarming or swimming plates supplemented with potassium phosphate buffer), images B/E show the inhibition of the swarming and respective swimming ability of PAO1 triggered by 5 µg/mL DlhR. Image C displays exemplarily a moderate inhibition of the swarming behavior of PAO1 triggered by 1 µg/mL DlhR.

3.2.1.4.2 Complementation experiments with *P. aeruginosa* PAO1 and external AHLs

Functional assays employed with purified DlhR protein proved its putative ability to quench QS in PAO1. To support these findings subsequent complementation experiments restoring the wild type motility phenotype of PAO1 under influence of DlhR were realized. *P. aeruginosa* PAO1 utilizes two different AHLs for controlling its motility like swarming, biofilm formation or pyocyanine production. Consequently, the AHLs 3-oxo-C12-HSL and C4-HSL were employed in this complementation assay. Swarming plates comprising 5 µg/mL DlhR protein were prepared as described in the previous section. 1 M AHL stock solutions were generated and dilution series were established in ethyl acetate ranging from 10^{-4} to 10^{-7} M. Then, 10 µL of each dilution of each AHL were spread over the DlhR containing swarming agar plates. After drying the plates, 1×10^8 cells of an overnight PAO1 culture were applied on the middle of the agar and incubation was carried out at 37°C for up to 24 h. Swarming plates lacking DlhR which were treated with AHLs and inoculated with PAO1 served as a positive control, agar plates supplemented with DlhR and not treated with AHLs served as a negative control. Results obtained for the complementation assay are summarized in Table 16 and shown in Figure 32 (VII.2.5.3 in appendix).

Table 16: Complementation experiments with PAO1, external AHLs and DlhR. (- : no swarming behavior, +++++ : strong swarming behavior, ++++ : constricted but visible swarming behavior, ++ : slight swarming behavior, + : min. swarming behavior).

AHL	Swarming behavior					
	Positive control (without DlhR)	Negative control (without AHL)	Dilution [M]			
			10^{-4}	10^{-5}	10^{-6}	10^{-7}
3-oxo-C12-HSL	++++	-	+++	+	++	-
C4-HSL	++++	-	+	+	+	-

Comparing the negative control to the swarming response of PAO1 to the different dilution steps of AHLs reveals that 3-oxo-C12-HSL was able to slightly restore the original swarming phenotype of PAO1, whereas complementation with C4-HSL hardly restored the inhibited swarming appearance of PAO1 triggered by DIhR. Nevertheless, complementation experiments using both AHLs in combination might deliver a more reliable result. The motility of PAO1 is regulated by a cascade of two different QS-regulated systems (*las* and *rhl*) thus, a combination of AHLs might be essential for a clear complementation of the motility phenotype of PAO1.

3.2.2 Gene *qsdR1* is involved in QQ of AI-1 molecules

The second QQ associated pNGR234b locus, *qsdR1*, was localized by various function-based assays on cosmid clone pWEB-TNC-C6. The genomic DNA fragment of NGR234 comprised by this clone was already identified by comparison in the ERGO database. Cosmid pWEB-TNC-C6 demonstrated to have a total size of 37.7 kb holding 33 ORFs. Among ORFs annotated as putative transporters or transposases and other ORFs with clear assigned functions, seven hypothetical proteins were present on pWEB-TNC-C6. Nevertheless, ORF NGR_b16870 stood out with its annotated function as a metal-dependent hydrolase providing a first indication of its affiliation to metallohydrolases of the AHLase domain. However, all hypothetical proteins had to be taken into account and since direct cloning of all these proteins would be time-consuming, subcloning was performed to detect the QQ associated gene.

3.2.2.1 Subcloning and identification of candidate ORFs on pWEB-TNC-C6

The subcloning procedure was identical to the procedure carried out for cosmid clone pWEB-TNC-B2. Restriction enzyme *HindIII* delivered pWEB-TNC-C6 fragments between 3-7.5 kb which were suitable for subcloning into *HindIII* linearized pTZ19R. All generated subclones of pTZ19R with pWEB-TNC-C6 *HindIII* fragments were isolated and verified by restriction analysis. Initial motility assays in *E. coli* XL1 blue host (II.7.3.2) were employed to identify subclones featuring a possible QQ activity. Using this assay one subclone (pTZ19R::fr55) could be uncovered being responsible for an altered swarming behavior of *E. coli* XL1 blue. Restriction analysis revealed that this subclone contained a 5.5 kb large *HindIII* insert of pWEB-TNC-C6. Furthermore, a detailed sequence and ORF analysis was established in order to identify all ORFs present on the 5.5 kb fragment of the subclone pTZ19R::fr55.

3.2.2.2 Sequence analysis and comparison to representatives of the AHLase group

To verify putative QQ associated ORFs present on the positively tested subclone pTZ19R::fr55, end-sequencing using the primer pair M13_20/M13_rev (Table 5) was employed. The obtained sequence data was compared to the genome of NGR234 within ERGO and revealed the presence of seven ORFs, NGR_b16830–NGR_b16890. All ORFs were examined in more detail using their AA sequence. Within the seven ORFs, NGR_b16870 revealed domains resembling signatures of the metallohydrolase family and therefore was considered to be the most probable candidate ORF on pTZ19R::fr55 attributed to the QQ activity of pWEB-TNC-C6. Consequently, first detailed sequence analyses should confirm this hypothesis before continuing with functional assays.

The NGR234 ORF NGR_b16870 (963 bp) encodes a 321-AA protein designated **QsdR1** (for **q**uorum sensing **s**ignal **d**egrading enzyme from *Rhizobium* sp. NGR234). The translational start codon of QsdR1 is preceded by a possible ribosome-binding site AGAGGA and possible -10 as well as -35 promoter sequences were identified according to previously reported rhizobia consensus promoter sequences (MacLellan *et al.* 2006). QsdR1 originating from pWEB-TNC-C6 is highly similar to a hypothetical protein of *Rhizobium etli* (RetIG_22662) with an E-value of $2e^{-124}$ and to a hypothetical protein of *Agrobacterium tumefaciens* (Atu4307) with an E-value of $1e^{-121}$. This protein belongs to hydrolases of the β -lactamase superfamily and is grouped to the class B of these enzymes requiring a bivalent metal ion (Zn^{2+}) for activity (Daiyasu *et al.* 2001). Although the NCBI database search only uncovered high homologies to rather conserved hypothetical proteins with β -lactamase domains, a direct comparison with known representatives of AHLases confirmed that QsdR1 is highly similar to the Aii2 hydrolase from an uncultured *Bacillus* sp., previously published by Carlier *et al.* 2003. Detailed alignment studies accomplished with BioEdit as well as BLAST results indicated two conserved regions among the QsdR1 sequence and the known AHLases (Figure 20).

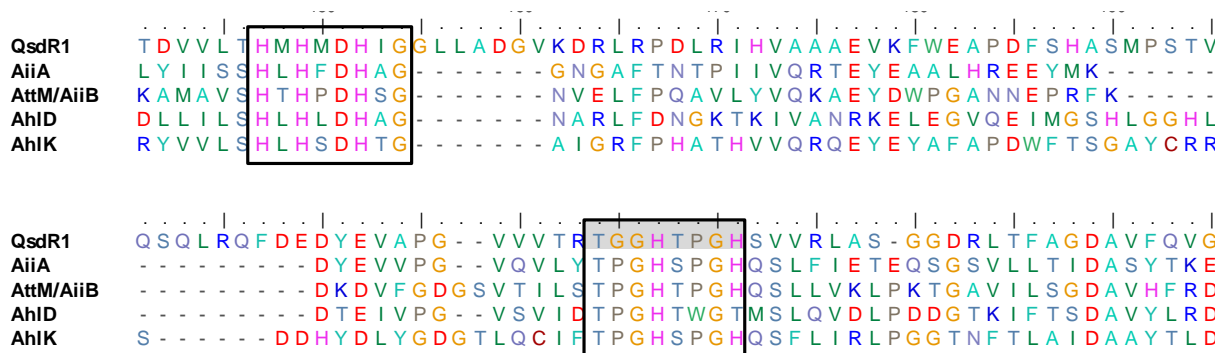


Figure 20: BioEdit alignment of QsdR1 and published AHLases sharing conserved regions. Positions of first AA in QsdR1: 135; AiiA: 98; AiiB/AttM: 123; AhlD: 111; AhlK: 98.

The two main conserved motifs comprised by AiiA homologous of the AHLase family are demonstrated in Figure 20 and highlighted by black boxes. The first short pattern represents the conserved “HXHX~DH” signature comprised by metallo- β -lactamases (I.2.3.1). This short sequence “¹⁴¹HMHMDHIG¹⁴⁸” was also identified in QsdR1. Beside the mentioned “HXHX~DH” region which is proposed to be a zinc-binding domain at least three other conserved residues (data not shown) are involved in successful binding of zinc and thus are crucial for its activity. Contrary to QsdR2, QsdR1 shares all these conserved residues and shares this feature with other representatives of the AHLase family. The second moderately conserved region (black box) with the respective AA sequence highlighted in gray was also found to be common among AiiA-related proteins. In addition to the first conserved region, QsdR1 also holds the second short sequence “²³⁶TGGHTPGH²⁴³”. Coherently, the sequence analysis of QsdR1 uncovered the presence of the two main AA motifs comprised by diverse representatives of the metallohydrolase family and thus delivered a first sequential association with a possible QQ activity. Nevertheless, to confirm these findings further functional assays are necessary.

3.2.2.3 Overexpression and purification of QsdR1

To accomplish function-based screenings using the purified QsdR1 protein, *qsdR1* had to be cloned into expression vector pET21a. A similar strategy of cloning and expression was followed as described for construct pET21a::*dlhR* (III.3.2.1.3). The respective primer pair *qsdR1_for/qsdR1_rev* (Table 5) was designed with *XhoI/NdeI* restriction sites and used to amplify *qsdR1*. Via subcloning into pSK+ and preparative digestion *qsdR1* gene was successfully ligated into expression vector pET21a, designated pET21a::*qsdR1*, and transformed into *E. coli* BL21 (DE3) cells. Prior to purification, the construct was verified by restriction and sequence analysis.

For the His-tag purification of construct pET21a::*qsdR1* optimal growth conditions were determined in small expression cultures (procedure as described previously for DlhR). Crude cell extracts were established by ultrasonication or French Pressure Cell, then purified using Protino® columns under native conditions and finally eluted with 5 mL 1x elution buffer. Establishing the purification from main expression cultures, a growth temperature of 17°C and an induction with 100 µM IPTG delivered a max. protein yield of 200-400 µg/mL. To subsequently use the QsdR1 protein for further activity assays, excess imidazole was removed from the protein eluate by dialysis against potassium phosphate buffer (pH 7.0). *E. coli* BL21 (DE3) with an empty pET21a vector served as a negative control and was incubated under identical conditions.

To verify the purity and the molecular weight of the His-tagged QsdR1 protein (36 kDa), separation by SDS-PAGE was employed. Additionally, to confirm a successful tagging of QsdR1 western blot analysis was accomplished after separating the protein by SDS-PAGE. Figure 21 displays the SDS-PAGE gel as well as the western blot carried out with QsdR1. Figure 21A shows the purified QsdR1 protein with a visible band at the corresponding molecular weight of ~36 kDa. Figure 21B demonstrates results obtained for the western blot staining where a clear band was detected at ~42 kDa. This notable shift from 36 kDa to 42 kDa obtained for the western blot might be caused by the change of buffers between SDS-PAGE and western blot.

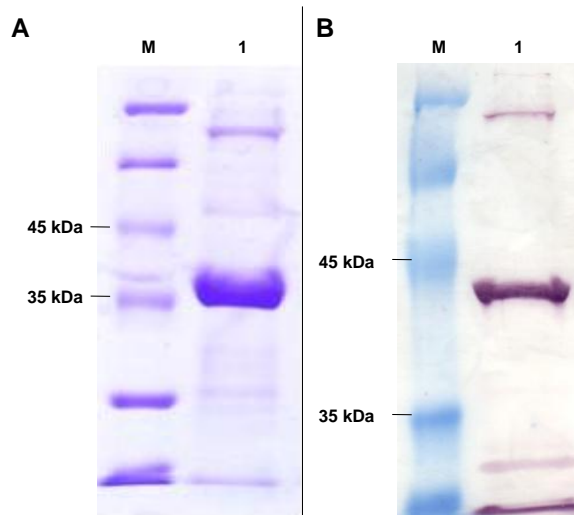


Figure 21: SDS-PAGE of overexpression and western blot analysis of QsdR1. (A) M: Protein marker #SM0431. **1:** 20 µL of eluate of pET21a::*qsdR1*. **(B) M:** Protein marker #SM0431. **1:** 20 µL of eluate of pET21a::*qsdR1* stained with western blot.

For further functional assays accomplished with the purified QsdR1, the protein solution was filtered sterile and concentrated when necessary.

3.2.2.4 Analysis of the QQ activity of QsdR1

The putative QQ activity of cosmid clone pWEB-TNC-C6 as well as subclone pTZ19R::fr55 was verified in initial function-based screenings. The corresponding gene *qsdR1*, possibly involved in AHL degradation, could be identified by detailed sequence and alignment studies. To support the previous results of QsdR1's ability to degrade AHLs, additional motility as well as activity assays had to be accomplished with the purified protein.

3.2.2.4.1 Inhibition of motility in *P. aeruginosa* PAO1

Purified QsdR1 protein extracts were established as specified earlier, filtered sterile and directly used for swarming as well as biofilm assays with PAO1. Different QsdR1 protein amounts ranging from 5 to 200 µg/mL were added to the prepared swarming agar before pouring the plates. After solidifying, 1×10^8 cells of an overnight culture of PAO1 were applied on the middle of the agar and plates were incubated at 37°C for up to 24 h. PAO1 inoculated on swarming agar supplemented with potassium phosphate buffer instead of protein served as a negative control. The evaluation of all tests carried out to determine the inhibitory effects of QsdR1 on PAO1's motility and to detect the min. protein content still influencing swarming in PAO1, resulted in an activity range of 50-200 µg/mL of the used protein. Assays accomplished with less than 50 µg/mL QsdR1 were inconsistent giving only partial or no inhibition. In Figure 22, images A and B depict results obtained for this motility assays. Where on the negative control plate PAO1 was not impaired in its ability to swarm, image B shows a clear inhibition of PAO1's swarming triggered by 50 µg/mL QsdR1.

Biofilm assays which were established as already described in II.7.4.2 were also employed with 5 to 200 µg/mL of QsdR1 protein extract (potassium phosphate buffer served as a negative control). After incubating the test tubes with PAO1 under specified conditions, biofilm production on glass surfaces was evaluated visually. Similar to swarming tests, a range of 50-200 µg/mL of the protein was optimal for a visible inhibition of biofilm formation. Figure 22 shows two test tubes monitoring the different appearances. While the left test tube demonstrates a continuous biofilm for the negative control, the right test tube depicts a less developed, porous biofilm influenced by 50 µg/mL of QsdR1.

3.2.2.4.2 Pigment inhibition assay with *C. violaceum* ChV2

The biosynthesis of pigment violacein in *C. violaceum* ChV2 is dependent on QS. Strain ChV2 does not require external AHLs to be added to the medium for production of violacein because it produces its own AHL. Consequently, when AHLs are degraded in the present medium by the putative QQ protein QsdR1, no violacein production takes place (medium

remains white). The ChV2 assay was accomplished as stated in II.7.5.2. LB medium inoculated with different concentrations of a preculture of ChV2 was supplemented with 5-20 μg QsdR1 protein extract. H₂O as well as buffer served as a negative control. Surprisingly, no effect on the violacein production in ChV2 could be observed for the purified QsdR1 protein. Since the detailed sequence analysis of QsdR1 revealed homologies to zinc-dependent hydrolases of the β -lactamase superfamily, Zn²⁺ as a cofactor was tested for its effect on QsdR1's activity. Therefore, a ZnSO₄ solution was prepared and the assays were repeated with same QsdR1 protein amounts but supplemented with 2 mM ZnSO₄. The result demonstrated that only the addition of the cofactor Zn²⁺ activated QsdR1 and the subsequent degradation of the AHLs which led to an inhibition of violacein pigment production in ChV2. Negative buffer controls ensured that the inhibition effect resulted only from the activity of the QsdR1 and not substances present in the protein solution. Similar results were obtained for the inhibition assay accomplished with the protein and ChV2 on solid YDC medium (data not shown). Image D of Figure 22 shows exemplarily a section of the ChV2 microtiter plate assay where the first row gives the pigment production triggered by the buffer control, row two shows an unchanged pigment production when QsdR1 is present and row three shows QsdR1 activity triggered by cofactor Zn²⁺.

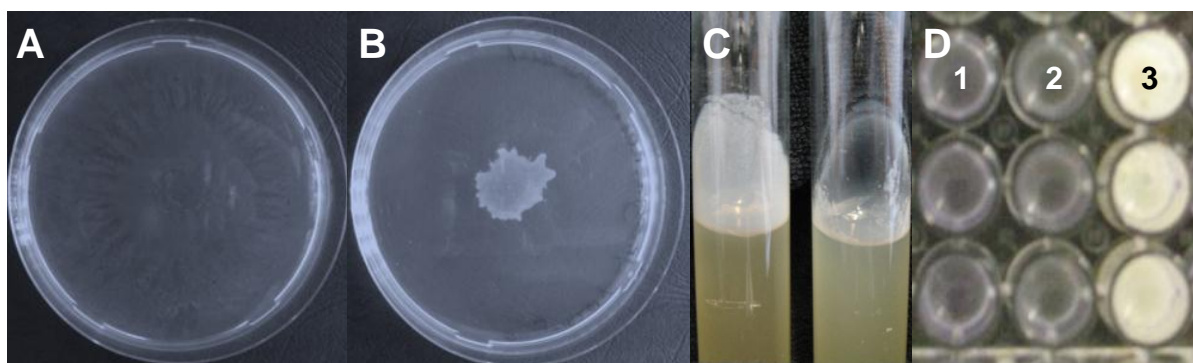


Figure 22: *P. aeruginosa* PAO1 swarming/biofilm assay and pigment inhibition in *C. violaceum* ChV2. (A) Potassium phosphate buffer control inoculated with PAO1 **(B)** Swarming plate supplemented with 50 $\mu\text{g}/\text{mL}$ QsdR1 prior to inoculation with PAO1. **(C)** Biofilm assay. Left: Test tube with potassium phosphate buffer inoculated with PAO1. Right: Test tube supplemented with 50 $\mu\text{g}/\text{mL}$ QsdR1 prior to inoculation with PAO1. **(D)** Pigment inhibition in ChV2. **Row 1:** Buffer control. **Row 2:** Unchanged pigment production in the presence of QsdR1. **Row 3:** Inhibited pigment production in the presence of QsdR1 and cofactor Zn²⁺.

The detected correlation between a cofactor and the activity of QsdR1 was only observed for assays carried out with ChV2. Neither the previous described motility assays nor the following β -galactosidase and HPLC-MS analyses demanded for the presence of such a cofactor in order to monitor an activity of QsdR1.

3.2.2.4.3 Determination of β -lactam degrading ability of QsdR1

Based on the close sequence similarity of QsdR1 to β -lactamase related proteins, a β -lactam antibiotic degradation assay was set up in order to test QsdR1 ability to utilize these substances. Therefore, the *qsdR1* gene was cloned into pET24c with previously described primers (*qsdR1_for/qsdR1_rev*, Table 5) using the same strategy as already employed for construction of pET21a::*qsdR1*. After transformation of pET24c::*qsdR1* into *E. coli* BL21 (DE3), the culture was plated onto LB agar containing 100 μ M IPTG and kanamycin. Small filter discs with different β -lactam antibiotics were placed on the agar surface. After an overnight incubation, the size of halos ranged from 2.8 cm for ceftriaxone to 1.5 cm for mezlocillin. The smallest halos were measured for penicillin G (1.2 cm) and cefadroxil (1.2 cm) demonstrating that QsdR1 has at least partially the ability to utilize β -lactam antibiotics (Table 19, VII.2.6). Nevertheless, no clear and distinct resistance to such antibiotics was observed in these tests using QsdR1. Therefore, further experiments focused more on the ability of QsdR1 to degrade AHL.

3.2.3 Biochemical characterization of QQ associated proteins, DIhR and QsdR1

Numerous function-based assays using biosensor strains like *A. tumefaciens* NTL4, *P. aeruginosa* PAO1, and *C. violaceum* ChV2 as well as additional screening procedures suggested that both loci comprised by pNGR234b were involved in modification or degradation of AHLs. Further enzyme activity assays using purified protein extracts of DIhR and QsdR1 should strengthen these findings and deliver precise data about the activity radius. In the context of this work initial rhizobial colonization experiments were accomplished to demonstrate that *dlhR* and *qsdR1* were able to affect plant root colonization. Lastly, DIhR and QsdR1 were subjected to HPLC-MS analysis to uncover the underlying cleaving mechanisms of these putative lactonases.

3.2.3.1 Verification of QQ effects of DIhR and QsdR1 by the β -galactosidase assay

AHL degradation triggered by DIhR and QsdR1 was quantified employing the β -galactosidase assay. Decrease of 3-oxo-C8-HSL was measured using the hydrolytic cleavage of ONPG substrate by the released β -galactosidase. Prior to overnight incubation with NTL4, 5 μ L of a 4.1×10^{-8} M 3-oxo-C8-HSL dilution were mixed with DIhR and QsdR1 protein extracts and incubated for 1.5 h at 30°C. For the reactions 2-10 μ g of recombinant DIhR protein and 4-30 μ g of recombinant QsdR1 were used to determine AHL degradation levels. Accumulated data from several repetitions displayed overlapping 3-oxo-C8-HSL degradation rates for both recombinant proteins. Protein levels of 4-10 μ g DIhR and QsdR1,

respectively showed the highest AHL decrease in the β -galactosidase assays and are summarized in Figure 23.

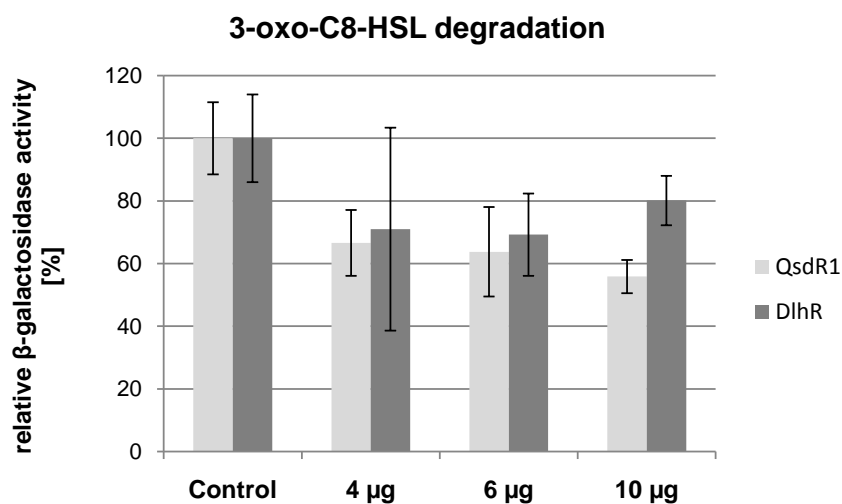


Figure 23: β -Galactosidase assay with NTL4. β -galactosidase activity in NTL4 after adding 3-oxo-C8-HSL and 4-10 μ g recombinant DIhR and QsdR1 protein extract. NTL4 without addition of 3-oxo-C8-HSL was employed as a positive control.

After a short incubation time with recombinant DIhR and QsdR1, the levels of detected 3-oxo-C8-HSL were significantly lower than those of the controls. No distinct or direct correlation between the applied recombinant protein amount and the degradation rate of AHLs could be measured. Nevertheless, a slight decrease of 3-oxo-C8-HSL with increasing QsdR1 amount was noticeable. In general, less than 73% of the added 3-oxo-C8-HSL could be detected after incubation with DIhR. The enzyme activity assay employed with recombinant and purified QsdR1 revealed an even more pronounced AHL degradation (Figure 23). In average, the β -galactosidase assays suggested that the QsdR1 degraded 40% of the added 3-oxo-C8-HSL revealing similar AHL reduction rates as already recorded for HitR and HydR but also for AldR and QsdR2. Consequently, these tests verified the ability of recombinant DIhR and QsdR1 to degrade 3-oxo-C8-HSL displaying a considerable degradation rate of more than 40%.

3.2.3.2 Characterization of DIhR and QsdR1 responsible for biofilm phenotypes in the rhizosphere

In the rhizosphere where nutrients and energy resources are limited, the strategy of AHL degradation was found to play a significant role in obtaining a competitive advantage in e.g. symbiosis over present microbes. Based on the functional and sequential findings of this research, it was found that NGR234 carries at least five QQ associated loci which might

facilitate its competition in mixed populations occurring in the rhizosphere. It was speculated that NGR234 carrying additional copies of the biochemically characterized proteins, DlhR and QsdR1, might enhance its competitive ability and be advantageous for its rhizosphere colonization. In order to test this hypothesis, NGR234 strains were constructed carrying extra copies of the two promising genes, *dlhR* and *qsdR1*, and were subjected to root colonization assays.

For the assembly of pBBR1MCS (hereafter pBBR) constructs, *dlhR* as well as *qsdR1* were PCR amplified from expression vectors pET21a::*dlhR* and pET21a::*qsdR1*, respectively using the T7 promoter/T7 terminator primer pair (Table 5). The purified PCR products were then ligated into *EcoRV* linearized pBBR vectors. Furthermore, to express *dlhR* and *qsdR1* in NGR234 cells under the control of pBBR P_{taq} promoter, only constructs harboring desired genes directed in line with the promoter were chosen for further assays. Obtained constructs pBBR::*dlhR* and pBBR::*qsdR1* were verified by sequencing and transformed via electroporation into NGR234 cells. NGR234 cultures harboring the constructs were established in liquid YEM medium supplemented with antibiotics or on YEM plates supplemented with antibiotics and congo red.

Primarily, the phenotype of NGR234 cells harboring extra copies of both genes was monitored. In Figure 24, images A-D demonstrate modified phenotypes of NGR234 expressing additional copies of *dlhR* and *qsdR1*. PCR based analysis revealed that although growing on YEM medium with chloramphenicol, red colored NGR234 mutants were lacking the desired constructs (images A/C). Only white appearing NGR234 colonies were harboring pBBR::*dlhR* (image A) or pBBR::*qsdR1* (image C). A similar phenotype could be monitored in liquid cultures where white and red NGR234 colonies were used to inoculate liquid YEM medium. Images B and D depict liquid cultures of NGR234 harboring pBBR::*dlhR* and pBBR::*qsdR1*, where B1 and D1 display white appearing colonies and B2 and D2 red appearing NGR234 colonies. Clearly, a difference in the composition of the cultures as well as biofilm formation and color could be noticed concluding that the expression of additional copies of *dlhR* and *qsdR1* influences the phenotype of NGR234. These cultures seemed to produce more cell material and extracellular polymeric substances, which might represent an advantage over other competitors in the rhizosphere. Consequently, only white appearing NGR234 mutants were employed for further rhizosphere assays.

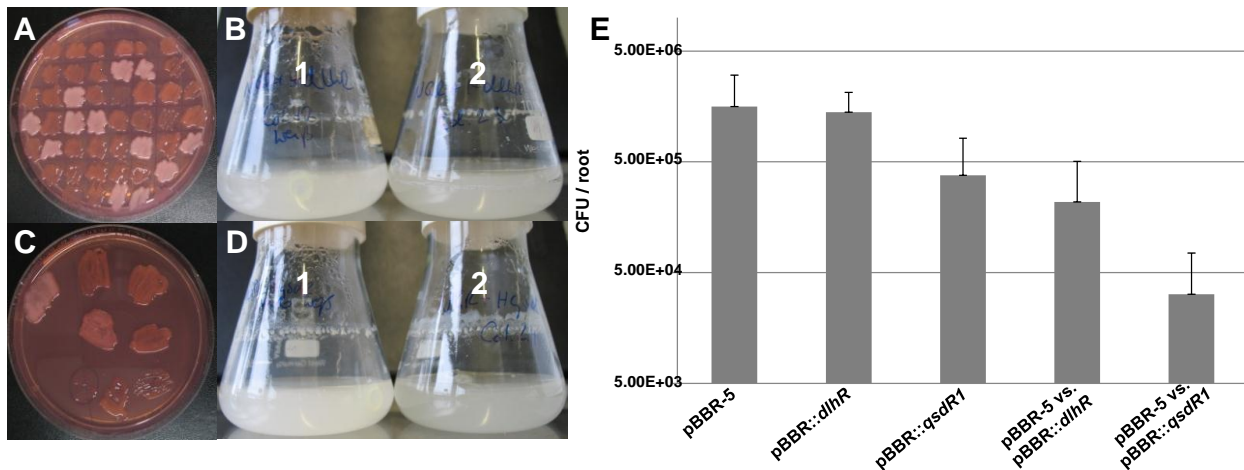


Figure 24: Biofilm phenotype of NGR234 in medium and the rhizosphere triggered by extra copies of *dlhR* and *qsdR1*. (A+C) NGR234 cells on YEM agar supplemented with congo red with a modified appearance of colonies triggered by extra copy of *dlhR* (A) and *qsdR1* (C). (B+D) Liquid cultures of NGR234 harboring constructs pBBR1::*dlhR* and pBBR1::*qsdR1*, B1/D1 were inoculated with white and B2/D2 with red appearing colonies. (E) Growth of NGR234 in the cowpea rhizosphere. Data represent mean numbers (CFU) of bacteria per root from a minimum of five replicates. From left to right: Control: pBBR-5 (NGR234 harboring the empty pBBR1MCS-5); pBBR::*dlhR* (NGR234 with extra copy of *dlhR* in pBBR1MCS); pBBR::*qsdR1* (NGR234 with extra copy of *qsdR1* in pBBR1MCS); pBBR-5 vs. pBBR::*dlhR* (competition experiments with NGR234 carrying control pBBR-5 versus NGR234 carrying pBBR::*dlhR*); pBBR-5 vs. pBBR::*qsdR1* (competition experiments with NGR234 carrying control pBBR-5 versus NGR234 carrying pBBR::*qsdR1*). The two last bars indicate the bacteria recovered carrying the extra copies of the corresponding QQ genes (i.e. *dlhR* and *qsdR1*). Bars indicate simple standard deviations.

Colonization tests were carried out on cowpea roots by inoculating each NGR234 mutant individually and in competition with the control strain (NGR234 harboring pBBR1MCS-5). Under the experimental conditions NGR234 grew and colonized the root most rapidly between three and six days after inoculation. Thus, after four days the plants were harvested and bacteria were recovered from developed roots. Bacterial numbers were quantified by measuring the colony forming units. These tests indicated that the control strain was most efficient in root colonization in all tested combinations (Figure 24E). While the strain carrying an extra copy of the *dlhR* gene was in general only slightly affected in its capability to colonize the root surface, the strain carrying the *qsdR1* gene was significantly affected in its rhizosphere colonization capability. Additional competition experiments confirmed these findings (Figure 24E, bars 3-4). In these tests the strains carrying extra copies of the *dlhR* or the *qsdR1* gene were outnumbered by the control strain and colonized the rhizosphere at a statistically significantly ($P \leq 0.01$) lower level. In fact the *qsdR1* strain was outnumbered by at least an order of magnitude by the control strain when coinoculated into the rhizosphere at equal numbers (CFU/mL), and the strain carrying extra copies of *dlhR* by a factor of 5-7. The experimental data suggest that both genes contribute to rhizosphere colonization fitness of NGR234 and are possibly involved in the degradation of plant-derived or microbial autoinducer molecules in the rhizosphere.

3.2.3.3 Uncovering the cleaving mechanisms of DIhR and QsdR1 by HPLC-MS analysis

The enzymatic degradation of AHLs by the recombinant proteins DIhR and QsdR1 was confirmed by the prior described enzyme activity assay. Nevertheless, cleavage or modification of such QS signal molecules can occur in different ways (lactone hydrolysis, amide bond hydrolysis, oxidoreduction) highlighted in the introduction (1.2.3). To detect the underlying cleavage mechanisms of AHL inactivation by recombinant DIhR and QsdR1, HPLC-MS analysis was performed in cooperation with the Institute for Organic Chemistry at the University of Tuebingen.

Therefore, 20 μ L of 3-oxo-C8-HSL were incubated with 0.005-0.3 mg/mL purified protein in 100 mM potassium phosphate buffer (for DIhR pH 7.5, for QsdR1 pH 7.0). After incubation and extraction, reaction products were analysed by HPLC-MS-DAD. To evaluate the spontaneous degradation of 3-oxo-C8-HSL, control experiments were accomplished with an inactive glycosyl transferase. The construct pET21a::*conT* comprising a glycosyl transferase with a frame shift was subjected to the same conditions and concentration of 3-oxo-C8-HSL. Repeated measurements with protein concentration of 0.01 mg/mL for DIhR and 0.1 mg/mL for QsdR1 indicated that the underlying mechanism of AHL degradation was a hydrolysis of the lactone ring of 3-oxo-C8-HSL (Figure 25).

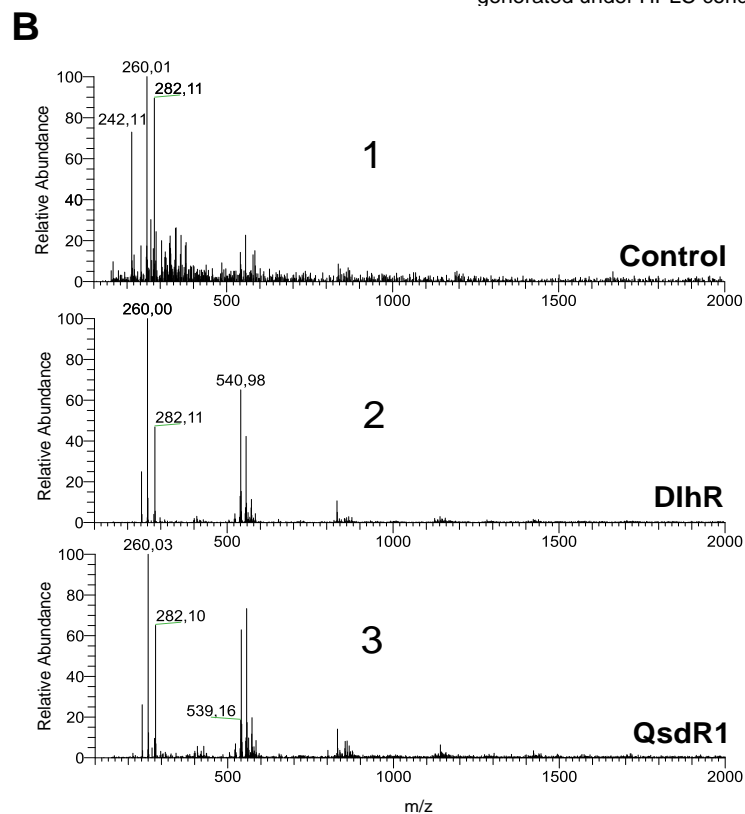
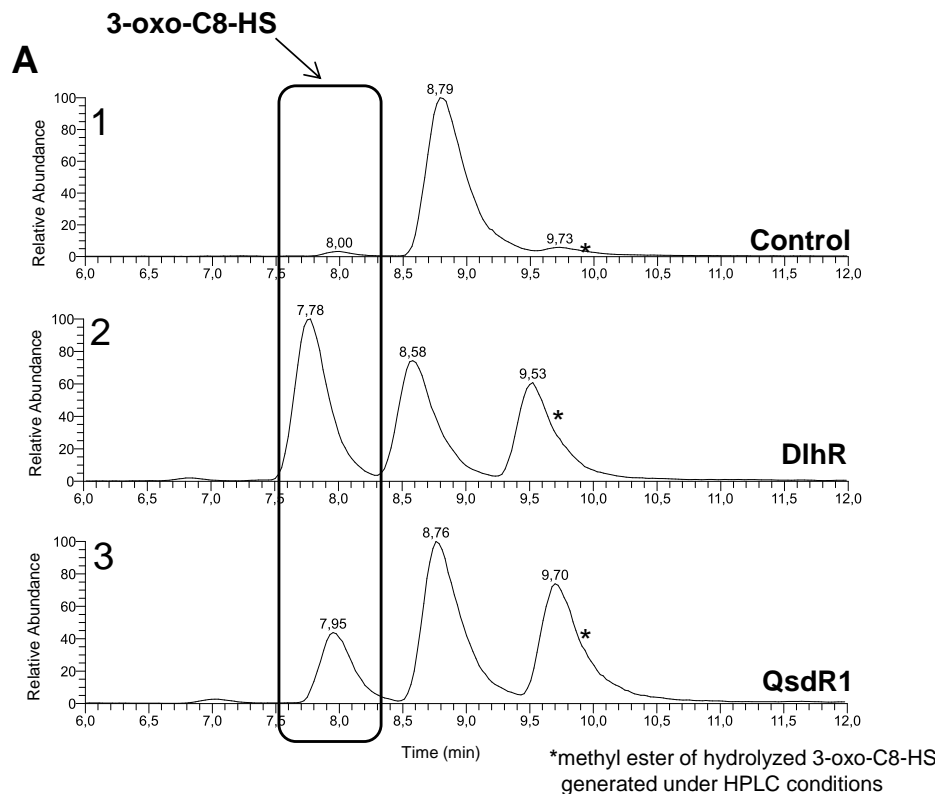


Figure 25: HPLC-MS analysis of recombinant DIhR and QsdR1. (A) HPLC-UV spectra recorded at 252 nm for 3-oxo-C8-HSL after incubation with control, DIhR, and QsdR1. **(B)** Respective mass spectra recorded for samples treated with either control protein, DIhR, or QsdR1. **(A1)** HPLC-UV chromatogram depicts the control incubated with 3-oxo-C8-HSL, displaying only one distinct peak at R_t 8.8 min for 3-oxo-C8-HSL. **(B1)** Mass spectrum of control (at R_t 8.0 min) showed the following ions: $[M+H]^+$ ion at an m/z of 242.1 (significant for this compound); $[M+H]^+$ ion at an m/z of 260.01 and $[M+Na]^+$ at an m/z of 282.1 (spontaneous degradation of 3-oxo-C8-HSL). **(A2)** HPLC-UV chromatogram for 3-oxo-C8-HSL incubated with DIhR showing the peak at R_t 7.8 min for the cleavage

product 3-oxo-C8-HS. The peak at R_t 8.6 min displays the unhydrolyzed 3-oxo-C8-HSL and a not relevant by-product (a methyl ester), which is only generated under HPLC conditions, was detected at R_t 9.6 min. **(B2)** Corresponding mass spectrum shows three characteristic ions: $[M+H]^+$ ion at an m/z of 260.0, a $[M+Na]^+$ ion at an m/z of 282.1 and a $[2M+Na]^+$ ion at an m/z of 540.2. **(A3)** HPLC-UV chromatogram of hydrolyzed 3-oxo-C8-HSL by QsdR1. The cleavage product was detected at R_t of 8.0 min, both peaks for the non-hydrolyzed form of 3-oxo-C8-HSL as well as the methyl ester were recorded for QsdR1 as well. **(B3)** Mass spectrum as already given for DIhR showed the characteristic ions ($[M+H]^+$ ion, a $[M+Na]^+$ ion and a $[2M+Na]^+$ ion at same m/z).

Determined by HPLC analysis and followed by mass spectrometry, the enzymatic 3-oxo-C8-HSL degradation resulted in a mixture of 3-oxo-C8-HS (opened lactone ring) with a R_t of ~7.9 min and a methyl ester of hydrolyzed 3-oxo-C8-HS with a R_t of ~9.6 min, only generated under given HPLC conditions. Peaks detected at R_t of ~8.6 min display the unhydrolyzed 3-oxo-C8-HSL form. The 3-oxo-C8-HSL incubated with the control protein resulted in the detection of almost exclusively the non-hydrolyzed form of 3-oxo-C8-HSL. Panel A1 of Figure 25 shows the HPLC-UV spectrum at 252 nm for the control, displaying only one distinct peak at R_t 8.8 min, representing 3-oxo-C8-HSL. A peak showing the relative abundance of the hydrolyzed form was under the detection limit, consequently no significant lactone hydrolyzation linked to the control could be detected. The mass spectrum of the control (at R_t 8.0 min) showed a $[M+H]^+$ ion at an m/z of 242.1 significant for this compound. $[M+H]^+$ ion at an m/z of 260.01 and $[M+Na]^+$ at an m/z of 282.1 were also detected owing to spontaneous degradation of 3-oxo-C8-HSL (Figure 25, panel B1). Both proteins incubated with 3-oxo-C8-HSL were able to hydrolyze the lactone ring of this *N*-AHL. HPLC-UV spectra detected at 252 nm for DIhR and QsdR1 showed almost identical retention times for the cleavage product 3-oxo-C8-HS with the opened lactone ring. Peaks were detected at R_t 7.8 min for DIhR and at R_t 8.0 min for QsdR1 (Figure 25, panel A2 and A3). Relative abundance of the 3-oxo-C8-HS compound found for both proteins was considerably higher compared to the control, thus displaying a good enzymatic degradation of 3-oxo-C8-HSL by both QQ associated proteins. Mass spectra for the proteins show a characteristic $[M+H]^+$ ion at an m/z of 260.0, a $[M+Na]^+$ ion at an m/z of 282.1 and a $[2M+Na]^+$ ion at an m/z of 540.2 (Figure 25, panel B2 and B3).

In summary, the control incubated under identical conditions as chosen for DIhR and QsdR1 with 3-oxo-C8-HSL did not produce a peak at R_t of ~7.9 min, which is characteristic for the cleaved form, 3-oxo-C8-HS. The HPLC-UV as well as mass spectrum data for both recombinant proteins confirmed a lactonolytic enzyme activity, giving evidence that DIhR and QsdR1 act as true lactonases in NGR234.

IV. Discussion

In the last 40 years, various research groups addressed their scientific question to cell-to-cell communication of microorganisms. The phenomenon of QS was initially discovered in *Vibrio fischeri* in 1970 by Nealson and colleagues (Nealson *et al.* 1970). Since then QS in its diversity has been demonstrated in many different Gram-negative and Gram-positive bacteria employed to synchronize group behavior and regulate gene expression in populations. The ability to communicate via diverse QS systems obviously forced bacteria to evolve a strategy to rival with each other by means of QS and the involved signal molecules. This process called quorum quenching enables bacteria to protect themselves from antagonists and to disarm competitors, which would colonize their niches within a population. The QQ strategy of Gram-negative and Gram-positive bacteria was investigated intensively and attained importance as clinical relevant phenotypes of bacteria like *P. aeruginosa* and its biofilm production were associated with QS. Biofilms developing in lungs (cystic fibrosis) or on urine and heart catheters could be blocked using anti-QS agents produced by bacteria. Such harmful QS-regulated phenomena (e.g. biofilm formation) are not only restricted to human-bacterial interactions, but were also observed in animals and very prevalent in plant-microbe interactions. Consequently, the application of such QQ approaches became a novel, valuable strategy to limit bacterial infections in humans, animals and in plants.

The most interesting aspect of QQ lies in the nonlethal strategy, where only a limited selective pressure is used to regulate survival of bacteria. Especially in plant-microbe interactions, this QQ strategy is often adopted by plants to disarm harmful pathogenic partners but also employed by plant-associated nitrogen-fixing bacterial communities to counteract direct competitors, which otherwise would gain the upper hand in this symbiosis (1.2.5). Still, few is known about QS and QQ systems of these plant symbionts. One of the main speculations on the research field of QQ in plant-associated bacteria deals with the connection of the number and diversity of symbiotic plant hosts and the QQ-mediated defense mechanisms owned by such symbiotic microorganisms. The hypothesis is: The more different symbiotic interactions can be established between plant hosts and nitrogen-fixing bacteria, the more QQ defense mechanisms are held by these bacteria to obtain a competitive advantage over present symbiotic soil bacteria. This hypothesis can also be interpreted vice versa, the greater the QQ inventory of such symbionts is, the greater is their number of plant hosts.

The main subject of the present work was the α -proteobacterium *Rhizobium* sp. NGR234 with its extremely broad range of symbiotic partners. NGR234, a representative of the

rhizobia which form nitrogen-fixing nodules, can establish a symbiotic relationship with more than 120 different genera of legumes and even one nonlegume. This broad host range is unique and until today, no other microsymbiont was discovered holding as many symbiotic partners as NGR234. Therefore, this characteristic qualifies NGR234 as a suitable candidate organism to accomplish initial studies answering the question of its correlation between QQ and the wide range of plant hosts.

The goal of the present research was to describe and investigate the inventory of QQ systems and enzymes owned by NGR234. After completing the whole genome sequence of NGR234, comparative genomics provided first insights into mechanisms involved in communication. Additionally, sequence data obtained for transport as well as secretion associated machineries could illuminate further puzzles of its broad host range. The available data set of QS and QQ systems was extended using a function-based screening, revealing a surprisingly large number of QQ associated loci within the genome of NGR234. In this context, five QQ active loci could be identified, whereas two were biochemically characterized.

1. The number of secretion systems correlates to the host range of *Rhizobium* sp. NGR234

The detailed sequence and comparison analysis accomplished with the genome of NGR234 revealed that this microbe carries 132 genes associated with secretion and hereby portrays a unique candidate in the Rhizobiales order. The secretion of proteins based on type I (T1SS) and type II secretion systems (T2SS) plays an important role in the symbiosis of rhizobia and their eukaryotic hosts. Specialized secretion machines like the type III secretion apparatus (T3SS) are deployed by Gram-negative bacteria to translocate numerous effector proteins directly into the cytoplasm of their eukaryotic hosts (Marie *et al.* 2001). Type IV secretion systems (T4SS) were uncovered in the plant-associated microbe *Agrobacterium tumefaciens* to introduce parts of the Ti-plasmid into the plant host (Chen *et al.* 2002). Type V machines are employed as autotransporter systems and type VI secretion systems seem to be involved in stress sensing (Weber *et al.* 2009). Conclusively, a wealth of secretion apparatuses are participating in interactions between plant-associated bacteria and their hosts, thus a speculation on the correlation between the host range of rhizobia and the number of specialized protein secretion systems emerged. It is obvious that secretion, transport, and translocation of exoproteins into the surroundings are essential for a successful plant-microbe communication and interaction (Deakin and Broughton 2009). NGR234 constitutes

an outstanding candidate within the rhizobia carrying almost twice as much secretion related genes as found in other plant-associated microbes. The sequence-based findings on the variety of secretion related proteins in NGR234 might deliver first answers to its broad host range, as candidates like *S. meliloti* SM1021 or *R. leguminosarum* nodulate only a restricted number of plants, which is in line with their few secretion associated proteins. Compared to NGR234, *S. meliloti* and *R. leguminosarum* comprise less than half of the 132 proteins involved in secretion processes which might be a hint to their narrow host range (Schmeisser *et al.* 2009).

2. Quorum sensing in NGR234 and selected rhizobia

Diverse QS mechanisms were identified in several representatives of the *Rhizobiaceae* family (Gonzalez and Marketon 2003). *R. leguminosarum* bv. *viciae* possesses the best characterized and complex QS regulatory network, composed of Rai, Rhi, Cin and Tra (Wisniewski-Dye and Downie 2002). This QS circuit was shown to be responsible for the production of five AHLs varying in chain length, while other strains like *R. etli* CNPA512 synthesize up to seven different AHLs. Most of the underlying intertwined QS systems are in fact identified but still poorly understood. *B. japonicum* appears to be unique, because cell density-dependent processes were detected in experimental studies however, no AHL production could be demonstrated (Loh *et al.* 2002a). Instead, this microbe uses a different extracellular signal molecule (bradyoxetin). In order to investigate the QS circuits comprised by NGR234, comparative analyses using all published QS systems were employed. Direct comparisons with two close relatives, *S. meliloti* SM1021 and *S. fredii* USDA257, proved to be most suitable (Figure 26). While the mediterranean isolate *S. meliloti* SM1021 is only capable of nodulating three plant genera (Capela *et al.* 2006), and NGR234 originating from *Lablab purpureus* is able to undergo symbiosis with over 120 genera of legumes, *S. fredii* USDA257 isolated from a wild soybean constitutes the middle with 79 genera of legumes, displaying an exact subset of NGR234 plant hosts (Pueppke and Broughton 1999). USDA257 is of great interest and importance because it is closely related to NGR234 and shares a relatively high number of symbiotic partners. Unfortunately, the USDA257 genome project is not yet completed, which makes detailed alignment and comparative analyses very difficult.

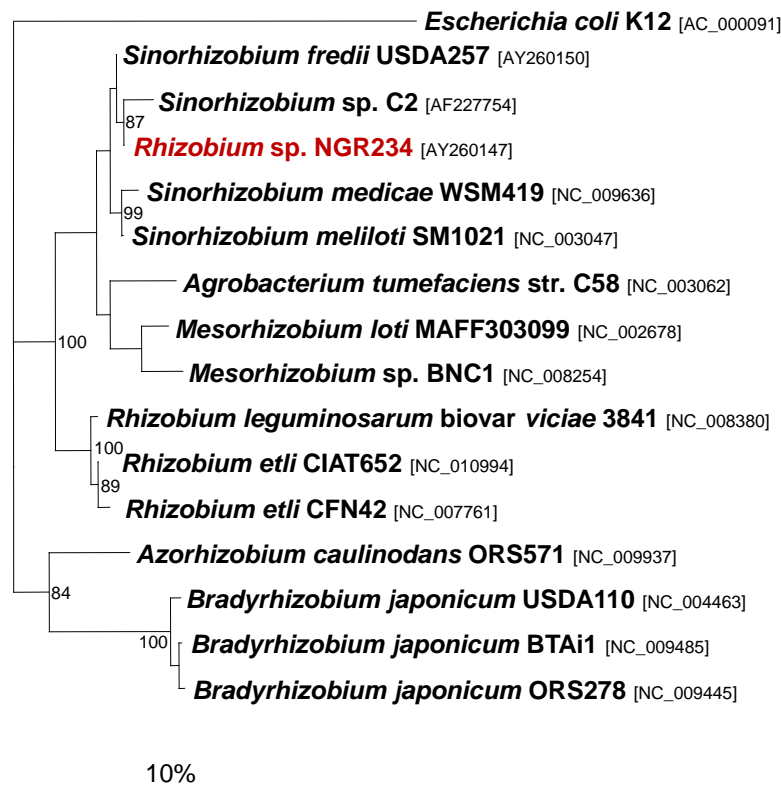


Figure 26: Phylogenetic relationships of rhizobia. 16S rRNA genes from selected rhizobial species as determined by Maximum Likelihood analysis. The percentage of bootstrap resamplings above 80 is indicated at the different nodes. The scale bar represents the expected number of changes per nucleotide position.

2.1. AHL-mediated cell-to-cell communication

The newly established genome sequence of NGR234 confirmed the presence of a TraI/TraR homolog on pNGR234a and additionally, uncovered a novel chromosome borne QS system not described before in NGR234. He and coworkers already indicated that NGR234 produces along with the characterized 3-oxo-C8-HSL two other AHL-like compounds, suggesting the presence of other AHL synthases elsewhere in the genome (He *et al.* 2003). Utilizing the large set of genomic data and other rhizobial genomes, one additional AHL synthase NgrI possibly responsible for the synthesis of one of the AHLs, could be identified. The corresponding regulator NgrR was also found in the genome of NGR234 (Schmeisser *et al.* 2009).

The localization of the CinI/R of *R. leguminosarum* and SinI/R system of *S. meliloti* SM1021 on the chromosomes of these organisms supported the obtained data of a novel QS system present on cNGR234 as well. The inverted order of synthase and regulator genes of the CinI/R system comprised by *R. leguminosarum* and the SinI/R system of *S. meliloti* SM1021 (Marketon and Gonzalez 2002) is identical to the NgrI/R, possibly arising from a shared

ancestor. Strain *S. fredii* USDA257 also holds homologous of this system, nevertheless an interpretation of the results is difficult due to the incomplete genome sequence. Using the ERGO database for further analysis of *ngrI/R* related genes revealed that only few rhizobial representatives appear to have a similar QS system (*R. etli* CFN42, *R. etli* CIAT652, and *Bradyrhizobium* BTA1). In other rhizobia comprised by ERGO individual AHL synthases and regulators were found but not in a cooperative manner (e.g. *Burkholderia glumae* BGR1, *Mesorhizobium loti*) (Yang *et al.* 2009). Additionally, the *NgrI/R* system holds a specific and outstanding feature. A nearby hypothetical protein (NGR_c16910) which is depicted in Figure 5 is possibly involved in regulation of the *NgrI/R* circuit. The ORF NGR_c16910 was found to have moderate homologies to *CinS* (*R. leguminosarum*) and the conserved hypothetical protein SMc00167 (*S. meliloti* SM1021) both localized upstream of the chromosome borne QS systems. Investigation on the *cin* and *rai* QS regulatory systems in *R. leguminosarum* proved that *cinS* together with a second gene regulates the expression of *rail/R* and other hierarchical genes. Edwards and colleagues could prove that *CinS* is translationally coupled to AHL synthase *CinI* and consequently mediates QS regulation in this microbe (Edwards *et al.* 2009). Based on the sequential homologies of the hypothetical protein NGR_c16910 to *cinS*, there were speculations about its similar function in NGR234 and within the *ngrI/R* QS system. Although, NCBI BLAST analyses revealed no significant similarities to characterized proteins, NGR_c16910 (proposed designation *ngrS*) could contribute to the regulation of *ngrI/R* and additionally mediate hierarchical genes and processes. Other orthologous of gene *cinS* were also identified in closely related rhizobia (e.g. *R. etli* CFN42, CIAT652) immediately downstream of the *luxI*-associated proteins. This is in line with the sequential findings of the chromosome borne *ngrI/R* related system in other rhizobia, moreover *cinS* supports the speculation of these microbes together with NGR234 that harbors an additional QS system with *ngrS* (Schmeisser *et al.* 2009).

Following up experimental studies of He (He *et al.* 2003), it was speculated that *NgrI* constitutes to the synthesis of the long-chain AHL rather than the short-chain AHL. Although, there is no experimental evidence, homologies to *CinI* of *R. leguminosarum* and *SinI* of *S. meliloti* SM1021 indicate that the AHL synthase *NgrI* might be responsible for the production of AHLs with chain lengths above 12 carbons. In strain *R. leguminosarum* the synthesis of the QS molecule 3-OH-C14:1-HSL was subscribed to the *cinI* locus (Lithgow *et al.* 2000; Schripsema *et al.* 1996). Detailed studies carried out with *SinI/R* identified several long-chain AHLs ranging from 12-18 carbons being synthesized in *S. meliloti* SM1021 (Barnett and Fisher 2006; Marketon and Gonzalez 2002; Marketon *et al.* 2003). Conclusively, it is most likely, that *NgrI* synthesizes long-chain AHLs.

Beside the Tral and NgrI synthase, the genome sequence of NGR234 did not reveal other additional AHL synthases. The remaining short-chain AHL mentioned by He and researchers (He *et al.* 2003) might be on the one hand a by-product of the long-chain AHL generated by NgrI or 3-oxo-C8-HSL modified by NGR234 itself. Another possibility could be that the comparative analysis of the NGR234 genome missed a putative AHL synthase, which might be due to the lack of similarities to already published AHL synthases. Nevertheless, copies of five LuxR-type response regulators featuring an autoinducer binding domain were found on pNGR234*b* and cNGR234. This rich inventory of putative response regulators might enable NGR234 to respond to many different AHLs produced by competitors in the rhizosphere.

2.2. AI-2 and AI-3 signaling systems can contribute to the broad host range of NGR234

Beside the interspecies AHL-based communication of NGR234 discussed already above, deeper insights into AI-2 and interkingdom signaling systems might deliver some missing links to describe, explain and understand NGR234's broad host range of symbiotic partners. The following chapters are addressed to AI-2 and AI-3-mediated signaling systems owned and possibly operated by NGR234.

2.2.1 AI-2-mediated signaling systems found in NGR234

Autoinducer 2 driven mechanisms are employed by bacteria to communicate on the interspecies level, allowing them to regulate gene expression in response to the composition of mixed bacterial populations. The AI-2 and its synthase gene *luxS* have been identified in different bacteria regulating behaviors like formation of biofilms (*Vibrio cholerae*, Xavier and Bassler 2005), motility (*Helicobacter pylori*, Rader *et al.* 2007) or bioluminescence (*Vibrio harveyi*, Schauder *et al.* 2001). In many other species, the role of AI-2 recognition and response is still unclear. Until today, in only three species, *V. harveyi*, *V. cholera* and *S. typhimurium*, AI-2 recognition as well as its signal relay could be determined in detail (Surette *et al.* 1999). Consequently, these systems are consulted to evaluate possible underlying AI-2 cascades. Genome wide analyses of *luxS* as well as other members of the AI-2 QS circuit were accomplished for NGR234, revealing surprising correlations. No orthologous of the AI-2 synthase gene *luxS* were found in the sequence of NGR234, speculating that this *Rhizobium* lacks the ability to produce its own AI-2 signal molecule. However, most of the components of the AI-2 circuit (e.g. LuxQ, LuxO) were found within the genome present in several copies, whereas LuxU as well as LuxP remained undiscoverable. Comparative and phylogenetic analyses on this universal signaling system accomplished in 2004 (Sun *et al.* 2004) support the sequence-based findings. Using 138 completed genomes

for their research, Sun and colleagues found that the gene *luxS* is widespread in bacteria (except for some parasites and symbionts), while most of these microbes lack the periplasmic binding protein LuxP and the signal relay protein LuxU. Both proteins were found by highly matches only within the *Vibrio* strains. They speculated that the response in the remaining bacteria to such AI-2 signals might be realized by the utilization of other components. The presence of the gene *luxS*, necessarily for the AI-2 production, is not required to enable bacteria to recognize and respond to AI-2. Experimental evidence for this correlation was already gathered using NGR234's close relative *S. meliloti* SM1021. This microbe lacks the AI-2 synthase gene *luxS*, nevertheless was able to respond to AI-2 present in the environmental medium (Pereira *et al.* 2008). The interesting study extended the speculations and hypotheses on the AI-2 communication of NGR234 and its importance. Because the production and release of AI-2 signal molecules is cell growth-dependent, these AI-2 signals store utilizable information for other present microbes (Galloway *et al.* 2011; Xavier and Bassler 2003). Presumably, NGR234 utilizes these AI-2 signals on the one hand to regulate its own gene expression to be capable of competing with antagonists and on the other hand to eliminate this signal from the environment. Experimental studies with *S. meliloti* SM1021 revealed that AI-2 functions as a signal molecule and not as a metabolite (Pereira *et al.* 2008). Consequently, this kind of interference with AI-2 QS systems must hold a benefit for NGR234 and its plant hosts.

2.2.2 AI-3 molecule based signaling systems

The bacterial-host conversation is an important aspect of symbiosis and is considered to be accomplished by an AI-3 molecule associated communication. Bacteria use beside AI-3 hormone like compounds known as epinephrine and norepinephrine to transmit their information to host cells. Furthermore, these autoinducer molecules are recognized by a two-component signal transduction system and transcriptional factors. Until today, this communication system was only uncovered in the human pathogen enterohemorrhagic *E. coli* O157:H7 but also observed in bacteria of the natural intestinal flora (Reading and Sperandio 2006; Walters and Sperandio 2006). The complex systems QseA/BC and QseD/EF are mainly composed of response regulators, sensor histidine kinases and transcriptional regulators. Taken together, these proteins are ubiquitous in bacteria consequently, similarities on a low level were also determined for NGR234. The present results obtained by the sequence-based approach can be misleading, as NGR234 carries at least 50 transcriptional regulators, as well as many copies of regulators and histidine kinases. Conclusively, the apparent similarities to QseA/BC and QseD/EF arose rather from sequence similarities than from actual homologies to the AI-3 QS system. Experimental evidence would enlighten the above stated speculations.

2.3. Correlation of QS-mediated communication in NGR234 and its number of symbiotic partners

Although, a novel AHL-based QS system could be identified and described in NGR234, the provided data only allows minor speculations about the broad host range of symbiotic partners. More focus should be put on the relatively high number of AHL response regulators owned by NGR234. The diversity of synthesized AHLs is very low, so NGR234 possibly uses the AHL-mediated communication system rather to recognize and respond to diverse AHLs secreted by its environment than to produce its own AHL. A similar observation was made for the AI-2 associated communication hold by NGR234. Although, NGR234 lacks the AI-2 synthase gene *luxS*, this microbe might possess the ability to sense and respond to AI-2 transmitted by diverse bacteria in populations found in environments like the rhizosphere. In this context, NGR234 might disrupt indirectly the communication of surrounding competitors by depleting the AI-2 concentration. The main speculation is that NGR234 tracks these indirect strategies to gain an advantage over other symbionts to establish a successful symbiosis with leguminous plants. Instead of actively producing signal molecules to communicate with prevalent bacteria, NGR234 passively uses the transmitted signals to alter and adapt its expression of crucial genes.

3. QQ in *Rhizobium* sp. NGR234

The presence of multiple QS systems utilized by diverse microorganisms inevitably led to the development of defense strategies to counteract harmful and unwanted interactions. Especially in the rhizosphere of plants, where a variety of microbes coact and rival for the symbiotic host, such QQ based strategies might provide a competitive advantage. These QS interfering strategies are employed by many plant symbionts for example to down regulate the expression of virulence genes involved in plant-microbe interactions of other present symbionts (Dong *et al.* 2004). The fact that microbes obtain the upper hand under such competing environmental conditions presumably correlates with the number of its symbiotic partners. Thus, detailed investigations combining sequence-based approaches with function-based screenings can deliver first answers to this question. Discovering novel QQ enzymes and circuits within the genomic information of symbiotic microbes might uncover the reason for a broad host range in their symbiotic interrelations.

3.1. Multiple QQ associated genes owned by NGR234 collaborate with its broad host range

Completing the whole genome of NGR234 provided access to numerous sequential data concerning the QQ inventory. The genome of NGR234 revealed the presence of 23 putative genes, which were associated with QQ (Table 14). Based on their annotation 18 of these 23 putative genes could be grouped to AHLases. Most of these ORFs showed the presence of the conserved motif “HXHX~DH”, other conserved residues as well as residues related to zinc-binding activity of AHLases were not considered in the context of the research. Nevertheless, based on the experimental findings for the two QQ associated ORFs *qsdR1* and *qsdR2*, the presence of such a conserved pattern allows the assumption that these ORFs might contribute to enzymatic AHL degradation by lactonolysis. Only five of these 18 identified ORFs were similar to previously published AHLases with identities ranging from 24% to 34% (in detail: ORF NGR_b16870 displayed an identity of 24% to Aii2, NGR_b15850 with 34% to AhIK, NGR_c03760 with 27% to Aii2, NGR_c05950 with 39% to AhID, and NGR_c06480 with 27% to QIcA). Although the identities were relatively low for these five ORFs, it was the first indication of ORFs associated with the function of AHLases in NGR234. The metal-dependent phosphohydrolase found on cNGR234 showed, in a direct comparison to QsdA, an AHL degrading phosphotriesterase discovered in *Rhodococcus erythropolis* W2 (Uroz *et al.* 2008), no significant correlation.

Although, the two ORFs (NGR_b22150 and NGR_c03800) resembling dienelactone hydrolase-like proteins did not provide any sequential similarities to published QQ enzymes, their predicted function strongly argued that these proteins could belong to lactonases. In natural environments, dienelactone hydrolases play a crucial role in microbial degradation of chloroaromatics, they catalyze dienelactone to maleyacetate in the chlorocatechol pathway (see also IV.3.3.2.1). Presumably these dienelactone hydrolase-like proteins might hold the ability to catalyze AHL molecules. Nevertheless, few is known about the AHL degrading function of such hydrolases. Until today, only BpiB07 was experimentally proved to interfere with bacterial QS systems (Schipper *et al.* 2009). Thus, there are only speculations about the AHL catalyzing function of both ORFs.

The remaining five ORFs were associated with amidases. Consequently, it was considered that these genes might be related to AHL amidases. In nature, amidases play a significant role in C-N bond formation and cleavage in prokaryotic organisms (Sharma *et al.* 2009). Conclusively, this group of enzymes might be involved in QQ processes by the cleavage of C-N bonds in AHL molecules.

In contrast to AHLases, the research field of AHL amidases is still emerging and only few studies offered experimental evidence for their enzymatic activity. However, the common characteristic of Ntn-hydrolases however could not be identified within the five ORFs.

To draw conclusions from the wealth of genes possibly involved in defense strategies in NGR234, other rhizobial representatives were consulted and analyzed upon their QQ inventory. Not only the close relatives *S. meliloti* SM1021 and *S. fredii* USDA257, but also the genomes of other plant symbionts were used to search for corresponding genes (Table 17). Surprisingly, the richness of QQ related genes is not limited to NGR234, although it has the highest number of 23 ORFs. Twenty copies of the NGR234 QQ associated genes were found within the genomes of *R. leguminosarum* bv. *viciae* 3841 and *S. fredii* USDA257. In 3841 the numerous QQ genes might contribute to the wealth of QS systems found in relative *R. leguminosarum* bv. *viciae*. The richness of AHL-mediated systems might possibly be transferred to 3841 and correlate to a high number of QQ related genes. Between 14 and 16 copies of the uncovered QQ associated genes were found within the genomes of *R. etli* CFN42, *M. loti* MAFF303099 and *B. japonicum* USDA110. Due to its narrow host range of symbiotic partners, it was expected that *S. meliloti* SM1021 carries the fewest number of QQ related genes, but this was not the case. Seventeen out of the 23 ORFs were identified in the genome of SM1021 (Table 17). A correlation between the phylogenetic distance of the rhizobial strains and their number of homologous QQ genes could not be observed. Beside these findings, no conclusions concerning the number of symbiotic partners and the direct correlation to the number of genes with a possible QQ activity could be drawn. The individual identities of these discovered ORFs range from $1e^{-205}$ (NGR_c10650 to SM1021) with a significant similarity to $1e^{-8}$ (NGR_c06480 to USDA110) completely unrelated. Around 75% of QQ related genes owned by NGR234 display significant analogs ($<e^{-50}$) within the other rhizobial genomes, for the remaining ORFs the similarity was too low to be considered as an analog. Best hits were monitored within the 20 copies of *S. fredii* USDA257. A more detailed analysis of single ORFs in the context of the presence and orientation of adjacent ORFs has to be established, to either support real similarities to NGR234's QQ genes or reject candidates due to their lack of homology. NGR234 carries more putative QQ genes than found in other rhizobial species. Nevertheless, the assumption that all these ORFs are functional is unlikely.

Table 17: QQ inventory of NGR234 and selected rhizobial microbes

ORF ID	Possible and/or annotated function	<i>S. meliloti</i> SM1021	<i>R. etli</i> CFN42	<i>R. leguminosarum</i> bv. <i>viciae</i> 3841	<i>M. loti</i> MAFF303099	<i>B. japonicum</i> USDA110	<i>S. fredii</i> USDA257
NGR_c10650	metallo- β -lactamase family protein	X	X	X	X	X	X
NGR_b16870	putative metallo- β -lactamase family protein	X	X	X		X	X
NGR_b15850	metallo- β -lactamase family protein	X	X	X	X	X	X
NGR_b12260	metallo- β -lactamase family protein	X	X	X	X		X
NGR_c22830	putative β -lactamase family protein	X	X	X	X	X	X
NGR_c27960	metal-dependent hydrolase	X	X	X		X	X
NGR_c05660	metallo- β -lactamase family protein	X	X	X	X	X	X
NGR_c03760	metallo- β -lactamase family protein	X	X	X	X	X	X
NGR_c05950	putative β -lactamase family protein			X	X	X	
NGR_c16020	metal-dependent hydrolase	X	X	X	X	X	X
NGR_c00430	putative metal-dependent hydrolase	X	X	X	X	X	X
NGR_c08460	metal-dependent phosphohydrolase	X	X	X			X
NGR_c06480	metal-dependent hydrolase					X	
NGR_c32270	putative β -lactamase family protein		X	X	X	X	X
NGR_c17430	metallo- β -lactamase family protein	X	X	X	X		X
NGR_c10940	metal-dependent hydrolase	X	X	X	X		X
NGR_b22150	dienelactone hydrolase-like		X	X			
NGR_c03800	dienelactone hydrolase-like	X		X	X		X
NGR_c01920	metal-dependent amidase	X		X			X
NGR_c28580	putative amidohydrolase	X				X	X
NGR_c27330	putative amidohydrolase family protein	X	X	X	X	X	X
NGR_c18520	putative amidohydrolase			X	X		X
NGR_c33720	amidohydrolase 2						X
Sum		17	16	20	15	14	20

3.2. The functional approach revealed a surprisingly high number of QQ related genes hidden in the genome of NGR234

The main goal of the present research was to investigate the QQ inventory of NGR234 using sophisticated methods on AHL degradation. Within this work, five NGR234-derived genes and loci could be identified and experimentally verified to interfere with AHL-based signal molecules. Two out of the five putative QQ genes were in part biochemically characterized. Different assays using biosensor strains to detect enzymatic AHL degradation were already implemented in various studies (D'Angelo-Picard *et al.* 2005; Musthafa *et al.* 2010; Schipper *et al.* 2009). In the *A. tumefaciens* NTL4 based assay using the *trai::lacZ* promoter fusion, the five cosmid clones repeatedly gave a positive result, which could be confirmed in motility assays in *E. coli*. The five genes and loci identified and linked to these QS inhibitory phenotypes were designated *aldR*, *dlhR*, *hitR-hydR*, *qsdR1* and *qsdR2*. As motility like swarming or swimming in *P. aeruginosa* PAO1 is QS-regulated by AHL signal molecules, this strain is frequently used to monitor QS inhibitory effects. Thus, PAO1 was subjected to motility assays with the five expressed genes, observing a strong reduced swarming and swimming behavior as well as a modified biofilm formation. Presumably, these monitored PAO1 phenotypes were a result of AHL degradation caused by the identified proteins. Furthermore, the hypothesis was supported by enzyme activity assays accomplished with crude cell extracts of pDrive vectors harboring *hitR-hydR*, *aldR* and *qsdR2* as well as recombinant and purified DIhR and QsdR1.

These experimental findings were in line with data derived from the sequence-based analyses, where *dlhR*, *qsdR1*, *qsdR2* and the *hitR-hydR* locus were already identified. Furthermore, combining this data set with experimental procedures, the list of potential QQ genes could be extended by gene *aldR*, which was only identified by function-based searches. To date, approximately 40 different QQ related enzymes were found, described and for the most part experimentally verified. Nevertheless, none of these researches used a preceding sequence analysis to uncover novel QQ associated enzymes, which were then verified using functional assays. Like published for AidH (Mei *et al.* 2010) or AhID (Park *et al.* 2003) and many other AHL degrading enzymes, such sequence analyses were only used to classify already identified genes and to align to available QQ proteins. The strategy pursued in the present study to elucidate the QQ inventory of NGR234 revealed to be more suitable, delivering a high number of candidates. It is noteworthy, that within the framework of the present research, three lactonases could be discovered in NGR234 (DIhR, QsdR1 and QsdR2) and additionally, two novel genes/loci (*aldR* and *hitR-hydR*) that had not been linked to QQ in earlier studies.

3.3. Wealth of loci involved in QQ is a unique feature of NGR234

The richness of ORFs linked to QQ activity in NGR234 raised the question of its uniqueness. Until today, no other microorganism proved to comprise as many QQ related ORFs as NGR234. Soil bacteria like *Agrobacterium tumefaciens*, *Ochrobactrum* sp. and *Rhodococcus erythropolis* also exhibited multiple AHL catabolic activities. The phytopathogen *A. tumefaciens* C58 expresses two lactonases, AttM and AiiB, located on the At and Ti plasmid, respectively (Carlier *et al.* 2003; Zhang *et al.* 2002). Both lactonases were found to play different biological roles, mainly modulating QS-regulated functions. AttM and AiiB are tightly intertwined with the regulatory QS cascade, thus contribute in combination with other signal molecules in *A. tumefaciens* C58 to the expression of virulence functions and in addition confer a selective advantage to this microbe in the tumor environment (Haudecoeur *et al.* 2009). In 2011, two studies provided experimental evidence that strain *Ochrobactrum* sp. was capable of inactivating various natural and synthetic AHL molecules. The first research on *Ochrobactrum* sp. A44 reported the AHL degradation by AiiO, an AHL acylase being able to utilize AHLs with chains ranging from C4 to C14 with and without 3-oxo or 3-hydroxy substitutions. A number of bacterial species (e.g. *V. paradoxus*) have been shown to employ AHL degradation to metabolize the resulting products as an environmental source of carbon (Leadbetter and Greenberg 2000). However, strain *Ochrobactrum* sp. A44 was not reported to metabolize AHL by-products thus, the purpose for AHL inactivation remains unknown (Czajkowski *et al.* 2011). The second publication employing *Ochrobactrum* sp. strain T63 reported on the identification and characterization of a novel AHLase, AidH, revealing no detectable homology to any of the known AHLases. Moreover, AidH showed to be highly similar to members of the α/β -hydrolases, thus representing the first reported AHLase within the group of these hydrolases (Mei *et al.* 2010).

Due to the broad AHL-degradation spectrum and rapid AHL inactivation of *Rhodococcus erythropolis* W2, this strain became of special interest. In the first report, strain W2 was shown to grow on AHLs as the sole carbon and energy source (preferring short-chain compounds) exhibiting an enzymatic AHL oxidoreductase and AHL amidolytic activity (Uroz *et al.* 2005). However, no speculations were stated on the biological role of both identified AHL degradation genes in W2. The second report could verify a gene involved in AHL degradation, encoding an AHLase unrelated to previously published QQ enzymes. Uroz *et al.* speculated about the role of QsdA in fatty acid metabolism, yet this was not experimentally verified. *R. erythropolis* W2 harboring three AHL degradation enzymes appears to be very well equipped to resist to Gram-negative soil competitors (Uroz *et al.* 2008).

To furthermore evaluate the richness of ORFs linked to QQ owned by NGR234, a direct comparison to closely related soil bacteria was accomplished. Several sequenced rhizobial genomes were used to conduct comparative analyses. The obtained data suggest, that rhizobial isolates appear to have several QQ genes encoded in their genomes and those appear to be present on the chromosomes or the larger megaplasmids but not on the symbiotic plasmids. A comparison revealed the presence of four out of the five NGR234 QQ genes in the *S. meliloti* SM1021 genome, however SM1021 lacks the *dlhR* locus. Also, *dlhR* as well as the *qsdR1* locus are missing in *M. loti* MAFF303099. Furthermore, an analysis of the nearly complete *S. fredii* USDA257 genome revealed that beside the *dlhR* gene, all NGR234 QQ genes were present in this close relative as well. These findings are in line with the sequence-based approach discussed earlier. Although, these rhizobial isolates have almost all copies of the experimentally verified QQ enzymes of NGR234, their functional evidence is still to be demonstrated. Thus, speculations about a similar richness of QQ related genes in these soil bacteria are more a guess than a concrete indication.

Translating and coining the striking findings for the above mentioned soil bacteria to NGR234's multiple loci involved in QQ, one might speculate, that comprising such a great arsenal of AHL degradative activities increases the potential of NGR234 to outcompete other symbionts. This hypothesis might deliver further answers to NGR234's broad host range of symbiotic partners and strongly indicates that equipped with these five QQ associated enzymes, NGR234 has a superior approach to a competitive environment.

3.3.1 Chromosomal loci *hitR-hydR*, *qsdR2* and *aldR* encode for novel lactone hydrolyzing enzymes

Three out of the five putative QQ genes were located on the chromosome, namely *hitR-hydR* locus, *qsdR2* and *aldR*. Using the PAO1 motility assay, the CV026 biosensor as well as enzyme activity assays, their QQ activity could be demonstrated. First sequence analyses revealed that only *qsdR2* exhibits a homology to published QQ enzymes. The *hitR-hydR* and *aldR* locus have not been reported to be involved in QS degrading or modifying activities, thus represent novel AHL hydrolyzing enzymes owned by NGR234.

3.3.1.1 Locus *hitR-hydR* reveals AHL degrading/modifying activity

Functional assays with subsequent sequence analyses identified the *hitR-hydR* locus on cosmid clone pWEB-TNC-A5 being responsible for the observed altered phenotypes in its *E. coli* XL1 blue host, as well as PAO1 and CV026. The genes *hitR* and *hydR* were sequentially overlapping, thus the operon as well as the single gene were monitored on AHL

degradation. Crude cell extracts of all three constructs showed considerable degradation rates for 3-oxo-C8-HSL as well as 3-oxo-C6-HSL. Since both ORFs did not reveal any sequence similarities to characterized QQ genes, AHL degradation rates were compared to BpiB01 published in 2009 (Schipper *et al.* 2009). BpiB01 revealed no conserved domains and was similar to a number of hypothetical proteins. For the ONPG assays, BpiB01 displayed an AHL degradation rate over 60%, whereas HitR and HydR demonstrated a rate over 50% (53-56%). Both genes were cloned into the pDrive vector and only crude cell extracts were employed for the ONPG assay, this must be mentioned while comparing the results to the purified protein BpiB01. However, HitR and HydR could establish degradation rates, where over 50% of the inserted AHLs were cleaved. Even more pronounced rates were monitored for tests accomplished with CV026 and 3-oxo-C6-HSL. The functional assays could prove that the two ORFs do not act as an operon, moreover are individually capable of AHL degradation. Sequence alignments with the deduced AA sequence of HitR did not indicate a relation to QQ associated proteins. Neither the C-terminal HIT-like domain nor the homologous proteins found in *S. meliloti* SM1021 uncovered such sequence similarities. Although found in many prokaryotes as well as in higher eukaryotes, the function of proteins belonging to the HIT family is still unknown. Thus, few speculations about the function of HitR as a putative QQ protein can be made. The predicted NUDIX hydrolase, HydR, also did not reveal any significant similarities to known and published QQ related hydrolases. Recent studies on NUDIX GDP-mannose hydrolases in *E. coli* demonstrated the structural importance of the NUDIX signature (Boto *et al.* 2011) and mentioned their role in the RcsC regulon linked to biofilm formation (Ferrières and Clarke 2003). The interrelation of biofilm formation and NUDIX hydrolases might also be a first indication for HydR and the function as a putative QQ enzyme. Nevertheless, experimental data is necessary to support these correlations.

Summarizing, the locus *hitR-hydR*, moreover both individual genes (*hitR* and *hydR*) showed to encode for proteins that are involved in AHL degradation and were verified in different functional assays. Regarding the weak similarities to other proteins and no sequential connections to published QQ genes, in the framework of this study, two novel QQ active proteins comprised by NGR234 were identified and partially characterized.

3.3.1.2 The metal-dependent hydrolase, QsdR2, is able to degrade AHL signal molecules

Within 12 hypothetical proteins comprised by cosmid clone pWEB-TNC-B9, one ORF stood out by its annotation as a metal-dependent hydrolase. Direct cloning and first motility as well as enzyme activity assays proved its ability to degrade AHLs. Although comparative analyses using various databases revealed homologies to conserved hypothetical proteins, no significant similarity to known AHLases of the metallohydrolase family could be identified. A clear inhibition of the swarming behavior of PAO1 as well as a considerable 3-oxo-C8-HSL degradation rate was monitored for crude cell extracts of construct pDrive::*qsdR2*.

QsdR2 was found to contain the conserved signature “HXHX~DH”, the essential motif of AHLase activity. The field of AHLases and their relevance in QQ associated processes is emerging in the past ten years, starting with the first lactonase activity found in *Bacillus* sp. 240B1 (Dong *et al.* 2000). The AiiA sequence, although not revealing any significant similarities to known enzymes, indicated the presence of a conserved “HXHX~DH” motif. This short region was found to be a characteristic of metallo- β -lactamases, glyoxalases II and arylsulfatases. The first two histidine residues of this motif were found to be involved in zinc-binding activity and the aspartic residue to participate in catalytic mechanisms (Carfi *et al.* 1995). Site directed mutagenesis of the AHLase motif in *Bacillus* sp. 240B1 revealed that the conserved aspartate and most of the histidine residues (beside the first histidine) are required for AiiA activity (Dong *et al.* 2000). Consequently, the activity of AHLases is dependent on, beside the “HXHX~DH” motif, other histidine and conserved residues (proline, glycine, aspartate, phenylalanine and glutamic acid, for a detailed review see Liu *et al.* 2005). Sequence alignments using QsdR2 and published representatives of the AHLases family (AiiA, AiiB/AttM, AhID and AhIK) revealed significant differences. Although harboring the “HXHX~DH” signature, all other activity relevant residues were absent in the deduced AA sequence of QsdR2 (Figure 12). Based on Dongs findings in 2000, the QsdR2 AHLase should not exhibit a lactonase activity (Dong *et al.* 2000). This is in contrast to the present work, which delivered experimental evidence of a measurable and reproducible QQ activity assigned to QsdR2.

Collectively, first sequence similarities to AHLases were supported by an inhibited motility of *E. coli* XL1 blue as well as PAO1 and were confirmed by reduced AHL levels in enzyme activity assays. Although QsdR2 comprises the zinc-binding motif common in AHLases, crucial conserved residues are absent in its sequence. Nevertheless, QsdR2 has definite QQ ability thus possibly displaying a new member of the lactonases of the metal-dependent hydrolase family.

3.3.1.3 AldR, an acetaldehyde dehydrogenase represents a novel lactone hydrolyzing enzyme

The chromosomal locus, *aldR*, was identified on cosmid clone pWEB-TNC-G2 using *in vitro* transposon mutagenesis. Although the sequence analysis of *aldR* did not reveal similarities to already published QQ proteins and to none of the other four QQ related proteins comprised by NGR234, the function of AldR could be verified using motility, as well as enzyme activity assays. AldR demonstrated the capability to interfere with diverse QS systems however, tests using 3-oxo-C8-HSL and 3-oxo-C6-HSL displayed rather low degradation rates compared to the remaining four active QQ genes. To support the low AHL degradation ability of AldR, more experimental data accomplished with the purified protein is needed.

The high sequence similarity of *aldR* to other acetaldehyde dehydrogenases in *S. meliloti* SM1021 or *R. etli* CFN42 does not allow other speculations about the function of this protein. The AA sequence of AldR features a highly conserved region counted to the NAD(P)⁺ dependent aldehyde dehydrogenase [EC 1.2.1.-] superfamily. These enzymes are counted to the oxidoreductases and normally catalyze the conversion of acetaldehyde into acetic acid (Lei *et al.* 2008). Oxidoreductases were already mentioned in the introduction to (1.2.4) to be able to modify AHL molecules, thereby leading to an inactivation of the signal. Based on the chemical structure of AHLs, acetaldehyde dehydrogenases could also function as oxidoreductases and inactivate the present AHLs. To date, only two such enzymes with oxidoreductase activity were biochemically characterized, thus only few information was accumulated on these AHL degrading enzymes (Chowdhary *et al.* 2007; Uroz *et al.* 2005). However, their mode of action is rather an indirect blockade of AHL-mediated cell-to-cell communication, thus might be not as efficient as the enzymatic degradation by lactonases and amidases. This fact leads to the assumption that AldR mediates enzymatic AHL degradation by the oxidoreductive way, which might explain the low conversion rate. Nevertheless, the accumulated data on the function of AldR on AHLs is not sufficient. Further analyses using for example HPLC-MS would deliver more reliable results on the enzymatic degradation way of AldR and would thereby extent the list of oxidoreductases.

3.3.2 Biochemical characterization of DIhR and QsdR1 located on the pNGR234b

The megaplasmid of NGR234 carries most of the genes associated with transport and polysaccharide synthesis and was already considered in earlier studies to play a crucial role in NGR234's broad host range (Schmeisser *et al.* 2009). Results from the previous described comparative studies on NGR234's QQ inventory revealed, that most of the discovered ORFs

were located on the cNGR234. Thus, the present research focused on QQ associated genes, *dlhR* and *qsdR1*, harbored by the pNGR234*b*. The biochemical characterization of the uncovered enzymes provides novel insights and more answers to the secret of the wide range of symbiotic partners of NGR234.

3.3.2.1 The dienelactone hydrolase, DlhR, constitutes a new member of the AHLases

Gene *dlhR* was found by a subcloning approach followed by various functional assays to be located on pWEB-TNC-B2 and responsible for QS inhibition. The ORF was annotated as a dienelactone hydrolase-like protein and was already uncovered in the sequence-based analysis. A previous research accomplished in our lab already reported on gene *bpiB07*, encoding a dienelactone hydrolase, being linked to QS inhibition and exhibiting a lactonolytic activity (Schipper *et al.* 2009). BpiB07 and DlhR could resemble the same function, but dienelactonases are structurally diverse and range in their function from metabolic process to QS. Because DlhR displays no domains indicating a putative QQ activity, the function of the discovered DlhR can only be elucidated by drawing conclusions to parallel reaction mechanisms found for related characterized enzymes. The role of dienelactone hydrolases [EC 3.1.1.45] in microbial degradation of chloroaromatics in natural environments was first described in 1985 (Ollis and Ngai 1985; Cámara *et al.* 2008). This protein catalyzes a step in metabolic conversion of chlorocatechols to β -keto adipate. The enol-lactone hydrolase [EC 3.1.1.24] coordinates a chemically analogous step in a similar pathway, thus the two hydrolytic reactions propose that these hydrolases share a common ancestor. Recent studies on conversion of 3-oxoadipate-enol-lactone into its linear product β -keto adipate by means of an enol-lactone hydrolase (ELH) represent a possible reaction way for the identified DlhR. As mentioned, these proteins share weak sequence similarities and the substrates for their reaction are very similar (Figure 27). Enzymes like ELH are involved in the processing of aromatic compounds (lactones) and therefore are targets in bioremediation of aromatic pollutants (Bains *et al.* 2011).

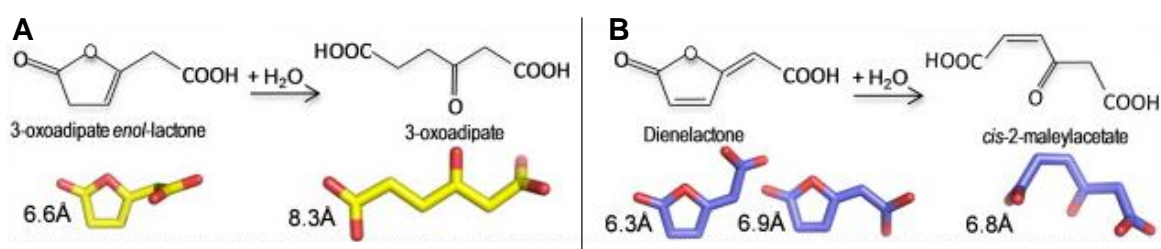


Figure 27: Reactions catalyzed by ELHs and dienelactone hydrolases with structure of substrates and products. (A) The reaction catalyzed by ELHs. (B) The reaction catalyzed by dienelactone hydrolases (Bains *et al.* 2011).

The comparison of the utilized substrate and its decomposition by ELHs and dienelactone hydrolases reveals surprising correlations. The chemical structure of ELH substrate 3-oxoadipate-enol-lactone shares high similarities to the substrate of the dienelactone hydrolase. Both proteins are able to hydrolyze the lactone ring of the corresponding substrates, which might be the missing link to the function of DIhR. The dienelactone hydrolase-like protein DIhR might hold the ability to catalyze the AHLs by enzymatically cleaving its lactone ring (lactonolysis). The comparative conclusions could be supported by the HPLC-MS analysis which was employed with AHL and purified DIhR, where DIhR was able to produce 3-oxo-C8-HS by hydrolyzing the 3-oxo-C8-HSL. Previous studies of Schipper *et al.* 2009 and Uroz *et al.* 2008 using HPLC-MS analysis proved to deliver reliable information about the enzymatic reaction of the promising proteins. Thus, HPLC-MS analysis of DIhR provided evidence for the lactonolytic way of AHL degradation.

Until today, BpiB07 is unique, no other dienelactone hydrolase associated enzymes were biochemically characterized or even reported. Conclusively, within the present research the experimental proof was provided by the functionality of DIhR as well as the elucidation of its enzymatic way of AHL degradation. These findings extend the number of AHLases. The DIhR protein is totally unrelated to the known bacterial AHLases, therefore represents the first novel QQ associated enzyme found in NGR234.

3.3.2.2 QsdR1 extends the list of functionally characterized AHLases of the metallo- β -lactamase family

QsdR1 originating from cosmid clone pWEB-TNC-C6 was identified within 33 ORFs based on its annotation as a metal-dependent hydrolase. In addition to previously described motility assays accomplished in *E. coli* XL1 blue and PAO1, QsdR1 was able to largely degrade 3-oxo-C8-HSL and 3-oxo-C6-HSL. Based on its sequence affinity to metallo- β -lactamases, it was speculated that QsdR1 catalyzes AHLs by lactonolysis, identical to AiiA, AhIK and QlcA. A series of functional assays was accomplished to support this hypothesis, finally a HPLC-MS analysis provided the proof.

In contrast to QsdR2, the sequence analysis of QsdR1 uncovered the highest similarity to Aii2 from uncultured *Bacillus* sp. published in 2003 (Carrier *et al.* 2003). Further comparison of QsdR1 to AiiA, AhID and QlcA exhibited 23%, 25% and 21% identities in the deduced AA sequences respectively, constituting a rather low degree of AA sequence identity and similarity. The active side (metal ion center) of AHLases binds two zinc ions and is coordinated by seven residues including the "HXHX~DH" pattern. The two first histidine residues of this motif together with the further distant third histidine are proposed to bind one

Zn²⁺, whereas the last histidine residue of the conserved pattern (~DH) coordinates the second Zn²⁺. Since QsdR1 shares the common zinc-binding sequence motif within the metallo-β-lactamases, it is possible that the purified protein requires a metal ion (Zn²⁺) for its activity. However, different controversial reports have been published regarding the metal content of an active AHLase and also the classification of AHLases to the metallohydrolases. On the one hand, studies were accomplished concerning the kinetics of AHLases, which postulated supported by experimental results, that AHLases although harboring a zinc-binding site, do not rely on zinc or other metals (Wang *et al.* 2004). On the other hand, strong evidence on the necessity of zinc was reported by Kim and colleagues (Kim *et al.* 2005) and by the research group of Thomas (Thomas *et al.* 2005). Both publications presented that the AHLase from *B. thuringiensis* is a metalloenzyme and requires the presence of zinc to form an active enzyme. Still, further studies are needed to determine whether AHLases comprising such a “HXHX~DH” motif are strict zinc proteins or contain a mixed metal-dinuclear site like glyoxalases II (Zang *et al.* 2001). Besides the active site for zinc-binding, the deduced AA sequence of QsdR1 holds similarities to a second rather moderate conserved signature within the AHLases (Figure 20). The “¹⁶⁵HTPGHTPGH¹⁷³” is similar to the zinc-binding motif and was found to comprise the third histidine residue located about 60 AA downstream of the first conserved motif, coordinating the metal ion center. Additionally, QsdR1 shares other mentioned conserved residues with the AHLase family. Although prior researches state that AHLases require zinc for its activity, this was not valid for QsdR1. Biosensor assays employed with CV026 proved the need of Zn²⁺, but the majority of the functional screenings did not demand for supplementation with metal ions. Tests accomplished in cooperation with the group of Prof. Schmitz-Streit using *E. coli* harboring an AHL reporter fused to a suicide gene (data no shown) did not reveal significant differences in deployed cofactors. Thus, more experimental evidence is necessary to estimate the zinc dependency of QsdR1. The AHL degradation capability of QsdR1 was verified and this protein showed to be very potent. Nevertheless, one might speculate about even more pronounced degradation rates when supplementing the reactions with different cofactors, especially with Zn²⁺. Findings of Wang and colleagues are in line with the results obtained for QsdR1 and its necessity of a metal ion. Still, there are speculations about the “HXHX~DH” sequence acting as a zinc-binding site in some AHLases enzymes but not in others. Further experimental evidence is needed to evaluate these hypotheses.

Finally, joining all obtained data and the HPLC-MS analysis for QsdR1 which confirmed an lactonolytic activity, these results give strong evidence that the QsdR1 protein acts as a true lactonase and until today was not described for NGR234.

3.3.3 DIhR and QsdR1 associated with biofilm phenotypes in the rhizosphere

In various rhizobial strains, such important processes like resistance, virulence factor production, antibiotic production, swarming, biofilm formation and nodulation are QS-regulated and inevitably play a role in plant-host interactions (Gao *et al.* 2005). Switching on and especially off such QS-regulated systems by interfering with the crucial signal molecules might play a great role in symbiotic and pathogenic bacterial interactions. Rhizobia equipped with a wealth of AHL degrading enzymes could enhance the successful competition in the rhizosphere and gain the upper hand in the symbiotic relationship. The importance of lactonases in such competing environments was already proven in earlier studies accomplished with AiiA in strain *B. thuringiensis*. Using *aiiA*-mutants, the role of AiiA in rhizosphere colonization as well as for its survival in the soil was proven (Park *et al.* 2008). Additionally, the introduction of *aiiA* genes in plants and bacterial pathogens supported the role of the lactonase in plant-microbe interactions (Dong *et al.* 2000; Dong *et al.* 2001; Dong *et al.* 2004). The findings, that NGR234 comprised a wealth of genes attributed to QQ activity and the previously mentioned experimental evidence on the role of AiiA during interactions of plant-associated bacteria, led to *in situ* experiments with DIhR and QsdR1. The hypothesis, that NGR234 equipped with additional copies of biochemically characterized enzymes, DIhR and QsdR1, would be more competitive in its natural niche, could not be demonstrated. Nevertheless, in competitive colonization of roots in the rhizosphere of cowpea plants, extra copies of *dIhR* and *qsdR1* strongly contributed to the colonization capability of NGR234. The expected effect that NGR234 equipped with more than the already discovered five QQ related loci would gain the upper hand in competition was not observed. Data from this study emphasizes the ecological importance of QQ during root colonization in NGR234.

4. Concluding remarks and outlook

The unique feature of *Rhizobium* sp. NGR234 to nodulate over 120 legumes and one nonlegume raised the question of the involvement of secretion, QS and QQ processes in establishing a symbiosis with a wide range of host partners. The wealth of secretion apparatuses found within the genome of NGR234 suggests that this symbiont, compared to closely related rhizobia, is more specialized on secretion, transport and translocation of proteins, which are essential for a successful plant-microbe interaction. The focus of the present research was put on the regulation of QS in NGR234 as well as its inventory of QQ associated genes, which may serve for mechanisms to optimize plant-host interactions. One novel QS system along with several AHL response regulator genes was uncovered, proposing its ability to communicate with other symbionts present in the rhizosphere and furthermore owning genes for an AHL dependent response. The advantage to sense various bacterial species in environments like the soil enables NGR234 to rapidly regulate gene expression to consequently gain the upper hand in competition. Supported by the presented results, the wealth of genes linked to QQ activity in NGR234 even stronger contributes to a competitive advantage. The inventory of QQ proteins constitutes an important feature of symbionts and is possibly needed during rhizosphere colonization and growth in soil. The role of all five QQ genes in NGR234 in the environment remains unclear, however current findings indicate that AHL degrading enzymes are diverse in bacteria and can contribute to its performance in the rhizosphere. Consequently, there is a direct correlation between the number of QQ associated genes and the range of plant hosts, which undergo a symbiotic relationship with NGR234.

Future work has to focus on the further determination and evaluation of the richness of QQ in NGR234. The previously presented sequence-based approach already paved the way for subsequent analyses. Nevertheless, a functional verification of these numerous genes is necessarily to speculate about the real QQ inventory of NGR234.

In addition, the role of the diverse QQ loci found within the genome of NGR234 has to be evaluated under the viewpoint of competition for the plant host within the ecological niche. More insights into the regulation of QS and QQ in representatives of the *Rhizobiaceae* in the context of their symbiotic partners would deliver relevant data and expand this emerging research field.

V. Abstract

Rhizobium sp. NGR234 belongs to the α -proteobacteria and is a unique representative of rhizobia forming nitrogen-fixing nodules with more legumes than any other microsymbiont. Many of the processes and genes necessary for an effective symbiosis were identified, but still there are significant gaps with respect to the bacterial interaction to fill and communication mechanisms to understand.

Within this research, the full genome sequence of *Rhizobium* sp. NGR234 was established, uncovering many striking features. The 6.9-Mbp genome is composed of the 3.93-Mbp chromosome (cNGR234), the 2.43-Mbp megaplasmid (pNGR234*b*) and the 0.54-Mbp symbiotic plasmid (pNGR234*a*). A total of 6,394 ORFs were assigned on the NGR234 genome, whereas 27% of the ORFs were related to genes with unknown function. Among many other remarkable features, a surprisingly high number of 132 proteins spread over the three replicons are linked to secretory processes, giving evidence that NGR234 encodes for more different secretion systems than any other known *Rhizobium*. Additionally, systems linked to QS AI synthesis and quenching of such QSautoinducers could be discovered. Beside the AHL synthase Tral and the response regulator TraR present on the pNGR234*b*, a second possible QS system composed of NgrI/NgrR located on the chromosome was identified. Detailed sequence analyses uncovered not only a novel AHL synthase but also several putative AHL degrading enzymes spread in the genome of NGR234. Altogether 23 ORFs were found by similarity search against public databases being possibly involved in QQ processes. To confirm the surprisingly high number of genes linked to degradation of autoinducer 1 molecules, a function-based approach was implemented. A previously published screening protocol using *A. tumefaciens* NTL4 was employed to verify candidate clones from a NGR234 genomic cosmid clone library. The genome wide functional analysis revealed the presence of five loci that consistently gave a positive result. Two of these loci were located on pNGR234*b* and three were encoded by cNGR234. The corresponding ORFs of all cosmid clones could be localized by the combination of subcloning, transposon mutagenesis and NCBI BLAST analyses. The identified genes were designated *dlhR*, *qsdR1*, *qsdR2*, *aldR* and *hitR-hydR*. One main goal of the research was to verify the functional QQ activity of all genes and to characterize in detail the most promising genes present on pNGR234*b*. Consequently, heterologous expression and purification were realized for DIhR and QsdR1. DIhR resembles a bacterial dienelactone hydrolase while QsdR1 shows high similarities to a metallo- β -lactamase, comprising two conserved motifs attributed to AHLases. The QQ impact of both purified proteins was investigated using biosensor strains *A. tumefaciens* NTL4, *P. aeruginosa* PAO1 and *C. violaceum* CV026. In all strains,

QS-dependent processes like swarming and violacein production as well as biofilm formation were reproducibly inhibited by both enzymes. Recombinant DIhR and QsdR1 investigated with the ONPG assay confirmed the ability to hydrolytically degrade 3-oxo-C8-HSL. In general, less than 73% of the employed AHL were detected for DIhR and a more pronounced degradation of AHLs (down to 40%) was measured for QsdR1. Furthermore, experimental data from competitive colonization of roots in the rhizosphere of cowpeas showed that extra copies of *dlhR* and the *qsdR1* gene strongly contributed to plant root colonization fitness of NGR234, emphasizing the ecological importance of QQ during root colonization of seedlings (i.e. biofilm formation). Finally, to uncover the underlying cleaving mechanism of AHL degradation by both proteins, HPLC-MS analysis was employed. The HPLC-UV as well as mass spectra for DIhR and QsdR1 confirmed lactonolytic activity, giving evidence that both proteins act as true lactonases that had not being described for NGR234 or in earlier QQ studies.

VI. References

- Arpigny, J. L. and Jaeger, K. E. (1999).** Bacterial lipolytic enzymes: classification and properties. Biochem J **343**(1): 177-83.
- Bains, J., Kaufman, L., Farnell, B. and Boulanger, M. J. (2011).** A Product Analog Bound Form of 3-Oxo adipate-enol-Lactonase (PcaD) Reveals a Multifunctional Role for the Divergent Cap Domain. J Mol Bio **406**(5): 649-58.
- Barnett, M. J. and Fisher, R. F. (2006).** Global gene expression in the rhizobial-legume symbiosis. Symbiosis **42**: 1-24.
- Bassler, B. L., Wright, M., Showalter, R. E. and Silverman, M. R. (1993).** Intercellular signalling in *Vibrio harveyi*: sequence and function of genes regulating expression of luminescence. Mol Microbiol **9**(4): 773-86.
- Bassler, B. L., Wright, M. and Silverman, M. R. (1994).** Multiple signalling systems controlling expression of luminescence in *Vibrio harveyi*: sequence and function of genes encoding a second sensory pathway. Mol Microbiol **13**(2): 273-86.
- Bauer, W. D. and Mathesius, U. (2004).** Plant responses to bacterial quorum sensing signals. Curr Opin Plant Biol **7**(4): 429-33.
- Bever, J. D. and Simms, E. L. (2000).** Evolution of nitrogen fixation in spatially structured populations of *Rhizobium*. Heredity **85**(4): 366-72.
- Bijtenhoorn, P., Schipper, C., Hornung, C., Quitschau, M., Grond, S., Wieland, N. and Streit, W.R. (2011).** BpiB05, a novel metagenome-derived hydrolase acting on *N*-acylhomoserine lactones (N-AHLs)." J Biotechnol, accepted.
- Boto, A. N., Xu, W., Jakoncic, J., Pannuri, A., Romeo, T., Bessman, M. J., Gabelli, S. B. and Amzel, L. M. (2011).** Structural studies of the Nudix GDP-mannose hydrolase from *E. coli* reveals a new motif for mannose recognition. Proteins: Structure, Function, and Bioinformatics 10.1002/prot.23069.
- Bradford, M. M. (1976).** A rapid and sensitive method for the quantitation of microgram quantities of protein utilizing the principle of protein-dye binding. Anal Biochem **72**: 248-54.
- Brelles-Marino, G. and Bedmar, E. J. (2001).** Detection, purification and characterisation of quorum-sensing signal molecules in plant-associated bacteria. J Biotechnol **91**(2-3): 197-209.
- Cámara, B., Marín, M., Schlömann, M., Hecht, H.-J., Junca, H. and Pieper, D. H. (2008).** trans-Dienelactone hydrolase from *Pseudomonas reinekei* MT1, a novel zinc-dependent hydrolase. Biochemical and Biophysical Research Communications **376**(2): 423-28.
- Capela, D., Filipe, C., Bobik, C., Batut, J. and Bruand, C. (2006).** *Sinorhizobium meliloti* Differentiation During Symbiosis with Alfalfa: A Transcriptomic Dissection. Mol Plant Micro **19**: 363-72.
- Carfi, A., Pares, S., Duee, E., Galleni, M., Duez, C., Frere, J. M. and Dideberg, O. (1995).** The 3-D structure of a zinc metallo-beta-lactamase from *Bacillus cereus* reveals a new type of protein fold. Embo J **14**(20): 4914-21.
- Carlier, A., Uroz, S., Smadja, B., Fray, R., Latour, X., Dessaux, Y. and Faure, D. (2003).** The Ti plasmid of *Agrobacterium tumefaciens* harbors an *attM*-paralogous gene, *aiiB*, also encoding *N*-Acyl homoserine lactonase activity. Appl Environ Microbiol **69**(8): 4989-93.
- Castang, S., Chantegrel, B., Deshayes, C., Dolmazon, R., Gouet, P., Haser, R., Reverchon, S., Nasser, W., Hugouvieux-Cotte-Pattat, N. and Doutheau, A. (2004).** *N*-Sulfonyl homoserine lactones as antagonists of bacterial quorum sensing. Bioorg Med Chem Lett **14**(20): 5145-49.

- Chen, C. N., Chen, C. J., Liao, C. T. and Lee, C. Y. (2009).** A probable aculeacin A acylase from the *Ralstonia solanacearum* GMI1000 is *N*-acyl-homoserine lactone acylase with quorum-quenching activity. BMC Microbiol **9**: 89.
- Chen, L., Chen, Y., Wood, D. W. and Nester, E. W. (2002).** A New Type IV Secretion System Promotes Conjugal Transfer in *Agrobacterium tumefaciens*. J Bacteriol **184**(17): 4838-45.
- Chester, N. and Marshak, D. R. (1993).** Dimethyl sulfoxide-mediated primer T_m reduction: a method for analyzing the role of renaturation temperature in the polymerase chain reaction. Anal Biochem **209**(2): 284-90.
- Chowdhary, P. K., Keshavan, N., Nguyen, H. Q., Peterson, J. A., Gonzalez, J. E. and Haines, D. C. (2007).** *Bacillus megaterium* CYP102A1 oxidation of acyl homoserine lactones and acyl homoserines. Biochemistry **46**(50): 14429-37.
- Czajkowski, R. and Jafra, S. (2009).** Quenching of acyl-homoserine lactone-dependent quorum sensing by enzymatic disruption of signal molecules. Acta Biochim Pol **56**(1): 1-16.
- Czajkowski, R., Krzyżanowska, D., Karczewska, J., Atkinson, S., Przysowa, J., Lojkowska, E., Williams, P. and Jafra, S. (2011).** Inactivation of AHLs by *Ochrobactrum* sp. A44 depends on the activity of a novel class of AHL acylase. Environ Microbiology Reports **3**(1): 59-68.
- D'Angelo-Picard, C., Faure, D., Penot, I. and Dessaux, Y. (2005).** Diversity of *N*-acyl homoserine lactone-producing and -degrading bacteria in soil and tobacco rhizosphere. Environ Microbiology **7**(11): 1796-1808.
- Daiyasu, H., Osaka, K., Ishino, Y. and Toh, H. (2001).** Expansion of the zinc metallo-hydrolase family of the beta-lactamase fold. FEBS Lett **503**(1): 1-6.
- de Nys, R., Wright, A. D., König, G. M. and Sticher, O. (1993).** New halogenated furanones from the marine alga *Delisea pulchra* (cf. *fimbriata*). Tetrahedron **49**(48): 11213-20.
- Deakin, W. J. and Broughton, W. J. (2009).** Symbiotic use of pathogenic strategies: rhizobial protein secretion systems. Nat Rev Micro **7**(4): 312-20.
- Dong, Y. H., Wang, L. H., Xu, J. L., Zhang, H. B., Zhang, X. F. and Zhang, L. H. (2001).** Quenching quorum-sensing-dependent bacterial infection by an *N*-acyl homoserine lactonase. Nature **411**(6839): 813-17.
- Dong, Y. H., Wang, L. Y. and Zhang, L. H. (2007).** Quorum-quenching microbial infections: mechanisms and implications. Philos Trans R Soc Lond B Biol Sci **362**(1483): 1201-11.
- Dong, Y. H., Xu, J. L., Li, X. Z. and Zhang, L. H. (2000).** AiiA, an enzyme that inactivates the acylhomoserine lactone quorum-sensing signal and attenuates the virulence of *Erwinia carotovora*. Proc Natl Acad Sci USA **97**(7): 3526-31.
- Dong, Y. H. and Zhang, L. H. (2005).** Quorum sensing and quorum-quenching enzymes. J Microbiol **43**: 101-9.
- Dong, Y. H., Zhang, X. F., Xu, J. L. and Zhang, L. H. (2004).** Insecticidal *Bacillus thuringiensis* silences *Erwinia carotovora* virulence by a new form of microbial antagonism, signal interference. Appl Environ Microbiol **70**(2): 954-60.
- Draganov, D. I., Teiber, J. F., Speelman, A., Osawa, Y., Sunahara, R. and La Du, B. N. (2005).** Human paraoxonases (PON1, PON2, and PON3) are lactonases with overlapping and distinct substrate specificities. J Lipid Res **46**(6): 1239-47.
- Duggleby, H. J., Tolley, S. P., Hill, C. P., Dodson, E. J., Dodson, G. and Moody, P. C. (1995).** Penicillin acylase has a single-amino-acid catalytic centre. Nature **373**(6511): 264-68.

- Edwards, A., Frederix, M., Wisniewski-Dye, F., Jones, J., Zorreguieta, A. and Downie, J. A. (2009).** The *cin* and *rai* quorum-sensing regulatory systems in *Rhizobium leguminosarum* are coordinated by ExpR and CinS, a small regulatory protein coexpressed with CinI. J Bacteriol **191**(9): 3059-67.
- Federle, M. J. and Bassler, B. L. (2003).** Interspecies communication in bacteria. J Clin Invest **112**(9): 1291-99.
- Ferrières, L. and Clarke, D. J. (2003).** The RcsC sensor kinase is required for normal biofilm formation in *Escherichia coli* K-12 and controls the expression of a regulon in response to growth on a solid surface. Mol Microbiology **50**(5): 1665-82.
- Flavier, A. B., Ganova-Raeva, L. M., Schell, M. A. and Denny, T. P. (1997).** Hierarchical autoinduction in *Ralstonia solanacearum*: control of acyl-homoserine lactone production by a novel autoregulatory system responsive to 3-hydroxypalmitic acid methyl ester. J Bacteriol **179**(22): 7089-97.
- Freiberg, C., Fellay, R., Bairoch, A., Broughton, W. J., Rosenthal, A. and Perret, X. (1997).** Molecular basis of symbiosis between *Rhizobium* and legumes. Nature **387**(6631): 394-401.
- Frezza, M., Castang, S., Estephane, J., Soulere, L., Deshayes, C., Chantegrel, B., Nasser, W., Queneau, Y., Reverchon, S. and Doutheau, A. (2006).** Synthesis and biological evaluation of homoserine lactone derived ureas as antagonists of bacterial quorum sensing. Bioorg Med Chem **14**(14): 4781-91.
- Fuqua, C., Parsek, M. R. and Greenberg, E. P. (2001).** Regulation of gene expression by cell-to-cell communication: acyl-homoserine lactone quorum sensing. Annu Rev Genet **35**: 439-68.
- Fuqua, C. and Winans, S. C. (1996).** Conserved *cis*-acting promoter elements are required for density-dependent transcription of *Agrobacterium tumefaciens* conjugal transfer genes. J Bacteriol **178**(2): 435-40.
- Fuqua, W. C. and Winans, S. C. (1994).** A LuxR-LuxI type regulatory system activates *Agrobacterium* Ti plasmid conjugal transfer in the presence of a plant tumor metabolite. J Bacteriol **176**(10): 2796-806.
- Galloway, W. R. J. D., Hodgkinson, J. T., Bowden, S. D., Welch, M. and Spring, D. R. (2011).** Quorum Sensing in Gram-Negative Bacteria: Small-Molecule Modulation of AHL and AI-2 Quorum Sensing Pathways. Chemical Reviews **111**(1): 28-67.
- Gao, M., Chen, H., Eberhard, A., Gronquist, M. R., Robinson, J. B., Rolfe, B. G. and Bauer, W. D. (2005).** *sinI*- and *expR*-dependent quorum sensing in *Sinorhizobium meliloti*. J Bacteriol **187**(23): 7931-44.
- Givskov, M., de Nys, R., Manefield, M., Gram, L., Maximilien, R., Eberl, L., Molin, S., Steinberg, P. D. and Kjelleberg, S. (1996).** Eukaryotic interference with homoserine lactone-mediated prokaryotic signalling. J Bacteriol **178**: 6618-22.
- Gonzalez, J. E. and Keshavan, N. D. (2006).** Messing with bacterial quorum sensing. Microbiol Mol Biol Rev **70**(4): 859-75.
- Gonzalez, J. E. and Marketon, M. M. (2003).** Quorum sensing in nitrogen-fixing rhizobia. Microbiol Mol Biol Rev **67**(4): 574-92.
- Grossman, A. D. (1995).** Genetic networks controlling the initiation of sporulation and the development of genetic competence in *Bacillus subtilis*. Annu Rev Genet **29**: 477-508.
- Hanzelka, B. L. and Greenberg, E. P. (1996).** Quorum sensing in *Vibrio fischeri*: evidence that S-adenosylmethionine is the amino acid substrate for autoinducer synthesis. J Bacteriol **178**(17): 5291-94.

- Haudecoeur, E., Tannires, M. I., Cirou, A. I., Raffoux, A. I., Dessaux, Y. and Faure, D. (2009).** Different Regulation and Roles of Lactonases AiiB and AttM in *Agrobacterium tumefaciens* C58. Molecular Plant-Microbe Interactions **22**(5): 529-37.
- He, X., Chang, W., Pierce, D. L., Seib, L. O., Wagner, J. and Fuqua, C. (2003).** Quorum sensing in *Rhizobium* sp. strain NGR234 regulates conjugal transfer (*tra*) gene expression and influences growth rate. J Bacteriol **185**(3): 809-22.
- Henke, J. M. and Bassler, B. L. (2004).** Bacterial social engagements. Trends Cell Biol **14**(11): 648-56.
- Hentzer, M., Wu, H., Andersen, J. B., Riedel, K., Rasmussen, T. B., Bagge, N., Kumar, N., Schembri, M. A., Song, Z., Kristoffersen, P., Manefield, M., Costerton, J. W., Molin, S., Eberl, L., Steinberg, P., Kjelleberg, S., Hoiby, N. and Givskov, M. (2003).** Attenuation of *Pseudomonas aeruginosa* virulence by quorum sensing inhibitors. Embo J **22**(15): 3803-15.
- Hoagland, D. R. and Arnon, D.I. (1950).** The water-culture method for growing plants without soil. California Agricultural Experiment Station Circular (347): 1-32.
- Hoang, T. T. and Schweizer, H. P. (1999).** Characterization of *Pseudomonas aeruginosa* enoyl-acyl carrier protein reductase (FabI): a target for the antimicrobial triclosan and its role in acylated homoserine lactone synthesis. J Bacteriol **181**(17): 5489-97.
- Holloway, B. W., Krishnapillai, V. and Morgan, A. F. (1979).** Chromosomal genetics of *Pseudomonas*. Microbiol Rev **43**(1): 73-102.
- Huang, J. J., Han, J. I., Zhang, L. H. and Leadbetter, J. R. (2003).** Utilization of acyl-homoserine lactone quorum signals for growth by a soil pseudomonad and *Pseudomonas aeruginosa* PAO1. Appl Environ Microbiol **69**(10): 5941-49.
- Huang, J. J., Petersen, A., Whiteley, M. and Leadbetter, J. R. (2006).** Identification of QuiP, the product of gene PA1032, as the second acyl-homoserine lactone acylase of *Pseudomonas aeruginosa* PAO1. Appl Environ Microbiol **72**(2): 1190-97.
- Hughes, D. T. and Sperandio, V. (2008).** Inter-kingdom signalling: communication between bacteria and their hosts. Nat Rev Microbiol **6**(2): 111-20.
- Janssens, J. C., Steenackers, H., Robijns, S., Gellens, E., Levin, J., Zhao, H., Hermans, K., De Coster, D., Verhoeven, T. L., Marchal, K., Vanderleyden, J., De Vos, D. E. and De Keersmaecker, S. C. (2008).** Brominated furanones inhibit biofilm formation by *Salmonella enterica* serovar Typhimurium. Appl Environ Microbiol **74**(21): 6639-48.
- Kendall, M. M., Rasko, D. A. and Sperandio, V. (2007).** Global Effects of the Cell-to-Cell Signaling Molecules Autoinducer-2, Autoinducer-3, and Epinephrine in a *luxS* Mutant of Enterohemorrhagic *Escherichia coli*. Infect Immuno **75**: 4875-84.
- Kim, M. H., Choi, W. C., Kang, H. O., Lee, J. S., Kang, B. S., Kim, K. J., Derewenda, Z. S., Oh, T. K., Lee, C. H. and Lee, J. K. (2005).** The molecular structure and catalytic mechanism of a quorum-quenching *N*-acyl-L-homoserine lactone hydrolase. Proc Natl Acad Sci USA **102**(49): 17606-11.
- Kleerebezem, M., Quadri, L. E., Kuipers, O. P. and de Vos, W. M. (1997).** Quorum sensing by peptide pheromones and two-component signal-transduction systems in Gram-positive bacteria. Mol Microbiol **24**(5): 895-904.
- Kovach, M. E., Elzer, P. H., Hill, D. S., Robertson, G. T., Farris, M. A., Roop, R. M. 2nd and Peterson, K. M. (1995).** Four new derivatives of the broad-host-range cloning vector pBBR1MCS, carrying different antibiotic-resistance cassettes. Gene **166**(1): 175-76.
- Krysciak, D., Schmeisser, C., Preuss, S., Riethausen, J., Quitschau, M., Grond, S. and Streit, W. R. (2011).** Multiple loci are involved in quorum quenching of autoinducer I molecules in the nitrogen-fixing symbiont (*Sino*-) *Rhizobium* sp. NGR234. Appl Environ Microbiol **55**(15): 5089-99.

- Lazizzera, B. A. and Grossman, A. D. (1998).** The ins and outs of peptide signaling. Trends Microbiol **6**(7): 288-94.
- Leadbetter, J. R. and Greenberg, E. P. (2000).** Metabolism of acyl-homoserine lactone quorum-sensing signals by *Variovorax paradoxus*. J Bacteriol **182**(24): 6921-26.
- Lei, Y., Pawelek, P. D. and Powlowski, J. (2008).** A Shared Binding Site for NAD⁺ and Coenzyme A in an Acetaldehyde Dehydrogenase Involved in Bacterial Degradation of Aromatic Compounds. Biochemistry **47**(26): 6870-82.
- Lin, Y. H., Xu, J. L., Hu, J., Wang, L. H., Ong, S. L., Leadbetter, J. R. and Zhang, L. H. (2003).** Acyl-homoserine lactone acylase from *Ralstonia strain* XJ12B represents a novel and potent class of quorum-quenching enzymes. Mol Microbiol **47**(3): 849-60.
- Lithgow, J. K., Wilkinson, A., Hardman, A., Rodelas, B., Wisniewski-Dye, F., Williams, P. and Downie, J. A. (2000).** The regulatory locus *cinRI* in *Rhizobium leguminosarum* controls a network of quorum-sensing loci. Molecular Microbiology **37**(1): 81-97.
- Liu, D., Lepore, B. W., Petsko, G. A., Thomas, P. W., Stone, E. M., Fast, W. and Ringe, D. (2005).** Three-dimensional structure of the quorum-quenching *N*-acyl homoserine lactone hydrolase from *Bacillus thuringiensis*. Proc Natl Acad Sci USA **102**(33): 11882-87.
- Loh, J., Carlson, R. W., York, W. S. and Stacey, G. (2002a).** Bradyoxetin, a unique chemical signal involved in symbiotic gene regulation. PNAS **99**(22): 14446-51.
- Loh, J., Pierson, E. A., Pierson, L. S., Stacey, G. and Chatterjee, A. (2002b).** Quorum sensing in plant-associated bacteria. Curr Opin Plant Biol **5**(4): 285-90.
- Lonn-Stensrud, J., Petersen, F. C., Benneche, T. and Scheie, A. A. (2007).** Synthetic bromated furanone inhibits autoinducer-2-mediated communication and biofilm formation in oral streptococci. Oral Microbiol Immunol **22**(5): 340-46.
- Luo, Z. Q., Clemente, T. E. and Farrand, S. K. (2001).** Construction of a derivative of *Agrobacterium tumefaciens* C58 that does not mutate to tetracycline resistance. Mol Plant Microbe Interact **14**(1): 98-103.
- Lyon, G. J., Mayville, P., Muir, T. W. and Novick, R. P. (2000).** Rational design of a global inhibitor of the virulence response in *Staphylococcus aureus*, based in part on localization of the site of inhibition to the receptor-histidine kinase, AgrC. Proc Natl Acad Sci USA **97**(24): 13330-35.
- MacLellan, S. R., MacLean, A. M. and Finan, T. M. (2006).** Promoter prediction in the rhizobia. Microbiology **152**(6): 1751-63.
- Manfield, M., Rasmussen, T. B., Henzter, M., Andersen, J. B., Steinberg, P., Kjelleberg, S. and Givskov, M. (2002).** Halogenated furanones inhibit quorum sensing through accelerated LuxR turnover. Microbiology **148**(Pt 4): 1119-27.
- Marie, C., Broughton, W. J. and Deakin, W. J. (2001).** *Rhizobium* type III secretion systems: legume charmers or alarmers? Current Opinion in Plant Biology **4**(4): 336-42.
- Marketon, M. M., Glenn, S. A., Eberhard, A. and Gonzalez, J. E. (2003).** Quorum sensing controls exopolysaccharide production in *Sinorhizobium meliloti*. J Bacteriol **185**(1): 325-31.
- Marketon, M. M. and Gonzalez, J. E. (2002).** Identification of Two Quorum-Sensing Systems in *Sinorhizobium meliloti*. J Bacteriol **184**(13): 3466-75.
- Marketon, M. M., Gronquist, M. R., Eberhard, A. and Gonzalez, J. E. (2002).** Characterization of the *Sinorhizobium meliloti sinR/sinI* Locus and the Production of Novel *N*-Acyl Homoserine Lactones. J Bacteriol **184**(20): 5686-95.

- Martinelli, D., Grossmann, G., Sequin, U., Brandl, H. and Bachofen, R. (2004).** Effects of natural and chemically synthesized furanones on quorum sensing in *Chromobacterium violaceum*. BMC Microbiol **4**: 1-25.
- Mathesius, U., Mulders, S., Gao, M., Teplitski, M., Caetano-Anolles, G., Rolfe, B. G. and Bauer, W. D. (2003).** Extensive and specific responses of a eukaryote to bacterial quorum-sensing signals. Proc Natl Acad Sci USA **100**(3): 1444-49.
- McClean, K. H., Winson, M. K., Fish, L., Taylor, A., Chhabra, S. R., Camara, M., Daykin, M., Lamb, J. H., Swift, S., Bycroft, B. W., Stewart, G. S. and Williams, P. (1997).** Quorum sensing and *Chromobacterium violaceum*: exploitation of violacein production and inhibition for the detection of *N*-acylhomoserine lactones. Microbiology **143**(12): 3703-11.
- Mei, G. Y., Yan, X. X., Turak, A., Luo, Z. Q. and Zhang, L. Q. (2010).** AidH, an alpha/beta-hydrolase fold family member from an *Ochrobactrum* sp. strain, is a novel *N*-acylhomoserine lactonase. Appl Environ Microbiol **76**(15): 4933-42.
- Miller, M. B. and Bassler, B. L. (2001).** Quorum sensing in bacteria. Annu Rev Microbiol **55**: 165-99.
- Molina, L., Constantinescu, F., Michel, L., Reimann, C., Duffy, B. and Defago, G. (2003).** Degradation of pathogen quorum-sensing molecules by soil bacteria: a preventive and curative biological control mechanism. FEMS Microbiol Ecol **45**(1): 71-81.
- Morohoshi, T., Shiono, T., Takidouchi, K., Kato, M., Kato, N., Kato, J. and Ikeda, T. (2007).** Inhibition of quorum sensing in *Serratia marcescens* AS-1 by synthetic analogs of *N*-acylhomoserine lactone. Appl Environ Microbiol **73**(20): 6339-44.
- Morrison, N. A., Hau, C. Y., Trinick, M. J., Shine, J. and Rolfe, B. G. (1983).** Heat curing of a sym plasmid in a fast-growing *Rhizobium* sp. that is able to nodulate legumes and the nonlegume *Parasponia* sp. J Bacteriol **153**(1): 527-31.
- Musthafa, K. S., Ravi, A. V., Annapoorani, A., Packiavathy, I. S. and Pandian, S. K. (2010).** Evaluation of anti-quorum-sensing activity of edible plants and fruits through inhibition of the *N*-acylhomoserine lactone system in *Chromobacterium violaceum* and *Pseudomonas aeruginosa*. Chemotherapy **56**(4): 333-39.
- Nealson, K. H., Platt, T. and Hastings, J. W. (1970).** Cellular control of the synthesis and activity of the bacterial luminescent system. J Bacteriol **104**(1): 313-22.
- Ng, W. L. and Bassler, B. L. (2009).** Bacterial quorum-sensing network architectures. Annu Rev Genet **43**: 197-222.
- Oinonen, C. and Rouvinen, J. (2000).** Structural comparison of Ntn-hydrolases. Protein Sci **9**(12): 2329-37.
- Ollis, D. L. and Ngai, K. L. (1985).** Crystallization and preliminary x-ray crystallographic data of dienelactone hydrolase from *Pseudomonas* sp. B13. J Biol Chem. **260**: 9818-19.
- Overbeek, R., Larsen, N., Walunas, T., D'Souza, M., Pusch, G., Selkov, E. Jr., Liolios, K., Joukov, V., Kaznadzey, D., Anderson, I., Bhattacharyya, A., Burd, H., Gardner, W., Hanke, P., Kapatral, V., Mikhailova, N., Vasieva, O., Osterman, A., Vonstein, V., Fonstein, M., Ivanova, N. and Kyrpides, N. (2003).** The ERGO genome analysis and discovery system. Nucleic Acids Res **31**(1): 164-71.
- Park, S. J., Park, S. Y., Ryu, C. M., Park, S. H. and Lee, J. K. (2008).** The role of AiiA, a quorum-quenching enzyme from *Bacillus thuringiensis*, on the rhizosphere competence. J Microbiol Biotechnol **18**(9): 1518-21.
- Park, S. Y., Kang, H. O., Jang, H. S., Lee, J. K., Koo, B. T. and Yum, D. Y. (2005).** Identification of extracellular *N*-acylhomoserine lactone acylase from a *Streptomyces* sp. and its application to quorum quenching. Appl Environ Microbiol **71**(5): 2632-41.

- Park, S. Y., Lee, S. J., Oh, T. K., Oh, J. W., Koo, B. T., Yum, D. Y. and Lee, J. K. (2003).** AhlD, an *N*-acylhomoserine lactonase in *Arthrobacter* sp., and predicted homologues in other bacteria. *Microbiology* **149**(6): 1541-50.
- Parsek, M. R., Val, D. L., Hanzelka, B. L., Cronan, J. E. Jr. and Greenberg, E. P. (1999).** Acyl homoserine-lactone quorum-sensing signal generation. *Proc Natl Acad Sci USA* **96**(8): 4360-65.
- Passador, L., Cook, J. M., Gambello, M. J., Rust, L. and Iglewski, B. H. (1993).** Expression of *Pseudomonas aeruginosa* virulence genes requires cell-to-cell communication. *Science* **260**(5111): 1127-30.
- Pechere, J. C. (2001).** Azithromycin reduces the production of virulence factors in *Pseudomonas aeruginosa* by inhibiting quorum sensing. *Jpn J Antibiot* **54**(Suppl C): 87-89.
- Pereira, C. S., McAuley, J. R., Taga, M. E., Xavier, K. B. and Miller, S. T. (2008).** *Sinorhizobium meliloti*, a bacterium lacking the autoinducer-2 (AI-2) synthase, responds to AI-2 supplied by other bacteria. *Molecular Microbiology* **70**(5): 1223-35.
- Persson, T., Hansen, T. H., Rasmussen, T. B., Skinderso, M. E., Givskov, M. and Nielsen, J. (2005).** Rational design and synthesis of new quorum-sensing inhibitors derived from acylated homoserine lactones and natural products from garlic. *Org Biomol Chem* **3**(2): 253-62.
- Pirhonen, M., Flego, D., Heikinheimo, R. and Palva, E. T. (1993).** A small diffusible signal molecule is responsible for the global control of virulence and exoenzyme production in the plant pathogen *Erwinia carotovora*. *Embo J* **12**(6): 2467-76.
- Pueppke, S. G. and Broughton, W. J. (1999).** *Rhizobium* sp. strain NGR234 and *R. fredii* USDA257 share exceptionally broad, nested host ranges. *Mol Plant Microbe Interact* **12**(4): 293-318.
- Rader, B. A., Campagna, S. R., Semmelhack, M. F., Bassler, B. L. and Guillemin, K. (2007).** The Quorum-Sensing Molecule Autoinducer 2 Regulates Motility and Flagellar Morphogenesis in *Helicobacter pylori*. *J Bacteriol* **189**: 6109-17.
- Rasmussen, T. B., Manefield, M., Andersen, J. B., Eberl, L., Anthoni, U., Christophersen, C., Steinberg, P., Kjelleberg, S. and Givskov, M. (2000).** How *Delisea pulchra* furanones affect quorum sensing and swarming motility in *Serratia liquefaciens* MG1. *Microbiology* **146**(12): 3237-44.
- Reading, N. C. and Sperandio, V. (2006).** Quorum sensing: the many languages of bacteria. *FEMS Microbiol Lett* **254**(1): 1-11.
- Redfield, R. J. (2002).** Is quorum sensing a side effect of diffusion sensing? *Trends Microbiol* **10**(8): 365-70.
- Reimann, C., Ginet, N., Michel, L., Keel, C., Michaux, P., Krishnapillai, V., Zala, M., Heurlier, K., Triandafillu, K., Harms, H., Defago, G. and Haas, D. (2002).** Genetically programmed autoinducer destruction reduces virulence gene expression and swarming motility in *Pseudomonas aeruginosa* PAO1. *Microbiology* **148**(4): 923-32.
- Ren, D., Sims, J. J. and Wood, T. K. (2001).** Inhibition of biofilm formation and swarming of *Escherichia coli* by (5Z)-4-bromo-5-(bromomethylene)-3-butyl-2(5H)-furanone. *Environ Microbiol* **3**(11): 731-36.
- Reverchon, S., Chantegrel, B., Deshayes, C., Doutheau, A. and Cotte-Pattat, N. (2002).** New synthetic analogues of *N*-acyl homoserine lactones as agonists or antagonists of transcriptional regulators involved in bacterial quorum sensing. *Bioorg Med Chem Lett* **12**(8): 1153-57.
- Romero, M., Diggle, S. P., Heeb, S., Camara, M. and Otero, A. (2008).** Quorum quenching activity in *Anabaena* sp. PCC 7120: identification of AiiC, a novel AHL-acylase. *FEMS Microbiol Lett* **280**(1): 73-80.

- Sambrook, J. a. R., D.W. (2001).** Molecular Cloning: A Laboratory Manual. 3re ed. Cold Spring Harbor Laboratory Press, Cold Spring Harbor, New York.
- Schaefer, A. L., Hanzelka, B. L., Eberhard, A. and Greenberg, E. P. (1996).** Quorum sensing in *Vibrio fischeri*: probing autoinducer-LuxR interactions with autoinducer analogs. J Bacteriol **178**(10): 2897-901.
- Schauder, S., Shokat, K., Surette, M. G. and Bassler, B. L. (2001).** The LuxS family of bacterial autoinducers: biosynthesis of a novel quorum-sensing signal molecule. Mol Microbiol **41**(2): 463-76.
- Schipper, C. (2009).** Quorum Quenching und Anti-Biofilm Strategien aus Metagenom -Isolierung und Charakterisierung Quorum Sensing inhibierender Proteine aus Genbanken direkt isolierter Umwelt-DNA. Dissertation.
- Schipper, C., Hornung, C., Bijtenhoorn, P., Quitschau, M., Grond, S. and Streit, W. R. (2009).** Metagenome-derived clones encoding two novel lactonase family proteins involved in biofilm inhibition in *Pseudomonas aeruginosa*. Appl Environ Microbiol **75**(1): 224-33.
- Schmeisser, C., Liesegang, H., Krysciak, D., Bakkou, N., Le Quere, A., Wollherr, A., Heinemeyer, I., Morgenstern, B., Pommerening-Roser, A., Flores, M., Palacios, R., Brenner, S., Gottschalk, G., Schmitz, R. A., Broughton, W. J., Perret, X., Strittmatter, A. W. and Streit, W. R. (2009).** *Rhizobium* sp. strain NGR234 possesses a remarkable number of secretion systems. Appl Environ Microbiol **75**(12): 4035-45.
- Schripsema, J., de Rudder, K. E., van Vliet, T. B., Lankhorst, P. P., de Vroom, E., Kijne, J. W. and van Brussel, A. A. (1996).** Bacteriocin small of *Rhizobium leguminosarum* belongs to the class of *N*-acyl-L-homoserine lactone molecules, known as autoinducers and as quorum sensing co-transcription factors. J Bacteriol **178**(2): 366-71.
- Seraphin, B. (1992).** The HIT protein family: a new family of proteins present in prokaryotes, yeast and mammals. DNA Seq **3**(3): 177-79.
- Sharma, M., Sharma, N. and Bhalla, T. (2009).** Amidases: versatile enzymes in nature. Reviews in Environmental Science and Biotechnology **8**(4): 343-66.
- Shepherd, R. W. and Lindow, S. E. (2009).** Two dissimilar *N*-acyl-homoserine lactone acylases of *Pseudomonas syringae* influence colony and biofilm morphology. Appl Environ Microbiol **75**(1): 45-53.
- Smith, K. M., Bu, Y. and Suga, H. (2003).** Library screening for synthetic agonists and antagonists of a *Pseudomonas aeruginosa* autoinducer. Chem Biol **10**(6): 563-71.
- Soto, M. J., Sanjuan, J. and Olivares, J. (2006).** Rhizobia and plant-pathogenic bacteria: common infection weapons. Microbiology **152**(11): 3167-74.
- Sperandio, V., Torres, A. G., Jarvis, B., Nataro, J. P. and Kaper, J. B. (2003).** Bacteria-host communication: the language of hormones. Proc Natl Acad Sci USA **100**(15): 8951-56.
- Stephenson, K., Yamaguchi, Y. and Hoch, J. A. (2000).** The mechanism of action of inhibitors of bacterial two-component signal transduction systems. J Biol Chem **275**(49): 38900-4.
- Streit, W. R., Joseph, C. M. and Phillips, D. A. (1996).** Biotin and other water-soluble vitamins are key growth factors for alfalfa root colonization by *Rhizobium meliloti* 1021. Mol Plant Microbe Interact **9**(5): 330-38.
- Streit, W. R., Schmitz, R. A., Perret, X., Staehelin, C., Deakin, W. J., Raasch, C., Liesegang, H. and Broughton, W. J. (2004).** An evolutionary hot spot: the pNGR234*b* replicon of *Rhizobium* sp. strain NGR234. J Bacteriol **186**(2): 535-42.
- Sun, J., Daniel, R., Wagner-Dobler, I. and Zeng, A. P. (2004).** Is autoinducer-2 a universal signal for interspecies communication: a comparative genomic and phylogenetic analysis of the synthesis and signal transduction pathways. BMC Evol Biol **4**: 1-36.

- Surette, M. G., Miller, M. B. and Bassler, B. L. (1999).** Quorum sensing in *Escherichia coli*, *Salmonella typhimurium*, and *Vibrio harveyi*: A new family of genes responsible for autoinducer production. Proc Natl Acad Sci USA **96**: 1639-44.
- Taga, M. E. and Bassler, B. L. (2003).** Chemical communication among bacteria. Proc Natl Acad Sci USA **100**(Suppl 2): 14549-54.
- Tateda, K., Comte, R., Pechere, J. C., Kohler, T., Yamaguchi, K. and Van Delden, C. (2001).** Azithromycin inhibits quorum sensing in *Pseudomonas aeruginosa*. Antimicrob Agents Chemother **45**(6): 1930-33.
- Teplitski, M., Mathesius, U. and Rumbaugh, K. P. (2011).** Perception and degradation of *N*-acyl homoserine lactone quorum sensing signals by mammalian and plant cells. Chem Rev **111**(1): 100-16.
- Teplitski, M., Robinson, J. B. and Bauer, W. D. (2000).** Plants secrete substances that mimic bacterial *N*-acyl homoserine lactone signal activities and affect population density-dependent behaviors in associated bacteria. Mol Plant Microbe Interact **13**(6): 637-48.
- Thomas, P. W., Stone, E. M., Costello, A. L., Tierney, D. L. and Fast, W. (2005).** The quorum-quenching lactonase from *Bacillus thuringiensis* is a metalloprotein. Biochemistry **44**(20): 7559-69.
- Trinick, M. J. (1980).** Relationships amongst the fast-growing rhizobia of *Lablab purpureus*, *Leucaena leucocephala*, *Mimosa* spp., *Acacia farnesiana* and *Sesbania grandiflora* and their affinities with other rhizobial groups. Journal of Applied Microbiology **49**(1): 39-53.
- Uroz, S., Chhabra, S. R., Camara, M., Williams, P., Oger, P. and Dessaux, Y. (2005).** *N*-Acylhomoserine lactone quorum-sensing molecules are modified and degraded by *Rhodococcus erythropolis* W2 by both amidolytic and novel oxidoreductase activities. Microbiology **151**(10): 3313-22.
- Uroz, S., Dessaux, Y. and Oger, P. (2009).** Quorum sensing and quorum quenching: the yin and yang of bacterial communication. ChemBiochem **10**(2): 205-16.
- Uroz, S., Oger, P., Chhabra, S. R., Camara, M., Williams, P. and Dessaux, Y. (2007).** *N*-acyl homoserine lactones are degraded via an amidolytic activity in *Comamonas* sp. strain D1. Arch Microbiol **187**(3): 249-56.
- Uroz, S., Oger, P. M., Chapelle, E., Adeline, M. T., Faure, D. and Dessaux, Y. (2008).** A *Rhodococcus qsdA*-encoded enzyme defines a novel class of large-spectrum quorum-quenching lactonases. Appl Environ Microbiol **74**(5): 1357-66.
- Viprey, V., Rosenthal, A., Broughton, W. J. and Perret, X. (2000).** Genetic snapshots of the *Rhizobium* species NGR234 genome. Genome Biol **1**(6): Research 0014.1-14.17.
- Wahjudi, M., Papaioannou, E., Hendrawati, O., van Assen, A. H., van Merkerk, R., Cool, R. H., Poelarends, G. J. and Quax, W. J. (2011).** PA0305 of *Pseudomonas aeruginosa* is a quorum quenching acyl homoserine lactone acylase belonging to the Ntn hydrolase superfamily. Microbiology 10.1099/mic.0.043935-0
- Walters, M., Sircili, M. P. and Sperandio, V. (2006).** AI-3 synthesis is not dependent on *luxS* in *Escherichia coli*. J Bacteriol **188**(16): 5668-81.
- Walters, M. and Sperandio, V. (2006).** Autoinducer 3 and epinephrine signaling in the kinetics of locus of enterocyte effacement gene expression in enterohemorrhagic *Escherichia coli*. Infect Immun **74**(10): 5445-55.
- Wang, L. H., Weng, L. X., Dong, Y. H. and Zhang, L. H. (2004).** Specificity and enzyme kinetics of the quorum-quenching *N*-Acyl homoserine lactone lactonase (AHL-lactonase). J Biol Chem **279**(14): 13645-51.

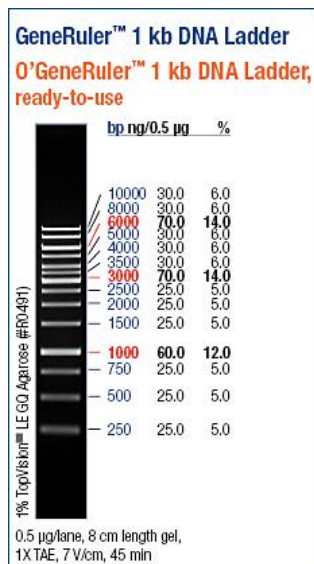
- Waters, C. M. and Bassler, B. L. (2005).** Quorum sensing: cell-to-cell communication in bacteria. Annu Rev Cell Dev Biol **21**: 319-46.
- Weber, B., Hasic, M., Chen, C., Wai, S. N. and Milton, D. L. (2009).** Type VI secretion modulates quorum sensing and stress response in *Vibrio anguillarum*. Environmental Microbiology **11**(12): 3018-28.
- Wisniewski-Dye, F. and Downie, J. A. (2002).** Quorum-sensing in *Rhizobium*. Antonie Van Leeuwenhoek **81**(1-4): 397-407.
- Wu, H., Song, Z., Hentzer, M., Andersen, J. B., Molin, S., Givskov, M. and Hoiby, N. (2004).** Synthetic furanones inhibit quorum-sensing and enhance bacterial clearance in *Pseudomonas aeruginosa* lung infection in mice. J Antimicrob Chemother **53**(6): 1054-61.
- Xavier, K. B. and Bassler, B. L. (2003).** LuxS quorum sensing: more than just a numbers game. Curr Opin Microbiol **6**(2): 191-97.
- Xavier, K. B. and Bassler, B. L. (2005).** Interference with AI-2-mediated bacterial cell-cell communication. Nature **437**(7059): 750-53.
- Yang, F., Wang, L. H., Wang, J., Dong, Y. H., Hu, J. Y. and Zhang, L. H. (2005).** Quorum quenching enzyme activity is widely conserved in the sera of mammalian species. FEBS Lett **579**(17): 3713-17.
- Yang, M., Sun, K., Zhou, L., Yang, R., Zhong, Z. and Zhu, J. (2009).** Functional analysis of three AHL autoinducer synthase genes in *Mesorhizobium loti* reveals the important role of quorum sensing in symbiotic nodulation. Canadian Journal of Microbiology **55**(2): 210-14.
- Yarwood, J. M., Bartels, D. J., Volper, E. M. and Greenberg, E. P. (2004).** Quorum sensing in *Staphylococcus aureus* biofilms. J Bacteriol **186**(6): 1838-50.
- Yates, E. A., Philipp, B., Buckley, C., Atkinson, S., Chhabra, S. R., Sockett, R. E., Goldner, M., Dessaux, Y., Camara, M., Smith, H. and Williams, P. (2002).** N-acylhomoserine lactones undergo lactonolysis in a pH-, temperature-, and acyl chain length-dependent manner during growth of *Yersinia pseudotuberculosis* and *Pseudomonas aeruginosa*. Infect Immun **70**(10): 5635-46.
- Zang, T. M., Hollman, D. A., Crawford, P. A., Crowder, M. W. and Makaroff, C. A. (2001).** *Arabidopsis* Glyoxalase II Contains a Zinc/Iron Binuclear Metal Center That Is Essential for Substrate Binding and Catalysis. J.Biol.Chem. **276**: 4788-95.
- Zhang, H. B., Wang, L. H. and Zhang, L. H. (2002).** Genetic control of quorum-sensing signal turnover in *Agrobacterium tumefaciens*. Proc Natl Acad Sci USA **99**(7): 4638-43.
- Zhang, L., Murphy, P. J., Kerr, A. and Tate, M. E. (1993).** *Agrobacterium* conjugation and gene regulation by N-acyl-L-homoserine lactones. Nature **362**(6419): 446-48.

VII. Appendix

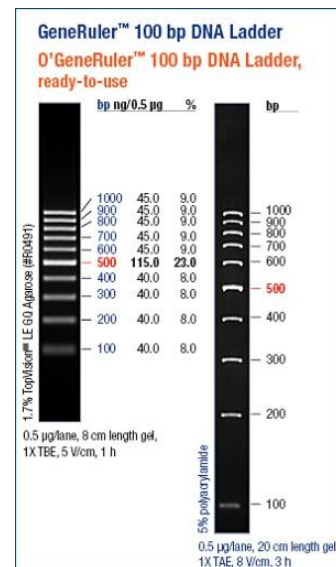
1. Molecular markers

1.1. Gene Ruler (Fermentas, St-Leon-Rot, Germany)

GeneRuler™ 1 kb DNA Ladder

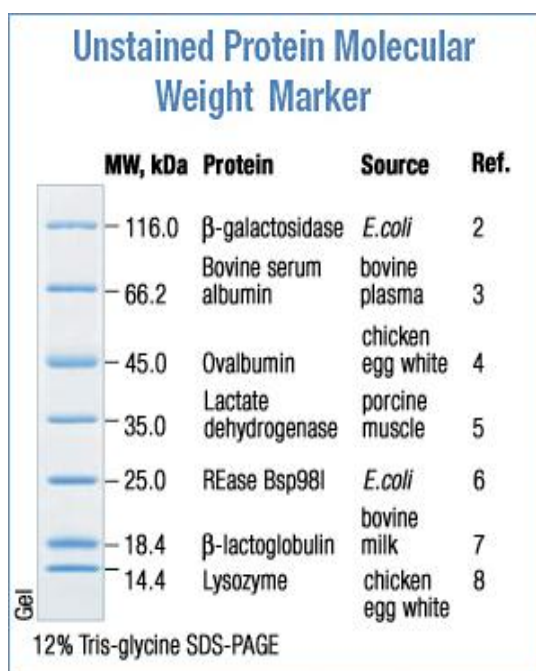


GeneRuler™ 100 bp DNA Ladder

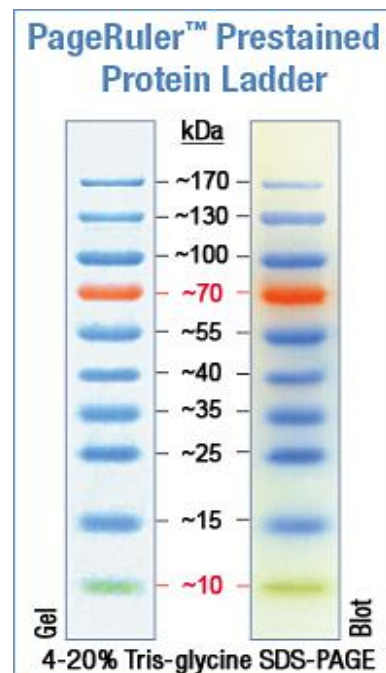


1.2. Protein marker (Fermentas, St-Leon-Rot, Germany)

Protein PageRuler™ (#SM0431)



Prestained Protein Ladder™ (#SM0671)



2. Additional figures and tables

2.1. Calibration curve for determination of protein content after Bradford 1976

Prior to the measurement of the protein content, a calibration curve was generated using different concentrations of BSA (bovine serum albumin), therefore 1, 0.5, 0.25 and 0.125 mg/mL BSA were measured. The calculated calibration line is given below.

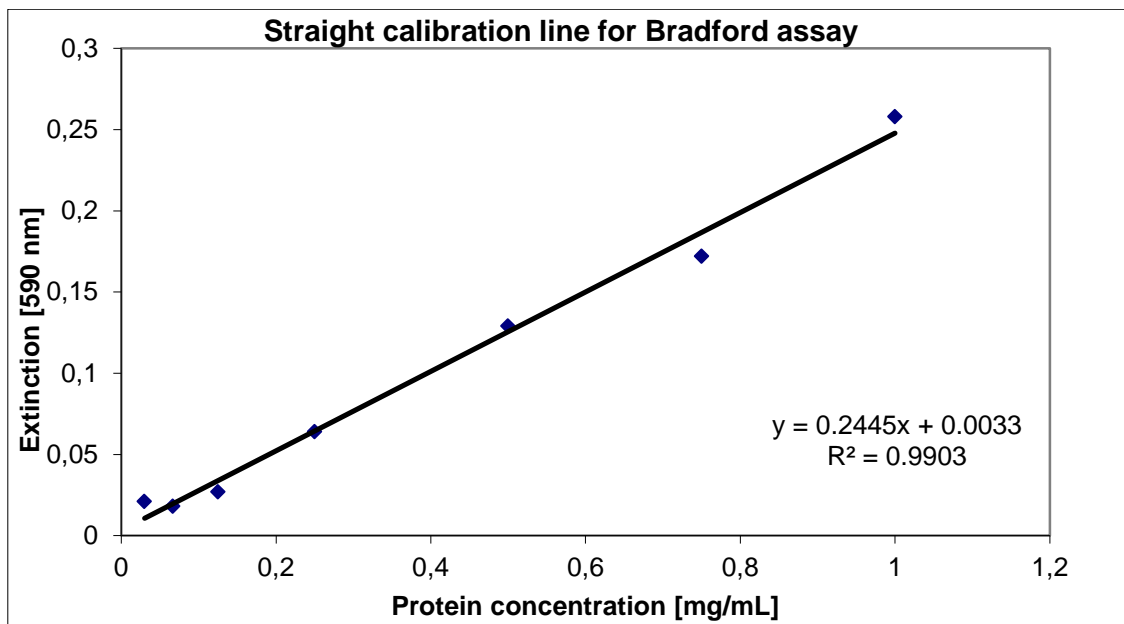


Figure 28: Straight calibration line for determination of protein content by the Bradford assay.

2.2. Evaluation scheme for swarming / swimming motility

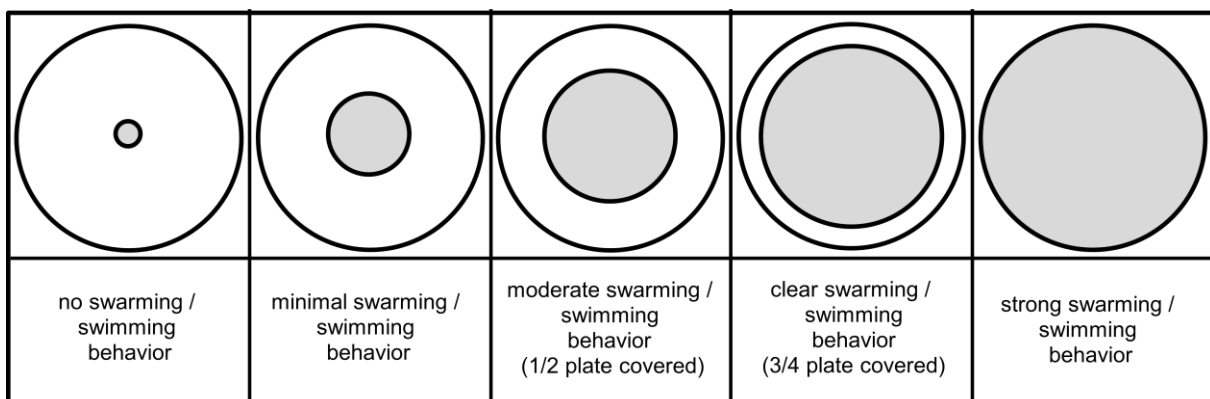


Figure 29: Definition of the motility of *E. coli* XL1 blue and of *P. aeruginosa* PAO1 on agar plates.

2.3. Summary of hydrolases found in *Rhizobium* sp. NGR234

Using the sequence-based screening for putative QQ genes, several hydrolases were selected based on their annotation. The putative QQ genes are summarized in Table 18.

Table 18: Hydrolases found in the genome of NGR234 by sequence analysis

ORF ID	Annotated/predicted function	Size of protein (no.of AA)
NGR_c10830	putative hydrolase	208
NGR_c28340	putative esterase/hydrolase	349
NGR_c16700	putative hydrolase	251
NGR_c17080	probable hydrolase	306
NGR_b05590	putative hydrolase or acyltransferase (alpha/beta-hydrolase superfamily)	314
NGR_b05410	putative esterase of the alpha/beta-hydrolase superfamily	261
NGR_b21240	beta-ketoadipate enol-lactone hydrolase	273
NGR_c08550	putative hydrolase	203
NGR_c04450	putative hydrolase	392
NGR_b15930	probable hydrolase	219
NGR_b14140	putative esterase of the alpha/beta-hydrolase fold	205
NGR_c21350	hydrolase of the alpha/beta fold family	318
NGR_c05550	putative hydrolase	221
NGR_c08180	putative hydrolase	300

2.4. Calculation of the coverage of the NGR234 cosmid clone library

To determine the extent of the cosmid clone library as well as its coverage of the NGR234 genome, several calculations had to be accomplished using the following formula:

$$N = \ln(1-P) / \ln(1-f)$$

N : required number of cosmid clones

P : desired probability

f : proportion of the genome contained in a single clone

This formula was used to determine the optimal number of clones required to ensure with a certain probability that any given DNA sequence is contained within the genomic library. The first generated cosmid clones comprised insert sizes ranging from 33-42 kb and had an experimentally determined insert rate of 95%. The calculation of the optimal number of clones was realized with an averaged insert size of 37.5 kb and an expected probability of 95%:

$$N = \ln(1-0.95) / \ln(1 - [3.75 \times 10^4 \text{ bases} / 6.9 \times 10^6 \text{ bases}])$$

$$N = 549.71 = \sim \mathbf{550 \text{ clones}}$$

A minimum of 600 clones had to be established within the library to reach the optimal number of clones considering also empty clones. Consequently, a total of 603 cosmid clones were generated, ensuring a 95% probability of a given DNA sequence of NGR234 being contained within the library composed of 33-42 kb DNA fragments.

For the calculation of the coverage of the NGR234 genome by obtained cosmid clones, the formula was converted:

$$N = \ln(1-P) / \ln(1-f) \iff$$

$$P = 1 - (1-f)^N$$

$$P_{33 \text{ kb}} = 1 - (1 - [3.3 \times 10^4 \text{ bases} / 6.9 \times 10^6 \text{ bases}])^{603} = 0.944 = \mathbf{94.4\%}$$

$$P_{37.5 \text{ kb}} = 1 - (1 - [3.75 \times 10^4 \text{ bases} / 6.9 \times 10^6 \text{ bases}])^{603} = 0.963 = \mathbf{96.3\%}$$

$$P_{42 \text{ kb}} = 1 - (1 - [4.2 \times 10^4 \text{ bases} / 6.9 \times 10^6 \text{ bases}])^{603} = 0.975 = \mathbf{97.5\%}$$

Coverage of the cosmid library was calculated based on the lower/upper limit of insert sizes as well as the average insert size of 37.5 kb. Concluding, the constructed NGR234 cosmid

clone library, when using the averaged insert size, covers at least 96.3% of the 6.9 Mbp NGR234 genome. Considering lower/upper limits of insert sizes, the overall coverage of NGR234's genome ranges between 94.4% and 97.5%.

2.5. Additional figures of motility assays accomplished in *E. coli* XL1 blue and *P. aeruginosa* PAO1

2.5.1 Motility assays carried out with pDrive::*qsdr2*

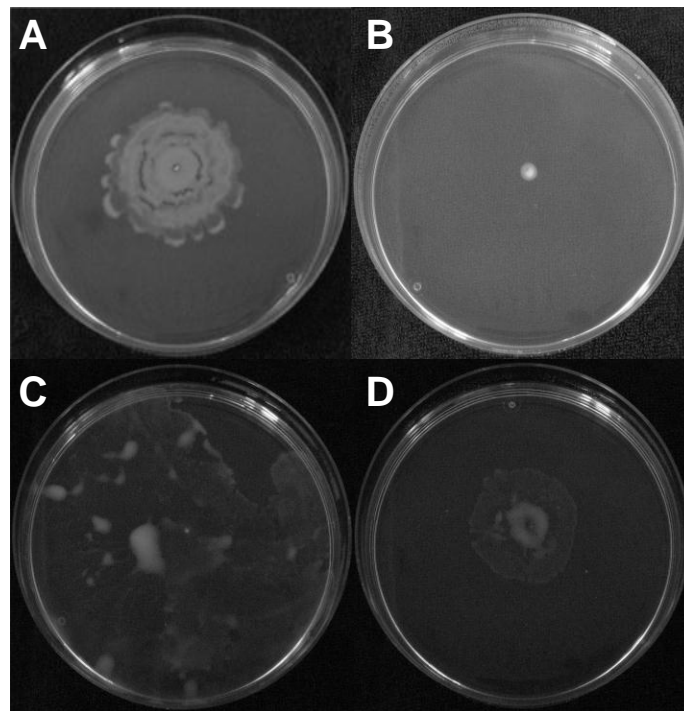


Figure 30: Motility assays accomplished with pDrive::*qsdr2* in *E. coli* XL1 blue and PAO1. (A) Control: *E. coli* XL1 blue cells without vector. (B) *E. coli* XL1 blue harboring pDrive::*qsdr2*. (C) Control: PAO1 cells on swarming plate without supplements. (D) Crude cell extract of pDrive::*qsdr2* with PAO1.

2.5.2 Motility assays carried out with pDrive::*aldR*

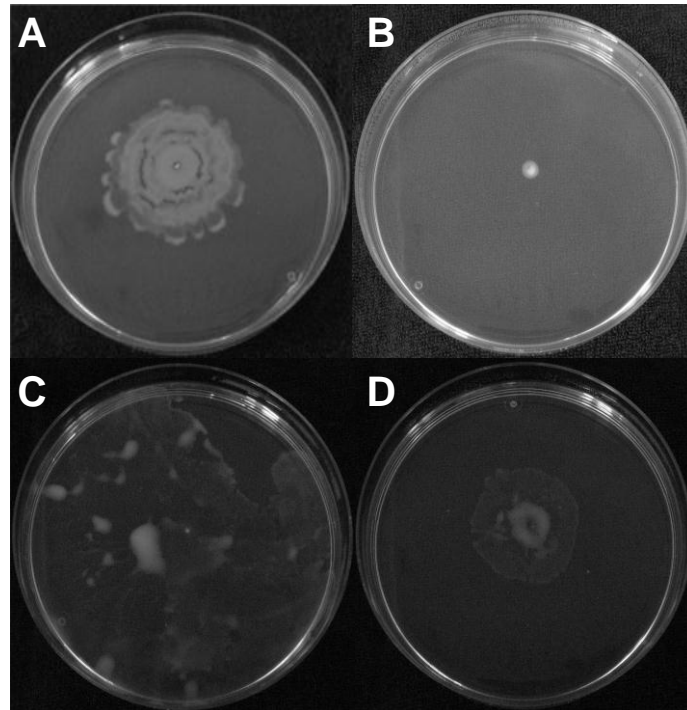


Figure 31: Motility assays accomplished with pDrive::*aldR* in *E. coli* XL1 blue and PAO1. (A) Control: *E. coli* XL1 blue cells without vector. (B) *E. coli* XL1 blue harboring pDrive::*aldR*. (C) Control: PAO1 cells on swarming plate without supplements. (D) Crude cell extract of pDrive::*aldR* with PAO1.

2.5.3 Complementation experiments with DIhR, PAO1 and external AHLs

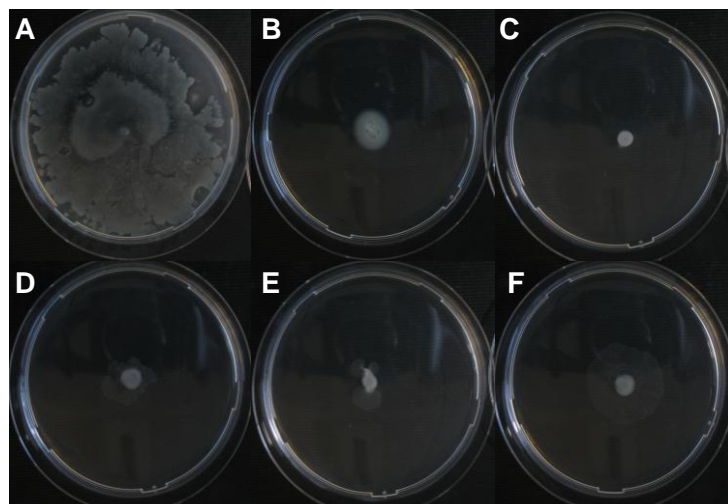


Figure 32: Complementation assay with 3-oxo-C8-HSL and 5 µg/mL DIhR. (A) Positive control: PAO1 without protein and AHLs. (B) Negative control: PAO1 inhibited swarming behavior triggered by 5 µg/mL DIhR. (C) PAO1 swarming behavior with DIhR and 10 µL 3-oxo-C8-HSL (10^{-7} M). (D) PAO1 swarming behavior with DIhR and 10 µL 3-oxo-C8-HSL (10^{-6} M). (E) PAO1 swarming behavior with DIhR and 10 µL 3-oxo-C8-HSL (10^{-5} M). (F) PAO1 swarming behavior with DIhR and 10 µL 3-oxo-C8-HSL (10^{-4} M).

2.6. β -Lactam degradation assay with *E. coli* XL1 blue harboring pET24c::*qsdR1*

Table 19: β -Lactam degradation assay with pET24c::*qsdR1*

β -Lactam antibiotic	Abbreviation	Diameter [cm]
Amoxicillin	AML10	1.8
Mezlocillin	MEZ30	1.5
Penicillin G	P5	1.2
Ceftriaxone	CRO30	2.85
Cefaclor	CEC30	1.7
Ceftriaxone	CRO30	2.8
Ceftributen	CFT30	2.5
Cefamandole	MA30	2
Cefoxitin	FOX30	2.4
Cefadroxil	CFR30	1.2
Cefetrazidol	CAZ10	2.15

3. Detailed listing of ORFs identified on cosmid clones

3.1. ORFs identified on pWEB-TNC-A5

ORF ID	Annotated/predicted function
NGR_c35340	N-acetylglucosamine-6-phosphate deacetylase
NGR_c35350	copper homeostasis protein
NGR_c35360	ROK family protein
NGR_c35370	putative glutamyl-tRNA amidotransferase subunit A protein
NGR_c35380	putative membrane protein
NGR_c35390	SlyX-like protein
NGR_c35400	basic membrane lipoprotein
NGR_c35410	peptide methionine sulfoxide reductase A 1
NGR_c35420	hypothetical protein
(NGR_c35430)	RNA)
NGR_c35440	putative ABC transporter-like, ATP-binding protein
NGR_c35450	hypothetical protein
NGR_c35460	activator of Hsp90 ATPase 1 family protein
NGR_c35470	hypothetical protein contains putative phospholipid-binding domain
NGR_c35480	auxin efflux carrier
NGR_c35490	branched-chain-amino-acid aminotransferase
NGR_c35500	cytochrome C, class I

NGR_c35510	3-deoxy-D-manno-octulosonate cytidyltransferase
NGR_c35520	prephenate dehydratase PheA
NGR_c35530	hypothetical protein
NGR_c35540	putative glyoxalase/bleomycin resistance protein/dioxygenase
NGR_c35550	putative transcriptional regulator
NGR_c35560	predicted NUDIX hydrolase
NGR_c35570	putative histidine triad (HIT) protein
NGR_c35580	DNA polymerase III, subunits gamma and tau
NGR_c35590	putative cytoplasmic protein
NGR_c35600	recombination protein, RecR
NGR_c35610	putative lytic murein transglycosylase
NGR_c35620	putative outer membrane protein, OmpA/MotB domain protein
NGR_c35630	ErfK/YbiS/YcfS/YnhG family protein
NGR_c35640	putative transmembrane transport protein
NGR_c35650	putative cytoplasmic protein
NGR_c35660	transcription termination factor, NusA
NGR_c35670	ribosomal protein L7Ae family protein
NGR_c35680	translation initiation factor IF-2
NGR_c35690	ribosome-binding factor A
NGR_c35700	tRNA pseudouridine synthase B
NGR_c35710	signal transduction histidine kinase
NGR_c35720	30S ribosomal protein S15
NGR_c35730	polyribonucleotide nucleotidyltransferase

3.2. ORFs identified on pWEB-TNC-B2

ORF ID	Annotated/predicted function
NGR_b21920	putative transport protein
NGR_b21930	putative kinase
NGR_b21940	putative ATP-binding component of a transport system
NGR_b21950	putative integral membrane protein
NGR_b21960	probable amino acid ABC transporter, permease protein
NGR_b21970	putative oxidoreductase
NGR_b21980	probable amino acid ABC transporter, substrate-binding protein
NGR_b21990	type III effector HRP-dependent outers
NGR_b22000	ribulose biphosphate carboxylase large chain (EC 4.1.1.39)
NGR_b22010	putative GntR family transcriptional regulator
NGR_b22020	hypothetical protein
NGR_b22030	oxidoreductase, putative glucose-fructose oxidoreductase

NGR_b22040	probable ribose ABC transporter, permease protein
NGR_b22050	probable ribose ABC transporter, ATP-binding protein
NGR_b22060	putative lipoprotein
NGR_b22070	ribose ABC transporter, periplasmic ribose-binding protein
NGR_b22080	hypothetical protein
NGR_b22090	transcriptional regulator, AraC family
NGR_b22100	putative isoquinoline 1-oxidoreductase alpha subunit
NGR_b22110	putative oxidoreductase beta subunit
NGR_b22120	hypothetical protein
NGR_b22130	hypothetical protein
NGR_b22140	transcriptional regulator, AraC family
NGR_b22150	hypothetical protein
NGR_b22160	senescence marker protein-30 (SMP-30)
NGR_b22170	putative GntR family transcriptional
NGR_b22180	dTDP-glucose 4,6-dehydratase
NGR_b22190	probable NTP pyrophosphohydrolase protein, MuT/nudix family
NGR_b22200	conserved hypothetical protein
NGR_b22210	putative transcriptional regulator, AbrB family

3.3. ORFs identified on pWEB-TNC-B9

ORF ID	Annotated/predicted function
NGR_c15790	putative tetracycline resistance protein
NGR_c15800	predicted multidrug efflux protein
NGR_c15810	phosphopantetheine adenyltransferase (EC 2.7.7.3)
NGR_c15820	peptidyl-prolyl cis-trans isomerase, cyclophilin type (EC 5.2.1.8)
NGR_c15830	peptidyl-prolyl cis-trans isomerase, cyclophilin type (EC 5.2.1.8)
NGR_c15840	S-adenosylmethionine tRNA ribosyltransferase-isomerase (EC 5.-.-.-)
NGR_c15850	queuine tRNA-ribosyltransferase (EC 2.4.2.29)
NGR_c15860	hypothetical protein
NGR_c15870	putative short chain dehydrogenase/reductase family member
NGR_c15880	hypothetical protein
NGR_c15890	putative transmembrane protein
NGR_c15900	hypothetical protein
NGR_c15910	putative ErfK/YbiS/YhnG oxidoreductase
NGR_c15920	2,5-dichloro-2,5-cyclohexadiene-1,4-diol dehydrogenase (EC 1.1.1.-)
NGR_c15930	probable transporter
NGR_c15940	hypothetical protein
NGR_c15950	adenylate cyclase (EC 4.6.1.1)

NGR_c15960	putative transposase of disrupted insertion sequence
NGR_c15970	carboxy-terminus of predicted integrase/transposase
NGR_c15980	putative transposase number 1 for insertion sequence NGRIS-4i
NGR_c15990	putative transposase number 2 for insertion sequence NGRIS-4i
NGR_c16000	amino-terminus of predicted integrase/transposase
NGR_c16010	amino-terminus of predicted integrase/transposase
NGR_c16020	metal-dependent hydrolase
NGR_c16030	deoxyribonuclease (EC 3.1.21.-)
NGR_c16040	methionyl-tRNA synthetase (EC 6.1.1.10)
NGR_c16050	hypothetical protein
NGR_c16060	DNA polymerase III, delta prime subunit
NGR_c16070	thymidylate kinase (EC 2.7.4.9)
NGR_c16080	penicillin binding protein
NGR_c16090	lipoprotein
NGR_c16100	hypothetical protein
NGR_c16110	putative exported molybdopterin cofactor-containing protein
NGR_c16120	putative exported molybdopterin cofactor-containing protein
NGR_c16130	putative transmembrane b-type cytochrome protein
NGR_c16140	pentapeptide MXKDX repeat protein
NGR_c16150	ECF family sigma factor
NGR_c16160	putative transmembrane protein
NGR_c16170	HpcH/HpaI aldolase
NGR_c16180	phosphoribosylaminoimidazole-succinocarboxamidesynthase PurC
NGR_c16190	phosphoribosylformylglycinamide synthase PurS
NGR_c16200	phosphoribosylformylglycinamide synthase I (FGAMsynthase I) PurQ
NGR_c16210	lipoprotein, putative
NGR_c16220	oxidoreductase, short chain dehydrogenase/reductase family
NGR_c16230	putative transcriptional regulator, GntR family
NGR_c16240	hypothetical protein

3.4. ORFs identified on pWEB-TNC-C6

ORF ID	Annotated/predicted function
NGR_b16700	WD-repeat protein, beta transducin-like protein
NGR_b16710	hypothetical protein
NGR_b16720	hypothetical protein
NGR_b16730	oleandomycin glycosyltransferase (EC 2.4.1.-)
NGR_b16740	hypothetical protein
NGR_b16750	putative ATP-binding protein of disrupted insertion sequence

NGR_b16760	Trm23a-like transposase, carboxy-terminus
NGR_b16770	putative transposase number 1 for insertion sequence NGRIS-4i
NGR_b16780	putative transposase number 2 for insertion sequence NGRIS-4i
NGR_b16790	putative transposase number 4 for insertion sequence NGRIS-4i
NGR_b16800	Trm23a-like transposase, amino-terminus
NGR_b16810	putative lipoprotein
NGR_b16820	hypothetical protein
NGR_b16830	two component sensor-kinase
NGR_b16840	putative NodW, Nodulation protein
NGR_b16850	putative two-component response regulator protein
NGR_b16860	C4-dicarboxylate transport transcriptional regulatory protein
NGR_b16870	metal-dependent hydrolase (EC 3.-.-.)
NGR_b16880	NmrA family protein
NGR_b16890	Cupin domain protein
NGR_b16900	LysE type translocator
NGR_b16910	putative transcriptional regulator, AsnC/Lrp family
NGR_b16920	Riboflavin-specific deaminase
NGR_b16930	hypothetical protein
NGR_b16940	NTP pyrophosphohydrolase, MutT family
NGR_b16950	hypothetical protein
NGR_b16960	hypothetical protein
NGR_b16970	putative ABC-transporter ATP-binding protein
NGR_b16980	putative ABC transport system, permease protein
NGR_b16990	probable polyamine ABC transporter, permease protein
NGR_b17000	putative amino acid ABC transporter, periplasmic solute-binding protein
NGR_b17010	NIPSNAP superfamily
NGR_b17020	probable aldehyd dehydrogenase

3.5. ORFs identified on pWEB-TNC-G2

ORF ID	Annotated/predicted function
NGR_c23380	putative transmembrane protein
NGR_c23370	putative transmembrane protein
NGR_c23360	hypothetical protein
NGR_c23350	MoxR family protein
NGR_c23340	hypothetical protein
NGR_c23330	NTP pyrophosphohydrolase, MutT family
NGR_c23320	polyA polymerase family protein

NGR_c23310	hypothetical protein
NGR_c23300	Adenine phosphoribosyltransferase (EC 2.4.2.7)
NGR_c23290	MaoC domain protein
NGR_c23280	MaoC-like dehydratase
NGR_c23270	putative GTP-binding protein
NGR_c23260	ATP-dependent Clp protease adaptor protein, ClpS
NGR_c23250	putative transcriptional regulator, LysR family
NGR_c23240	putative transcriptional regulator, LysR family
NGR_c23230	conserved hypothetical protein
NGR_c23220	peptidyl-tRNA hydrolase (EC 3.1.1.29)
NGR_c23210	ABC transporter, substrate binding protein [amino acid]
NGR_c23200	GGDEF family protein
NGR_c23190	50S ribosomal protein L25
NGR_c23180	50S ribosomal protein L25
NGR_c23170	putative transcriptional regulator, Fis family
NGR_c23160	putative transposase for insertion sequence NGRIS-10
NGR_c23150	acetaldehyde dehydrogenase 2 (EC 1.2.1.3)
NGR_c23140	conserved hypothetical protein
NGR_c23130	YD repeat protein

VIII. Abbreviations

3-oxo-C6-HSL	<i>N</i> -(3-oxohexanoyl)-L-homoserine lactone
3-oxo-C8-HSL	<i>N</i> -(3-oxooctanoyl)-L-homoserine lactone
3-oxo-C12-HSL	<i>N</i> -(3-oxododecanoyl)- L-homoserine lactone
3841	<i>R. leguminosarum</i> bv. <i>viciae</i> 3841
A	Ampere
A.	<i>Agrobacterium</i>
AA	Amino acid
ACP	Acyl carrier protein
AHL	Acyl homoserine lactone
AHLase	AHL lactonase
AI	Autoinducer
AI-1	Autoinducer 1
AI-2	Autoinducer 2
AI-3	Autoinducer 3
AIP	Autoinducer peptide
AldR	Acetaldehyde dehydrogenase from NGR234
Amp	Ampicillin
ANU265	<i>Rhizobium</i> sp. ANU265
APS	Ammonium persulfate
AT	<i>Agrobacterium tumefaciens</i> medium
B.	<i>Bacillus</i>
B.	<i>Bradyrhizobium</i>
BCIP	5-bromo-4-chloro-3'-indolyphosphate p-toluidine salt
bidest	Bidistilled
bp	Base pairs
BSA	Bovine serum albumin
°C	Degree Celsius
C4-HSL	<i>N</i> -(butanoyl)-L-homoserine lactone
C	Carbon

C.	<i>Chromobacterium</i>
CFN42	<i>Rhizobium etli</i> CFN42
CFU	Colony forming units
ChV2	<i>Chromobacterium violaceum</i> ChV2
Cm	Chloramphenicol
conc.	concentrated
CV026	<i>Chromobacterium violaceum</i> CV026
Da	Dalton
DH5 α	<i>E. coli</i> DH5 α
Dl _h R	Dienelactone hydrolase from NGR234
DMF	Dimethylformamide
DMSO	Dimethyl sulfoxide
DNA	Desoxyribonucleic acid
dNTP	Desoxyribonucleotide-5'-triphosphate
DPD	4,5-dihydroxy-2,3-pentanedione
e	e-Value
<i>E.</i>	<i>Escherichia</i>
EC	European Commission number
<i>E. coli</i>	<i>Escherichia coli</i>
E-Cup	Eppendorf cup
EDTA	Ethylendiaminetetraacetate
e.g.	For example (exempli gratia)
EHEC	Enterohemorrhagic <i>E. coli</i>
ELH	Enol-lactone hydrolase
EPI100	<i>E. coli</i> EPI100
<i>et al.</i>	<i>et alii</i> (and others)
EtOH	Ethanol
g	Gram
GC	Guanine and cytosine content
GDSL	Conserved motif of esterases and lipases
Gm	Gentamycin

h	Hour
H ₂ O _{bidest}	Double distilled water
HitR	Histidine triad protein from NGR234
His-tag	Histidine ₆ -tag
HPLC	High performance liquid chromatography
HSL	Homoserine lactone
HydR	Hydrolase from NGR234
i.e.	id est/that is
IPTG	Isopropyl-β-D-1-thiogalactopyranoside
k	Kilo (10 ³)
Kac	Potassium acetate
Kan	Kanamycin
kb	Kilo base pairs
kDa	Kilo Dalton
L	Liter
LB	Luria Bertani
LEW	Lysis equilibration wash buffer
m	Milli (10 ⁻³)
M	Mole (mol/L)
mA	Mili ampere
μ	Micro (10 ⁻⁶)
<i>M.</i>	<i>Mesorhizobium</i>
MAFF303099	<i>M. loti</i> MAFF303099
max.	Maximum
Mbp	Mega base pairs
MCS	Multiple cloning site
MetOH	Methanol
mg	Milligram
μg	Microgram
μL	Microliter
μF	Microfarad

min	Minute
min.	Minimum
mL	Milliliter
mM	Milli mole
mol	Molar
MS	Mass spectrometry
MWCO	Molecular weight cut off
n	Nano (10^{-9})
N	Normal mole
NBT	nitro-blue tetrazolium chloride
NCBI	National Center for Biotechnology Information
NF	Not found
NGR234	<i>Rhizobium</i> sp. NGR234
nm	Nanometer
nt	Nucleotide
NTL4	<i>Agrobacterium tumefaciens</i> NTL4
Ntn	N-terminal nucleophilic hydrolase domain
NUDIX	N-ter. NADH pyrophosphatase/C-ter. NADH pyrophosphatase
OD	Optical density
OD ₆₀₀	Optical density at wavelength 600 nm
ONPG	<i>ortho</i> -nitrophenyl- β -D-galactopyranoside
ORF	Open reading frame
<i>P.</i>	<i>Pseudomonas</i>
PAO1	<i>Pseudomonas aeruginosa</i> PAO1
PAGE	Polyacrylamide electrophoresis
pBBR	pBBR1MCS
pBBR-5	pBBR1MCS-5
PCR	Polymerase chain reaction
<i>Pfu</i>	<i>Pyrococcus furiosus</i>
PON	Paraoxonase
psi	Pound per square inch

pSK+	pBluescript II SK+
PTE	Phosphotriesterase
PVDF	Polyvinylidene fluoride
QQ	Quorum quenching
QS	Quorum sensing
QsdR	Quorum sensing degrading protein from NGR234
R	Resistance
<i>R.</i>	<i>Rhizobium</i>
<i>R.</i>	<i>Rhodococcus</i>
RNA	Ribonucleic acid
RNAse	Ribonuclease
Rif	Rifampicin
rpm	Rounds per minute
RT	Room temperature
R _t	Retention time
SAM	S-adenosyl methionine
SDS	sodium dodecyl sulfate
sec	Second
SM1021	<i>Sinorhizobium meliloti</i> SM1021
Sp	Spectinomycin
<i>sp.</i>	Species
T1SS	Type one secretion system
T2SS	Type two secretion system
T3SS	Type three secretion system
T4SS	Type four secretion system
TAE	Trisacetate-EDTA
T _{ann}	Annealing temperature
<i>Taq</i>	<i>Thermus aquaticus</i>
TE	Tris-EDTA
TEMED	N,N,N',N'-Tetramethylene ethylene diamine
Tet	Tetracycline

TFF	Tangential flow filtration
T _m	Melting temperature
Tris	Tris-(hydroxymethylene)-aminoethane
TBST	Tris buffered saline with Tween
TY	TY medium
U	Unit
USDA257	<i>Sinorhizobium fredii</i> USDA257
USDA110	<i>B. japonicum</i> USDA110
UV	Ultraviolet
V.	<i>Variovorax</i>
V	Volt
v/v	Volume per volume
WT	Wild type
w/v	Weight per volume
X-Gal	5-bromo-4-chloro-3-indolyl-β-D-galactopyranoside
XL1 blue	<i>E. coli</i> XL1 blue
YDC	<i>Chromobacterium</i> medium
YEM	Yeast mannitol medium

Abbreviations of AA

A	Ala	Alanine	M	Met	Methionine
C	Cys	Cysteine	N	Asn	Asparagine
D	Asp	Aspartic acid	P	Pro	Proline
E	Glu	Glutamic acid	Q	Gln	Glutamine
F	Phe	Phenylalanine	R	Arg	Arginine
G	Gly	Glycine	S	Ser	Serine
H	His	Histidine	T	Thr	Threonine
I	Ile	Isoleucine	V	Val	Valine
K	Lys	Lysine	W	Trp	Tryptophan
L	Leu	Leucine	Y	Tyr	Tyrosine

Acknowledgements

First of all I would like to thank Prof. Dr. Wolfgang Streit for giving me the opportunity to accomplish my work in his group, for providing me this spectacular research topic and for his support throughout the last four years. I would like to thank Prof. Dr. Bernward Bisping for agreeing to be the second assessor of my PhD thesis and PD Dr. Andreas Pommerening-Röser for his support during the administration.

Furthermore, I would like to acknowledge Dr. Christel Vollstedt for the scientific support of my work as well as the manuscripts, her practical experience and her patience. Further, I wish to thank Jun. Prof. Dr. Mirjam Perner for fruitful scientific discussions, her motivation and her help with language problems.

I wish to thank my girls from the office - Janine Maimanakos, Jennifer Chow and Stefanie Böhnke - for their support in lab routine, the great atmosphere and team spirit as well as for the uncountable funny moments. It was a pleasure to be a part of this "girl's office". Further, I would like to thank Arkadius Ozimek for his support and motivation during this time as well as being a great lab companion and a very good friend.

In the last four years, I have benefited from the never ending helpfulness of Angela Jordan and Martina Schmidt. Thank you very much for your continuous support in every day lab routine and your excellent practical experience (which helped me a lot with our special friend NGR234).

I would like to thank my colleagues for proofreading parts of the PhD thesis. Thanks to Arkadius Ozimek, Christian Utpatel, Claudia Hornung, Mariita Rodriguez, Sabine Zumbrägel. Further, I wish to thank all colleagues that accompanied me during the time in Duisburg and Hamburg. I have benefited from a great lab team full of practical experience, deep knowledge, helpfulness, commitment and friendship. It was a wonderful time.

Last but not least, I would like to thank my boyfriend and my best friends for their motivation, patience and their help in many situations during the practical lab time and the final phase of my PhD thesis.

Finally, and most importantly, I wish to thank my family, my grandparents, my parents and my brother, for their continuous support throughout the years and especially for giving me the opportunity to study and accomplish a doctorate. Thank you very much - this work is for you.